

**Manipulating the *Chlamydomonas reinhardtii* Phosphate
overplus response for Biological Phosphorus Recovery from
Wastewater**

Laura Tatiana Zúñiga Burgos

Submitted in accordance with the requirements for the degree of
Doctor of Philosophy

The University of Leeds
School of Civil Engineering
School of Molecular and Cellular Biology

September 2023

The candidate confirms that the work submitted is her own and that appropriate credit has been given within the thesis where the reference has been made to the work of others.

This copy has been supplied on the understanding that it is copyright material and that no quotation from the thesis may be published without proper acknowledgement.

Acknowledgements

I would like to express my sincere gratitude to my supervisors Dr Miller Alonso Camargo-Valero and Professor Alison Baker, for believing in my potential as a researcher and for giving me the opportunity to work on this beautiful project, where both fundamental and applied sciences can be connected with the shared vision, that interdisciplinarity will help to achieve real change in this world. During my PhD experience at the University of Leeds, their supervision, advice, reviews and constant support, made a significant contribution to my personal and academic development. Without them, this thesis could not have been produced the way it is.

I also wish to express my gratitude and appreciation to the technical and laboratory management staff of the School of Civil Engineering (Dr David Elliot, Emma Tidswell and Morgan McGowan), the School of Chemical and Process Engineering (Dr Adrian Cunliffe and Mrs Karine Alves), the Faculty of Biological Sciences (Dr Iain Manfield – Biomolecular interactions, Dr Ruth Hughes – Bioimaging facilities). I thank you all for your assistance with my laboratory work and insightful discussions. I also thank Dr Stephen Slocombe, for sharing his expertise in algal biology with me and providing advice in the development of my laboratory skills, and to Dr Franja Prosenc for being a great support during the last year of my PhD. To my fellow PhD students, especially to my friends Johan Andres Pasos-Panqueva, Angie Lamprea-Pineda, Angela Bayona-Valderrama, and Hannah Robinson, with whom I shared a PhD journey full of emotions and challenges. I thank you all for the memorable moments that I will keep with me forever.

To Professor Adolfo Saiardi from University College of London (UCL). I thank you for providing a great one-to-one training experience on polyphosphate analysis techniques, contributions and insightful discussions. The learning obtained during this visit led to a very fruitful collaboration, which represents a large part of the work presented in this thesis.

I gratefully acknowledge the financial support given by the School of Civil Engineering, University of Leeds and the GCRF Water Security and Sustainable Development Hub.

I want to give special thanks to Dr Johana Husserl for her mentorship and support. We will finally become 'colleagues' as you said. To my best friends Joan, Alejandra and Marisol, thank you for always reminding me who I am. To Max, thank you for being that 'grumpy friendly face' and becoming that word 'love' in this place. Your constant presence, kindness and pragmatic ways helped me to keep the PhD crisis under control. Finally, this thesis is dedicated to the women who raised me and sacrificed so much to help me pursue my dreams.

Esta tesis está dedicada a mis abuelitas Francisca y Rosita, y a mi madre Ángela:

No tengo como agradecerles todo lo que han hecho por mí.

Abstract

Global dependency on phosphate (P) rich rock mining to produce inorganic phosphorus fertilisers has broken the balance of the phosphorus cycle and is threatening our ability to achieve food and water security. The predicted phosphorus scarcity crisis due to the imminent depletion of P-rock reserves represents one of the biggest challenges for humanity, as phosphorus is irreplaceable to sustain life on Earth. At the same time, nutrient-rich agricultural runoff and sewage discharges are generating an excessive load of nutrients into water bodies. This is triggering the eutrophication of aquatic ecosystems at a scale never seen before. To protect water resources, strict nutrient discharge limits have been set by local environmental agencies, particularly in Europe, the UK and North America, where limits are revised on a regular basis. For that reason, current P control systems struggle to comply with the P discharge limits; in addition, they do not facilitate P recovery and reuse. Microalgae may offer a solution as they grow naturally in wastewater, taking up nutrients in the process, but their vulnerability to changes in environmental conditions limits their use to reliably control P at wastewater treatment plants.

Chlamydomonas reinhardtii and microalgae in general, can exhibit a P overplus response when transferred from P-deprived to P-replete conditions. This is the overaccumulation of P in the form of polyphosphate (polyP) granules. Understanding the factors that influence microalgal P overplus could be key to enhancing the robustness of P recovery in wastewater treatment systems using algae-based technologies. In this thesis, a quantitative method to analyse polyP in *Chlamydomonas* was developed and used along with more qualitative methods to follow changes in polyP and other physiological parameters during P-depletion and repletion. The results show that polyP content in algal cells is the key physiological parameter to monitor during P-deprivation, as the lowest in-cell polyP content triggers a bigger P overplus response upon P resupply. During P resupply, the successful P recovery depends on both P uptake and biomass growth. While supplying all nutrients rather than P alone, did not affect polyP accumulation, it promoted biomass growth which led to a complete removal of P from the media in 12 h. These results contribute to better future design of P recovery systems from wastewaters using P overplus response in microalgae.

This work provides further evidence of the PSR1 transcription factor of *C. reinhardtii* as the most important regulator of P homeostasis. The experimental comparison between PSR1 overexpression and PSR1 knockout strains led to

the determination that PSR1 is a key component of polyP synthesis and hence of P overplus responses.

Real-life application of the research findings about the P overplus phenomenon requires a deeper understanding of microalgal P metabolism in terms of P sensing, P uptake, polyP synthesis and turnover.

Table of contents

Acknowledgements	ii
Abstract	iii
Table of contents	v
List of Figures	x
List of Abbreviations	i
List of Publications and Contributions	vi
Chapter 1 Introduction	1
1.1 Phosphorus is crucial to food, energy and water security.....	1
1.2 Microalgae can help to fix the broken P cycle	2
1.3 The black box: The metabolism behind the P overplus response of microalgae.....	4
1.4 Project Aim, Scope and Objectives	6
1.5 Structure of the thesis.....	7
Chapter 2 Literature Review	9
2.1 The paradox of the phosphorus cycle.....	9
2.1.1 Global effects of the broken phosphorus cycle.....	12
2.2 Wastewater as a potential P source	13
2.2.1 Traditional physicochemical and biological approaches for P control and recovery.....	14
2.2.2 P recovery from digestate in EBPR-based WWTWs.....	17
2.2.3 Alternative cost-effective biological approaches for P control and recovery	18
2.2.4 The use of photosynthetic microorganisms for sophisticated nutrient control in wastewater treatment.....	23
2.2.5 Recycling of P removed from wastewater as P-rich microalgal biomass.....	24
2.2.6 When technology is not enough: Performance and challenges of MBWTs	26
2.3 Phosphate Physiology of Microalgae.....	27
2.3.1 Phosphate biochemical composition of microalgal cells.....	27
2.3.2 The phosphate overplus response and/or luxury phosphate uptake of microalgae	31
2.3.3 Methods for the analysis of Microalgal polyphosphates	34
2.4 <i>Chlamydomonas reinhardtii</i> as a model organism to study microalgae P metabolism	38
2.4.1 Phosphate sensing.....	40

2.4.2	Phosphate scavenging/sparing and acclimation	42
2.4.3	Phosphate transport.....	43
2.4.4	Polyphosphate synthesis.....	44
2.4.5	Polyphosphate turnover	45
2.4.6	Similarities and differences of microalgae with yeast and plants P metabolism	46
2.5	Research gaps	47
Chapter 3 Materials and Methods		48
3.1	<i>Chlamydomonas reinhardtii</i> strains	48
3.2	Cultivation media and solutions.....	49
3.2.1	Tris Acetate Phosphate (TAP) media.....	50
3.2.2	Tris Acetate (TA) media	51
3.2.3	Media supplements.....	51
3.3	Microalgal cultivation	52
3.3.1	Long-term storage.....	52
3.3.2	Starter cultures.....	52
3.3.3	Inoculation.....	52
3.3.4	Phosphorus deprivation.....	52
3.3.5	Phosphorus repletion	52
3.3.6	Monitoring Bacterial Contamination	53
3.4	Culture analysis.....	53
3.4.1	Optical Density	53
3.4.2	Cell counting and size	54
3.4.3	Chlorophyll concentration.....	55
3.4.4	DAPI staining and Confocal microscopy	56
3.5	Media analysis.....	56
3.5.1	pH	57
3.5.2	Phosphate concentration in the media	57
3.5.3	Ion Chromatography (IC-MS).....	58
3.6	Biomass analysis.....	58
3.6.1	Biomass concentration.....	59
3.6.2	Total Phosphate content in the biomass	59
3.6.3	Elemental analysis (CHNS).....	60
3.6.4	Polyphosphate analysis.....	61
3.6.5	Western Blot Analysis	67
3.7	Data analysis.....	70

3.7.1	Growth and Nutrient uptake rates	70
3.7.2	Data visualisation and Statistical significance	71
3.7.3	Principal Component Analysis.....	71
Chapter 4 Phosphate deprivation and overplus: What parameters prime <i>Chlamydomonas reinhardtii</i> for enhanced polyphosphate accumulation?		72
4.1	Introduction.....	72
4.2	Objectives.....	73
4.3	The study of P deprivation in <i>C. reinhardtii</i>	73
4.3.1	<i>C. reinhardtii</i> can sustain the same initial growth rate under P deprivation compared to P-replete cells	73
4.3.2	P-deprived <i>C. reinhardtii</i> sustains growth due to ability to mobilise internal inorganic P reserves.....	77
4.3.3	RNA, the second largest pool of P in <i>C. reinhardtii</i> is degraded upon longer P deprivation	81
4.3.4	Ammonium and sulphate removal from the media is not affected by P deprivation in <i>C. reinhardtii</i>	82
4.4	The study of P overplus in <i>C. reinhardtii</i>	85
4.4.1	P deprivation and subsequent resupply as KPO_4 does not affect biomass growth in <i>C. reinhardtii</i>	85
4.4.2	Longer P-deprivation does not always mean bigger P overplus in <i>C. reinhardtii</i>	87
4.4.3	Unique polyP dynamics are shown for <i>C. reinhardtii</i> during phosphate overplus.....	90
4.4.4	Phosphate overplus was accompanied by an unexpected IP_6 surplus pattern	91
4.4.5	<i>C. reinhardtii</i> phosphate overplus did not affect the removal of ammonium or sulphate from the media.....	92
4.5	Results summary and discussion	95
Chapter 5 The effect of nutrients other than P on <i>Chlamydomonas reinhardtii</i> phosphate overplus response		101
5.1	Introduction.....	101
5.2	Objective	102
5.3	First P overplus experiment.....	102
5.3.1	P repletion together with all other nutrients triggered biomass growth	102
5.3.2	PolyP accumulation during P overplus is not influenced by the availability of other nutrients apart from P	105
5.3.3	RNA recovery occurs only upon P repletion together with all nutrients in 96 h P-deprived cultures.....	107

5.3.4	Biomass growth upon TAP repletion resulted in enhanced nutrient removal	108
5.4	Second P overplus experiment.....	116
5.4.1	Reduced biomass growth observed in P-deprived cultures supplied of P with excess nutrients	116
5.4.2	PolyP accumulation pattern altered in P-deprived cells supplied with P with both excess and diluted nutrients	118
5.4.3	RNA recovery was still dependent on nutrient availability in the second P overplus experiment	121
5.4.4	Reduced phosphate removal observed in the second P overplus experiment.....	122
5.4.5	Negative effect on P overplus observed in second P overplus experiment with excess nutrient supply.....	126
5.5	Results summary and discussion	128
Chapter 6 PSR1 is a key component of polyphosphate synthesis during the phosphate overplus response in <i>Chlamydomonas reinhardtii</i>		134
6.1	Introduction.....	134
6.2	Objective	135
6.3	Overexpression of PSR1 induces luxury phosphate uptake in <i>C. reinhardtii</i>	135
6.3.1	Non-native PSR1 was successfully detected in transgenic strains.....	135
6.3.2	Overexpression of the PSR1 transcription factor does not alter the growth and viability of <i>C. reinhardtii</i>	136
6.3.3	Levels of biomass phosphate follow transgene PSR1 protein expression pattern, leading to enhanced P accumulation ...	138
6.3.4	Enhanced phosphate removal is achieved under nitrogen-replete conditions via PSR1 overexpression	139
6.3.5	Polyphosphate dynamics under PSR1 overexpression reveal insights into P-recycling processes within the cells	142
6.3.6	Assessing the potential effect of PSR1 overexpression on cell volume under phosphate non-limiting conditions	145
6.3.7	Magnesium, rather than calcium, is the potential counterion, assisting PSR1 overexpression strains with increased uptake of phosphate	146
6.4	Assessing the effect of PSR1 on <i>C. reinhardtii</i> P overplus	146
6.4.1	<i>C. reinhardtii</i> growth abnormal in <i>psr1-1</i> mutant but not affected by PSR1 overexpression during P overplus	146
6.4.2	P overplus response was also observed when PSR1 is overexpressed in <i>C. reinhardtii</i>	150

6.4.3	RNA content pattern not affected by PSR1 overexpression during P overplus	152
6.4.4	PSR1 overexpression enhanced phosphate removal efficiency during P overplus	154
6.5	Results summary and discussion	158
Chapter 7 General Discussion and Conclusions		170
7.1	The use of reliable qualitative and quantitative polyP analysis tools in microalgae.....	170
7.2	What physiological parameter of P deprivation is better for studying P overplus?	175
7.3	What is the importance of nutrients other than P in the P overplus response?.....	177
7.4	PSR1 and P overplus in <i>C. reinhardtii</i>	182
7.5	Conclusions and Recommendations	184
7.5.1	Conclusions.....	184
7.5.2	Recommendations and further research	186
References.....		189
Appendix.....		219

List of Figures

Figure 2.1 Summary of the phosphorus cycle.	11
Figure 2.2 The evolution of energy-intensive wastewater treatment.....	16
Figure 2.3 Energy generation and nutrient recovery opportunities from sludge in WWTWs.....	17
Figure 2.4 Microalgae/Bacteria consortia in WSPs.....	19
Figure 2.5. Stack tubular PBR (Algae PARC Wageningen University) ..	24
Figure 2.6 Comparison of wastewater treatment approaches.	27
Figure 2.7 <i>Chlamydomonas reinhardtii</i> cell structure and morphology.	39
Figure 2.8 The in-cell processes behind the P overplus response of <i>C. reinhartii</i>	40
Figure 3.1 PSR1 construct in <i>C. reinhardtii</i> 8-27, 8-42 and 8-2 strains..	48
Figure 3.2 Malachite green phosphate assay after Ppx1 treatment of <i>C. reinhartii</i> 2 µg RNA.	64
Figure 3.3 PAGE gel polymerisation in 24 cm Hoefer cast.....	66
Figure 3.4 <i>C. reinhardtii</i> polyP visualisation on PAGE stained with Toluidine Blue.	67
Figure 4.1 <i>C. reinhardtii</i> biomass growth during control and P- deprivation experiment.	74
Figure 4.2 <i>C. reinhardtii</i> cell volume in control and P-deprivation experiment.....	77
Figure 4.3 Phosphate accumulation of <i>C. reinhardtii</i> during the control and P-deprivation experiment.	78
Figure 4.4 PAGE polyP visualisation with equal loading of dry biomass from control and P-deprivation experiment.	80
Figure 4.5 RNA content in the biomass variation during the P- deprivation experiment in <i>C. reinhardtii</i>	81
Figure 4.6 Nutrient removal from the media during the control and P- deprivation experiment.	83
Figure 4.7 <i>C. reinhardtii</i> biomass growth during P overplus upon KPO ₄ repletion.....	86
Figure 4.8 Phosphate accumulation of <i>C. reinhardtii</i> during P overplus upon KPO ₄ repletion.....	88
Figure 4.9 RNA content in biomass of P-deprived and KPO ₄ repleted <i>C. reinhartii</i> during P overplus.....	90
Figure 4.10 PAGE with polyP migration during P-deprivation and P repletion as KPO ₄	91
Figure 4.11 Nutrient removal from the media during P overplus upon KPO ₄ repletion.....	93

Figure 4.12 A suggested model on the effect of the P deprivation length on microalgal P overplus.	97
Figure 5.1 <i>C. reinhardtii</i> biomass growth during P overplus after resuspension in TAP media.....	103
Figure 5.2 Phosphate accumulation of <i>C. reinhardtii</i> during P overplus upon TAP repletion.....	106
Figure 5.3 PAGE with polyP migration during P deprivation and P repletion as KPO ₄ or TAP media.....	107
Figure 5.4 RNA content in biomass of 24 h and 96 h P-deprived <i>C. reinhardtii</i> during P overplus.....	108
Figure 5.5 Phosphate, ammonium and sulphate concentration in the media during P overplus of 24 h and 96 h P-deprived cultures...	110
Figure 5.6 PCA analysis of the effect of P-deprivation and nutrient availability on P overplus in <i>C. reinhardtii</i>	114
Figure 5.7 <i>C. reinhardtii</i> biomass growth after P supply in the second P overplus experiment.....	117
Figure 5.8 <i>C. reinhardtii</i> P overplus response after P supply in the second P overplus experiment.....	120
Figure 5.9 RNA content in <i>C. reinhardtii</i> biomass during P overplus after P supply in the second P overplus experiment.	121
Figure 5.10 Phosphate, ammonium and sulphate removal from the media by <i>C. reinhardtii</i> after P supply in the second P overplus experiment.....	123
Figure 5.11 PCA analysis of the effect of P-deprivation and nutrient availability during the second P overplus experiment in <i>C. reinhardtii</i>	125
Figure 5.12 Effect of N:P and S:P ratio on polyP fold increase in P overplus experiments.....	127
Figure 6.1 Transgene PSR1 was still detected in PSR1 overexpression strains 8-27 and 8-42.	136
Figure 6.2 <i>C. reinhardtii</i> growth not affected by PSR1 overexpression.	137
Figure 6.3 PSR1 overexpression enhanced total phosphate accumulation in <i>C. reinhardtii</i>	139
Figure 6.4 Nutrient removal from the media of PSR1 overexpression strains (8-27, 8-42 and 8-2) and the non-transformed control (UVM4).	141
Figure 6.5 DAPI-polyP timeline of PSR1-OE and its background UVM4.	143
Figure 6.6 Distribution of cell volumes of the non-transformant control UVM4 and the PSR1 overexpression strain 8-27 over time.....	145
Figure 6.7 Effect of PSR1 knockout or overexpression on <i>C. reinhardtii</i> growth during P-deprivation and repletion.	148

Figure 6.8 Phosphate accumulation of PSR1 overexpression strain and <i>psr1-1</i> mutant during P-deprivation and repletion.....	151
Figure 6.9 RNA variation in biomass of PSR1 overexpression strain and <i>psr1-1</i> mutant during P-deprivation and repletion.....	154
Figure 6.10 Nutrient removal from the media by the PSR1 overexpression strain and <i>psr1-1</i> mutant, during P-deprivation and repletion.....	155
Figure 6.11 Heatmap of key genes involved in P metabolism differentially expressed in PSR1-OE strains.	163
Figure 7.1 A vision of P-deprivation and P repletion steps in P recovery from wastewater using microalgae P overplus response.	187

List of Tables

Table 3.1 <i>Chlamydomonas reinhardtii</i> strains used throughout this project.....	49
Table 3.2 Tris Acetate Phosphate (TAP) recipe.....	50
Table 3.3 Cell size estimates from cell counting pictures, using Fiji software.....	54
Table 3.4 PAGE recipe according to the gel concentration.	65
Table 4.1 Growth parameters calculated during control and P-deprivation experiment.	76
Table 4.2 Biomass carbon and nitrogen composition in control and P-deprivation experiment.	84
Table 4.3 Growth parameters of P-deprived <i>C. reinhardtii</i> after KPO ₄ repletion.....	87
Table 4.4 Biomass carbon and nitrogen content during P overplus upon KPO ₄ repletion.....	94
Table 5.1 Growth parameters of TAP repleted <i>C. reinhardtii</i> during P overplus.....	104
Table 5.2 Phosphate removal performance according during the P overplus experiment according to P-deprivation and P repletion type.	109
Table 5.3 Nutrient uptake rates of <i>C. reinhardtii</i> cells during P overplus according to P-deprivation state and P repletion type.....	112
Table 5.4 Biomass composition of <i>C. reinhardtii</i> 24 h after resuspension in TAP media during P overplus.....	115
Table 5.5 Growth parameters during <i>C. reinhardtii</i> P overplus after P supply in the second P overplus experiment.....	118
Table 5.6 Nutrient uptake rates of <i>C. reinhardtii</i> cells observed in the second P overplus experiment.....	124
Table 5.7 Differences between P overplus response in first and second experiments.....	132
Table 6.1 Growth rates estimated for the PSR1 overexpression strains and the non-transformant control.	137
Table 6.2 Maximum nutrient uptakes observed in the non-transformant control and the PSR1 overexpression strains.....	142
Table 6.3 Summary of observations of polyP dynamics from composite Figure 6.5.....	144
Table 6.4 Increase of biomass concentration after P-deprivation of PSR1 overexpression and <i>psr1-1</i> mutant.	149
Table 6.5 Growth parameters of PSR1 overexpression strain and <i>psr1-1</i> mutant after P repletion.....	149

Table 6.6 Fold change of polyP content after P-deprivation affected in PSR1-OE strain.	150
Table 6.7 Difference in RNA content of PSR1 overexpression and <i>psr1-1</i> mutant during P-deprivation.....	153
Table 6.8 Changes in nutrient uptake rates by PSR1 overexpression strain and <i>psr1-1</i> mutant, compared to the control.	157

List of Figures in Appendix

Figure A 1 Polyphosphate quantification of <i>C. reinhardtii</i> in proportion to RNA.....	219
Figure A 2 PAGE polyP visualisation with equal loading of RNA from P-deprivation experiment.	220
Figure A 3 PAGE with polyP migration during 24 h P deprivation and P repletion as KPO ₄ or TAP media.....	221
Figure A 4 PAGE with polyP migration during 96 h P deprivation and P repletion as KPO ₄ or TAP media.....	222
Figure A 5 Confocal images of DAPI stained cells taken after 48 h of cultivation.....	223
Figure A 6 Confocal images of DAPI stained cells taken after 72 h of cultivation.....	224
Figure A 7 Confocal images of DAPI stained cells taken after 144 h of cultivation.....	225

List of Tables in Appendix

Table A 1 Changes in nutrient uptake rates by PSR1 overexpression strain and psr1-1 mutant, compared to the control.	226
---	-----

List of Abbreviations

π	pi coefficient
ADP	Adenosine 5'-disphosphate
APS	Ammonium persulphate
<i>A. thaliana</i>	<i>Arabidopsis thaliana</i>
ATP	Adenosine 5' triphosphate
BBM	Bold's Basal Media
C	Carbon
<i>C. reinhardtii</i>	<i>Chlamydomonas reinhardtii</i>
<i>C. vulgaris</i>	<i>Chlorella vulgaris</i>
CHNS	Elemental analysis (Carbon/ Hydrogen/ Nitrogen/ Sulphur)
°C	Degrees Celsius
CO ₂	Carbon Dioxide
DAPI	4',6-diamidino-2-phenylindole
ddH ₂ O	Distilled deionised water
DEPC	Diethyl Pyrocarbonate
dia	Diametre
DIPP	Diphosphoinositol polyphosphate phosphohydrolase
DNA	Deoxyribonucleic acid
DO	Dissolved Oxygen
DTT	Dithiothreitol
dw	Dry weight of biomass
EBPR	Enhanced biological phosphorus removal
ECL	Enhanced chemiluminescence
EDTA	Ethylenediaminetetraacetic acid
Em	Emmision
EPS	Extracellular polymeric substances
Ex	Excitation

FI	Fold increase
<i>g</i>	Relative centrifugal force
GAOs	Glycogen accumulative organisms
GDP1	Putative phosphodiesterase 1
GFP	Green fluorescent protein
h	hour
HAB	Harmful Algal Blooms
HDAC	Histone deacetylase
HEPES	4-(2-hydroxyethyl)-1-piperazineethanesulfonic acid
HRP	Horseradish peroxidase
HRT	Hydraulic retention time
IC-MS	Ion Chromatography
IFDC	International Centre for Soil Fertility and Agriculture Development
IP ₆	Inositol Hexakisphosphate
IP ₇	Inositol pyrophosphate 7
IPs	Inositol polyphosphates
IPY1	Inorganic Pyrophosphatase
KPO ₄	1 M Potassium phosphate solution made of both K ₂ HPO ₄ and KH ₂ PO ₄
kt	kilotons
L	Litre
LMICs	Low Middle Income Countries
LPB1	Low Phosphate Bleaching 1 gene
LRL1	Lipid Remodelling Regulator 1
M	Molar
mA	milliampere
μ _{max}	Maximum growth rate
MBWT	Microalgae-based wastewater treatment
μg	micrograms

mg	milligrams
min	minutes
μL	microlitre
mL	millilitre
μM	micromolar
μmol m ⁻² s ⁻¹	Units of light intensity (micromole per square meter per second)
mM	millimolar
MPa	Megapascal
Mt	Million metric tons
Myb	Myeloblastosis DNA binding domain
N	Nitrogen
N:P	Nitrogen to Phosphorus molar ratio
NH ₄ -N	Ammonium expressed as nitrogen (14.01 g/mol)
nm	nanometres
NMR	Nuclear Magnetic Resonance
O ₂	Oxygen
OD750nm	Optical Density (Absorbance at 750nm of wavelength)
OrG	Orange G Dye
P	Phosphate (PO ₄)
P1BS	PHR1-binding sequence
PAGE	Polyacrylamide Gel Electrophoresis
PAOs	Polyphosphate accumulative organisms
PAPs	Purple Acid Phosphatases
PBR	Photobioreactors
PCA	Principal component analysis
PCR	Polymerase chain reaction
PG	Phosphatidylglycerol
PHAs	Polyhydroxyalkanoates
PHR1	<i>A. thaliana</i> Phosphate starvation response 1

PI	Protein Inhibitors
P _m	Mineral phosphorus
PNPase	Polynucleotide phosphorylase
PO ₄ -P	Phosphate expressed as P (30.97 g/mol)
polyP	Polyphosphate
PPE	Personal protection elements
PP-IPs	Inositol pyrophosphates
PPK	Polyphosphate kinase
PPN1	Endopolyphosphatase 1
PPX1	Exopolyphosphatase 1
Ppx1	Recombinant exopolyphosphatase 1 enzyme
Pre1	Preliminary stock solution
PSR1	<i>C. reinhardtii</i> Phosphate Starvation Response 1
PSR1-OE	PSR1 overexpression
RNA	Ribonucleic acid
rpm	Revolutions per minute
<i>S. cerevisiae</i>	<i>Saccharomyces cerevisiae</i>
s	seconds
S	Sulphur
S:P	Sulphur to Phosphorus molar ratio
SDS	Sodium dodecyl sulfate
SDS-PAGE	SDS-polyacrylamide gel electrophoresis
SE	Standard Error
SPX	SPX Protein Family
SQDG	Sulfoquinovosyldiacylglycerol
SRT	Solid retention time
TA	Tris Acetate media
TAP	Tris Acetate Phosphate media
TBS-T	Tris Buffered Saline with Tween
TE	Trace Element solution

TEM	Transmission Electron Microscopy
TEMED	N, N, N-Tetramethylethlenediamine
TOR	Target of Rapamycin
Total P	Total phosphate
V	Volts
v/v	volume/volume
VFAs	Volatile fatty acids
VIP1	Vegetative Insecticidal Protein 1
vs.	versus
VTC	Vacuolar Transporter Chaperone
w/v	weight/volume
w/w	weight/weight
WSPs	Waste stabilization ponds
WWTWs	Wastewater treatment works
YFP	Yellow fluorescence protein (Venus)

List of Publications and Contributions

In the following list are referenced the work presented in this thesis that have been carried out at least in part by a person other than me, including experimental design, data collection or analysis.

I am an author on two publications with other authors which include data produced and analysed by me and included in my thesis.

- Research paper: joint first author

Slocombe, S.P., Zúñiga-Burgos, T., Chu, L., Mehrshahi, P., Davey, M.P., Smith, A.G., Camargo-Valero, M.A. and Baker, A. 2023. Overexpression of PSR1 in *Chlamydomonas reinhardtii* induces luxury phosphorus uptake. *Frontiers in Plant Science*. 14. doi: <https://doi.org/10.3389/fpls.2023.1208168>

Contribution: The data shown in **Figure 6.2 - Figure 6.5, Table 6.1, and Figure A 5 - Figure A 7** of my thesis corresponds to my contribution to this published work as seen in Figure 1B, Figure 2A-E, Table 1 (growth rates), supplementary Figure 6A-C, supplementary Figure 7 and Supplementary Figure 8 of the published paper. The data from **Figure 6.11** of my thesis is derived from my re-analysis of the list of key P metabolism genes differentially expressed by PSR1 overexpression strains in the RNA sequencing analysis performed by Dr Slocombe.

- Review paper: co-author

Slocombe, S.P., Zúñiga-Burgos, T., Chu, L., Wood, N.J., Camargo-Valero, M.A. and Baker, A. 2020. Fixing the Broken Phosphorus Cycle: Wastewater Remediation by Microalgal Polyphosphates. *Frontiers in Plant Science*. 11(982). doi: <https://doi.org/10.3389/fpls.2020.00982>

Contribution: **Figure 2.6** of this thesis was adapted from our review paper. This figure was part of my contribution to this publication.

- Unpublished work:

All the gels in the figures of this thesis showing polyacrylamide electrophoresis (PAGE) of polyphosphate samples were run by Prof. Adolfo Saiardi, University College London with RNA samples prepared by me, from experiments designed and conducted by me. These figures are: **Figure 3.4, Figure 4.4, Figure 4.10** (which is a cut version of **Figure 5.3**) and **Figure A 2 - Figure A 4**.

Chapter 1 Introduction

1.1 Phosphorus is crucial to food, energy and water security

The increasing global demand for phosphorus and high dependency on phosphate rock minerals in the supply chain, is creating pressure on our society to change the current vision of 'Exploit-Consume-Waste'. The phosphorus cycle, which usually takes millions of years to transform reactive forms of phosphorus (e.g., phosphates) into stable reserves (phosphate rock) has become linear due to the indiscriminate mining of (P)-rich rock for fertiliser production and subsequent net accumulation of reactive forms of phosphorus in the environment (Elser and Bennett, 2011). This practice is a threat to global phosphate rock reserves (and supply) and has a high energy demand for fossil fuels, as does its refinery, purification process and transport to suppliers and farmers (Childers et al., 2011). We face a future phosphorus scarcity crisis, as all living organisms rely on phosphorus to live. Inorganic fertilisers derived from P-rich rock are applied to crops in unsustainable ways to cope with the increasing global food demand, which causes huge P losses from soil to water streams (Hart et al., 2004, Carpenter, 2008). Approximately 50% of agricultural soils are P-limited and thus, they rely on the application of mined P fertilisers, as P is the second most important inorganic element for plant growth (after nitrogen) (Demay et al., 2023, Lynch, 2019).

Paradoxically, solid wastes and wastewater generated by human activities are loaded with phosphorus, but they are usually disposed to land or left partially untreated and discharged to water streams (Jarvie et al., 2006). Surface water bodies, which are a source of clean water, are suffering from eutrophication and threaten water quality and accessibility. The UK government guidance recommends that rivers should not exceed an annual average concentration of 0.1 mg P/L (DEFRA-UK). However, wastewater treatment works (WWTWs) in the UK are allowed to discharge untreated sewage after certain periods of high rainfall. The UK government and water regulators have been accused of breaking the law over how sewage release has been monitored and regulated¹. Communities are organising campaigns to take their complaints to Parliament as the perception is that the UK Government is not doing 'enough' to achieve nutrient neutrality^{2 3}. Thus, the eutrophication of water ecosystems in the UK is

¹ Esme Stallard Jonah Fisher and Sophie Woodcock 'Government may have broken law over sewage - watchdog', BBC news, 2023

² 'River Wye tributary pollution above targets, campaigners claim', BBC news, 2023

³ Ione Wells & Sam Francis, 'Ministers propose scrapping pollution rules to build more homes', BBC news, 2023

definitely a topical matter in environmental and social policy. Public concerns are absolutely valid, as approximately two-thirds of the world population is affected by water scarcity, and governments are pushed to agree on very strict P discharge consents (0.1-1 mg/L) to protect water resources (Leaf, 2018, Todo and Sato, 2002, Sternlieb and Laituri, 2010, Mekonnen and Hoekstra, 2016). This increases wastewater treatment costs as more sophisticated technologies (usually high-energy-intensive processes) are often implemented to meet regulated parameters. Traditional WWTWs are already complex and energy-intensive and do not facilitate P recovery (Cordell et al., 2011). In the case of industrialised countries, there are enough resources and installed capacity to achieve wastewater treatment goals, but the urgent need is for such processes to be more cost-effective, less fossil-fuel dependent and sustainable in the long run. In contrast, low- and middle-income (LMIC) countries are far behind regarding service coverage, suitable infrastructure to cope with increase wastewater discharges and have fewer resources to enforce and comply with high standards of nutrient control facilities, including phosphorus control and recovery (von Sperling and Augusto de Lemos Chernicharo, 2002).

1.2 Microalgae can help to fix the broken P cycle

In the search for alternatives to phosphorus control and recovery at wastewater treatment works, natural wastewater treatment systems like wastewater stabilisation ponds (WSPs) have been considered as a cost-effective option (Johnson et al., 2007, Mara, 2006). This is due to the low maintenance and operation costs, especially in developing countries (Mara, 2013, von Sperling and Augusto de Lemos Chernicharo, 2002, Von Sperling, 2007). These systems make use of the naturally occurring symbiotic relationship between bacteria and microalgae to remove organic matter and nutrients from wastewater via biological uptake (Von Sperling, 2007, Camargo Valero et al., 2010). Microalgae are photosynthetic microorganisms which grow naturally in wastewater. Microalgae capture carbon dioxide and accumulate nutrients, like nitrogen and phosphorus, with the power of sunlight via photosynthesis processes. Therefore, microalgae are a promising alternative to energy-intensive WWTWs, however, open systems like WSPs are very susceptible to climate conditions (Abis and Mara, 2003). Overall, not enough research has been done on assessing the influence of environmental factors on P removal processes by microalgae. Far more research has been undertaken within a cold/temperate/arctic climate context than it has been done for tropical environments as it coincides with interests of the 'Global North' (Powell et al., 2011, Powell et al., 2008, Sells et al., 2018, Cheregi et al., 2019). The great

majority of tropical environments coincide within the territory of LMICs or 'Global South', where there may be different types of barriers (political, socio-economical, etc.) (Sathya et al., 2023, Chrispim et al., 2019, Mara, 2013, Confraria et al., 2017).

Microalgae-based wastewater treatment (MBWT) systems are promising both as 1) a sophisticated tool to achieve strict nutrient discharge consents to control eutrophication, whilst producing high-value products, with the use of engineered systems - i.e., photobioreactors (PBRs) (Slompo et al., 2020, Borowitzka, 2013), and also as 2) a suitable option for resource-limited rural and urban communities to reduce the impact of moderated nutrient discharges to water streams by cost-effective means like WSPs (Bunce et al., 2018, Mara, 2013). MBWT offers an alternative to recycle these nutrients for the benefit of these communities, according to their potential and technological boundaries (energy crops fertilisation, biofuel production, etc.) (Coppens et al., 2016). Van Puijenbroek et al. made an assessment of the predicted progress and challenges of nitrogen and phosphorus removal from wastewater for the next few decades, and found that for LMICs with high population growth, the impacts of inadequate nutrient control approaches will be severe and cause deterioration of water quality (van Puijenbroek et al., 2019). This evidences a need to direct efforts to help these communities developing simple and cost-effective strategies for nutrient control and recovery, for which MBWT is promising. To achieve the goal of simplicity and cost-effectiveness of MBWT, further research needs to focus on each context of application. Microalgae are vulnerable to environmental conditions (e.g. nutrient concentration in wastewater, temperature, light/dark regime, etc.), which can change considerably for each case scenario/location. Therefore, the design of MBWT needs to consider the effect of environmental factors on nutrient removal efficiency and quality of microalgal biomass produced. Microalgae grown in wastewater have been mostly considered for their biofuel potential due to their lipid content (Hu et al., 2008). However, microalgal biofuels are still not cost competitive with petroleum based fuels. Moreover, the land demanded for biofuel production conflicts with that of food production (Ángeles et al., 2019). Thus, in the context of the phosphorus cycle, it makes more sense to use nutrient-rich microalgal biomass to return phosphate to land (Solovchenko et al., 2016).

Microalgae-based P biofertilisers have a slower nutrient release rate than P-rich rock fertilisers (Mulbry et al., 2005, Chu et al., 2020b, Coppens et al., 2016). Thus, the use of microalgae-based biofertilisers may not only decrease the P discharge to water streams due to runoff but is also more adapted to the P

uptake rate of plants in crops (Mulbry et al., 2005). Nonetheless, the choice of microalgae byproducts will depend on the context. For instance, in tropical countries like Colombia and Brazil in Latin America, large portions of land are being dedicated to the production of energy crops in the form of monocultures (Martínez Londoño et al., 2016). Sugarcane cultivation for biofuel production (bioethanol) is going through a yield decline mostly because of soil degradation caused by long-term monoculture and intensive application of inorganic fertilisers (Garside et al., 2005). In the South American context, the affordability of P-rich rock fertilisers represents a socioeconomic challenge, which drives inequity levels across small and large farm holdings. In this context, the problem begins with access to expensive industrial fertilisers when soils start to run out of nutrients and low-cost options like manures are not available (de Sousa et al., 2015, FAO, 2019); under such circumstances, produced microalgae biomass from MBWT may offer an alternative to inorganic fertilisers, as an organic fertiliser to support soil health and crop nutrient demand. In temperate climate countries like the UK, and most of Europe, there are no phosphate rock reserves (Cooper and Carliell-Marquet, 2013). This means that agricultural production depends on imported P fertilisers, which generates a high vulnerability to supply disruption or price increase (van Dijk et al., 2016). At the same time, poor soil quality is affecting the two most important field crops, wheat and oilseed rape. This is due to the loss of soil organic carbon caused by the intensive application of industrial fertilisers and soil losses. Soil organic carbon plays an important role in maintaining soil structure and storing nutrients. Organic matter-deficient soils lead to increased nutrient and soil losses to water bodies. Therefore, microalgae biomass, which is a source of nutrients (nitrogen, phosphorus and carbon), may offer a solution by recovering the nutrient storage capacity of soils by restoring organic carbon levels (Alobwede et al., 2019).

1.3 The black box: The metabolism behind the P overplus response of microalgae

The use of microalgae technology for P recovery currently faces its biggest challenge in the gap of understanding microalgal P metabolism.

Microorganisms like microalgae, bacteria and yeasts exhibit a phosphate overplus response when transferred from culture media with low to high P concentration levels (Solovchenko et al., 2019a). Microalgae can also perform luxury P uptake when deprived of nutrients other than P (Powell et al., 2009). Both processes involve a transient overaccumulation of in-cell P as polyphosphates (polyP), but there is not clear understanding of the mechanistic

differences between these two phenomena (Solovchenko et al., 2019b, Slocombe et al., 2020). Microalgae can build up an approximate 2-6 fold increase in their P biomass content, mostly due to polyP accumulation, as a consequence of a period of nutrient deprivation followed by P re-supply, (Plouviez et al., 2021).

It is believed that the microalgae P overplus phenomenon can be a solution to fix the broken phosphorus cycle, as it relies mostly on phosphate levels (Slocombe et al., 2020). Currently, there is no conclusive evidence on the conditions leading to high P recovery yields in MBWTs using P overplus capacity. The problem starts with the inconsistency in the methodologies to analyse microalgal polyphosphate accumulation dynamics which are the direct measurement of P overplus (Martin and Mooy, 2013, Werner et al., 2007, Aitchison and Butt, 1973). Hence, no biological questions regarding P overplus can be addressed without the development of reproducible polyphosphate analysis tools in microalgae.

For instance, it is commonly assumed that longer periods of P deprivation maximise in-cell P surplus upon refeeding, but the actual criteria to determine the length of the P deprivation is not well defined – i.e., some studies use periods without specific or mechanistic biological variables (Aitchison and Butt, 1973, Solovchenko et al., 2019a, Plouviez et al., 2023b, Lavrinovičs et al., 2022). For example, an arbitrary 3-day period of P-deprivation using an experimental design with limited algal species, and set environmental factors, may have promoted a high P overplus performance under those conditions, but may be too short or too long for a different experimental set up. Thus, physiological parameters of P-deprivation are preferred, as they can be adapted to different scenarios. Some studies used the time of cessation of growth, or the time to reach the lowest in-cell P concentration (Solovchenko et al., 2019b, Aitchison and Butt, 1973). Moreover, the effect of other nutrients on microalgal P overplus has been overlooked – i.e., P recovery in MBWTs depends on the N:P ratio (Beuckels et al., 2015) and other nutrients like magnesium (Schönborn et al., 2001). Thus, a better understanding of how these factors affect P overplus responses may lead to a reliable design of MBWTs using this phenomenon.

Furthermore, reducing the gap in the knowledge of microalgal P metabolism also requires going beyond the physiological level. Physiological responses in microalgae are controlled and regulated by transcriptional and post-transcriptional processes which can differ in a species-dependent manner. However, the great majority of algal genomes have not been either sequenced or well annotated yet (Nelson et al., 2021). Many studies aimed at working with

microalgal strains collected directly from wastewater treatment systems as a means to be more realistic (Eladel et al., 2019, Han et al., 2014, Wen et al., 2017). However, these studies struggled to provide in-depth explanations behind the advantages or limitations of these strains to recover nutrients from wastewater, based only on physiological data. The genome of *Chlamydomonas reinhardtii*, which is a model organism for microalgal research, is well annotated and hence, plenty of molecular biology tools have been developed to increase the understanding of phosphorus regulation mechanisms (Craig et al., 2023, Salomé and Merchant, 2019).

In *C. reinhardtii*, 'Phosphate Starvation Response 1' (PSR1) is an important transcription factor in the regulation of phosphate metabolism (Wykoff et al., 1999). Mutants lacking the expression of PSR1 were defective in their response to P deprivation (Shimogawara et al., 1999). Furthermore, Bajhaiya et al. reported that PSR1 overexpression in *C. reinhardtii* enhanced phosphate and starch accumulation under both 'high P' and 'low P' conditions (Bajhaiya et al., 2016). These findings suggest that PSR1 also has an important role in regulating the P overplus response of *C. reinhardtii*. Understanding how PSR1 intervenes in this phenomenon could lead to future strategies for the manipulation of these phenomena to enhance algal biomass P accumulation and nutrient removal from wastewater.

1.4 Project Aim, Scope and Objectives

This project aims to broaden and deepen the current knowledge of polyphosphate accumulation in microalgae, as a direct measurement of their phosphate overplus response. Specifically, one key goal is the standardisation of an experimental design to study P-deprivation and subsequent P repletion, to investigate the key parameters affecting polyP accumulation, microalgal biomass growth and nutrient removal, which is needed to produce reproducible results within the research community. This will contribute to expanding our knowledge across different algal species and cultivation conditions that are closer to real operation conditions at wastewater treatment systems using microalgal P overplus phenomena to control and recover phosphate. This study also seeks to determine the role of the phosphate starvation response transcription factor of *C. reinhardtii* in its P overplus response.

There is a lack of robust evidence regarding the potential differences between the concept of microalgal luxury phosphate uptake and phosphate overplus response. The following research questions so far still remain unanswered: 1) Are luxury P uptake and P overplus responses mechanistically different? and 2) are these responses triggered by different environmental factors? Therefore, to

improve our current understanding of luxury P uptake and phosphate overplus response, this research work reports the results from a series of lab-based approaches to monitor polyphosphate accumulation in the green microalgae *C. reinhardtii*, when subjected to P-deprivation and P-repletion conditions, separately. The P overplus experiment consisted of P-deprivation followed by P repletion. These experiments were designed and conducted to elucidate how the manipulation of P-deprivation, nutrient availability and PSR1 regulation, provide suitable conditions for polyphosphate accumulation, biomass growth and P removal from the media during P overplus. The results from this work will help as a guide to future research, aiming at the development of a robust and reliable MBWT system using the microalgae P overplus phenomena to meet P discharge consents, and consequently producing P-rich microalgal biofertilisers to help fixing the broken phosphorus cycle.

The following objectives were designed for this project:

1. To understand physiological responses to P deprivation and their relationship with the P overplus phenomena in *C. reinhardtii*.
2. To implement reliable analytical methods to quantify and characterise in-cell polyphosphate in *C. reinhardtii* and understand its dynamics during P overplus.
3. To assess the role of nutrient availability, other than P, on P overplus at the P repletion stage using *C. reinhardtii*
4. To evaluate the role of the PSR1 transcription factor on the phosphate overplus response of *C. reinhardtii*.

1.5 Structure of the thesis

The structure of this thesis comprises, apart from this introductory section, six further chapters as follows: Chapter 2 – Literature Review, which is focused on 1) the relevance of the broken phosphorus cycle to food and water security, 2) the challenges of the current and alternative microalgae-based approaches for P recovery from wastewater and 3) the knowledge and gaps regarding microalgae P metabolism. Chapter 3 – Materials and Methods: describes in detail all the methodology as well as the illustration of the experimental design to test: 1) Physiological changes in P-deprived *C. reinhardtii* against non-P-deprived cultures, 2) the effect of the P-deprivation period, nutrient availability, or the PSR1 overexpression vs its knockout on P overplus, and 3) the induction of P overplus or luxury P uptake by PSR1 overexpression in *C. reinhardtii*.

In chapters 4-6, I report on the results from these experiments according to their contribution towards the project objectives and compare these results with

previous studies. Chapter 4 - Phosphate deprivation and overplus: What parameters prime *Chlamydomonas reinhardtii* for enhanced polyphosphate accumulation?: includes the successful application of polyP qualitative and quantitative analysis tools for the determination of two physiological factors of P-deprivation. The effect of these physiological factors on P overplus is tested and new polyphosphate and inositol hexakisphosphate (IP₆) dynamics are revealed. Chapter 5 - The effect of nutrients other than P on *Chlamydomonas reinhardtii* phosphate overplus response: exhibits the difference between P repletion as 'P only' against repletion with all nutrients, in terms of biomass growth, polyphosphate accumulation and nutrient removal. The change in the 'all nutrient' repletion methodology provided insights which may be relevant to the application of P overplus for P recovery in WWTWs. Chapter 6 - PSR1 is a key component of polyphosphate synthesis during the phosphate overplus response in *Chlamydomonas reinhardtii*: reveals the capacity of PSR1 overexpression to activate a phosphate overplus response without previous P-deprivation conditions and the opposite effects of PSR1 overexpression versus PSR1 knockout on P deprivation and repletion.

Chapter 7 – General Discussion and Conclusions, this chapter summarises the results obtained as part of the research work undertaken and their contribution to our understanding of *Chlamydomonas reinhardtii* phosphate overplus response. The new evidence obtained in this work is linked to the potential application of this phenomenon to biologically recover P from wastewater and highlights future areas of research and recommendation.

Chapter 2 Literature Review

2.1 The paradox of the phosphorus cycle

Due to its high chemical reactivity, mineral forms of phosphorus (P_m) are not widely found. As a nutrient source, their contribution in the bio-, geo-, chemical cycle of phosphorus differs from other nutrient cycles, such as nitrogen (N) and carbon (C), as P_m is not linked to a gaseous phosphorus phase (Ashley et al., 2011). As it is shown in **Figure 2.1A**, the natural state of P_m consists of apatite minerals in the lithosphere which took around 10 to 15 million years to form as sediments in oceans and freshwaters. Apatite minerals are biologically unavailable for living organisms (Sonzogni et al., 1982). Phosphate (P), which is the bioavailable form of phosphorus, becomes available when it is released from apatite minerals via chemical weathering in the soil formation process, or when it is transferred from terrestrial to aquatic ecosystems in the form of eroded soil that is dissolved through riverine runoff (Yuan et al., 2018). Therefore, living organisms rely on the processes that allow phosphorus to be bioavailable to survive (Solovchenko et al., 2019a). After N, P is the second most frequent macronutrient that limits plant growth. This is mainly because living organisms contain different cellular compounds containing phosphorus (e.g. Nucleic acids, phospholipids, proteins, etc.). P plays an important role in many natural processes as well (Ashley et al., 2011). In small concentrations, it represents a vital component of the aquatic ecosystems, enhancing biological productivity (Melia et al., 2017). Once bioavailable, P becomes part of organic cycles, through living organisms. P is mobilised from soils to plants and animals and then returns to the soil where it is taken up by plants through a process called mineralization (Yuan et al., 2018).

However, the P cycle has been transformed with the input of human activities involving: P-rich rock extraction, crop fertilisation, livestock production with manure generation and food consumption leading to waste production (Cordell et al., 2009). The impact of these activities is reflected in the acceleration of P transfers between land and water (**Figure 2.1B**). Extracted P from mining is processed into fertilisers that are exported around the globe to be directly applied to crops. Commercial agriculture companies harvest those crops, which are then transported to different areas and traded for food production and consumption. P circulates all around these traded areas, either as a fertiliser or as a component of harvested crops. This creates a bigger need to apply fertilisers each time crops are harvested to prepare the soil for the next production cycle and to keep with global food demand (Yuan et al., 2018). Once the food is consumed, P is excreted from our bodies in urine and faeces,

directly into wastewater (Cordell et al., 2009). P extracted and circulated never comes back to the place it was taken from and this results in the P cycle becoming linear. Thus, the consequence of human alterations to the P cycle is the increased speed of the cycle phases that would naturally take millions of years to come through and further renew the P source. All living organisms rely on P to survive and hence, finding a way to fix the broken cycle of P is a matter of global importance (Solovchenko et al., 2016).

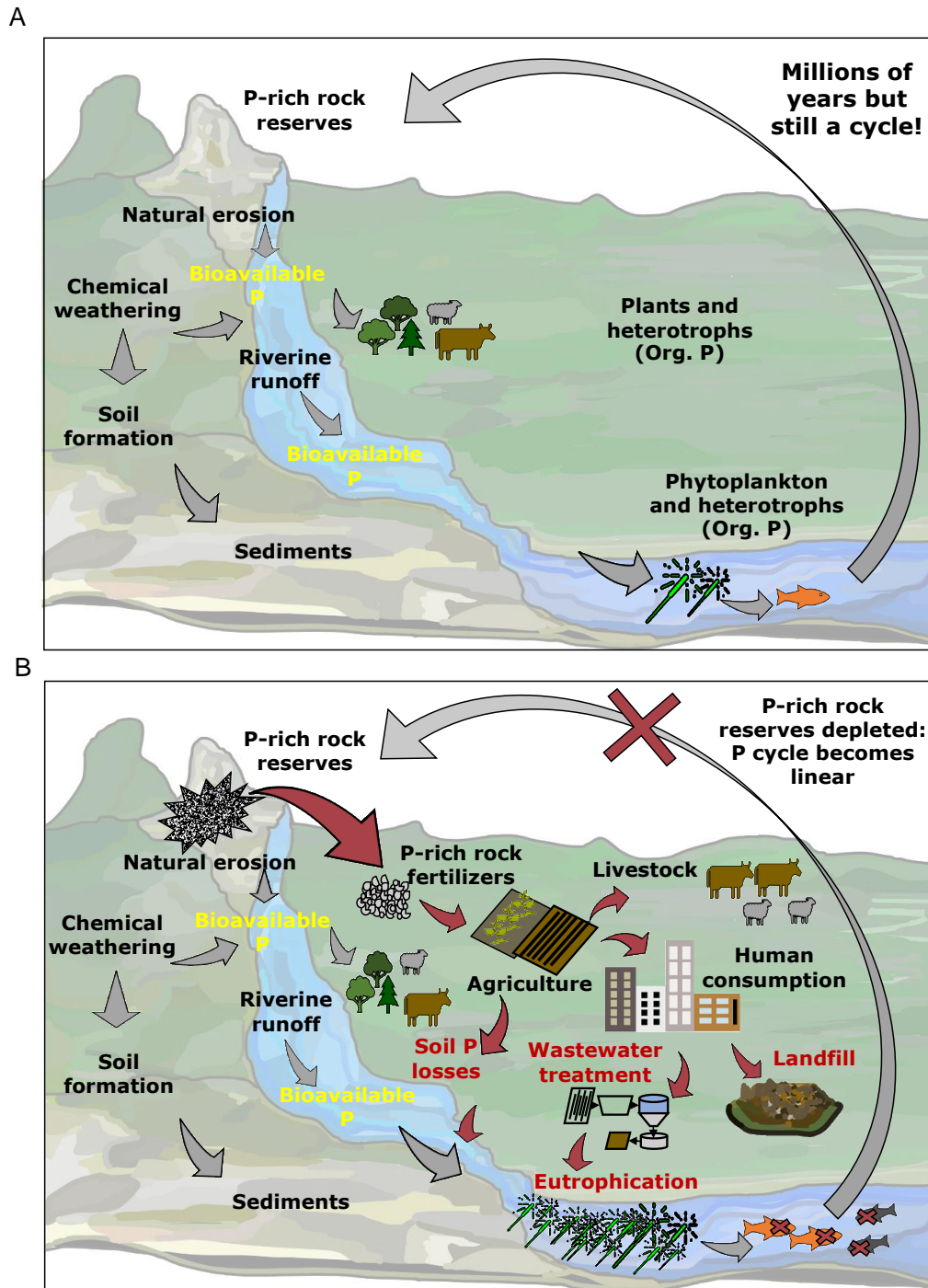


Figure 2.1 Summary of the phosphorus cycle. A Representation of the natural process by which P becomes bioavailable. P-rich rock composed of apatite minerals took millions of years to form. Chemical weathering and natural erosion cause the release of P, which becomes part of the soil and sediments. Plants, algae and microbes generate biomass by taking P as a macronutrient. This biomass is ingested by heterotrophic organisms. In aquatic environments, P becomes bioavailable when P soil particles are disseminated by riverine runoff from the land. B Human alterations to the P cycle. Exacerbated mining of P-rich rock to produce inorganic fertilisers, causes an increase of soil P losses to water streams. Fertilisers are used for food or livestock production. Once consumed, the P ends up as solid waste in landfills or wastewater. Inadequate management of lost P causes eutrophication. Figure adapted from Yuan et al. (2018).

2.1.1 Global effects of the broken phosphorus cycle

Human alterations to the phosphorus cycle have generated consequences for all the different processes where phosphorus is involved. However, the biggest threats that this problem poses for our society are the following:

1. The **problem of a future phosphorus scarcity** is a consequence of the mining of P-rich rock from reserves that take such a long time to form (Yuan et al., 2018). The International Centre for Soil Fertility and Agriculture Development (IFDC) last report, estimated the worldwide phosphate rock reserves to be around 60.000 million metric tons (Mt) instead of 16.000 Mt (which was the amount estimated before), based on inferred reserves (Ashley et al., 2011). However, these 'new' reserves have not been confirmed yet and do not remove the threat of phosphorus scarcity. Another important factor is the quality of the remaining reserves, which may be lower in P concentration and higher in radioactive compounds and heavy metals concentration (Cordell et al., 2009).
2. Phosphorus scarcity represents a serious **threat to food security**. Worldwide human population relies on P to sustain its food demand as agriculture depends on P fertilisers that are produced in large part from P-rich rock (Solovchenko et al., 2016). Since P is irreplaceable in food production, P scarcity could lead to a food security crisis (Ashley et al., 2011). It also brings concern about the geographical distribution of P-rich rock sources. Globally, P-rich rock reserves are concentrated in particular regions. Morocco holds approximately 73% of the global reserves, following by China, Algeria and the United States. Such geographical distribution of P sources increases other countries' geopolitical vulnerability (El Wali et al., 2019). The UK and other European countries rely on imported P fertilisers for agriculture (Cooper and Carliell-Marquet, 2013). For this reason, many European organisations are working on the development of new strategies to overcome P import dependency, by promoting an emphasis on the role of P recycling and recovery as an alternative to P rich minerals (van Dijk et al., 2016). For instance, Latin American and Caribbean nations are already struggling with P supply (Nyamangara et al., 2020), as local farmers struggle to cope with an increased demand for food as the soils lose their nutrient content. As developing countries with lower economic incomes, many of these farmers cannot afford to buy imported P-rich rock fertilisers. Therefore, in some cases, the use of organic fertilisers in the form of manure, for example, is more commonly used to cope with food demand (Appleton and Notholt, 2002, Rao et al., 2004). However,

its use as an organic fertiliser means that delivered phosphorus will not be readily bioavailable for plants (Holford, 1997) and can also represent a risk to public health, as they might get contaminated with pathogens (Nicholson et al., 2005), heavy metals (Zhao et al., 2014) and antibiotics (Li et al., 2015).

3. The unsustainable use of extracted phosphate rock, in the form of applied fertilisers generates a load of P leakage to groundwater. Inorganic fertilisers have a high solubility that plants cannot fully cope with when absorbing the nutrients from the soil (Schachtman et al., 1998). This means that a high portion of P is wasted and ends up by runoff into water streams, causing **eutrophication** (Talboys et al., 2016). This is the elevated nutrient concentration (e.g. N and P) in lakes, estuaries, and coastal areas. The effects of these high nutrient loads are the generation of algal/cyanobacterial blooms that are harmful to fishes and cover the water surface, thus limiting access to oxygen from the atmosphere. The dissolved oxygen (DO) in the river is consumed by the decomposition of organic matter, causing hypoxic conditions that are not tolerable by aquatic forms of life (Elser, 2012). The effects are chronic, and it may take years for a river to reduce P levels and recover biodiversity even with the strictest conservation practices (Yuan et al., 2018). In addition, phosphate excretion by human beings increases P discharge in domestic wastewater. Whether climate change acts as an aggravator of the problem of harmful algal blooms (HAB) in eutrophicated water streams is a subject of debate as different studies reach opposite conclusions (Hallegraeff et al., 2021, Mejbil et al., 2023). However, it seems that the effect of climate change on the occurrence of HAB should be evaluated on a case-to-case level, as Hallegraeff et al. (2021) showed that the pattern of HABs varied across different regions.

2.2 Wastewater as a potential P source

The threat of eutrophication and inadequate wastewater management affecting the quality of aquatic ecosystems has created a need to develop stringent regulations for P discharge, which increases capital and operational and maintenance costs at WWTWs. The EU Urban Wastewater Directive 91/271, Water Framework Directive (2000/60/EC) and the UK Environment Agency have consent for a maximum annual average P discharge level of 1 mg/L, which means that some WWTWs will have to achieve P effluent concentrations under 0.1 mg/L (Yulistyorini, 2016, DEFRA-UK, UK-Environment-Agency, 2019). WWTWs in the UK are required to handle approximately 55 kilotons (kt)

of P per year from municipal wastewater, which is equivalent to 71% of imported fertilisers, 77.5 kt P. Handling of P inputs to WWTWs has represented an average investment of £80 billion since 1989 (Cooper and Carliell-Marquet, 2013). With upcoming more stringent P discharge consents, there is a need to consider more cost-effective alternatives to current WWTWs. In the context of the broken phosphorus cycle, wastewater represents a potential source of P. Once recovered, P can be returned to the land as a biofertiliser. However, the fate of recovered P is determined by the method of P removal used at WWTWs. This section reviews the current approaches for P control and recovery.

2.2.1 Traditional physicochemical and biological approaches for P control and recovery

One of the most common physicochemical techniques for P removal is chemical precipitation. Phosphate is a trivalent anion and thus, can be readily easy to precipitate, using di-valent or trivalent salts of iron (Fe), aluminium (Al) or calcium (Ca). These salts form complexes with both the organic and inorganic fractions of P by coagulation/crystallisation where flocs and salts are formed. Consequently, flocs and insoluble salts are removed by sedimentation in the form of sludge (Nassef, 2012). The process has sufficient levels of efficiency especially at $\text{pH} > 9.5$, where virtually all free phosphate (orthophosphate) will precipitate, for instance as hydroxyapatite ($\text{Ca}_5(\text{PO}_4)_3\text{OH}$) when lime (CaCO_3) is chosen as coagulant agent. However, the most relevant disadvantage is that it requires chemical additions that increase treatment costs (Ruzhitskaya and Gogina, 2017). Alternatively, a process of electrochemical coagulation of phosphate does not require chemical addition as it involves the use of stainless-steel cathodes and stable semiconductor anodes to stimulate phosphate precipitation (Cid et al., 2018). However, the main constraint of physicochemical-based approaches is the generation of large amounts of sludge not suitable for reuse due to the low bioavailability of the recovered P, which is strongly bound to the metallic salts (Qiu and Ting, 2014, Melia et al., 2017).

The bioavailability of the phosphorus in the sludge can be achieved with biological treatment. The enhanced biological phosphorus removal (EBPR) with activated sludge systems, for example, consists of the use of polyphosphate accumulative organisms (PAOs) (Melia et al., 2017, Ong et al., 2016). EBPR is based on enhancing PAOs ability to perform polyP accumulation, beyond that required for survival (a process known as luxury phosphorus uptake). PolyPs are polymers of ten to hundreds of orthophosphate residues linked by phosphoanhydride bonds (Kulaev et al., 2005). Polyphosphate is retained within

the cells as an energy reserve for maintenance or to provide a competitive advantage over ordinary heterotrophic bacteria, a reason why PAOs tend to outcompete other organisms.

- **PAOs activity in WWTWs**

The EBPR process requires alternating anaerobic and aerobic/anoxic conditions (Jeyanayagam, 2005, Tarayre et al., 2016). In the anaerobic phase, PAOs consume available volatile fatty acids (VFA) as carbon storage in the form of polyhydroxyalkanoates (PHAs), using ATP (Adenosine triphosphate) as an energy source. ATP is produced from the hydrolysis of accumulated polyP, releasing orthophosphate (soluble P). Then the aerobic phase leads to the oxidation of PHAs, a process that releases energy that can be used for P uptake. Since the uptake rate in the aerobic phase is greater than the amount of released orthophosphate under the anaerobic phase, P accumulation is achieved (Bunce et al., 2018). Therefore, P is removed from wastewater as it goes from the liquid to solid phase and becomes part of the sludge that is removed by sedimentation (Du et al., 2012).

The literature highlights *Candidatus Accumulibacter phosphatis* as the PAO most responsible for EBPR. Their full genome sequence is available, which allows the study of the metabolic pathways associated with P accumulation (Camejo et al., 2019). Other putative PAOs found in WWTWs include *Acintobacteria* sp., *Pseudomonas* sp., *Paracoccus* sp. and some *Enterobacter* sp. The biochemical machinery to perform P accumulation is well-studied in bacteria (Achbergerová and Nahálka, 2011, Günther, 2011, Albi and Serrano, 2016). The most important enzymes involved in the process are the polyphosphate kinase (PPK), which catalyses the elongation of the polyP chain, and the exopolyphosphatase (PPX), which removes a phosphate group at the end of the polyP chain (Albi and Serrano, 2016, Rashid and Kornberg, 2000, Kawakoshi et al., 2012).

- **Progress and challenges of EBPR**

The EBPR process stability and reliability remain a challenge as standards for the cultivation of these microorganisms have not been established and just a few microorganisms have been isolated for further research. Different factors like stricter P discharge limits or sudden increase in P concentration in coming wastewater, make the addition of a carbon source and calcium and magnesium salts necessary, which incurs additional costs to the EBPR process (Qiu and Ting, 2014, Izadi et al., 2021). Furthermore, PAOs might be outcompeted by glycogen accumulative organisms (GAOs) for the carbon substrate. These organisms grow in the same environment as PAOs and represent one of the

main causes of deterioration of the EBPR process as they do not contribute to the P removal (Günther, 2011).

As shown in **Figure 2.2**, the current energy-intensive WWTWs have come to accumulate a subset of processes for the removal of C, N and P (Heterotrophic bacteria, nitrifying bacteria, PAOs, etc.). This is not a sustainable approach, as it requires a larger footprint and flexible capacity to deliver on-demand wastewater treatment to growing human populations. Furthermore, nitrate is recirculated from the final effluent as a substrate for denitrifying bacteria to produce gaseous N and nitrous oxide, the latter being a potent greenhouse gas and also a major scavenger of ozone (Wunderlin et al., 2012). Some of the released phosphate in the EBPR also needs to be recirculated to the nitrification and heterotrophic organic matter removal steps as a substrate to avoid the use of additives. Additionally, organic carbon may be added to the EBPR process as the levels of organic carbon at this step would be already low, and are required for PAOs phosphorus metabolism (**Figure 2.2**). These parts of the process add complexity to the operation and maintenance of the system.

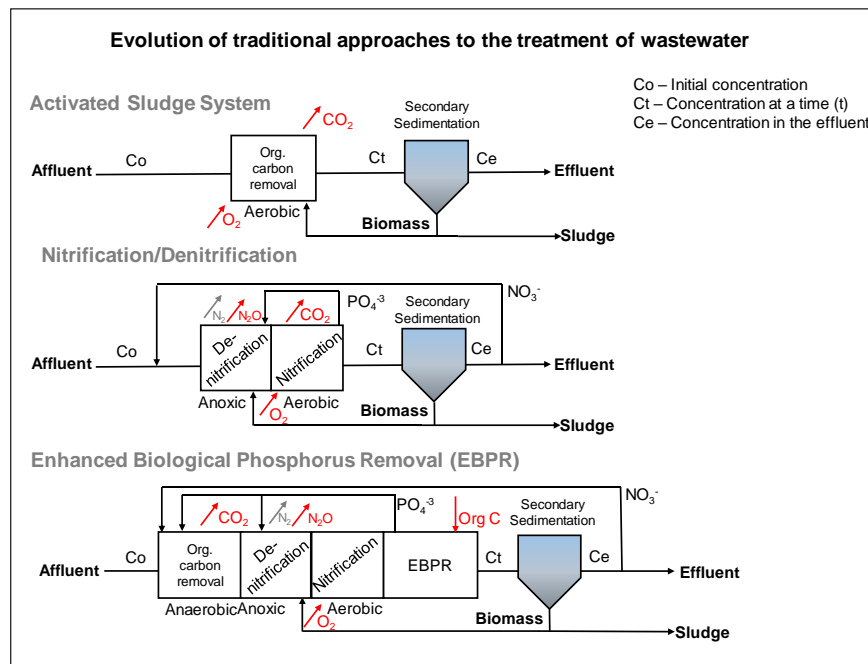


Figure 2.2 The evolution of energy-intensive wastewater treatment. The additive characteristic of current approaches in WWTWs for C, N and P removal is energy-intensive, complex and unsustainable. The activated sludge system was developed to remove organic matter. Secondary treatment included the N removal via nitrification and denitrification and P via the EBPR process. In red, are greenhouse gas emissions and steps where carbon source or oxygen provision is required, which increases the treatment costs (££).

2.2.2 P recovery from digestate in EBPR-based WWTWs

The phosphate recovery process is achieved by producing struvite from the anaerobic digestion (AD) product of sludge generated at the wastewater treatment facility as shown in **Figure 2.3**. Struvite precipitation has been the most studied process for the recovery of phosphate and ammonia. Magnesium salts are added to the digested liquor to form a compound called magnesium ammonium phosphate or struvite ($\text{MgNH}_4\text{PO}_4 \cdot 6\text{H}_2\text{O}$), which is insoluble and precipitates (Monfet et al., 2018). The precipitate can be further used as a slow-release biofertiliser. Slow-release fertilisers are considered those with a delayed time of inorganic nutrient release to match crop plants nutrient uptake rate, thus reducing nutrient-rich runoff from soils to water. As a fertiliser struvite provides magnesium and ammonia to the soil, which are also considered important plant nutrients (Talboys et al., 2016). Despite being to date one of the best ways to recover and reuse P from wastewater, this process incurs additional operational and maintenance costs. It requires the addition of magnesium salts and can generate an unwanted accumulation of struvite within the reactor, which may affect P recovery rates (Nättorp et al., 2019).

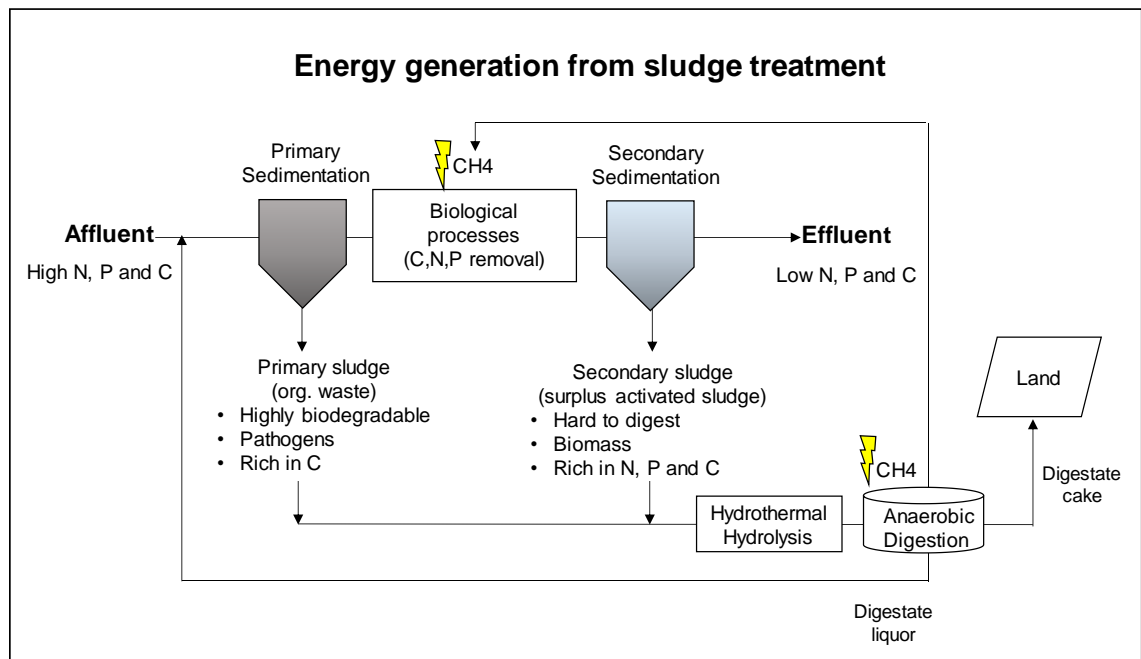


Figure 2.3 Energy generation and nutrient recovery opportunities from sludge in WWTWs. Hydrothermal hydrolysis and AD of primary and secondary sludge produced at WWTWs produce biogas, which supports on-site energy demand. The liquid phase from the AD process is usually recirculated to the WWTWs, while the solid phase is treated and then disposed of in landfills.

Comparable to struvite is the calcium phosphate (Ca-P) precipitation from the digester liquor, which creates a form of P that is similar to that found in apatite minerals extracted from P-rich rock, which is more useful for industrial

applications (Melia et al., 2017). In general, struvite and recovered Ca-P represent acquired benefits from EBPR processes, however, they are limited to WWTWs that include biological treatment and industrial P-rich wastewaters (Nättorp et al., 2019). Struvite production from chemical precipitation processes is not recommended as the removed P is strongly bounded to cations (Ohtake and Tsuneda, 2019).

2.2.3 Alternative cost-effective biological approaches for P control and recovery

A Wastewater Stabilization Pond (WSP) is the simplest form of wastewater treatment. In their most basic form, the process consists of a pond where wastewater is left for a period of time, long enough so natural processes can achieve organic matter stabilization (Von Sperling, 2007). Biological wastewater treatment in the form of (WSPs) represents one of the broader alternatives for smaller populations (Sells et al., 2018). This is mainly because it is fairly easy to construct and can be designed to be cost-effective (Powell et al., 2008). WSPs take advantage of the naturally occurring symbiotic relationship between microalgae and bacteria in water streams. As shown in **Figure 2.4**, heterotrophic bacteria metabolise organic carbon from wastewater in the presence of oxygen for both growth and energy, producing carbon dioxide (CO₂). CO₂ is utilised by microalgae for photosynthesis, growth and the production of oxygen (O₂), which supports bacterial activity (Acién Fernández et al., 2018). Microalgae are photosynthetic eukaryotic microorganisms that can grow photoautotrophically, photoheterotrophically, chemoheterotrophically or mixotrophically, depending on the algal species (Abdulsada, 2014, Abreu et al., 2022). Microalgae are widely used for wastewater treatment. The most common species found in wastewater are *Chlorella* sp., *Scenedesmus* sp. and *Chlamydomonas* sp. These species are the most studied for nutrient control in WWTWs (Von Sperling, 2007, Powell et al., 2008).

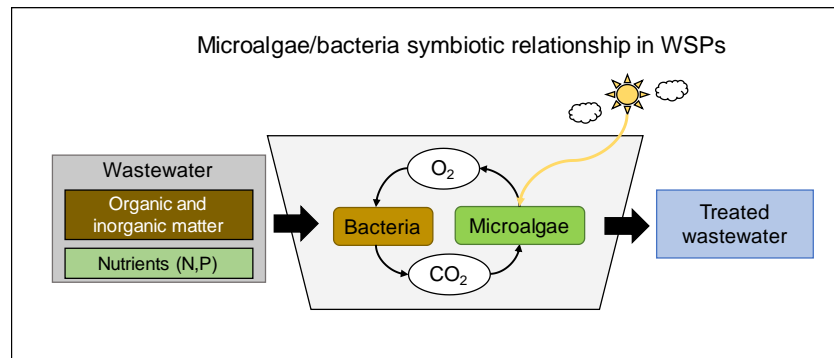


Figure 2.4 Microalgae/Bacteria consortia in WSPs. The organic and inorganic carbon coming from wastewater is metabolised by heterotrophic bacteria, a process that requires O₂ and produces CO₂. Microalgae use the produced CO₂ as a carbon source and light for photosynthesis, growth and the production of O₂, which supports bacterial activity.

- Microalgal activity in WSPs

P removal by microalgae in WSP relies on two different processes: 1) Microalgae consume CO₂ from both the atmosphere and produced by heterotrophic bacteria during respiration. CO₂ consumption increases the pH in WSPs (Von Sperling, 2007). An increase in the pH leads to the precipitation of phosphates due to the formation of complexes with metal cations like Ca⁺², Mg⁺ and Fe⁺². 2) Production of microalgal biomass drives the uptake of both P and N. In the case of P, in-cell accumulation of phosphate beyond that required for growth is possible due to the synthesis of polyphosphate (Slocombe et al., 2020). Microalgae P metabolism allows this microorganism to cope with both high and low concentrations of P found in wastewater. However, depending on the environmental conditions, microalgae may require a longer hydraulic retention time¹ (HRT) compared to traditional WWTWs (Solovchenko et al., 2016, Powell et al., 2008).

- Performance and challenges of WSPs

WSPs require a fairly simple operation and little or no equipment, as they rely on natural processes. The need for a long HRT creates the need for very large areas of land (Von Sperling, 2007). The WSPs offer an efficient treatment in terms of organic matter and pathogen removal, however, for nutrient control, this is not the situation (Sells et al., 2018). In the case of P, the removal rates are highly variable, due to seasonal changes in the environmental factors that interact with WSPs (Mbwele, 2006, Picot et al., 1992). Therefore, understanding

¹ Hydraulic retention time is a parameter widely used in the design on wastewater treatment systems to determine the minimum time that a 'mass' of wastewater needs to be retained at each stage of the process to achieve the treatment goal.

how environmental factors affect these processes is important for the design of WSPs with the capacity to meet P discharge consents.

- **Effect of environmental factors on microalgae P removal**

Temperature has a positive effect on microalgal growth and P uptake. Martínez et al. reported nitrogen and phosphate removal rates of over 90% and high biomass productivity of *Scenedesmus* sp. grown in a secondary wastewater treatment effluent between 20-30°C (Martínez et al., 2000). Powell et al. reported higher P removal at higher temperatures (~25°C), when cultivating a microalgal inoculum mainly composed of *Scenedesmus* sp. in synthetic wastewater, which explains at least one possible cause for the seasonal variation of P removal in WSPs (Powell et al., 2008). Varying temperatures under 15°C had no effect in the Schmidt et al. study, using also synthetic wastewater (Schmidt et al., 2016). At temperatures below 20°C, the challenge is more related to the growth and survival of microalgae, however, this seems to be correlated to photoperiod based on the findings of Delgadillo-Mirquez et al. stud, using a microalgal-bacteria consortia and primary wastewater effluent (Delgadillo-Mirquez et al., 2016). At 5°C they found no microalgal growth, which is also consistent with the results of the Roleda et al. report. In the Roleda et al. study no cell division of microalgae was observed at 10°C, when cultivating *Thalassiosira pseudonana*, *Odontella aurita*, *Nannochloropsis oculata*, *Isochrysis galbana*, *Chromulina ochromonoides* and *Dunaliella tertiolecta* in F/2 synthetic media (Roleda et al., 2013). However, better P removal rates at higher temperatures might be just linked to the increase in biomass production rather than an increase in the in-cell P content per biomass.

Higher light intensity coincided with more polyphosphate and biomass accumulation under cultivation in synthetic wastewater media (Powell et al., 2009). However, this also meant less P content per biomass produced. On the other hand, Sforza et al. found *Nannochloropsis salina* cultivated in synthetic media to have a higher specific growth rate under a light intensity of 150 $\mu\text{mol m}^{-2} \text{s}^{-1}$, but the maximum P content was observed with lower specific growth rate in the cultures grown with a light intensity of 750 $\mu\text{mol m}^{-2} \text{s}^{-1}$ (Sforza et al., 2018). In the case of WSPs, light intensity varies seasonally and decreases exponentially with the depth of the pond, meaning that the deeper the ponds are, the lower the P removal will be. Thus, the biggest areas are required to achieve lower depth of the ponds. At the same time, low-depth WSPs favour CO₂ losses to the atmosphere, instead of inorganic carbon uptake by microalgae (Acién et al., 2017). Light provision is possible to favour P removal but incurs high extra costs to a process intended to offer cost-effectiveness.

Photoperiod determines the light/dark regime and has an important role in microalgae growth (photosynthesis and respiration) and nutrient metabolism (Belkoura et al., 2006, Krzemińska et al., 2014, Yulistyorini, 2016). Generally speaking, the longer the light regime is, the more biomass will be produced for almost every algal species. However, based on the Krzemińska et al. report, the effects of photoperiod on microalgal biomass production vary among microalgal species with some preferring continuous light, or 12 h:12 h light/dark regime (Krzemińska et al., 2014). Lee et al. found that the elongation of the dark cycle in photoperiod is advantageous for organic matter metabolism but not for N and P removal. In their study, *Coelastrum microporum* was cultivated in municipal wastewater coming from anaerobic digester treating sludge from both primary and secondary wastewater treatment (Lee et al., 2015). These results were consistent with Zhang et al. observation that *Scenedesmus dimorphus* grown in Bold's Basal Media (BBM), required at least 16 h of light for nitrogen and 20 h of light for P removal (Zhang et al., 2015). Furthermore, Yulistyorini observed that *Chlamydomonas reinhardtii* achieved a comparable P biomass accumulation to that of continuous light-grown cultures when grown with a photoperiod of 16 h:8 h when supplied with initial N and P concentrations of 200 mg/L and 100 mg/L, respectively. Such nutrient concentrations are comparable to those found in digestate generated at WWTWs (Yulistyorini, 2016). However, municipal wastewater concentrations of N and P are expected around ~40 mg/L and ~9 mg/L, respectively (Di Capua et al., 2022, Ragsdale, 2007, Qadir et al., 2020). The manipulation of both temperature and photoperiod can compensate for a decreased P quota (Shatwell et al., 2014).

Nutrient availability influences P removal by microalgae. Ruiz et al. found that decreasing the P concentration in the influent, coincided with a higher reduction of the P levels in the media while conserving the biomass production in *Chlorella vulgaris* grown in filtered urban wastewater (Ruiz et al., 2011). However, these results are not consistent with other reports. For instance, Sforza et al. found that higher P levels in the media resulted in an increased uptake of P by *Nannochloropsis salina* and Powell et al. reported higher P accumulation as polyP at higher P concentrations in synthetic wastewater (Sforza et al., 2018, Powell et al., 2009). Microalgae growth increases with higher nutrient concentrations in the media which consequently, enhances P removal. Nonetheless, microalgae can also adapt and grow in wastewater, even when there is a high variation in the concentration of nutrients, and can assist in the nutrient control process (Wang et al., 2010).

Apart from N and P, other nutrients may influence microalgae growth if they are limiting, and hence, P removal. For instance, Sells et al. studied the variation in

the organic load (C) and the cation concentration, to examine its effect on the cellular P content of an inoculum dominated by the *Scenedesmus* genus, collected from a WSP. The organic load had a negative effect on cellular P content, as it promoted heterotrophic growth, in contrast with the negligible influence of the cation concentration (Sells et al., 2018). This was unexpected as cations like calcium have a role in the stability of in-cell polyP (Diaz et al., 2009).

pH. As mentioned before, when microalgal consumption of CO₂ exceeds replenishment, pH increases and induces inorganic P to precipitate with cations, which may be removed from wastewater (Von Sperling, 2007). Larsdotter et al., observed higher P removal rates in microalgae hydroponic cultures at higher pH, due to both chemical precipitation and higher algal production (Larsdotter et al., 2010). In Sells et al. study, a pH of 7-8 was observed together with a lower cellular P content, than that of microalgae cultured at a pH of 8-9, and this was attributed to the increased biomass yield at lower pH (Sells et al., 2018). In WWTWs, pH is a very important parameter to be monitored, rather than manipulated, because its maintenance is not cost-effective.

Microalgae/bacteria consortia in WWTWs. As shown in **Figure 2.4**, microalgae and bacteria can form a symbiotic relationship that is favourable for wastewater organic matter and nutrient removal (Delgadillo-Mirquez et al., 2016). The success of such consortia may rely on the availability of these organisms to 'clump' together. Su et al. cultivated a wastewater-derived culture composed of filamentous cyanobacteria and bacteria in municipal wastewater. Under the microscope, they observed that this cooperative system is formed when bacteria get attached to the cyanobacteria filaments, and this also supports the settling ability of the cyanobacterial/bacterial biomass in the form of flocs (Su et al., 2011). Some species of microalgae are filamentous, thus it can be speculated that clumping of microalgal and bacterial cultures is also possible (Liu et al., 2020a). For P removal, previous studies have found a strong correlation between the performance of the algae/consortia and the N:P ratio (Chevalier and de la Noüe, 1985, Lee et al., 2015). However, this correlation can be very variable (5 to 30 N:P) and dependent on other factors like photoperiod and algal species (Choi and Lee, 2015). Other reports focused on the dynamics of competitive behaviour between bacteria and microalgae growth (Natrah et al., 2014, Fukami et al., 1997). González-Camejo et al. found that the bacteria/algae ratio was dependent on light intensity and temperature, and the type of bacteria that form the consortia. For example, the presence of nitrifying bacteria has a negative effect on nitrogen removal, since they compete with microalgae for ammonium, which is usually the nitrogen source preferred

by some microalgae species, although some species may prefer nitrate (González-Camejo et al., 2018, Wood, 2020, Hellebust and Ahmad, 1989, Podevin et al., 2015, Arumugam et al., 2013).

Crimp et al. did a comprehensive study of microalgal P uptake in 15 WSPs distributed in 8 sites in New Zealand, with cool temperate, warm temperate and subtropical conditions. Among the parameters monitored over a year, only rainfall and P concentration influenced biomass P content. These findings were unexpected since variables like temperature (4.2-27.9°C) and solar radiation were not significant (Crimp et al., 2018). A study by Schmidt et al. complemented that of Crimp et al., as it aimed at understanding P uptake by *Chlorella vulgaris* and *Chlamydomonas reinhardtii*, when grown in synthetic wastewater, under 'cold' (10-15°C) conditions. They also observed that the initial P concentration had a positive effect on the biomass P concentration (Schmidt et al., 2016).

Evidence on P removal by microalgae in wastewater stabilisation ponds has been largely collected from comparing differences between pond inlet and outlet characteristics and correlating that with environmental and operational conditions, which perpetuates the "black box" approach used to study engineered systems. That substantially limits current availability to fully understand what is really controlling algal P uptake and how microalgae respond to changing environmental and operational conditions.

2.2.4 The use of photosynthetic microorganisms for sophisticated nutrient control in wastewater treatment

WSPs are a common form of low-cost wastewater treatment and climate conditions are an important factor to consider for their design. When regulated parameters in the final discharge cannot be met, a highly engineered, closed MBWTs system may offer an alternative. Photobioreactors (PBRs) are a type of enclosed, suspended system, used for microalgae cultivation (Li et al., 2019). There are many subtypes of PBRs (panel, tubular, column, soft frame, hybrid PBRs, membrane PBRs etc.), from which, the most commonly used at industrial scale are the tubular PBRs. They have lower volume-to-surface ratios, which allow higher biomass concentrations than those achieved by WSPs. PBRs are efficient for microalgal cultivation, however, they are preferably used for the production of high-value-added products that can afford the considerably high costs and energy consumption of tubular PBRs which may consist of several connected loops (see **Figure 2.5**) (Płaczek et al., 2017). The high costs may come from the high HRT that PBRs require to avoid biomass losses, making the solid retention time (SRT) dependent on the HRT. (Luo et al., 2018). PBRs have

also been found to have poor settlement rates, leading to important biomass losses, and harvesting issues. As enclosed systems, they promote microalgal biofilm formation over the structure's surface, which may reduce light penetration and photosynthesis (Płaczek et al., 2017).



Figure 2.5. Stack tubular PBR (Algae PARC Wageningen University)

For this type of technology, downstream processes are already available to facilitate harvesting of algal biomass. Although these may be expensive, accounting for approximately 30% of the total biomass production costs (Singh and Dhar, 2006, Gutiérrez et al., 2015, Uduman et al., 2010, Molina Grima et al., 2003). WSPs represent a more affordable alternative for P recovery, but the P removal efficiency is currently lower than that of more sophisticated and energy-intensive technologies like EBPR or chemical precipitation, as the resulting algal biomass leave the systems within the final effluent. This characteristic is only beneficial if the final effluent is reuse in agricultural irrigation, as both treated water and algal biomass is used to support crops. Therefore, despite microalgal wastewater remediation has been applied using WSPs, this approach is yet far from replacing current processes applied at large WWTWs. More research work is needed to improve design and operation and maintenance conditions of both WSPs and PBRs, as well as optimum design parameters for P control and recovery.

2.2.5 Recycling of P removed from wastewater as P-rich microalgal biomass

The main advantage of MBWTs against EBPR in terms of P recovery performance is that it does not require chemical addition to support N and P removal. Biomass obtained from MBWT can be valorised as a slow-release biofertilizer, which is fully bioavailable to crops and soil biome. MBWT processes can also be steered towards the production of other final products, with different levels of quality depending on the downstream processing set for

the resulting biomass depending on its quality and quantity (Acién Fernández et al., 2018).

Microalgae are a rich source of carbohydrates, lipids, proteins, pigments and vitamins. Coppens et al. reported the benefits of using microalgae as an organic slow-release fertiliser in the cultivation of tomatoes (Coppens et al., 2016). Improved quality of the fruits, measured as an increase in sugar and carotenoid content, was observed when microalgal-bacterial flocs were used to fertilise tomato crops. However, lower tomato yields were obtained which highlights the need to optimise parameters for either the microalgal-bacterial flocs processing, application and/or cultivation conditions (Coppens et al., 2016). Another study by Dineshkumar et al. analysed the impact of algal-biofertilisers on rice growth and productivity and found a positive performance of rice plants in terms of plant growth, seed yield and biological activity and chemical characteristics of soils, when fertilised with a combination *Chlorella vulgaris* and *Spirulina platensis* dry algal biomass (Dineshkumar et al., 2018). Schreiber et al. tested the use of dried versus wet *C. vulgaris* biomass as a biofertiliser for wheat cultivation in different substrates (Schreiber et al., 2018). They observed that wheat plants had vigorous growth compared with that obtained with mineral fertiliser application when using either dry or wet algal biomass. However, their discussion highlights the economic barrier of the costs of mineral fertilisers versus the costs of microalgal fertilisers, which creates a barrier to establishing algal biofertilisers in the agricultural sector (Schreiber et al., 2018).

There are few studies of algal fertiliser applications where wastewater treatment was involved (Renuka et al., 2016, Mulbry et al., 2007). Wuang et al., assessed the suitability of *S. platensis* to both bioremediate aquaculture wastewater and examined the use of algal biomass as biofertiliser to leafy vegetables. *S. platensis* efficiently removed ammonium and nitrate, N being the only monitored nutrient. For crop performance, their results showed a range of efficiencies among tested vegetable types, but highlighted microalgal biomass as an effective micronutrient donor. The levels of N, P, and potassium (K) in microalgal biomass were lower compared to chemical fertiliser. However, the levels of different micronutrients like calcium, iron, selenium, manganese and zinc, which appear in low concentrations but higher than in chemical fertilisers, play key roles in plant growth and metabolism (Wuang et al., 2016). Microalgae fertilisers bring additional benefits to improve soil quality in contrast with mineral fertilisers, which are a major cause of erosion and nutrient losses when used extensively (Dineshkumar et al., 2018, Gonçalves et al., 2023). However, one possible constraint of using wastewater-grown algal biomass for crop fertilisation is the possibility of soil pollution with heavy metal traces above the

consented limits, which has not been well studied and no risk assessments have been made (Renuka et al., 2016). Hence, microalgae biomass produced at WWTWs could be applied as a biofertiliser for the production of energy crops instead of food crops. This would avoid the possible risk to public health associated with micropollutants present in harvested algal biomass from municipal wastewater treatment facilities. However, further research and risk assessments are needed to establish 'best practices'.

2.2.6 When technology is not enough: Performance and challenges of MBWTs

While a part of the field focuses on developing new technologies to improve the performance and reliability of MBWTs, not strong evidence in published literature has aimed at overcoming the gap of uncertainty in the use of photosynthetic microorganisms for nutrient control and recovery in WWTWs, and this represents one of the biggest barriers this strategy faces. The uncertainty comes from the gap in the knowledge of microalgal in-cell P metabolism. Thus, acquiring a deep understanding of this process can help to improve design and performance of WSP systems and retrofit conventional WWTWs. Operation and maintenance costs can be reduced by just increasing the understanding of the biological processes behind this technology.

Both sophisticated (PBR) and simple (WSP) alternatives are forms of MBWT. MBWTs are still far from being a perfect solution for wastewater treatment as their performance is clearly susceptible to changes in environmental conditions. Nevertheless, MBWTs have the potential to turn current WWTWs 'greener'.

Figure 2.6 shows a comparison between a conventional WWTW designed for biological nutrient control (EBPR) and a MBWT system for nutrient control. While both systems, with the current technologies, may produce undesirable products, the MBWT can be designed as a greener technology in terms of emissions and by-products. The future of wastewater treatment in the form of MBWT relies on a better understanding of the mechanisms that allow microalgae to cope with nutrients in wastewater and how these mechanisms are regulated by microalgae.

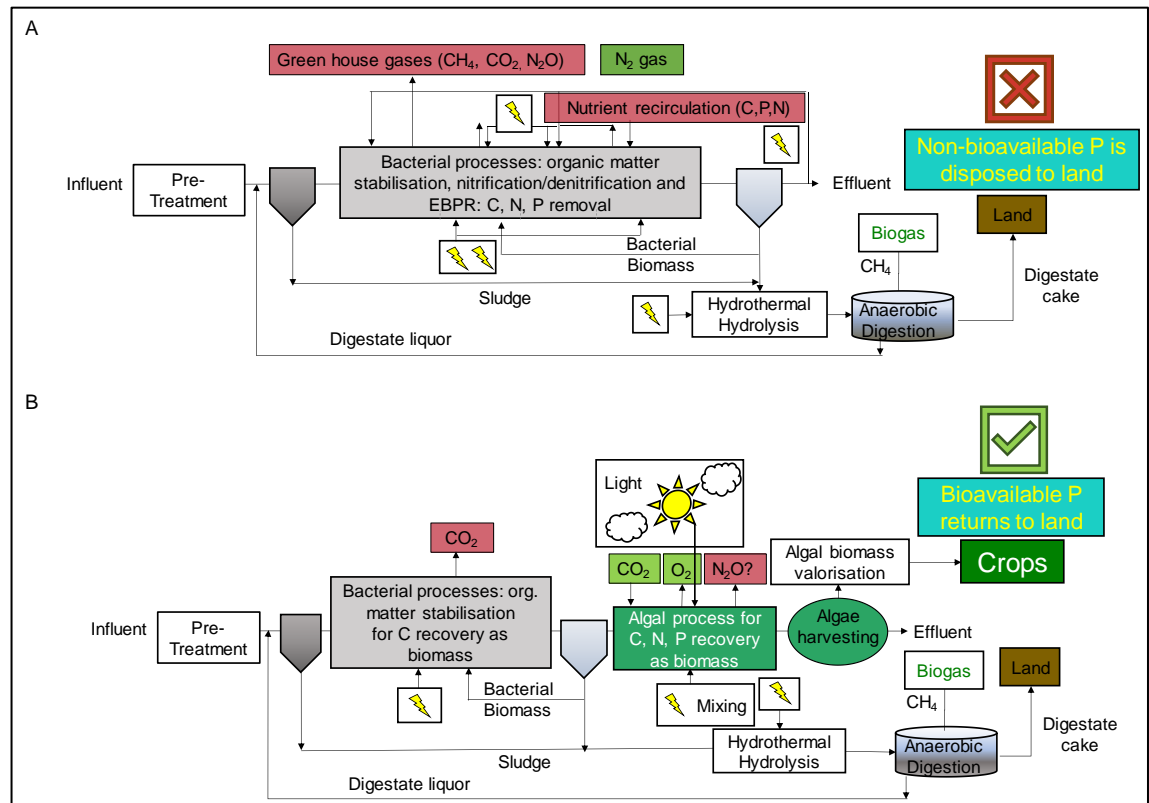


Figure 2.6 Comparison of wastewater treatment approaches. A

Conventional WWTW combining denitrification and EPBR processes after primary sedimentation and B A proposed substitution of these steps with an MBWT in the form of a microalgae/bacteria consortium. Undesirable products such as important greenhouse gases (e.g. CO₂, N₂O), energetically wasteful steps and costly/non-renewable inputs (e.g. supplements: organic C) or wasteful outputs (e.g. N₂, NO₃⁻) are shown in red. Products or steps that are beneficial or that can be potentially renewable are shown in green along with biogas, biofuels and value products. Downstream anaerobic digestion steps are indicated for both processes resulting in the production of methane and fertilisers. Figure adapted from (Slocombe et al., 2020).

2.3 Phosphate Physiology of Microalgae

P is an irreplaceable element for living organisms, including microalgae. Within the cells, phosphate can be found in organic forms, as it makes part of important cellular components, including the genetic material, DNA/RNA, and phospholipids, and inorganic forms (polyP, free phosphate) (Dyhrman, 2016). Due to the intrinsically slow characteristic of the natural phosphorus cycle (see section 2.1), P_m is not readily available to living organisms. This represented an opportunity for microalgae, whose evolution assisted in the development of a unique P metabolism that helps them cope with uncertain P environments.

2.3.1 Phosphate biochemical composition of microalgal cells

Microalgae cells synthesise several molecules that contain phosphate. These molecules serve different purposes within the cells and can be split into two groups, organic and inorganic P components.

- Organic pools of P

The most important organic compounds that contain phosphate are nucleic acids (DNA/RNA) that store all of the microalgal (and any other living form) genetic and transcript information (Dyhrman, 2016). However, compared to RNA, DNA stability may be more important to preserve as it contains the very base of the microalgal genome. RNA, otherwise, has a very dynamic function and is synthesised and degraded constantly (Raven, 2013). RNA role is to assist in the process of protein synthesis by encoding distinct types of RNAs (messenger RNA-mRNA, ribosomal RNA- rRNA, and transfer RNA-tRNA). However, rRNA accounts for 85% of total P in RNA, which indicates that ribosomes are the main source of non-storage P in microalgal cells (Flynn et al., 2010). Couso et al. observed a reduction of ribosomal proteins RPS6 and RPL37 under P-deprivation, as a response to the activation of autophagy in *C. reinhardtii* (Couso et al., 2017). A proteomics study by Plouviez et al. showed that the green microalgae *C. reinhardtii* reduces its abundance of proteins involved in ribosome structure and synthesis, and translation, after exposure to P-depleted conditions (Plouviez et al., 2023a). These results were consistent with previous transcriptomic studies in *C. reinhardtii* and other microalgae species like *Nannochloropsis oceanica* and *Thalassiosira pseudonana* (Mühlroth et al., 2017, Dyhrman et al., 2012, Plouviez et al., 2021). The Plouviez et al. proteome data also showed the transfer from P depleted to P replete conditions and observed an increase in the abundance of the same proteins that showed a decrease during P deplete conditions (ribosome structure and synthesis, and translation) (Plouviez et al., 2023a). Under no nutrient limitation, microalgae follow the maximum growth rate (μ_{max}) hypothesis (Rees and Raven, 2021). The growth rate hypothesis indicates that the rate at which ribosomes are produced follows the biomass growth rate for different organisms (Elser et al., 2003). Simultaneously, when environmental conditions are limiting for growth, organisms (not just microalgae) will make use of the bulk of rRNA to sustain growth (Flynn et al., 2010, Allen and Gillooly, 2009). In this sense, the hypothesis indicates that biomass P content is mostly dominated by changes in RNA (mostly rRNA) (Raven, 2013). Rees et al corroborated the strong relationship between maximum specific growth rate (μ_{max}) and biomass P content. However, RNA was not the only P-rich molecule correlated with the increase in μ_{max} (Phospholipids, polyphosphate and to a lesser extent DNA). Moreover, they found that the μ_{max} hypothesis was true for microalgae but not for cyanobacteria. Bacteria have up to seventeen copies of the rRNA operon which makes these organisms keep a constant 50% RNA, relative to its biomass total phosphate content, during the period of μ_{max} . This indicates that in

cyanobacteria (prokaryotes), RNA is the largest pool of phosphate. In contrast, in microalgae the largest pool of P is polyP (35% of total P), followed by RNA (25% of total P) (Rees and Raven, 2021).

Phospholipids are essential components of the cellular membrane of microalgae and also represent a reservoir of P (Mühlroth et al., 2017, Dyhrman, 2016). Manisali et al. reported a decrease in the phospholipid content of *Nannochloropsis oculata* when cultures depleted phosphate from the media (Manisali et al., 2019). In *Chlamydomonas reinhardtii*, P limitation promotes the partial replacement of phospholipids with sulpholipids as a P-sparing response (Hidayati et al., 2019, Raven, 2013, Van Mooy et al., 2009). As observed by Rees et al., the phospholipid content of microalgae also increased in relation to μ_{max} . Phospholipid contribution to the total P content of microalgae (14%) is higher than that of cyanobacteria (3%) (Rees and Raven, 2021). For microalgae, phospholipids are components of cell membranes and organelles. This characteristic and the difference in RNA dynamics mentioned before, suggest that cyanobacteria and microalgae, although both are photosynthetic microorganisms, have different P-sparing mechanisms.

Inositol polyphosphates (IPs) are a class of P-rich molecules present in all eukaryotes (Lorenzo-Orts et al., 2020). In yeast and plants, IPs have several roles (i.e, P storage, P starvation signalling, DNA repair, autophagy, environmental stress responses and ribosome biogenesis) (Wild et al., 2016, Azevedo and Saiardi, 2017, Jia et al., 2023, Lorenzo-Orts et al., 2020, Rees and Raven, 2021, Raboy, 2020). However, in microalgae, the role of these molecules has not been explored to the same degree of depth as for yeast and plants. In *Chlamydomonas* sp., potential roles in calcium-dependent deflagellation were observed for IP₃ (Yueh and Crain, 1993). The more phosphorylated forms of IPs (IP₅₋₈) have been identified in *Chlamydomonas reinhardtii*, *Chlorella vulgaris* and *Chlorella sorokiana*, and their connection with carbon metabolism and photosynthesis regulation was reported (Couso et al., 2016, Morales-Pineda et al., 2023, Couso et al., 2020, Couso et al., 2021). As Couso et al. showed in their latest study, CO₂-mediated IPs synthesis enhanced phosphate storage in *Chlorella* sp. (Morales-Pineda et al., 2023). Thus, in microalgae IPs are believed to be involved in P signalling (like in yeast) rather than P storage (like in plants). In plants, inositol hexakisphosphate (IP₆), also called phytate or phytic acid is the major storage form of P (Raboy, 2020).

Adenosine triphosphate (ATP) is another organic P component of microalgal cells. Considered the cell energy currency, ATP is involved in many processes involving phosphorylation and dephosphorylation mechanisms (Dyhrman, 2016) (Geider and Roche, 2002). ATP is the P-donor of polyphosphate, the main

inorganic storage form of P (Tani et al., 2009). Sanz-Luque et al. found that polyphosphate accumulation is a mechanism of *C. reinhardtii* to avoid inhibition of electron transport in the mitochondria and the chloroplast, under sulphate deprivation (Sanz-Luque et al., 2020). As explained by Sanz-Luque et al., acclimation responses are energy-demanding (e.g. sulphate, phosphate, etc.). Thus, ATP is not a storage source of organic P, as it is a vital component of energy homeostasis in microalgal cells.

- Inorganic pools of P

Microalgae had to evolve to cope with fluctuating levels of phosphate in the environment. As mentioned earlier (section 2.2.1), polyphosphates are the molecules that microalgae and other organisms (e.g., yeast, bacteria) synthesise to store phosphate beyond what it is needed for growth (Albi and Serrano, 2016). It seems that this molecule was first described for microalgae in 1960s by Miyachi and Tamiya, who suggested that the role of polyphosphate was similar to that in yeast (P storage) (Miyachi and Tamiya, 1961).

Polyphosphate represents the main form of inorganic P in microalgal cells, with a chain length in the range of 2-1,000 phosphate units (Christ et al., 2020b). It accounts for approximately 35% of the total biomass phosphate (Rees and Raven, 2021). Several functions have been described for this polymer, due to its polyanion characteristic, similar to that of ATP. The storage of phosphate in the form of polyP could be explained as a strategy to reduce the risk of unbalancing the delicate equilibrium of P-based biological reactions, due to very high uptake rates of P (Solovchenko et al., 2019a, Dyhrman, 2016).

Polyphosphate is stored in vacuole-like organelles called acidocalcisomes which are membrane-enclosed organelles that accumulate polyP in the form of granules and sequester calcium and metals (Goodenough et al., 2019). Due to its high electron density, polyP co-localises with cations like calcium (Ca^{2+}) and magnesium (Mg^{2+}) in acidocalcisomes (Siderius et al., 1996, Tsednee et al., 2019). Having a counterion helps to provide stability to this polymer (Ruiz et al., 2001). Therefore, other than a P reserve, polyP is a cation chelator assisting in the resistance to heavy metals (Komine et al., 2000, Andreeva et al., 2014). It is also considered a source of energy (Van Mooy et al., 2009). Polyphosphate may also act as a regulator of enzyme activity and adaptation to stress responses and late-growth phases (Kulaev and Kulakovskaya, 2000, Goodenough et al., 2019). In microalgae, polyP is mostly accumulated in acidocalcisomes, although it has also been found in the cell wall during late growth stages or cytokinesis, where it has a presumed role in protecting daughter cells upon cell cycle completion, against pathogens (Werner et al., 2007). Polyphosphate is synthesised during P-replete conditions and mobilised

during P-deplete conditions (Solovchenko et al., 2020, Solovchenko et al., 2019a). This particular dynamic led to uncovering the phenomena of phosphate overplus response and/or luxury P uptake in microalgae.

2.3.2 The phosphate overplus response and/or luxury phosphate uptake of microalgae

The phosphate overplus or 'overcompensation' phenomena was first studied in yeast around 1960s, (Liss and Langen, 1962), but was identified a couple of decades earlier as a response to P limitation in the yeast *Saccharomyces cerevisiae* (Schmidt et al., 1946). P overplus is the term mostly used to describe the enhanced accumulation of phosphate in the form of polyphosphate after supplying P to P-deprived cells (Voelz et al., 1966). In microalgae, this phenomenon was first studied in detail by Aitchison and Butt (Aitchison and Butt, 1973).

Furthermore, microalgae can also accumulate more phosphate than is needed for growth when exposed to another type of stress, when P is not a limiting factor (sulphur or nitrogen stress, etc.) (Chu et al., 2020a, Harold, 1966, Aksoy et al., 2014, Goodenough et al., 2019, Kuesel et al., 1989). This response has been named luxury P uptake (Fitzgerald and Nelson, 1975, Bolier et al., 1992). In our last review (Slocombe et al., 2020), it was highlighted that P overplus and luxury P uptake were two different phenomena in microalgae, in agreement with Eixler et al. and Powell et al. (Eixler et al., 2006, Powell et al., 2009). However, in published literature, luxury P uptake has also been referred to as the capacity of P-deprived microalgae to accumulate P after P is resupplied (Solovchenko et al., 2019a, Solovchenko et al., 2019b). Therefore, diverted interpretations of what luxury P uptake and P overplus responses really are, represent a limitation within the research community working in this field.

There have been several studies on the response of microalgae or cyanobacteria to P supply after a period of P deprivation, named either P overplus or luxury P uptake. Aitchison and Butt's study observed in *Chlorella vulgaris*, that polyP accumulation was enhanced by increasing the time of P-deprivation (0 h – 36 h) before P resupply as resuspension in fresh media (3 mM P ~ 100 mg PO₄-P/L). They also observed that polyP levels would decrease during the exponential growth phase (under P-replete conditions), which was consistent with Harold's study in *Aerobacter aerogenes* (Harold, 1966). Moreover, Aitchison and Butt reported that under P deprivation, *Chlorella vulgaris* cells were able to mobilise internal P reserves to sustain the growth observed during this period (Aitchison and Butt, 1973). Sicko and Jensen deprived the cyanobacteria *Plectomena boryanum* of phosphate for 5 days,

followed by biomass harvesting and resuspension in fresh media (10 mg PO_4/L). They observed that *P. boryanum* cells reduced their P content to 0.76 microgram per million cells during P-deprivation, and then exhibited a 25-fold increase in its total P content after P supply (Sicko-Goad and Jensen, 1976). Eixler et al. used *C. vulgaris* to study its P overplus response by avoiding centrifugation of biomass to initiate P-deprivation and P repletion. Centrifugation of biomass may have a mechanical stress effect on the cells (Scarsella et al., 2012). Instead, they diluted a preculture of *C. vulgaris* to initiate a P-deprivation period of 72 hours, which was followed by a P supply with a potassium phosphate solution. Eixler et al. studied P overplus response when increasing P concentration during repletion using P-deprived cells cultured in up to 0.16 mM P (Eixler et al., 2006). The result from Eixler et al. study was consistent with Sforza et al., who cultivated *Nannochloropsis salina* for 5 days with a low concentration of P (5 mg $\text{Na}_2\text{HPO}_4 \cdot \text{H}_2\text{O}/\text{L}$), to generate P-depleted cultures. P-depleted cultures exhibited a higher accumulation of phosphate and polyphosphate when inoculated in fresh media with 150 mg $\text{Na}_2\text{HPO}_4 \cdot \text{H}_2\text{O}/\text{L}$, compared to 5, 50 and 100 mg $\text{Na}_2\text{HPO}_4 \cdot \text{H}_2\text{O}/\text{L}$ (Sforza et al., 2018). Solovchenko et al. tried to build on previous works by stating that the lack of consistency leading to slow progress in the understanding of luxury P uptake in microalgae was due to (1) previous studies not depleting the internal P reserved of microalgal cultures before repletion and (2) the lack of advanced laboratory techniques for the study of this phenomena in microalgae (Solovchenko et al., 2019a). In their study, *C. vulgaris* cells were P-deprived until biomass growth ceased for three consecutive days and then harvested and resuspended in fresh media (0.4 mM P) (Solovchenko et al., 2019b). Up to date, this is the first and only published work in which a physiological parameter of P deprivation, instead of an arbitrary time period, was used in an experimental design of P overplus in microalgae. Plouviez et al. cultivated *Chlamydomonas reinhardtii* in a medium containing 1 mg P/L for 5 days (considered P-depleted cultures), followed by a supply of P as potassium phosphate (10 mg P/L ~ 0.33 mM P). They corroborated the capacity of *C. reinhardtii* to perform P overplus. However, their transcriptomic data did not show signs of replacement of phospholipids with sulpholipids (Manisali et al., 2019). This indicates that the P depletion process in their experiment was not enough to activate phosphate deprivation responses in this microalga (Plouviez et al., 2021). Lavrinovičs et al. chose *C. vulgaris* to test the effect of P-deprivation length (0-10 days) and observed that a 10-day period of P-deprivation with low initial biomass concentration (0.2-1.5 g dry biomass/L) had improved P removal from the media and polyP accumulation. However, an AI-based approach in this same study, suggested that a one-day P-deprivation period with low initial biomass

concentration at the time of P resupply would achieve the highest performance (Lavriničs et al., 2022). These results were consistent only for the period of P-deprivation, with those obtained by Plouviez et al. (Plouviez et al., 2023b). Plouviez et al. tested the effect of initial biomass and P concentration and P-deprivation period length on *C. reinhardtii* P overplus. They found that higher initial biomass (0.17-0.57 grams dry biomass/L) and P concentration (0-20 mg P/L), generated higher total P accumulation during P overplus. Consistently with Aitchison and Butt study, Plouviez et al. also observed that a longer period of P-deprivation (0-4 days) was correlated with a bigger P overplus (Plouviez et al., 2023b, Aitchison and Butt, 1973). Interestingly, Lobakova et al. reported on *Micractinium simplicissimum*, which could be the first exception of microalgal P overplus (Lobakova et al., 2023). This species did not have abnormal behaviour when cultivated under P-deprived or P-replete conditions, separately. However, when *M. simplicissimum* was P repleted (800 mg PO₄/L) after a period of P-deprivation of three consecutive days after cell division ceased, it displayed intolerance to the P gradient. These results suggest that P overplus might not occur in all microalgae as previously assumed.

So far, most studies on luxury P uptake or P overplus have been done in the green microalgae *Chlorella vulgaris* due to its fast growth and wide use in the microalgal research field (Krienitz et al., 2015). Also, all the studies mentioned above were performed under controlled conditions and synthetic cultivation media. Lavriničs et al. evaluated the performance of *Desmodesmus communis*, *Tetradesmus obliquus* and *Chlorella protothecoides* when P-deprived for 7 and 14 days. They chose those periods of P-deprivation to ensure near-complete to total depletion of polyphosphate before P resupply. Although, it is not clear if polyP content after P-deprivation was measured. The P-deprived cultures were inoculated in primary and secondary wastewater treatment effluent (Lavriničs et al., 2020). As mentioned previously (**Figure 2.3**), the difference between primary and secondary wastewater treatment effluent is that the first one is more nutrient-rich than the second. Lavriničs et al. showed that none of these species was particularly more effective for P overplus as they exhibited different advantages and disadvantages in terms of growth, P removal and polyP accumulation. However, they highlighted the implications of using wastewater for the study of P overplus: high variations in the nitrogen to phosphorus ratios, pH, and organic load (Lavriničs et al., 2020). In a later study, Lavriničs et al. used the species *T. obliquus*, *Botryococcus braunii*, *C. vulgaris* and *Ankistrodesmus falcatus*, for their ability to grow in wastewater. In that study, the four species were P-deprived for 3 and 5 days before being inoculated in secondary wastewater treatment effluent. From

this experiment, Lavrinovičs et al. reported that *C. vulgaris* had the best P overplus and biomass growth performances. *B. braunii*, which showed no differences according to the P-deprivation periods tested, was suggested as a promising alternative for its good biomass growth and nutrient removal rate (Lavrinovičs et al., 2021). As far as I can tell, Lavrinovičs et al. studies, are among the first to suggest the potential importance of other nutrients apart from P (i.e., Nitrogen to phosphorus ratio) on the performance of wastewater treatment systems using microalgal P overplus.

2.3.3 Methods for the analysis of Microalgal polyphosphates

The direct measurement of P overplus or luxury P uptake is polyphosphate accumulation. As pointed out by Solovchenko et al., one of the main gaps in the study of these phenomena is the availability of advanced techniques or reproducibility of commonly used techniques to analyse polyphosphate in microalgae (Solovchenko et al., 2019a). Most, if not all, methodologies for polyP analysis have been developed for yeast, and some have been adapted successfully to microalgae. The analysis of polyP, depending on the research aim, may be used to determine different characteristics of the polymer in a specific sample (Christ et al., 2020b):

1. Total phosphate content in the biomass is not a direct measurement of polyphosphate, as it provides the quantification of all P-containing forms in the biomass (inorganic and organic). However, in microalgae, this method has been used as an approximation to detect polyphosphate accumulation during P overplus (Plouviez et al., 2023b, Plouviez et al., 2021, Plouviez et al., 2022). Total phosphate in the biomass can be obtained after a complete hydrolysis of extracted dry microalgal biomass with the combination of a strong acid, an oxidising reagent, and heat to release all phosphate (Koistinen et al., 2020). Released phosphate can be quantified using common colourimetry methods like blue ascorbic acid method and malachite green assays (Carter and Karl, 1982, Murphy and Riley, 1962, Rodriguez et al., 1994).
2. Total polyP quantification can be subdivided into the methods that require or do not require previous polyP extraction. PolyP extraction with trichloroacetic or perchloric acid is used to disrupt the cells, and this is followed by subsequent and time-consuming extractions with sodium perchlorate or sodium hydroxide (Liss and Langen, 1962, Kulaev et al., 1966, Aitchison and Butt, 1973). Alternatively, polyP can be extracted by using commonly used methods to extract nucleic acids like RNA, due to the shared properties of both molecules (Neef and Klädde, 2003). Once

extracted polyP can be quantified by colourimetry at an absorbance of 630 nm, after staining with toluidine blue O (Lavriničs et al., 2020, Lavriničs et al., 2021). Toluidine blue O is a metachromatic dye which stains nucleic acids in blue and polyP in pink (Au - Loss et al., 2011). However, the quality of the results may be affected by the presence of nucleic acids in the samples, which are also stained by toluidine blue O (Christ et al., 2020b). Quantification may also be achieved by digesting extracted polyP as mentioned above for total phosphate content in biomass (Powell et al., 2009). However, if the extraction of high-purity polyP is not achieved, the digestion process will lead to the quantification of other P-containing compounds (Christ et al., 2020b). The gold standard for polyP extraction and quantification was developed by Bru et al. (Bru et al., 2017). In this method, polyP and RNA are extracted using the phenol-chloroform method, followed by treatment with a recombinant exopolyphosphatase (ScPpx1), purified from the yeast *Saccharomyces cerevisiae*. This enzyme has specific polyphosphatase activity, which means that it only degrades polyphosphate (Wurst and Kornberg, 1994). The product of the digestion, which occurs at a temperature of 37 degrees Celsius, contains all free phosphate (orthophosphate) released from polyP. Finally, quantification of phosphate released from polyP may be achieved with absorption spectroscopy.

To avoid polyP extraction, nuclear magnetic resonance (NMR) can be used. This method, which is widely used in physical sciences, uses a magnetic probe to identify the unique spin properties of atomic nuclei. Therefore, ^{31}P NMR is a non-destructive method that has been used in microalgae with the capacity to identify all P-containing compounds (Hebeler et al., 1992, Kuesel et al., 1989). However, ^{31}P NMR detects polyphosphates and other molecules based on the class of bonds, and thus it might not distinguish molecules that contain phosphoanhydride bonds as polyP (Bru et al., 2017). Also, the presence of cation complexes according to pH variations can cause chemical shifts in the polyP signal in ^{31}P NMR (Sianoudis et al., 1986). Alternatively, live cells can be stained with 4',6-diamidino-2-phenylindole (DAPI) and polyP can be quantified by absorbance or fluorescence spectroscopy (Sforza et al., 2018, Kolozsvari et al., 2014). DAPI is commonly used for the staining of DNA (emission maxima 461 nm) (Kapuscinski, 1995). A shift in the spectrum of the same sample can be used to stain polyP (emission maxima of 525 nm), due to the shared polyanion characteristic of both DNA and polyP (Aschar-Sobbi et al., 2008b). A Raman confocal microscopy method has been recently developed to quantify

polyphosphate in microalgae and obtained highly similar results compared to the gold standard (Moudříková et al., 2017). Raman microscopy identifies a signal that is recognizable for polyP, by measuring the light scattering ability of the compound of interest and generating a unique spectrum (Christ et al., 2020b). Raman microscopy was used to study the P overplus response of *C. vulgaris* (Solovchenko et al., 2019b).

3. The polyphosphate chain length distribution of a sample can be determined by polyacrylamide gel electrophoresis (PAGE). Electrophoresis of polyacrylamide gels loaded with RNA/polyP samples offers an opportunity to qualitatively assess polyphosphate chains extracted in an RNA sample. Polyphosphate is a polyanionic compound and thus, migrates vertically in the opposite direction of the negative electrode, likewise RNA and other P-rich compounds in the sample like inositol polyphosphates (Losito et al., 2009, Lonetti et al., 2011). Furthermore, polyP migration will depend on the length (molecular weight) of the polymer. After migration, PAGE can be stained with toluidine blue O or for more sensitivity, DAPI is used. This method may be used to determine whether a sample contains mostly long, medium, or short-chain polyP, or if it is heterogeneous (parameter of polydispersity). PAGE has been used in *C. reinhardtii* and *C. vulgaris* recently (Sanz-Luque et al., 2020, Yi-Hsuan et al., 2023). PAGE can also be used to analyse inositol polyphosphate dynamics, which would be valuable to understand more of how these biomolecules participate in microalgae P metabolism. Alternatively, chromatography may also be used to determine polyP chain length distribution from extracted samples. This method allows the separation of a mixture of different polyP chain lengths with approximately 10 units of difference (Christ et al., 2020b).
4. Cellular localisation of polyP and its morphology can only be achieved by non-destructive methods that involve microscopy imaging of live or fixed cultures. Raman confocal microscopy was successfully used to detect, quantify, and localise polyP, lipids, and starch in *C. vulgaris* and *Desmodesmus quadricauda* (Moudříková et al., 2021, Moudříková et al., 2017). However, this technique is very complex and relies on the assumption that the culture is homogenous (Moudříková et al., 2017). Raman microscopy may not be the best technique to study P overplus in microalgae since the effect on the cells due to P deprivation can disturb the quality of the result. Microalgae cells have morphological changes when undergoing P-deprivation, which could affect the calibration of the

Raman microscopy settings (Bajhaiya et al., 2016). Confocal microscopy of DAPI-stained cells may provide information about the localisation and shape of polyP granules as has been shown in *C. reinhardtii* (Slocombe et al., 2023). DAPI is a light-sensitive dye and thus, appropriate standardisation of the confocal imaging and processing must be considered. An alternative to confocal microscopy is transmission electron microscopy (TEM). Granules of polyphosphate can be indirectly identified as electron-dense bodies. TEM has been used to analyse the structure of polyP granules in *C. reinhardtii* (Aksoy et al., 2014, Goodenough et al., 2019), *C. vulgaris* (Solovchenko et al., 2019b) and other microalgae (Shebanova et al., 2017). If sophisticated confocal (Raman) or electron microscopes are not available, light microscopy can offer an alternative to enable polyP visualisation. Light microscopy was used to localise polyP in *C. reinhardtii* cells stained with lead nitrate and ammonium sulphide (Plouviez et al., 2021). In this technique, the polyphosphate counterions (e.g. calcium or magnesium) are replaced by lead ions. Black staining of polyP granules is obtained as lead sulphite is generated (Bolier et al., 1992).

5. Polyphosphate counterions like calcium or magnesium can be quantified from extracted polyP samples using atomic absorption spectrometry or inductively coupled plasma optical emission spectrometry (Christ et al., 2020b). The purity must be high to ensure that any cations identified are indeed a counterion of polyP. Otherwise, polyP counterions can also be detected by combining TEM with X-ray microanalysis. This technique was used in *C. reinhardtii* to identify calcium colocalization with polyP bodies (Ruiz et al., 2001)

The methodologies mentioned above have been developed for the study of polyP and have been tested in microalgae. From these techniques, only a few have been used to study luxury P uptake or P overplus in microalgae. Those studies have mostly focused on total P or polyP quantification and localisation of polyP granules. For polyP quantification, the most reliable and specific methods seemed to be Raman microscopy and biochemical ScPpx1 assay. Moreover, it is important to make use of alternative techniques to generate information about other parameters of polyP that will drive the microalgal polyphosphate field forward. Parameters like polyP chain length distribution or average chain length, and structure of polyP (linear, cyclic, etc.), have been mostly neglected in microalgae studies, but have provided valuable insights into P metabolism in yeast (Christ et al., 2020b). For instance, thanks to the good understanding of polyP metabolism in yeast, methods have been developed for

the production of food-quality grade polyP from yeast (Christ et al., 2020a). One attempt to produce long-chain polyP (with a high demand in the medical field) from *C. vulgaris*, has been very recently published (Yi-Hsuan et al., 2023). There is a great opportunity to make the most of the techniques recently developed to bring microalgal polyphosphates closer to the level of yeast. Improving the understanding of microalgal polyP will provide more suitable conditions for their use in medicine, agriculture, the food industry, etc. At the same time, this may help to promote P recovery from wastewater using microalgae, prevent eutrophication of water ecosystems and supply the demand for polyphosphates in the industry.

2.4 *Chlamydomonas reinhardtii* as a model organism to study microalgae P metabolism

P overplus and luxury P uptake responses have been studied in several microalgal species, where polyP was analysed together with other physiological parameters like biomass growth and P removal from the media. Physiological responses are controlled by transcriptional and post-transcriptional processes. However, molecular biology techniques are limited for microalgal species with little to no genomic information available. This represents a major gap in understanding the underlying mechanisms behind P overplus or luxury P uptake in microalgae.

The unicellular alga *Chlamydomonas reinhardtii* is considered a reference organism for microalgae research, serving as a model for other algae (Harris, 2001). This is because its reference genome has been fully sequenced, multiple strains have been identified and it has a haploid genome (Craig et al., 2023). The latter feature has led to the generation of hundreds of non-lethal mutants and consequently, a better understanding of its cell biology (Salomé and Merchant, 2019, Fauser et al., 2022). It was highlighted before that one of the main gaps in achieving cost-effective, robust and reliable MBWT constitutes the need for understanding the mechanisms of P uptake and their regulation, *Chlamydomonas reinhardtii* is seen as a suitable organism for the development of this project as a contribution to fulfilling this gap.

The morphology of *Chlamydomonas reinhardtii* is shown in **Figure 2.7**. *C. reinhardtii* is unicellular and has two flagella supported by basal bodies, which means they can move spatially in the growth media (Dutcher and O'Toole, 2016). The eyespot is responsible for photoreception, thus assisting in phototaxis of *C. reinhardtii* (Ueki et al., 2016). Cells are oval-shaped and measure ~5-10 µm, although their volume has been fitted to that of a sphere

(Hillebrand et al., 1999). *C. reinhardtii* has a cell wall, however, there are laboratory strains that carry cell wall mutations and are cell wall deficient. These mutants are viable and are widely used for genetic modifications but might be more sensitive to stressors. The chloroplast occupies two-thirds of the cell and contains the pyrenoid, where Rubisco is concentrated and has a role in the inorganic carbon concentration (Mackinder et al., 2016, Harris, 2001). Starch granules and plastoglobules are believed to contain lipids and thylakoid components (Engel et al., 2015). Acidocalcisomes are membrane-enclosed organelles that accumulate polyP in the form of granules and sequester calcium and other metals (Goodenough et al., 2019).

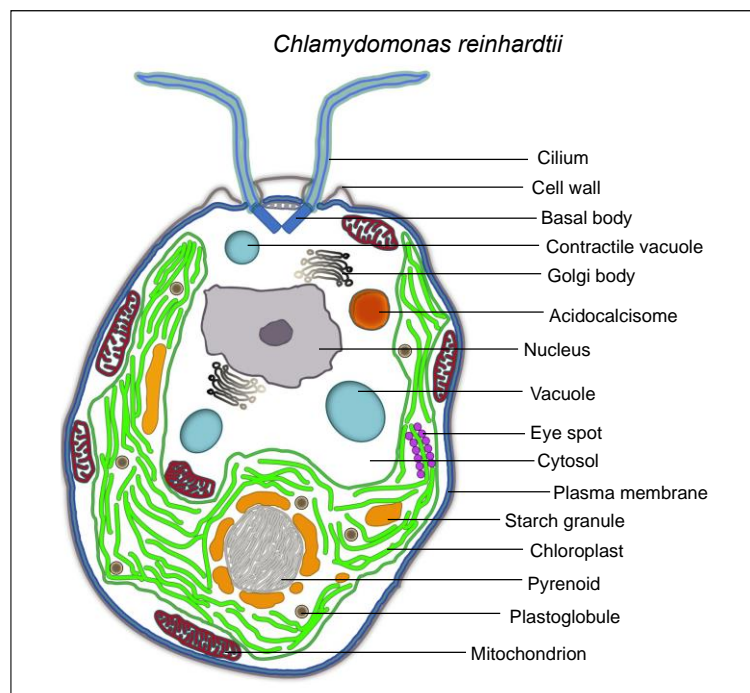


Figure 2.7 *Chlamydomonas reinhardtii* cell structure and morphology. Adapted from Harris et al. (Harris, 2001).

Despite having high efficiency in the transformation of foreign DNA into *C. reinhardtii* cells, a major obstacle is to further achieve the overall expression of transgenes from the *Chlamydomonas* nuclear genome (Neupert et al., 2009). This difficulty comes from the presence of non-conventional epigenetic suppression activities and/or a repressive chromatin structure (Schroda, 2019). The chromatin complex is found in the nucleus of eukaryotic cells and includes DNA, RNA, and protein; therefore, a repressed chromatin structure inhibits promoter accessibility and further transgene expression (Neupert et al., 2020). To overcome this problem, Neupert et al. isolated *C. reinhardtii* strains that have an enhanced capacity to accumulate fluorescence proteins expressed from nuclear transgenes. From this study, the strain called UVM4 resulted in high fluorescent protein expression levels (Neupert et al., 2009). This strain was

obtained by mutagenesis of *Chlamydomonas reinhardtii* *cw15 arg⁻* (also known as CC-4350) which is cell wall deficient and does not grow in arginine. It also harbours the *nit1* mutation, meaning that it does not grow on nitrate as a nitrogen source (Gallaher et al., 2015). The line UVM4 has been used for the high-level expression of various transgenes, which makes it suitable for the generation of over-expressor lines (Schroda, 2019).

With all the molecular techniques and information available for this species, *C. reinhardtii* can be considered a model for the study of microalgal P metabolism during its P overplus response (**Figure 2.8**). The next sections aim to provide an overall understanding of what is already known about *C. reinhardtii* P metabolism behind its P overplus response. For some of the yet unknown mechanisms, some assumptions or speculations are based on similarities of *C. reinhardtii* with yeast and vascular plants.

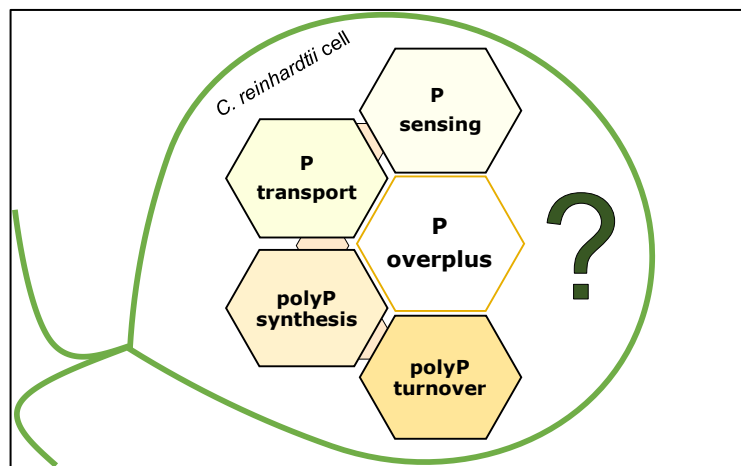


Figure 2.8 The in-cell processes behind the P overplus response of *C. reinhardtii*

2.4.1 Phosphate sensing

The first component of P metabolism, and specifically, P overplus is P sensing. *C. reinhardtii* cells need first need to sense 'low to no P' and 'high P' conditions, so the right response mechanism is activated. The most important element in P sensing uncovered so far is the phosphorus starvation response transcription factor (PSR1) (Moseley et al., 2006). PSR1 regulates Pi acquisition through the up or downregulation of various enzymes involved not only in P homeostasis but also in redox, photosynthesis and starch and lipid metabolism, among many others (Bajhaiya et al., 2016). PSR1 plays a key role in the regulation of genes involved in nutrient starvation responses. Shimogawara et al. elucidated the mechanisms that photosynthetic organisms like microalgae use to respond to P deprivation (Shimogawara et al., 1999). In their study, they isolated mutants of *C. reinhardtii* with an inefficient ability to acclimate to P limitation. Mutants that

were able to survive high concentrations of radioactive P (phosphorus radiolabelling) during starvation and mutants that were unable to accumulate extracellular phosphatase during P-replete conditions were isolated. The results highlighted the role of the PSR1 transcription factor in the response to the sense of low environmental P levels, and signal transduction of P deprivation to activate the cell machinery needed (Shimogawara et al., 1999). PSR1 is similar to the Phosphate-starvation response 1 factor (PHR1) in vascular plants (Rubio et al., 2001). These genes encode a nucleus-localised factor with a Myeloblastosis (Myb)-like DNA binding domain² (Moseley et al., 2006, Jiang et al., 2019). Although there are many similarities in the functions of both PSR1 and PHR1, there is far more understanding of the regulation of PHR1, which shows some features not associated with PSR1 function. For instance, PSR1 has glutamine-rich domains and PHR1 does not, PHR1 has sumoylation sites that are not present in PSR1 (Grossman, 2015). Interestingly while PHR1 binds to a palindrome sequence (5'-GNATATNC-3') called PHR1-binding sequence (P1BS) (Jiang et al., 2019), there is not enough proof that this sequence is ubiquitously the binding site of PSR1 in *C. reinhardtii* (assuming that it triggers its regulation by binding to DNA as PHR1) (Grossman, 2015). Bajhaiya et al. made an earlier assessment to determine if P1BS is a PSR1 binding site, however, their results are not conclusive as this sequence was found upstream of both known genes regulated or not regulated by PSR1 (Bajhaiya et al., 2016). Therefore, it is still unclear how PSR1 is activated and how it activates the P starvation response, in a phosphate-dependent way, in *C. reinhardtii*. PSR1 transcripts are upregulated under P-deprivation conditions (Moseley et al., 2006, Bajhaiya et al., 2016). When P is resupplied to P-deprived cells, to trigger a P overplus response, PSR1 transcripts are downregulated as shown in Plouviez et al. study (Plouviez et al., 2021). However, the mechanism behind PSR1 inhibition or downregulation under P-replete conditions is still unknown. In *Arabidopsis thaliana*, one of the model organisms for the study of vascular plants, the SPX1 gene was found to inhibit PHR1 in a phosphate-dependent way (Puga et al., 2014). The SPX domain is named after SYG1/Pho81/XPR1 proteins from yeasts and humans (Yao et al., 2014). SPX domains are found in many eukaryotic genes in fungi, algae, plants and humans (Wild et al., 2016). In plants, inositol pyrophosphate (IP₈) acts as the intracellular signal of P sufficiency, when it binds to the protein SPX1, which increases the affinity of the interaction of SPX1 with PHR1. SPX1/PHR1 interaction is believed to prevent PHR1 binding to DNA to activate downstream responses (Dong et al., 2019).

² MYB proteins contain from one to four conserved DNA-binding repeats and are divided into different classes based on the number of these repeats.

Suppression occurs by affecting PHR1 binding equilibrium with DNA (Qi et al., 2017). *C. reinhardtii* harbours a homolog of the SPX1 gene, but so far there is neither evidence of IP₈ binding to SPX1 nor of this complex interaction with PSR1.

2.4.2 Phosphate scavenging/sparing and acclimation

Under P-limiting or deprived conditions, *C. reinhardtii* and microalgae in general, release phosphatases and phosphodiesterases involved in the degradation of organic P compounds. Moseley et al. showed in *C. reinhardtii* that PSR1-dependent P starvation response induced an increase in the expression of genes involved in P scavenging like PHOX (alkaline pH optimum phosphatase). The PHOX protein was described by Quisel et al. study (Moseley et al., 2006, Quisel et al., 1996). Moreover, in *C. reinhardtii* purple acid phosphatases (PAPs) were identified for their role in degrading inositol hexakisphosphate (IP₆), also called phytate, when cultivated in the presence of IP₆ as the whole P source (Rivera-Solís et al., 2014). The work of Yehuda et al. highlighted the chloroplast DNA of *C. reinhardtii* as a P repository. In their study, the chloroplast polynucleotide phosphorylase (PNPase), consumes and generates phosphate in a PSR1-dependent way, and thus is believed to have a role in P recycling (Yehudai-Resheff et al., 2007). The low phosphate bleaching gene (LPB1), whose specific function remains unknown but is predicted to be localised in the chloroplast, is associated with cell survival under P-deprivation (Chang et al., 2005). Chang et al. developed *lpb1* mutants and found that, under P deprivation, *C. reinhardtii* cells had a 'usual' P starvation response (e.g. upregulation of phosphatases and P transporters), compared to the wild type. However, *lpb1* rapidly bleached and died after resuspension in P-free media, which indicates that LPB1 has a role in acclimation to P-deprived conditions (Chang et al., 2005). Furthermore, as mentioned in Section 2.3.1, under P deprivation, microalgae replace phospholipids with sulpholipids. In *C. reinhardtii*, P-deprivation led to the upregulation of a gene encoding a putative phosphodiesterase GDP1, involved in the degradation of phospholipids and the genes SQD1 and SQD3, required for sulpholipid sulfoquinovosyldiacylglycerol (SQDG) synthesis (Bajhaiya et al., 2016). This coincided with a reduction of the phospholipid phosphatidylglycerol (PG) observed by Riekhof et al. in P-deprived *C. reinhardtii* (Riekhof et al., 2003). Sanz-Luque and Grossman provided a possible explanation for the observations made by Chang et al. in the *lpb1* mutant. In *Arabidopsis*, a homolog of LPB1 encodes a UDP-glucose pyrophosphatase (UGP3), which is required for sulpholipids synthesis (Okazaki et al., 2009). If *C. reinhardtii* LPB1 function is as that of *Arabidopsis*, the *lpb1* mutant degrades PG but cannot replace them with SQDG, as it cannot

synthesise sulpholipids. PG are major components of the cell membrane and can only be replaced by sulpholipids due to their anionic character, which causes bleaching and cell death (Sanz-Luque and Grossman, 2023). The lipid remodelling regulator (LRL1) was found to assist membrane composition shift from PG to SQDG under P-deprivation (Hidayati et al., 2019).

2.4.3 Phosphate transport

Once the signal of 'high P' or 'low P' is activated, P acquisition is achieved by the upregulation of P transporters. Like in yeast, microalgae harbour genes encoding both low-affinity H^+/PO_4^{3-} (PTA) and high-affinity Na^+/PO_4^{3-} (PTB) transporters. In a PSR1-dependent way, PTA (1 and 3) and PTB transporters are downregulated and upregulated during P-deprived conditions, respectively (Bajhaiya et al., 2016, Moseley et al., 2006). PTA1 and PTA3 are hence, candidates of a low affinity uptake system under P-repleted conditions in *C. reinhardtii*. Both P uptake systems have a predicted location in the plasma membrane of *C. reinhardtii* (Wang et al., 2020).

Other genes involved in P metabolism in *C. reinhardtii* include PTC1, which is a homologue of the yeast *Saccharomyces cerevisiae* low-affinity Pi transporters PHO87, PHO90 and PHO91 (Wykoff and O'Shea, 2001). This gene was believed to resemble a low-affinity Pi transporter and to have a role in P sensing because low-affinity phosphate transporter defective mutants of *S. cerevisiae* showed a constitutive activation of the PHO regulon with no defects in Pi uptake, meaning that the mutants exhibited a de-repression of P response genes (Auesukaree et al., 2003). The Wang et al. study showed that PTC1 could have a role in P sensing, as they observed that the *ptc-1* mutant also exhibited a higher accumulation of polyP than its parental strain. Moreover, PTC1, which also has an SPX domain, is suggested to repress low P stress responses, as *ptc1-1* mutant exhibited higher transcriptional expression of PSR1, PTB2 and PHOX. Wang et al. results suggested that *C. reinhardtii* gene PTC1 is involved in phosphate transport outside the acidocalcisomes, polyP accumulation and P-deprivation-dependent signalling (Wang et al., 2021). Furthermore, *C. reinhardtii* harbours two homologues of the mitochondrial and chloroplast PHT transporters (PHT3 and PHT4, respectively), previously characterised in plants (Liu et al., 2020b, Zhu et al., 2012). A new publication from Tóth et al. confirmed that the PHT4-7 gene of *C. reinhardtii* encodes a chloroplast membrane phosphate transporter, which helps to maintain P homeostasis. The *pht4-7* mutant exhibited abnormal growth and lower tolerance to high light under P limitation, which appears to be due to ATP shortage (Tóth et al., 2023).

2.4.4 Polyphosphate synthesis

Once P is transported to the cell, it is stored in the form of polyphosphate granules. The synthesis of polyP by *C. reinhardtii* occurs through the VTC complex and is conjectured to be similar to that of yeast, as plants do not seem to synthesise polyphosphate (Lorenzo-Orts et al., 2020). In yeast, phosphate transported to the cell is needed to drive ATP synthesis which is the main donor of polyP. The terminal phosphate of ATP is transferred to the polyP chain, generating adenosine 5'-diphosphate (ADP) (Gerasimaitė and Mayer, 2016). Inositol polyphosphates are synthesised as a response to ATP fluctuation and bind to the SPX domain of the Vacuolar transporter chaperone (VTC) complex, which activates polyphosphate synthesis (Wild et al., 2016, Gerasimaite et al., 2017). In yeast, polyP synthesis occurs in the cytosolic side of the vacuolar membrane, but it is translocated to the acidocalcisomes where it elongates. This is believed to avoid the toxicity of cytosolic nascent short-chain polyP (Gerasimaitė et al., 2014). The polyP chain-length dynamics of microalgae are currently unknown, although the hypothesis is that polyP accumulation occurs similarly to that of yeast (Solovchenko et al., 2019a, Solovchenko et al., 2019b, Lobakova et al., 2023).

In *C. reinhardtii* the homologs of the polyP synthesizing enzyme VTC4 and the VTC1 protein of *S. cerevisiae* were essential for polyP synthesis and acclimation to sulphur deprivation (Aksoy et al., 2014, Sanz-Luque et al., 2020). Moreover, Cliff et al. found homologs of the VTC4 protein in 48 algal species and a model was used to predict its protein structure (Cliff et al., 2023). Interestingly, Sanz-Luque et al. uncover a new role of polyP in *C. reinhardtii* ATP homeostasis. Under nitrogen (N) and sulphur (S) deprivation, active electron flow in mitochondria and chloroplast is necessary and drives ATP synthesis. N and S deprivation cause growth arrest, and since the *vtc4-1* mutant cannot synthesise polyP, ATP levels accumulate and do not recycle to ADP. ADP is necessary to sustain the respiratory electron flow (Vermeaglio et al., 1990). Therefore, polyP synthesis from ATP helps to store excess P and maintain ATP levels, which highlights its role in maintaining electron transport in the mitochondria and chloroplast (Sanz-Luque et al., 2020). This study highlights the interaction between nitrogen, sulphur, and phosphorus metabolism in *C. reinhardtii*. For instance, it is known that S deprivation of microalgae causes the opposite effect as that of P deprivation, as sulpholipids are replaced by phospholipids (Moseley et al., 2009b). This response helps to sustain photosynthetic activity (Sato et al., 2017). The *lpb1* mutant of *C. reinhardtii* was slightly more resistant to S deprivation than to P-deprivation but still bleached. Meanwhile, deprivation of both P and S did not trigger cell

bleaching as ATP synthesis was reduced. This observation led Sanz-Luque and Grossman to suggest that PG are not as efficient as SQDGs at protecting the cells from the damage caused by S deprivation (Sanz-Luque and Grossman, 2023).

From this perspective, polyP synthesis serves as a phosphate repository, which helps to regulate ATP levels, especially during periods of nutrient deprivation (other than P). However, if polyP synthesis in *C. reinhardtii* resembles the same mechanisms observed in *S. cerevisiae*, ATP would require the synthesis of IP₃ to activate the VTC complex via its SPX domain. In *C. reinhardtii* a mutant of the Vegetative Insecticidal Protein (VIP1) protein, *vip1-1*, encodes an IP₆ kinase (Couso et al., 2016). *vip1-1* had reduced levels of the inositol pyrophosphates IP₇ and IP₈, putative precursors of VTC complex activation of polyP synthesis. The *vip1-1* mutant showed an impaired Target of Rapamycin (TOR) signalling. TOR is a protein kinase found in yeast, plants, animals and algae, and acts as an essential regulator of cell growth. This indicates that IPs synthesised by VIP are involved in cell growth regulation and signalling. Interestingly, in a later publication, Couso et al. showed that the activity of a component of TOR in *C. reinhardtii*, TORC1, was inhibited during P-deprivation in a PSR1-mediated way (Couso et al., 2020). PSR1 modulates the activity of one of the key components of the TORC1, the subunit LST8, which is required for TOR activation. Their proposed model suggests that the *psr1-1* mutant is defective in P-sensing or P-deprivation signalling, as TORC1 is an effector of PSR1 regulation. Couso et al. observed high and low levels of LST8 in the *psr1-1* mutant when grown in P-deprived and P-replete conditions, respectively (Couso et al., 2020). It is unknown whether PSR1 regulation of TORC1 influences VIP1-mediated IPs synthesis and hence, polyP synthesis. Sanz-Luque and Grossman suggest that polyP synthesis could be relevant to modulating TOR kinase activation. Their hypothesis, yet unexplored, is that the *vip1-1* mutant may have excess ATP levels. Excess ATP would be directed to other processes (related to growth), instead of IPs mediated polyP synthesis, via the TOR pathway (Sanz-Luque and Grossman, 2023).

2.4.5 Polyphosphate turnover

At this time, no proteins have been identified with a putative exopolyphosphatase function in *C. reinhardtii*. In yeast, there is more than one protein involved in polyphosphate degradation (Rao et al., 2009). The gene PPX1 encodes an exopolyphosphatase which can degrade very efficiently polyP chains from three to several hundreds (Wurst and Kornberg, 1994, Lichko et al., 2006). A polyphosphate kinase has a reversible function as it can

synthesise polyP from ATP and degrade it by transferring phosphate residues to ADP (Rao et al., 2009). Endopolyphosphatases like PPN1 in yeast, cleave long-chain polyP to generate shorter polyP chains (Lonetti et al., 2011, Lichko et al., 2010). Plouviez et al. RNA sequencing analysis of *C. reinhardtii* P overplus response led them to suggest that a gene encoding a diphosphoinositol polyphosphate phosphohydrolase (DIPP) could be involved in polyP turnover (Plouviez et al., 2021). In their subsequent proteome study, Plouviez et al. observed that only two proteins exhibited low abundance during P depletion of P-deprived *C. reinhardtii* cells: an inorganic pyrophosphatase (IPY1) and a Nudix hydrolase MutT / 8-oxo-dGTP diphosphatase (Plouviez et al., 2023a). However further research is needed to confirm their polyphosphatase activity.

2.4.6 Similarities and differences of microalgae with yeast and plants P metabolism

As discussed in the sections above, there are still many mechanisms of *C. reinhardtii* and microalgae overall P metabolism that are unknown to us. Microalgae are photosynthetic microorganisms, likewise cyanobacteria. Cyanobacteria are prokaryotes and have a similar P metabolism to that of other PAOs like *Escherichia coli* (Dyhrman, 2016). However, an example of a shared response to P-deprivation in cyanobacteria and microalgae is the replacement of phospholipids with sulpholipids (Dyhrman, 2016, Van Mooy et al., 2009, Reistetter et al., 2013). Nonetheless, microalgae are eukaryotes as they have both a mitochondrion and a chloroplast. It seems that the P metabolism of microalgae may be an intermediate (or hybrid) between that of yeasts and plants. *C. reinhardtii* for instance has been named 'the green yeast' (Rochaix, 1995). In terms of P metabolism, *C. reinhardtii* harbours some homologs with a putative function similar to the ones characterised in yeast for polyphosphate synthesis (see section 2.4.4). At the same time, *C. reinhardtii* is considered an organism for the study of plants, due to its similarities to the model *A. thaliana* (Gutman and Niyogi, 2004). P homeostasis regulation in *C. reinhardtii* may be closer to that of plants like *A. thaliana* as both harbour P deprivation response transcription factors (PSR1/PHR1). Since *C. reinhardtii* harbours a homolog of the SPX1 protein, P signalling could potentially be regulated via SPX1 binding to PSR1, likewise in *A. thaliana* (see section 2.4.1). Interestingly, SPX domains have a major role in yeast polyP synthesis, and homologs of the VTC complex in *C. reinhardtii* also have SPX domains. Therefore, research is needed to uncover the unexplored regulation of P metabolism (especially P signalling and polyP synthesis) via SPX domains, in *C. reinhardtii*. Lastly, researchers should

keep an open mind to the possibility that *C. reinhardtii* and microalgae in general, could have unique features of their P metabolism that are not necessarily related to yeast or plants.

2.5 Research gaps

Based on the literature reviewed, it was found that P overplus responses of microalgae are still far from being applied for the improvement of P control and recovery from wastewater. The first gaps found are (1) the imprecision in the use or knowledge of the concepts of luxury P uptake and P overplus in microalgae and (2) the lack of appropriate analytical techniques of microalgal polyphosphates. No biological questions regarding these two phenomena can be answered without the development of reproducible analytical techniques for polyP identification and characterisation. Polyphosphate is the direct measurement of luxury P uptake and P overplus. Once we have developed clear and robust analysis techniques of polyP in microalgae, we can proceed to study this phenomenon in a more reproducible way. For instance, the knowledge regarding how P-deprivation and not its time length, affect P overplus will drive more focus towards the physiological aspects indicating that microalgae are 'ready' to perform their best P overplus response. Moreover, wastewater is a fluctuating environment where P is present along with all other nutrients. Therefore, it is important to understand how nutrients other than P affect microalgal P overplus response. Understanding how both factors, P-deprivation, and nutrient availability, will contribute to the constitution of reliable design parameters of P overplus-based recovery systems in MBWTs.

Lastly, the role of *C. reinhardtii* PSR1 in regulating the response to P-deprivation has been widely assessed. P overplus depends on P-deprivation and yet, no direct connection has been made to the role of PSR1 in *C. reinhardtii* P overplus. Thus, assessing how this transcription factor affects polyP accumulation after P-deprived cells are repleted with P, will be an important contribution to the knowledge of *C. reinhardtii* P metabolism. This will drive the robust manipulation of microalgal P overplus for biological P recovery from wastewater.

Chapter 3 Materials and Methods

This chapter contains all relevant information regarding the research methodology used throughout the project, for the cultivation of *Chlamydomonas reinhardtii* for maintenance, and for the course of experiments, sample collection and treatment and analyses. The sections in this chapter are split into 1) The list of strains used, 2) Cultivation media and solutions used for each experimental treatment, 3) Microalgal cultivation conditions, 4) Culture analyses, 5) Media analyses and 6) Biomass analyses. Unless otherwise stated, all methods were conducted at the Faculty of Biological Sciences of the University of Leeds.

3.1 *Chlamydomonas reinhardtii* strains

The strains of *Chlamydomonas reinhardtii* used throughout the project are listed in **Table 3.1**. Most of the strains were purchased from the Chlamydomonas Resource Center, University of Minnesota, USA. The strain UVM4 was provided by Ralph Bock (Neupert et al., 2009). The genetically modified strains 8-27, 8-42 and 8-2 were designed and developed by Dr Lili Chu (Slocombe et al., 2023). The number of additional copies of the construct inserted in the genome (if larger than one), is yet to be determined (**Figure 3.1**). For all the experiments, three biological replicates of the designated strains were used.

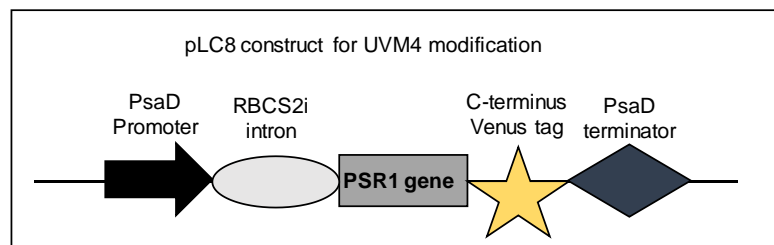











Figure 3.1 PSR1 construct in *C. reinhardtii* 8-27, 8-42 and 8-2 strains. The transgene PSR1 expression is controlled by the light-sensitive promoter PsalD. The RBCS2i intron enhances expression. The C-terminus Venus tag is used for the detection of the transgene PSR1. The PsalD terminator indicates the end of transcription for the construct.

Table 3.1 *Chlamydomonas reinhardtii* strains used throughout this project

Strain	Phenotype	Description
 CC-1690	'Wild type' mt+	Also referred to as 21gr (Sager, 1955)
 CC-125	'Wild type' mt+ <i>nit1 nit2</i>	Also referred to as 137c (Davies and Plaskitt, 1971)
 CC-5325	Thinner cell wall (<i>cw15</i> mt-)	Also referred to as CC-4533 or CMJ030 (Zhang et al., 2014). Background strain of the Chlamydomonas CliP mutant Library
 CC-4350	Cell wall deficient <i>cw15 nit1 nit2 arg7-8</i> mt+	Also referred as [Matagne 302] or CC-4350 <i>cw15-302</i> mt+ (Fernández and Matagne, 1984)
 UVM4	Cell wall deficient <i>cw15</i>	UV mutated strain used for high transgene expression levels (CC-4350 background)
 8-27	Cell wall deficient <i>cw15</i>	PSR1 overexpression strain (UVM4 background)
 8-42	Cell wall deficient <i>cw15</i>	PSR1 overexpression strain (UVM4 background)
 8-2	Cell wall deficient <i>cw15</i>	PSR1 overexpression strain (UVM4 background)
 <i>psr1-1</i>	mt-	CC-4267 <i>psr1-1</i> (CC-125 background), derived from original <i>psr1-1 cw15</i> strain (Shimogawara et al., 1999)

3.2 Cultivation media and solutions

The microalgal culture was in one of the following culture media alone or supplemented with the solutions listed below. Throughout the project, all growth media and solutions were prepared in distilled-deionised water (ddH₂O) and sterilised by autoclaving at 121°C for a minimum of 20 min before use.

3.2.1 Tris Acetate Phosphate (TAP) media

Tris Acetate Phosphate media (TAP) was prepared according to the Chlamydomonas Resource Center (University of Minnesota, USA). This media provides all nutrients in adequate balance to sustain biomass growth. The Hutner's trace element solution was replaced with a list of trace element solutions following Kropat et al. recipe, without selenium (Kropat et al., 2011). The recipe is listed in **Table 3.2**.

Table 3.2 Tris Acetate Phosphate (TAP) recipe

Preliminary stock 1	EDTA-Na₂ (125 mM)	- 13.959 g EDTA-Na₂ in approx. 250 mL dH₂O - Make to pH 8.0 using KOH (approx. 1.7 g; trace element grade) - Fill to 300 mL total with dH₂O
Preliminary stock 2	(NH ₄) ₆ Mo ₇ O ₂₄ (285 μM)	- 0.088 g (NH ₄) ₆ Mo ₇ O ₂₄ .4H ₂ O in dH ₂ O
Trace Element 1 (TE1)	EDTA-Na ₂ (25 mM)	50 mL Pre1 made up to 250 mL with dH ₂ O
Trace Element 2 (TE2)	(NH ₄) ₆ Mo ₇ O ₂₄ (285 μM)	- 25 mL Pre2 made up to 250 mL with dH ₂ O
Trace Element 3 (TE3)	Zn.EDTA (2.5 mM)	- 0.18 g ZnSO ₄ .7H ₂ O - 5.5 mL Pre1 - Make up to 250 mL with dH ₂ O
Trace Element 4 (TE4)	Mn.EDTA (6 mM)	- 0.297 g MnCl ₂ .4H ₂ O - 12 mL Pre1 - Make up to 250 mL with dH ₂ O
Trace Element 5 (TE5)	Fe.EDTA (20 mM)	2.05 g EDTA-Na ₂ - 0.58 g Na ₂ CO ₃ - Dissolve in approx. 150 mL dH ₂ O - 1.35 g FeCl ₃ .6H ₂ O - Make up to 250 mL with dH ₂ O
Trace Element 6 (TE6)	Cu.EDTA (2 mM)	- 0.085 g CuCl ₂ .2H ₂ O - 4 mL Pre1 - Make up to 250 mL with dH ₂ O
Potassium Phosphate (KPO₄)	Phosphate Buffer II	- 10.8 g K ₂ HPO ₄ - 5.6 g KH ₂ PO ₄ - Make up to 100 mL with dH ₂ O

A	Solution A	- 20 g NH ₄ Cl - 5 g MgSO ₄ .7H ₂ O - 2.5 g CaCl ₂ .2H ₂ O - Make up to 500 mL with dH ₂ O
Tris	Tris base – Trizma (1 M)	- 60.57 g Trizma - Make up to 500 mL with dH ₂ O (Buffers to pH 8.5)
TAP media	Add the following solutions to approx. 750 ml dH ₂ O - 20 mL Tris	
	- 1.0 mL KPO ₄	
	- 10.0 mL A	
	- 20.0 mL Tris	
	- 1.0 mL TE1	
	- 1.0 mL TE2	
	- 1.0 mL TE3	
	- 1.0 mL TE4	
	- 1.0 mL TE5	
	- 1.0 mL TE6	
	- 1.0 mL Glacial Acetic Acid	
	- Adjust to pH 7.0 using HCl/KOH - Makeup to 1 L with dH ₂ O	

3.2.2 Tris Acetate (TA) media

Tris Acetate media (TA) was used to trigger phosphorus starvation in *Chlamydomonas* strains. Thus, TA is prepared with the same recipe as TAP media, replacing the KPO₄ solution with 1 mL/L media of a 1.65M KCl solution, to keep potassium concentration the same as in TAP media.

3.2.3 Media supplements

TAP agar was supplemented with paromomycin (10µg/mL), for the transgenic strains 8-27, 8-42 and 8-2 to maintain the transgene in these strains.

Paromomycin was not used in liquid cultures during the experiments to prevent effects on biomass growth rates. To supply paromomycin, TAP media with agar was melted in a microwave and let to cool under 50°C of temperature, before adding paromomycin. The media was then poured into 30 mL universal tubes and left to solidify.

Arginine was supplied to TAP agar and liquid (before autoclaving) for the cultures of the arginine auxotrophic strain CC-4350 up to a concentration of 100 $\mu\text{g/ml}$. Arginine was also supplied to TAP or TA media for cultures of all strains (CC-1690, CC-125 and CC-5325), that were used in the same experiment with CC-4350 to keep the culture conditions equivalent for all the strains.

3.3 Microalgal cultivation

Inoculation and manipulation of microalgal cultures (agar or liquid) always took place within a laminar flow cabinet to sustain axenic conditions. For cultivation, an AG230 (Photo Systems Instruments, Czech Republic) was used. The cultures were kept at 25 °C and constant light at 100 $\mu\text{mol m}^{-2} \text{s}^{-1}$ of intensity. The liquid cultures were shaken at 160 rpm for all experiments. No additional CO_2 was provided apart from atmospheric CO_2 .

3.3.1 Long-term storage

Chlamydomonas reinhardtii strains were kept from 6-8 weeks on TAP Agar slopes. In some cases supplemented as stated in section 3.2.3.

3.3.2 Starter cultures

Liquid cultures were inoculated from agar cultures in 30 mL universal tubes containing 15 mL of TAP media. These cultures (referred to as Starter cultures) were left under controlled conditions (see above)

3.3.3 Inoculation

Inoculation was done by transferring a volume of cells from the starter culture to fresh media up to an initial optical density of $\text{OD}_{750\text{nm}}=0.005$.

3.3.4 Phosphorus deprivation

$\text{OD}_{750\text{nm}} 1.0$ cultures ($\text{OD}_{1.0}$) were harvested by centrifugation at 3000g for 10 min. The supernatant was discarded and the biomass was washed twice with fresh TA media (supplemented with arginine 10 $\mu\text{g/mL}$), before its final resuspension in fresh TA media (supplemented with arginine 10 $\mu\text{g/ mL}$).

3.3.5 Phosphorus repletion

Phosphate-deprived cultures were supplied with phosphorus as either 'P¹' only or together with all other nutrients in TAP media, both up to 1 mM P.

¹ Phosphate (PO_4) is referred throughout the project as 'P'.

In one experiment, phosphorus repletion with all nutrients together with P was done by harvesting centrifuged biomass (3000 x g for 10 min), discarding old media and resuspending in fresh TAP media, whereas 'P' only was fed as a calculated volume from the KPO_4 solution.

In another experiment, to avoid the effect of centrifugation, phosphorus repletion together with all nutrients was provided as a calculated volume from the KPO_4 solution to give a final concentration of 1mM and all other nutrients were supplied with a 5xTA solution to a known volume of culture (1:5 v/v). 'P' only repletion was supplied by adding a calculated volume from the KPO_4 solution and ddH₂O was added to make the same 1:5 dilution as for the TAP-supplemented cultures with the same final concentration of P (1mM).

3.3.6 Monitoring Bacterial Contamination

Although axenic practices were kept during all experiments, contamination of microalgal cultures at the end of each experiment was checked by plating 100 μ l of culture on Luria Bertani (LB) petri plates and incubated at room temperature, 30°C and 37°C, temperature to check for fungi, yeast or bacterial contamination, respectively. LB media provides suitable conditions for bacteria and yeast, but not for microalgae, thus it can be used as a tool to detect contamination of microalgal cultures.

Luria Bertani media composition is detailed below for 1 L (agar 15 g/L):

1. 10 g Tryptone
2. 5 g Yeast Extract
3. 10 g Sodium Chloride (NaCl)

3.4 Culture analysis

Cultivation during all experiments was monitored at the beginning of the sampling sessions using a Jenway 6715 UV/Vis spectrophotometer to monitor optical density. Spectrophotometry was also used to measure absorbances to calculate chlorophyll concentration. Growth was also measured in the culture by cell counting.

3.4.1 Optical Density

Optical density at an absorbance of 750nm was measured to monitor biomass growth in 1.5 mL polystyrene semi-micro cuvettes. Microalgal culture samples were diluted with ddH₂O to maintain the absorbance reading under 1.0 and were mixed before taking the reading in the spectrophotometer.

3.4.2 Cell counting and size

Cell counts were collected from fixed culture samples. Cells diluted between 10-50x and were fixed with a 5% glutaraldehyde and 10% formaldehyde solution in ddH₂O. 10 µL of fixed cells was loaded in duplicates on a Neubauer chamber and left for 45 seconds to settle. Cells were counted using an Olympus CK2 microscope with a CDPlan 40/0.6 160/0-2 Objective Len. Cell numbers were collected with a mechanical counter.

Cell concentration was calculated as follows:

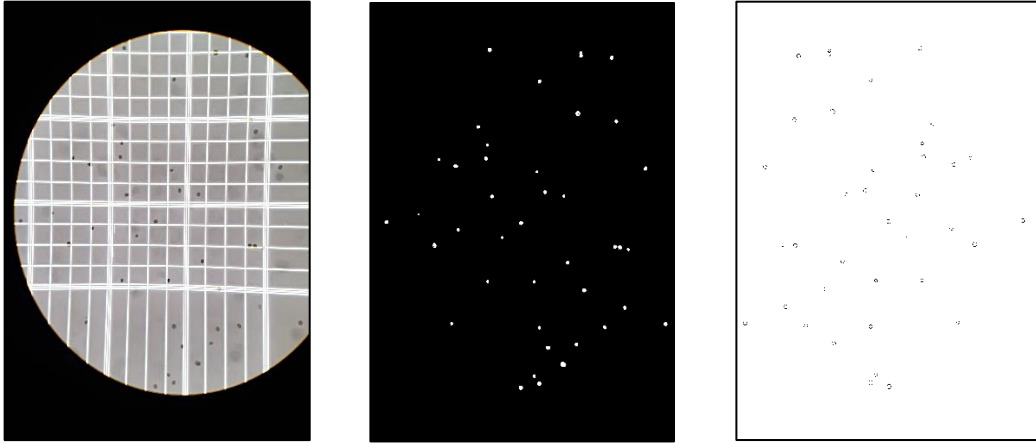
$$\text{Eq 1 Cell concentration} \left(10^6 \frac{\text{cells}}{\text{mL}} \right) = \frac{\text{average number of cells (top,bottom grid)}}{\text{volume of the grid}} = \frac{\text{number of cells} \cdot 10^{-6}}{1 \text{ mm} \cdot 1 \text{ mm} \cdot 0.1 \text{ mm}} = \frac{\text{number of cells} \cdot 10^{-6}}{10^4 \text{ mL}}$$

Cell size from cell counting pictures was estimated from photographs taken at the moment of cell number collection, using an iPhone 11 camera (12-megapixel wide lens and 12-megapixel ultra-wide lens), to estimate the cell size.

Fiji (ImageJ) software was used for the image processing of the photographs. The settings were used as shown in **Table 3.3**:

Table 3.3 Cell size estimates from cell counting pictures, using Fiji software.

Preparation	Processing	Analysing
Under the 'Analyze' tab	Under the 'Process' tab	Under the 'Analyze' tab
Set scale, using Neubauer chamber scale in µm	1. 'Binary' – 'Make Binary'	4. 'Analyze particles' to identify the cells within the expected range in µm ² and with a circularity not lower than 80%
Under the 'Process' tab, 'Enhance contrast' of cells against the background and then 'Subtract Background'	2. 'Noise' – 'Remove outliers' to get rid of traces of background	
	3. 'Binary' - 'Watershed'	



Cell volume was calculated as reported previously (Hillebrand et al., 1999). According to this study, *Chlamydomonas reinhardtii* cell volume resembles that of a sphere:

Eq 2

$$\text{Cell volume } (\mu\text{m}^3) = \frac{\pi}{6} \text{ dia}^3$$

Where,

π , is the pi coefficient

dia , is the measured diameter of the cell

3.4.3 Chlorophyll concentration

Chlorophyll quantification was calculated after solvent extraction. 0.1 – 1.0 mL of microalgal culture, according to the growth phase (0.1 mL for stationary cultures, ~0.2-0.5 mL for exponential growth cultures and 1.0 mL for early exponential growth cultures) was collected. The volume of the sample was controlled to avoid absorbance readings over the value of 1.0 for chlorophyll determination.

The collected sample was centrifuged at maximum speed (12000 g for 10 min) and the supernatant was discarded. The biomass pellet was resuspended in 1.0 mL of 80% (v/v) acetone / 20% (v/v) methanol by vortexing thoroughly, before centrifugation at maximum speed for 5 min, to remove all cellular debris. The supernatant was transferred to a glass cuvette and absorbances were obtained simultaneously at 646.6nm, 663.6nm and 750nm. Acetone and methanol solution were used as a blank to contrast the sample readings.

Chlorophyll concentration was determined as reported previously (Porra et al., 1989). Abs stands for the absorbance readings at the specific spectrum length (nm) minus the absorbance at 750nm:

Eq 3

$$Chl\ a\ \left(\frac{\mu g}{ml}\right) = \frac{12.25\ Abs_{663.6nm} - 2.55\ Abs_{646.6nm}}{sample\ volume\ (ml)}$$

Eq 4

$$Chl\ b\ \left(\frac{\mu g}{ml}\right) = \frac{21.31\ Abs_{646.6nm} - 4.91\ Abs_{663.6nm}}{samples\ volume\ (ml)}$$

Eq 5

$$Chl\ a + b\ \left(\frac{\mu g}{ml}\right) = \frac{17.76\ Abs_{646.6nm} + 7.34\ Abs_{663nm}}{sample\ volume\ (ml)}$$

3.4.4 DAPI staining and Confocal microscopy

DAPI (4',6-diamidino-2-phenylindole) is a fluorescent stain used commonly to stain DNA in live or fixed cells, which can also be used to stain polyphosphate granules within the cells. A culture sample volume of 200 μ L was taken, 2 μ L of 1 mM DAPI stain (Sigma) was added and left incubating in the dark for 4 h. Cells were fixed for 20 min by adding 4 μ L of 25% Glutaraldehyde (Sigma), and then flash frozen with liquid nitrogen at stored at -70°C.

30-50x cells of *C. reinhardtii* were visualised in a Zeiss LSM880 Upright Confocal Microscope (Carl Zeiss) with a Plan-Apochromat 63x/1.4 Oil DIC M27 objective. The filter for excitation (Ex) was Ex 405nm and emission (Em) was DAPI-DNA Em 420-475nm and DAPI-polyP Em 535-575nm.

6-8 z-stacks were taken for each cell. Image processing on software Fiji (Image J) was used to do a Z-projection of the z-stacks into one 2D image with all the polyphosphate granules (Schindelin et al., 2012). This software was also used to collect the diameter of the cells to calculate the cell volume as mentioned in section 3.4.2.

3.5 Media analysis

Culture samples were collected and biomass was harvested by centrifugation (3000g for 10 min). The supernatant (the media) was sterile filtered with a syringe filter system (0.22 μ m pore size) and stored in sterile 7 mL universal tubes at -20°C. Sterile filtration prevents further assimilation of nutrients by microalgae cells, which are retained in the filter, thus allowing to determine the concentration of nutrients at the specific time point when the sample was collected.

The media was used to obtain pH measurements and the concentration of both anion and cations.

3.5.1 pH

A Mettler Toledo FiveEasy™ pH meter was used to monitor the pH of filtered media samples.

3.5.2 Phosphate concentration in the media

Phosphate concentration in the media was obtained using the ascorbic acid blue molybdate assay, adapted from previously reported protocols (Koistinen et al., 2020) (Pierzynski, 2000). Before the tests all glassware was acid washed in 0.1M HCl overnight, the next day the glassware was washed in ddH₂O and left to dry overnight before use.

The following solutions (1-5) were prepared:

1. 2.5 M H₂SO₄ in ddH₂O
2. 2.75 g L⁻¹ Potassium antimonyl tartarate in ddH₂O
3. 40 g L⁻¹ Ammonium molybdate tetrahydrate in ddH₂O
4. 0.1 M Ascorbic acid in ddH₂O (Opaque bottle) in ddH₂O
5. 5 g L⁻¹ Phenolphthalein dissolved in ethanol 50% of total volume and topped up with ddH₂O

All reagents were kept at 4°C except for the sulphuric acid (H₂SO₄).

The assay began with frozen filtered supernatants being left to thaw at room temperature and then diluted between 1-100x in ddH₂O in 1.5 mL polystyrene cuvettes. To avoid the effect of high pH, phenolphthalein (solution 5) was used as an indicator. One drop of phenolphthalein (approx. 10 µl) was added to each cuvette, if a pink colour was formed, drops of sulphuric acid (solution 1) were added until the colour disappeared. Any additional volume added between solutions 1 and 5 was accounted for in the final calculation as a dilution factor.

A combined reagent was freshly prepared by mixing the solutions in the following order, at the beginning of each assay:

1. 500 mL L⁻¹ solution 1
2. 50 mL L⁻¹ solution 2
3. 150 mL L⁻¹ solution 3
4. 300 mL L⁻¹ solution 4

160 µL of a combined reagent (stable for 4 h) was added to 1 mL of diluted, pH-adjusted sample, tapped gently and left for 20 min before taking the absorbance reading at 880nm in a spectrophotometer (see section 3.4) against ddH₂O as a

blank. For every 10 samples, the blank absorbance reading was taken and adjusted once again at 0 for accuracy.

For each assay, the absorbance at 880nm of a calibration curve (0-24 $\mu\text{M PO}_4\text{-P}$) after 20 min of contact with the combined reagent, was taken. The calibration curve was made from a solution of 1 M KH_2PO_4 in ddH_2O .

A linear regression of the calibration curve (Abs880nm vs $\mu\text{M PO}_4$), was used to calculate the PO_4 concentration, which was then expressed as $\text{mg PO}_4\text{-P/L}^2$.

3.5.3 Ion Chromatography (IC-MS)

The concentration of anion and cations in the filtered media was determined by Ion Chromatography (IC-MS) using a Metrohm 850 Professional IC, with an 896 Detector at the Environmental Engineering Laboratory (School of Civil Engineering, University of Leeds) by the laboratory technicians Dr. David Elliot, Miss Emma Tidswell and Mr Morgan McGowan. The samples were diluted 10x before analysis, using ddH_2O).

For the cations, a Metrosep C4-100/4.0 column (kept at a constant temperature of 30°C) was used. 10 μL of sample was loaded with an injector at a flow rate of 0.9 ml/min with an injector pump (20 MPa of pressure), through the column.

For the anions, a Metrosep A Supp 5-150/4.0 column (kept at a constant temperature of 30°C) was used together with an RP2 Guard Column. 20 μL of samples were loaded with an injector at a flow rate of 0.7 ml/min with an injector pump (15 MPa of pressure).

The Metrohm IC used has a carousel (Metrohm 856 Professional Sample Processor) that allows to run 50 samples automatically, and organises the data in an Excel file with the concentrations measured for both anion and cations.

3.6 Biomass analysis

Fresh microalgal biomass samples were collected after phase separation of microalgal culture by centrifugation (3000g for 10 min). After removing the supernatant (media), the fresh pellets were resuspended in ddH_2O and transferred to a 1.5 mL microcentrifuge tube. Then, the pellets (for Biomass concentration, Elemental analysis (CHNS) and Polyphosphate) were washed twice with ddH_2O to remove any media components attached to the microalgal cell, before being flash frozen with liquid nitrogen and stored at -70°C . Fresh

² Throughout this project 'mg $\text{PO}_4\text{-P/L}$ ' refers to the concentration of phosphate obtained by colorimetry or IC-MS assays, expressed as P (30.97 g/mol). Similarly, mg $\text{NH}_4\text{-N/L}$ and mg $\text{SO}_4\text{-S/L}$, correspond to the IC-MS results expressed as N (14.01g/mol) and S (32.06 g/mol), respectively.

biomass samples collected for Western Blot analysis were used for protein extraction before being flash-frozen with liquid nitrogen and stored at -70°C.

3.6.1 Biomass concentration

Throughout the project, the volume of culture sample (mL) collected to determine biomass concentration was equivalent to 5/OD750nm. This ensured the dry biomass was kept in the range of 1.0-2.5 mg, which assists in the standardisation of the protocol. Before each experiment, empty pre-labelled 1.5 mL microcentrifuge tubes were weighed before sample collection.

Depending on the sample volume calculated, the samples were collected in 15 mL falcon tubes and transferred to pre-weighed 1.5 mL microcentrifuge tubes or directly into the pre-weighed 1.5 mL microcentrifuge tubes.

Biomass concentration (g dry weight/L) was obtained by drying fresh biomass pellets to collect their dry weight (dw). Fresh biomass pellets, were dried under vacuum in a SpeedVac Plus (SC210A – Thermo Savant Instruments) overnight. The weight was collected from the dry pellets before a second drying period (overnight) was conducted. The latter period of drying ensured no difference in the weight collected. Biomass concentration was calculated as follows:

Eq 6

$$\text{Biomass concentration} \left(g \frac{dw}{L} \right) = \frac{(\text{Tube} + \text{Dry pellet weight}) \text{ mg} - (\text{Pre weighed tube}) \text{ mg}}{\text{Volume of sample (mL)}}$$

3.6.2 Total Phosphate content in the biomass

Total Phosphate content in the biomass was measured from the dry pellets collected for biomass concentration (section **above**). The dry pellets were digested to release from the biomass, all inorganic phosphorus compounds and break all organic phosphorus compounds into free PO₄.

Complete digestion of dry biomass occurred after transferring 200 µL of oxidizing reagent to the 1.5 mL tubes containing the dry pellets. The oxidizing reagent is composed of 0.675 M H₂SO₄ and 50 g/L potassium persulfate (K₂S₂O₈) in ddH₂O. Digestion was conducted at 100°C for 60 minutes in a dry bath (Cole-Parmer BH-200). After this period, free PO₄ was released into the liquid phase. The samples were left to cool, diluted in ddH₂O, and assayed for PO₄-P concentration as detailed in section **3.5.2**.

Total phosphate content in the biomass (%PO₄-P,dw) was calculated as follows:

Eq 7

$$\begin{aligned} & \text{Total } PO_4 \text{ content in biomass } (\%PO_4 - P, dw) \\ &= \frac{\frac{mg PO_4 - P}{L} * 200 \mu l * 10^{-6} L}{mg dw} * 100\% \end{aligned}$$

Where

$\frac{mg PO_4 - P}{L}$, is the phosphate concentration measured from the digested pellets

$200 \mu l * 10^{-6} L$, is the volume of oxidizing reagent added to the dry pellet calculated in L

$mg dw$, is the dry weight of the sample collected in section **3.6.1**

3.6.3 Elemental analysis (CHNS)

Throughout the project, the volume of culture sample collected for Elemental analysis (CHNS) corresponded to 40/OD750nm. This practice allowed to collection of a minimum of 8-10 mg dw required for this analysis. The samples were collected in 15 mL or 50 mL falcon tubes and transferred to 1.5 mL microcentrifuge tubes. The fresh biomass pellets were washed, stored and dried as explained in section **3.6.1**. The dry samples were left in a desiccator before 2-3 mg of dry biomass sample was encapsulated in tin capsules, in duplicates.

The Elemental analysis (CHNS) was conducted at the Analytical Laboratory (School of Chemical and Process Engineering, University of Leeds) by the laboratory manager Dr. Adrian Cunliffe and the analytical technician Karine Alves Thorne. CHNS content in the dry biomass capsules was obtained using a Thermo Scientific Flash EA2000 organic elemental analyser. The capsules were fed in the furnace (900°C) under helium (BOC CP Grade). To induce combustion of the samples, oxygen (BOC Grade N5.0) was supplied for 5 s. The elemental analyser was calibrated with oatmeal and BBTOT standards (of known CHNS content). Quality control samples of barley flour (Elemental Microanalysis Ltd.) were used in duplicates to ensure the proper functioning of the instrument. The CHNS content is expressed separately for each element as %, dw.

3.6.4 Polyphosphate analysis

Polyphosphate analysis protocols used in *Chlamydomonas reinhardtii* were adapted from those developed in the yeast *Saccharomyces cerevisiae* with the training, help and guidance of Professor Adolfo Saiardi (Laboratory of Molecular and Cell Biology, UCL). These methods were used for the extraction of polyP from microalgal cells, its quantification and detection.

Throughout this project, the culture sample volume collected for polyP extraction corresponds to $10/\text{OD}_{750\text{nm}}$. This practice allowed for the protocol to be standardised in the laboratory. The collected sample was treated and stored as mentioned at the beginning of section 3.6.

3.6.4.1 RNA/polyP extraction

The phenol/chloroform method, used commonly for RNA extraction was used to extract polyP, due to the similarity of the polyP molecule to that of nucleic acids (RNA). The following reagents were prepared before the assay:

1. LETS buffer (0.1M LiCl, 10 mM Tris-HCl pH 8.0, 10 mM EDTA, 0.5% SDS)
2. Acidic phenol (pH 4.3-4.5) (Thistle Scientific Ltd)
3. Acid-washed glass beads (425-600 μm) (Sigma)
4. Chloroform (Sigma)
5. Pure ethanol pre-chilled at -20°C (VWR chemicals)
6. DEPC-water (1ml of Diethyl Pyrocarbonate in 1 L of ddH₂O, autoclaved)

Frozen biomass pellets were left to thaw on ice for approx. 15 min before 300 μL of LETS buffer were added to the sample tubes. The cells were resuspended completely by vortexing. Then 300 μL of acidic phenol and the equivalent of 300 μL acid-washed glass beads were added. The mixture (resuspended cells, acidic phenol and glass beads) was vortexed vigorously for 6 min using a TissueLyser LT (QIAGEN) and centrifuged at 3000g for 3 min. The supernatant was transferred to a new 1.5 mL microcentrifuge tube and 300 μL of chloroform was added. The samples were vortexed thoroughly for 15 s and centrifuged at 3000g for 3 min. The supernatant was transferred to a new 1.5 mL microcentrifuge tube and 750 μL of pre-chilled pure ethanol were added and mixed by flipping the tubes manually. The mixture (sample in pure ethanol) was kept at -20°C overnight to allow precipitation of RNA/polyP.

Precipitated samples were centrifuged at maximum speed (13000g for 10min). The supernatant was discarded and the tubes were left at 37°C for 10 min in a dry batch, to eliminate any residual ethanol. RNA/polyP was resuspended in

100 μL of DEPC-water, vortexed gently and left at 37°C for a further 10 min. The RNA concentration ($\mu\text{g}/\mu\text{L}$) was then measured using an ND-1000 Nanodrop. The extracted RNA/polyP samples were stored at -20°C.

RNA content in the biomass was expressed as %RNA,dw as follows:

Eq 8

$$\begin{aligned} & \text{RNA content in biomass (\%RNA, dw)} \\ &= \frac{\text{RNA concentration sample } \left(\frac{\mu\text{g RNA}}{\mu\text{L}} \right) * 100\mu\text{L} * 1000^{-1}\text{mg RNA}}{\text{Biomass concentration sample } \left(\frac{\text{mg dw}}{\text{mL}} \right) * \text{volume of sample (mL)}} * 100\% \end{aligned}$$

Where,

$\frac{\mu\text{g RNA}}{\mu\text{L}}$, is RNA concentration of the sample measured

100 μL , is the volume of DEPC water used to dilute precipitated RNA

1000⁻¹mg RNA, changes μg to mg of RNA

$\frac{\text{mg dw}}{\text{mL}}$, is the biomass concentration of the sample

volume of sample (mL), is the volume of sample taken, calculated as 10/OD750nm

3.6.4.2 Quantification

Quantification of polyphosphate was achieved by digestion of extracted RNA/polyP with a recombinant exopolyphosphatase (Ppx1) kindly provided by Professor Adolfo Saiardi (LMCB – UCL). This enzyme, endogenous from the yeast *Saccharomyces cerevisiae*, is responsible for degrading the Polyphosphate into free phosphate, which can be further quantified using colourimetry assays.

Digestion of RNA/polyP with Ppx1 was conducted in 1.5 mL microcentrifuge tubes at 37°C for 1 h, using a dry bath (Cole-Parmer BH-200). The reaction was prepared as follows:

5. 2 μg RNA
6. 2 μL Buffer 10X
7. 1 μL Ppx1 (Concentration ~ 100 ng/ μL)
8. Sterile ddH₂O up to 20 μL

The Buffer 10X (200 mM HEPES pH 6.8, 1 M KCl, 60 mM MgCl₂ and 10 mM DTT) was prepared in aliquots and kept at -20°C before analysis. The

enzymatic reaction was terminated by placing the reaction tubes on ice and adding 1 μL of 0.5 M EDTA pH 8.0.

Digested samples were assayed for their PO_4 concentration, using the malachite green assay. The following reagents were prepared before the assay:

- Malachite green solution
0.127g Malachite green oxalate (Alfa Aesar)
1.4 g polyvinyl alcohol (Alfa Aesar)
400 mL ddH₂O, stirred overnight and filtered using Whatman 1 filter paper
Solution kept at room temperature

- Molybdate solution
13.84 mg Ammonium molybdate tetrahydrate (BRAND)
44.8 mL concentrated H₂SO₄
ddH₂O up to 400 ml
Solution stored in the dark at 4°C

- Combined Molybdate/Malachite solution was prepared fresh before each assay (for 96 well, 8.6ml Molybdate solution and 6.4 mL Malachite solution)

1 μL of digested sample and 1 μL of undigested RNA sample were loaded, separately, in triplicates on a 96-well plate. Both samples (digested and undigested) were diluted 100x in ddH₂O. 100 μL of combined Molybdate/Malachite solution were loaded on each sample. The colour reaction takes place immediately (see **Figure 3.2**). Absorbance at 595nm \pm 5nm was read using a POLARstar OPTIMA plate reader (BMG Labtech) after the plates were shaken for 5s to further mix the sample with the combined solution. The absorbance readings were compared with those obtained from a calibration curve tested for each plate. The calibration curve was made from a solution of 1 M KH₂PO₄ in ddH₂O. The phosphate concentration ($\mu\text{M PO}_4\text{-P}$) was calculated using a polynomial regression (2 degrees) after plotting the calibration curve against the Abs660nm.

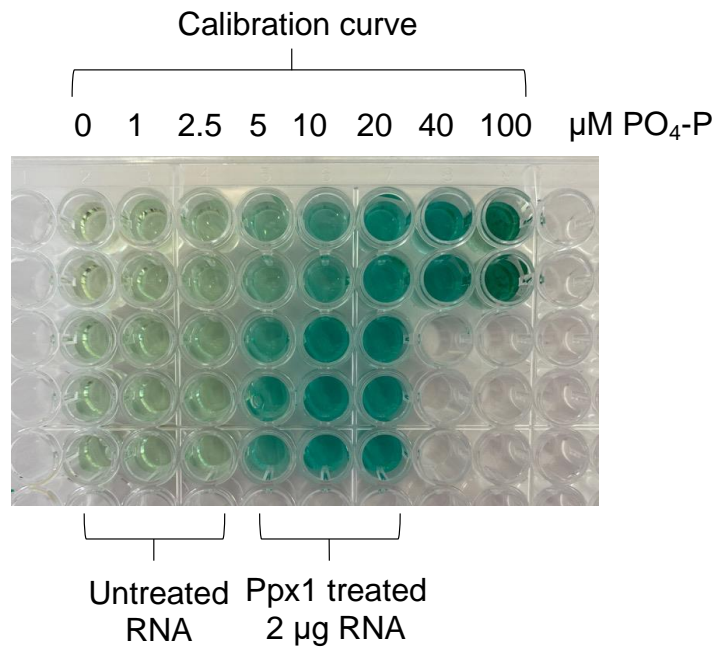


Figure 3.2 Malachite green phosphate assay after Ppx1 treatment of *C. reinhardtii* 2 μg RNA. Ppx1 degrades polyphosphate into free phosphate. Malachite green assay in 96 well plate shows differences in colourimetry in untreated vs. Ppx1 treated RNA, which can be quantified against a calibration curve for phosphate.

The concentration of phosphate was expressed as $\text{ng PO}_4\text{-P}/\mu\text{g RNA}$, to allow the subtraction of any phosphate detected in undigested samples, from the digested samples, for accuracy:

- 1 μL of undigested RNA used on 96-well plate has a specific RNA concentration in $\mu\text{g RNA}/\mu\text{L}$
- 1 μL of digested RNA used on a 96-well plate came from the Ppx1 reaction where 2 μg RNA was diluted in 20 μL of reaction volume

To compare Polyphosphate content with Total phosphate content in the biomass. Polyphosphate content was expressed as $\% \text{PO}_4\text{-P, dw}$:

Eq 9

$$\text{Polyphosphate } (\% \text{PO}_4 - \text{P, dw}) = \frac{\mu\text{g PO}_4 - \text{P}}{\text{mg RNA}} * 1000^{-1} \text{ mg} * \frac{\text{mg RNA}}{\text{mg dw}} * 100\%$$

Where,

$\frac{\mu\text{g PO}_4 - \text{P}}{\text{mg RNA}}$, is the polyphosphate content of the sample

1000^{-1} mg , to express polyphosphate in $\text{mg PO}_4 - \text{P}$

$\frac{\text{mg RNA}}{\text{mg dw}}$, is the RNA content in the biomass for this specific sample

3.6.4.3 Detection (PAGE)

Polyphosphate detection using polyacrylamide gel electrophoresis (PAGE) in *C. reinhardtii* RNA samples was conducted at the Laboratory of Molecular and Cell Biology at the University College of London, under the guidance of Professor Adolfo Saiardi, during a research visit. **All the PAGE shown in the results section (Chapters 4 and 5) were generated by Professor Adolfo Saiardi.**

The following reagents were prepared for PAGE:

- 40% Acrylamide/Bis-acrylamide 19:1 (Geneflow)
- 10X TBE buffer (For 1 L: 108 g Tris, 55 g Boric acid, 40 mL 0.5M Na₂EDTA pH 8.0. Top up to 1 Litre with ddH₂O)
- 10% Ammonium persulfate in ddH₂O (w/v)
- N, N, N-Tetramethylethylenediamine (TEMED, SIGMA)

The recipe for PAGE depends on the gel concentration. Higher gel concentration means slower migration of RNA/polyP. Throughout this project, 20% and 33.3% were used (**Table**).

Table 3.4 PAGE recipe according to the gel concentration.

Gel conc. (%)	40% Acr/Bis 19:1 (mL)	ddH ₂ O (mL)	10XTBE (mL)	10%APS (mL)	TEMED (μL)
20%	19.0	14.9	3.8	0.2	15
33.3%	31.7	2.2	3.8	0.2	30

The gel mixture was loaded in a 24 cm Hoefer cast, allowing the gel to polymerise as it is shown in **Figure 3.3**.

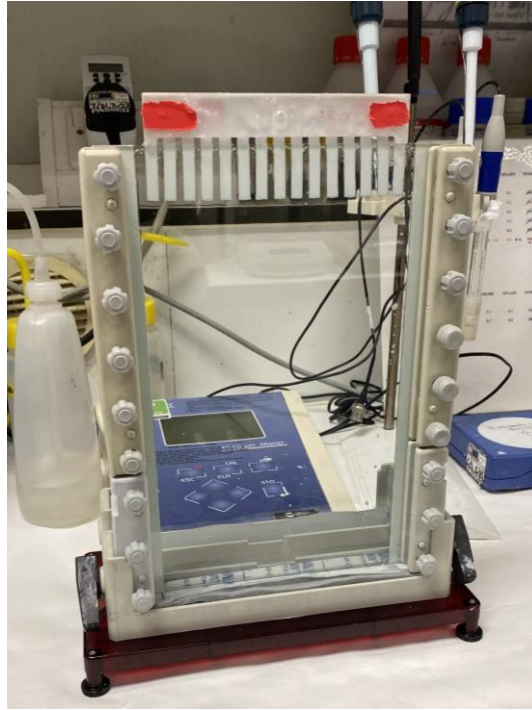


Figure 3.3 PAGE gel polymerisation in 24 cm Hoefer cast

The gel cast was positioned in a Tall Standard Dual Cooled Vertical Protein Electrophoresis Unit (Hoefer) with 6 L of 1X TBE buffer and pre-ran for 30 min at 330V and 6 mA. Then the RNA samples (equivalent to 20 μ g RNA) are loaded together with 10 μ L of migration dye (10 mM Tris-HCl pH 7.0, 1 mM EDTA, 30% glycerol, 0.1% Orange G) on each well. PAGE were run at 500 V and 4 mA overnight until the Orange G dye shows the bands just below half of the gel.

The gel was removed carefully from the cast and placed in a tray with a filtered staining solution (20% methanol, 2% glycerol, 0.05% Toluidine Blue) and shaken gently for 30 min. The gel was de-stained for 2h by changing the same solution without Toluidine Blue several times.

For visualisation, pictures were taken of the de-stained gels after white light exposure using a scanner (EPSON perfection 4990 Photo). **Figure 3.4** shows a representative picture of a Toluidine Blue stained PAGE containing *C. reinhardtii* RNA samples, showing polyphosphate migration. The blue background was removed from the picture, this shows that Toluidine blue O is a metachromatic dye that stains RNA in blue and polyP in red. The use of glass beads is necessary, independently of the absence or deficiency of a cell wall in *C. reinhardtii* cells.

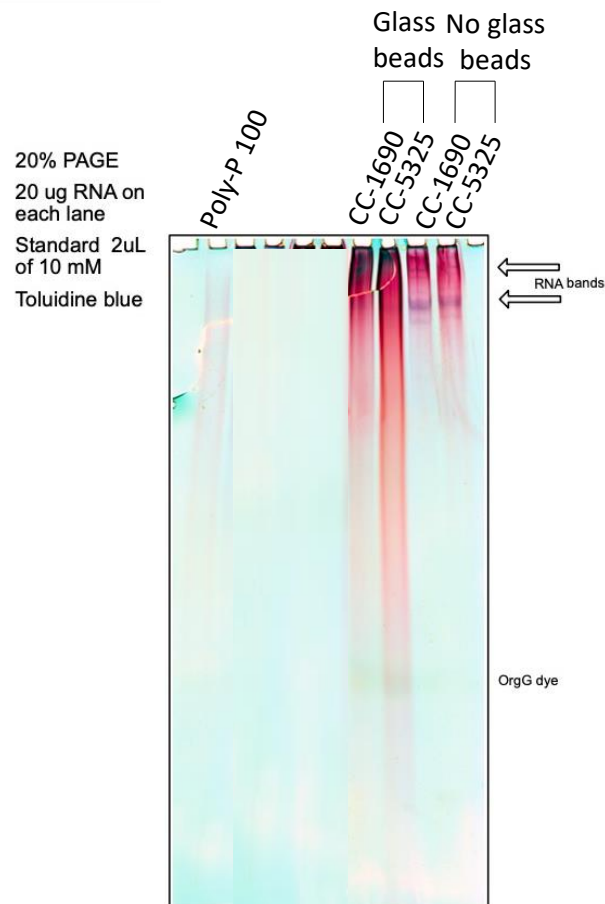


Figure 3.4 *C. reinhardtii* polyP visualisation on PAGE stained with Toluidine Blue. Representative 20% PAGE stained with Toluidine Blue (blue background removed using the scanner software). The gel shows a polyP100 standard at the left, followed by 20 μg RNA of exponential growth *C. reinhardtii* strains (CC-1690 and CC-5325), extracted with and without glass beads during the process of protocol standardisation

3.6.5 Western Blot Analysis

Western Blot analysis was used to detect the transgene protein expression of the transcription factor PSR1 in the PSR1 overexpression strains (Slocombe et al., 2023). The culture sample volume collected corresponded to 50 μg of Chlorophyll a+b (see section 3.4.3).

3.6.5.1 Protein extraction

The protocol for protein extraction from fresh microalgal pellets was adapted from Wittkopp, et al. (Wittkopp et al., 2017)

The following reagents were prepared before protein extraction.

- HEPES³ 6+PI
45 mL HEPES 6 (5mM HEPES pH 7.5 with KOH, 10 mM EDTA pH 7.5 with NaOH) + Protein Inhibitors 'PI'⁴ (450 µL 100mM Benzamide hydrochloride hydrate 100x, 450 µL PMSF 100X, 450 µL 6-Aminocaproic acid 100x)
- HEPES 6, PI, 0.1 M dithiothreitol (DTT), 0.1M Na₂CO₃ (800 µL HEPES+PI, 100 µL 1 M DTT, 100 µL 1 M Na₂CO₃)

The cells were harvested by centrifugation at 3000g for 10 min, the supernatant was discarded. 300 µL HEPES 6 + PI were added to resuspend the cells, transferred to a new 1.5 mL microcentrifuge tube and centrifuged at 5000 g for 2 min. The supernatant was removed without disturbing the pellet. 60 µL of HEPES 6 +PI + 0.1 M DTT + 0.1 M Na₂CO₃ were added to resuspend the protein lysate by pipetting and vortexing. The protein samples were flash-frozen with liquid nitrogen and stored at -70°C.

3.6.5.2 Protein preparation

The protein extract was left to thaw on ice before 40 µL of 5% SDS, and 30% Sucrose solution was added (the final concentration of the protein sample is equivalent to 0.5 µg Chlorophyll a+b/ µL). The equivalent volume of 10 µg of Chlorophyll was transferred to a 200 µL PCR tube and mixed with 1X loading buffer (4x Laemmli sample buffer Bio-Rad 1610747). The samples were boiled for 1 min at 99°C to denature the proteins, and centrifuge at 5000g for 1 min.

3.6.5.3 SDS-polyacrylamide gel electrophoresis (SDS-PAGE)

Proteins were resolved with SDS-PAGE electrophoresis. The following reagents were prepared:

- Tris buffer 8.8 (1.5 M Tris-HCl pH 8.8)
- Tris buffer 6.8 (0.5 M Tris-HCl pH 6.8)
- Acrylamide (30% Acrylamide/Bis-acrylamide (w/v)) (Severn Biotech Ltd 20-2100-05)
- 10% (w/v) Sodium dodecyl sulfate (SDS)
- 10% Ammonium persulfate (APS) (w/v)
- TEMED (Sigma 101125341)
- Running buffer 10X (For 1 L, 30g Tris, 144 g Glycine, 10 g SDS, pH 8.3)

³ 4-(2-hydroxyethyl)-1-piperazineethanesulfonic acid (HEPES)

⁴ Protein inhibitors (PI) were added to HEPES 6 fresh before protein extraction.

The SDS-PAGE consists of a separating gel (bottom) and a stacking gel (top), casted in a BIORAD. The concentration of the separating gel depends on the length of the protein of interest. In this project, 8% SDS-PAGE was used. For the stacking gel, 4% is commonly used. The reagents were mixed in the following order for the separating gel and left to polymerise. Then, the stacking gel was prepared and loaded on top of the separating gel. A well comb was inserted into the stacking gel and left to polymerise.

The well comb was removed from the polymerised gel and the gel was placed in a gel tank (Bio-Rad Mini Protean TGX) filled with 1X Running Buffer (Diluted from 10X). The boiled lysate was loaded on each well per sample. 4 μ L of a CSL-BBL Pre-stained Protein Ladder (Clever Scientific, UK stored in aliquots at -20°C) was loaded on one side of the gel. The SDS-PAGE were left to run at 150V for 1 h.

3.6.5.4 Protein transfer and blocking

SDS-PAGE was followed by the transfer of proteins to a membrane (also called blot). The following reagents were prepared:

- Ponceau S Red (0.1% (w/v) in 5% acetic acid, Sigma)
- Tris Buffered Saline with Tween (TBS-T)
20mM Tris-HCl, 150 mM NaCl, 0.1 % (v/v) Tween 20 pH 7.6
- Blocking solution (5% (w/v) low-fat dried milk in TBS-T)

Resolved proteins were transferred from the SDS-PAGE to a PVDF membrane (preactivated with methanol for 1 min), for 2 h at 70V in 1X Transfer buffer (25 mM Tris base, 192mM Glycine, 20 % methanol; pH 8.3) The membrane was briefly stained with Ponceau S Red, to confirm even loading of protein. The membrane was rinsed in ddH₂O and de-stained with TBS-T. The blot was incubated at room temperature and gently shaken, in blocking solution for 1 h.

3.6.5.5 Immunodetection

The PSR1 transgene protein in the PSR1 overexpression strains 8-27 and 8-42, was detected using the C-terminus Venus Tag inserted with the construct (see **Figure 3.1**) against the background strain UVM4 as a negative control as UVM4 does not harbour an endogenous Venus 'Yellow fluorescent protein' (YFP) protein.

Immunodetection was conducted using a primary anti-GFP antibody with a 1:5000 dilution in 3% low-fat dried milk in TBS-T (Abcam ab6556). To reduce the blot background (other proteins apart from the transgene PSR1), the anti-GFP antibody was preincubated at 4°C overnight, with a membrane containing

the protein extract from the background strain UVM4. The following day, the pre-incubated anti-GFP was used on the membranes containing the protein extracts of each PSR1 transgenic strain (8-27 and 8-42) (4°C, overnight). The membranes were washed 3x with TBS-T for 10 min at room temperature. Binding of Horseradish peroxidase (HRP)-conjugated secondary anti-Rabbit antibody (Jackson Immuno Research 111-035-144) with a 1:5000 dilution in 3% low-fat dried milk in TBS-T was conducted for 1 h at room temperature. Finally, the blots were washed 3x with TBS-T for 5 min, before enhanced chemiluminescence (ECL) detection with a SuperSignal™ West Pico Chemiluminescent Substrate (Thermo Scientific). Blots show exposure after 1.5 min.

3.7 Data analysis

3.7.1 Growth and Nutrient uptake rates

The growth rates and doubling times were calculated according to (Osundeko et al., 2013).

The specific growth rate ($\mu = h^{-1}$) was calculated for the exponential growth phase as follows:

Eq 10

$$\mu (h^{-1}) = \frac{\ln\left(\frac{y_1}{y_0}\right)}{t_1 - t_0}$$

Where:

y_0 and y_1 , are the biomass (g dw/L) or (cell concentration (10^6 cells/mL) if available) values at the beginning (t_0) and at the end (t_1) of the exponential, phase, respectively

The doubling time (h) was calculated as:

Eq 11

$$\text{Doubling time (h)} = \frac{\ln(2)}{\mu}$$

Where:

μ , is the specific growth rate (**Eq 10**)

The biomass productivity (g dw L⁻¹ h⁻¹) was calculated during the period of exponential growth as follows:

Eq 12

$$\text{Biomass productivity (g dw L}^{-1} \text{ h}^{-1}) = \frac{Cdw1 - Cdw0}{t1 - t0}$$

Where,

$Cdw0$ and $Cdw1$, are the biomass concentration values (g dw/L) the beginning ($t0$) and at the end ($t1$) of the exponential growth phase

The nutrient uptake rates (NUR = mg nutrient g dw⁻¹ h⁻¹) were calculated for each time segment from 0-24 h after P repletion in the P overplus experiment (section 3.3.5) as follows:

$$\text{NUR (mg nutrient g dw}^{-1} \text{ h}^{-1}) = \frac{\left(\frac{CNmedia_{ts1} - CNmedia_{ts0}}{Cdw_{ts0}} \right)}{ts1 - ts0}$$

Where,

$CNmedia_{ts0}$ and $CNmedia_{ts1}$, are the nutrient concentration in the media (mg nutrient/L) at the beginning ($ts0$) and at the end ($ts1$) of the time segment

Cdw_{ts0} , is the biomass concentration (g dw/L) at the beginning ($ts0$) of the time segment

$ts1 - ts0$, is the time segment difference (h)

3.7.2 Data visualisation and Statistical significance

Statistical significance tests were evaluated by one-way ANOVA and by Tukey HSD test with a p-value of 0.05, n=3). Two-way ANOVA (two factors) was used to analyse the effect of both P deprivation length and P repletion type together. Both data visualisation and statistical analysis were produced using the software OriginPro (Version 2021, OriginLab Corporation, Northampton, MA, USA).

3.7.3 Principal Component Analysis

For the multivariate principal component analysis (PCA), the average of the nutrient uptake rates and the initial nutrient concentration in the media for the strains (three biological replicates per strain) used in each experiment (first P overplus exp. CC-1690, CC-125, CC-5325 and CC-4350 and second P overplus exp. CC-1690 and CC-125) were used. The data was normalised by calculating the z-scores by subtracting the value from its mean and dividing it by the standard deviation. The eigenvalues generated by the PCA report led to the selection of the first two principal components as long as the eigenvalue is higher than one.

Chapter 4 Phosphate deprivation and overplus: What parameters prime *Chlamydomonas reinhardtii* for enhanced polyphosphate accumulation?

4.1 Introduction

The first objective of this chapter is to demonstrate that the monitoring of physiological parameters over time periods, may lead to a robust understanding of how P-deprivation affects P overplus in *C. reinhardtii*. The correlation between P-deprivation length and polyP accumulation during P overplus is unclear, due to the use of time periods (hours, days, etc.) as a reference parameter for the resupply of P in previous studies. This is due to the lack of standardised protocols and specific physiological markers, which makes different studies hard to compare and replicate and hinders mechanistic understanding of the overplus phenomenon. Thus, there is a need to develop reproducible physiological markers adaptable to different microalgal species, cultivation conditions, etc. Previous studies have suggested the optimum period of P deprivation to be either when growth ceases or biomass reaches its lowest P content. I wanted to determine whether either of these physiological parameters has an enhanced effect on P overplus. I evaluated this hypothesis by 1) standardising an experimental design of P-deprivation and P overplus in four strains of *C. reinhardtii* and 2) monitoring the fate of phosphate as it is accumulated in the biomass.

Also, even though P overplus is the overaccumulation of polyP, previous literature has failed to provide a reliable quantification of polyP that fits into the P mass balance of the microalgal culture. The second objective of this chapter is to show the application of two polyP analysis methods, commonly used in the yeast *S. cerevisiae*, to *C. reinhardtii*: 1) Colorimetry assay of Ppx1 treated RNA samples and 2) Toluidine Blue staining of polyP resolve by PAGE. The first method allows the quantification of polyP and is fitted in the mass balance of P. The second provides a tool for qualitative visualisation of polyP and detection of the length of the polyP chain. I used this tool to observe the dynamics of the accumulated polyP pool and to test the hypothesis formulated by Solovchenko et al., that polyP is accumulated as a long-chain polymer during microalgal P overplus (Solovchenko et al., 2019a, Solovchenko et al., 2019b, Lobakova et al., 2023).

Lastly, one of the main gaps in the knowledge of microalgal P metabolism is how polyP synthesis occurs. As mentioned earlier in section 2.4.4 (Chapter 2 Literature Review), the synthesis of polyP by *C. reinhardtii* occurs through the

VTC complex and its regulation is conjectured to be similar to that of *S. cerevisiae* (Wild et al., 2016). In budding yeast it is believed that inositol pyrophosphates (PP/IPs) production responding to ATP fluctuation triggers polyP synthesis. The binding of IPs to the SPX domain of the VTC complex presumably is responsible for activating polyP synthesis (Sanz-Luque et al., 2020, Lonetti et al., 2011, Gerasimaite et al., 2017). However, *C. reinhardtii*, strikingly differs from yeast regarding general polyP metabolism. For instance, a key enzyme the exopolyphosphatase Ppx1, has no homologs in microalgae (Wurst et al., 1995, Plouviez et al., 2023a). Since inositol hexakisphosphate (IP₆) can also be visualised via PAGE, and it is a precursor of the synthesis of PP/IPs, this chapter will evaluate the hypothesis that the IP₆ detection pattern should match that of polyP during P overplus, reaffirming the role of IPs in polyP synthesis.

4.2 Objectives

1. To understand physiological responses to P deprivation and their relationship with the P overplus phenomena in *C. reinhardtii*.
2. To implement reliable analytical methods to quantify and characterise in-cell polyphosphate in *C. reinhardtii* and understand its dynamics during P overplus.

4.3 The study of P deprivation in *C. reinhardtii*

4.3.1 *C. reinhardtii* can sustain the same initial growth rate under P deprivation compared to P-replete cells

To determine the physiological parameter(s) of P deprivation that are correlated with the highest P overplus response in *C. reinhardtii*, I monitored different growth parameters in four strains, cultivated under P-deprivation conditions and compared these to cells cultivated under non-deprived conditions ('control'). The strains CC-1690, CC-125, CC-5325 and CC-4350, obtained from the *Chlamydomonas* Resource Center were selected due to their broad use in *Chlamydomonas* sp. research. The strain CC-1690 has been used for the *Chlamydomonas* Genome Project (Craig et al., 2023). CC-125 is one of the oldest and most widely used wild-type strains (Pröschold et al., 2005), and is the background of many mutants. CC-5325 is the background of the Clip mutant library and was thought to be cell wall deficient (Li et al., 2016) until Zhang et al. concluded that it has a comparable intact cell wall to that of CC-1690 but thinner (Zhang et al., 2022). Lastly, the cell wall deficient strain CC-4350 is widely used due to its high transformation efficiency (Neupert et al., 2009).

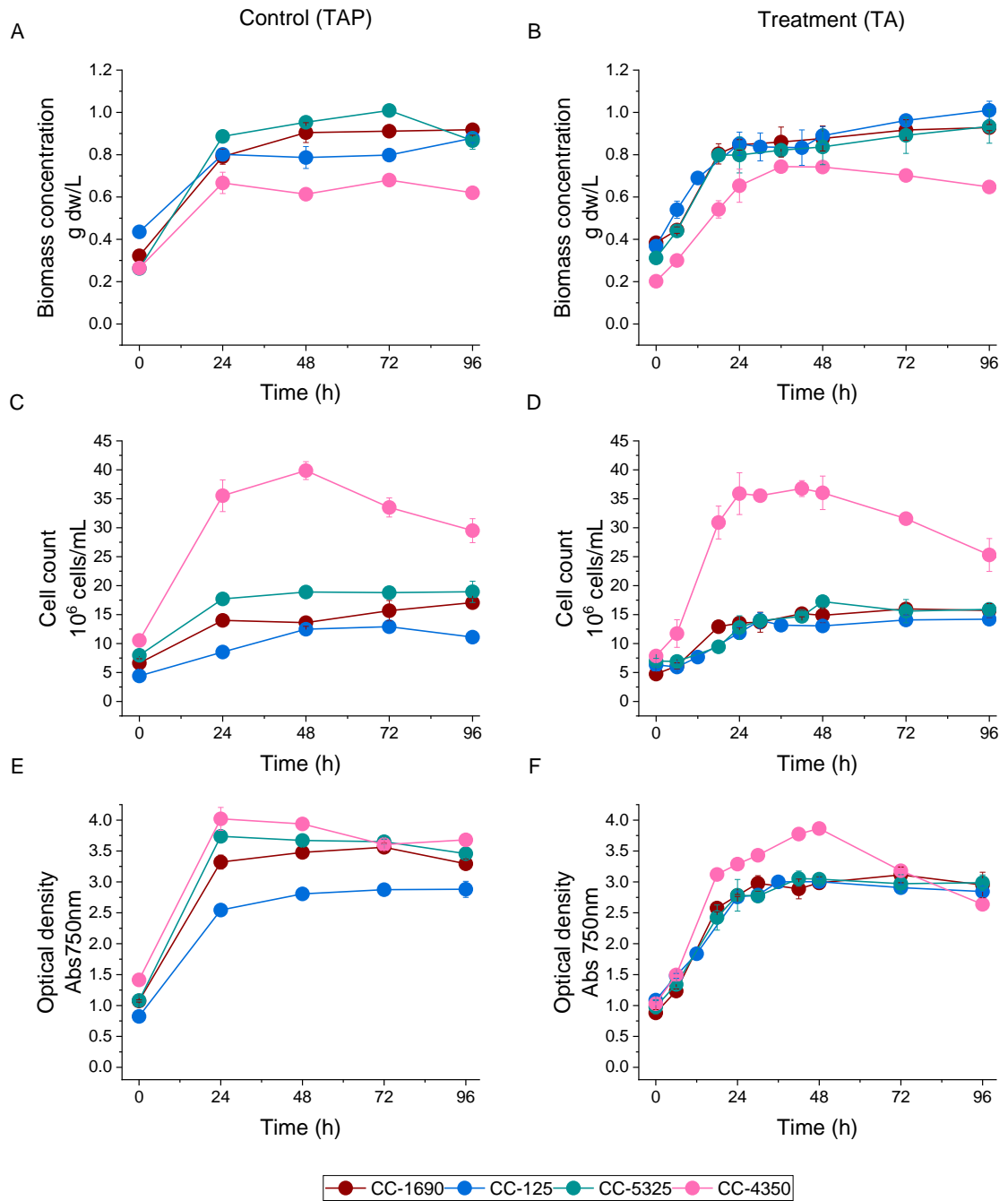


Figure 4.1 *C. reinhardtii* biomass growth during control and P-deprivation experiment. For the strains CC-1690, CC-125, CC-5325 and CC-4350, growth was not altered when mid-exponential cells were resuspended in TA media. Mid-exponential cells were resuspended in TAP media (Left column) or TA media (Right column). A-B Biomass concentration (g dw/L), C-D Cell count (10⁶ cells/mL) and E-F Optical density (Absorbance 750nm).

In these *C. reinhardtii* strains, I examined biomass, cell number and optical density, after resuspending mid-exponential growing ($OD_{750nm}=1.0$) cells in P-free (TA) or TAP media (**Figure 4.1**). Pre-cultivation of *C. reinhardtii* until $OD_{750nm}=1.0$ is needed to ensure that all cells are at the same growth and metabolic stage before control (resuspension in TAP) and treatment (resuspension in TA) experiments started. No differences were observed in the growth patterns of *C. reinhardtii* cells between P-deprived and non-P-deprived cultures. One of the objectives of this experiment was to determine the time when growth terminates, which occurred at the 24 h time-point. After this time, all the cultures reached a stationary growth phase. The different parameters of growth (growth rates, doubling times and biomass productivity) are summarised in (**Table 4.1**). For all four strains, growth continues at the same rate, 24 h after resuspension, independently of P availability in both TA and TAP (p-value=0.66). The results allowed me to confirm that growth ended after 24 h under both P-deprived and control conditions and suggest that factors other than P are limiting growth. In terms of biomass productivity, no difference was observed in P deprivation compared to the control experiment (p-value=0.85). The four strains produced approx. 0.47 g dw/L during the first 24 h, in both experimental conditions. Doubling times were significantly shorter for the strain CC-4350 (p-value= 4.76×10^{-4}). This strain is characterized by having smaller cells than the other strains, which I validated by estimating the cell biovolume (**Figure 4.2**) from pictures collected at the time of cell counting (see **Chapter 3** Materials and Methods section **3.4.2**), and requires a considerably higher number of cell division cycles to generate biomass (Chlamydomonas Resource Center).

P deprivation has been shown to trigger cells *C. reinhardtii* cells to increase in size due to starch accumulation as shown in (Bajhaiya et al., 2016), or lipids for other microalgae (Hu et al., 2008, Liu and Benning, 2013). However, larger cells were only observed for the strain CC-5325 after resuspension in TA media (p-value= 8.85×10^{-4}). Since the experiments were run under continuous illumination, it is not expected that cells will have a synchronised circadian rhythm and hence a greater variation in cell size is likely (Craigie and Cavalier-smith, 1982, Zones et al., 2015).

Table 4.1 Growth parameters calculated during control and P-deprivation experiment. Mid-exponential cells were resuspended in TAP media (Control) or TA media (Treatment). Values average (n=3) \pm SE, calculated during exponential growth (24 h) as shown in section 3.7.1 in **Chapter 3** Materials and Methods

A		
Specific growth rate		
(h⁻¹)		
Strain	Control (TAP)	Treatment (TA)
CC-1690	0.037 \pm 0.002	0.032 \pm 0.002
CC-125	0.027 \pm 0.002	0.032 \pm 0.003
CC-5325	0.051 \pm 0.001	0.041 \pm 0.002
CC-4350	0.038 \pm 0.003	0.044 \pm 0.004
Average	0.038 \pm 0.005	0.037 \pm 0.003

B		
Doubling time		
(h)		
Strain	Control (TAP)	Treatment (TA)
CC-1690	24.2 \pm 5.0	20.1 \pm 3.1
CC-125	25.2 \pm 2.8	24.1 \pm 2.2
CC-5325	20.9 \pm 2.7	25.9 \pm 2.2
CC-4350	13.8 \pm 1.2	11 \pm 1.2
Average	21.0 \pm 2.6	20.3 \pm 3.3

C		
Biomass productivity		
(g dw L⁻¹ h⁻¹)		
Strain	Control (TAP)	Treatment (TA)
CC-1690	0.021 \pm 0.002	0.019 \pm 0.001
CC-125	0.018 \pm 0.001	0.020 \pm 0.002
CC-5325	0.027 \pm 0.001	0.020 \pm 0.002
CC-4350	0.018 \pm 0.002	0.019 \pm 0.002
Average	0.021 \pm 0.002	0.020 \pm <0.001

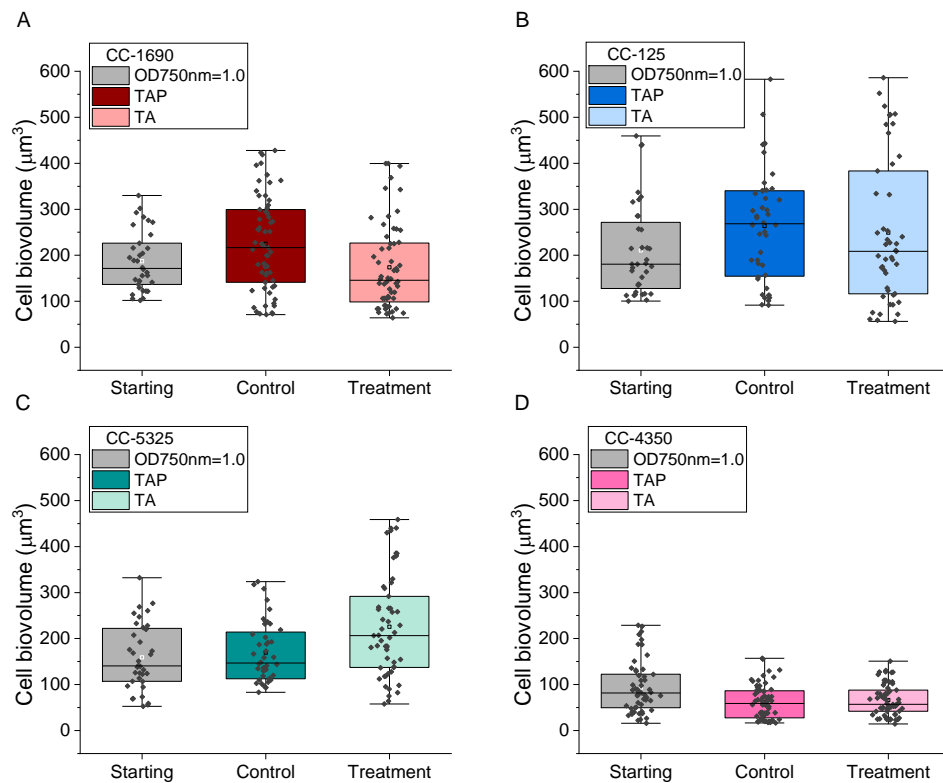


Figure 4.2 *C. reinhardtii* cell volume in control and P-deprivation experiment. CC-4350 cells are approximately half the size of the strains CC-1690, CC-125 and CC-5325. Mid-exponential cells ($\text{OD}_{750\text{nm}}=1.0$) were resuspended in TAP media (Control) or TA media (Treatment). Cell biovolume (μm^3) data was collected for the 24 h time point after resuspension. A CC-1690, B CC-125, C CC-5325 and D CC-4350 ($n=30-50$ cells).

4.3.2 P-deprived *C. reinhardtii* sustains growth due to ability to mobilise internal inorganic P reserves

Next, I aimed to identify the dynamics of the internal pools of P that allow P-deprived *C. reinhardtii* to sustain growth at the same rate as non-P-deprived cells. To do so, I applied a polyP quantification method commonly used in the yeast *Saccharomyces cerevisiae* (Lonetti et al., 2011) in *C. reinhardtii*. In this method, RNA extraction is followed by recombinant Ppx1 treatment to degrade all polyphosphate into free phosphate, which can be quantified using malachite green assay (see **Chapter 3 Materials and Methods section 3.6.4**). I expressed polyP as a proportion of dry biomass (dw) (**Figure 4.3A-B**). Biomass concentration (g dw/L) was stable after growth ceased in both control and treatment experiments (**Figure 4.1A and B**). Expressing polyP in proportion to a stable parameter like dry biomass allows the determination of reliable patterns of change. When there was no P-deprivation (**Figure 4.3A**), I observed that the strain CC-5325 kept accumulating polyP throughout the control experiment.

This strain contrasted with the other strains, which maintained a stable polyP content of approx. 1.0% PO₄-P,dw (0.75% PO₄-P,dw for CC-4350). CC-5325 and CC-4350 are the strains with the highest and lowest content of polyP, respectively. For P-deprived cultures, a rapid decrease in the polyP content was observed, which reached a plateau at the 24 h time point, for all the strains (Figure 4.3B).

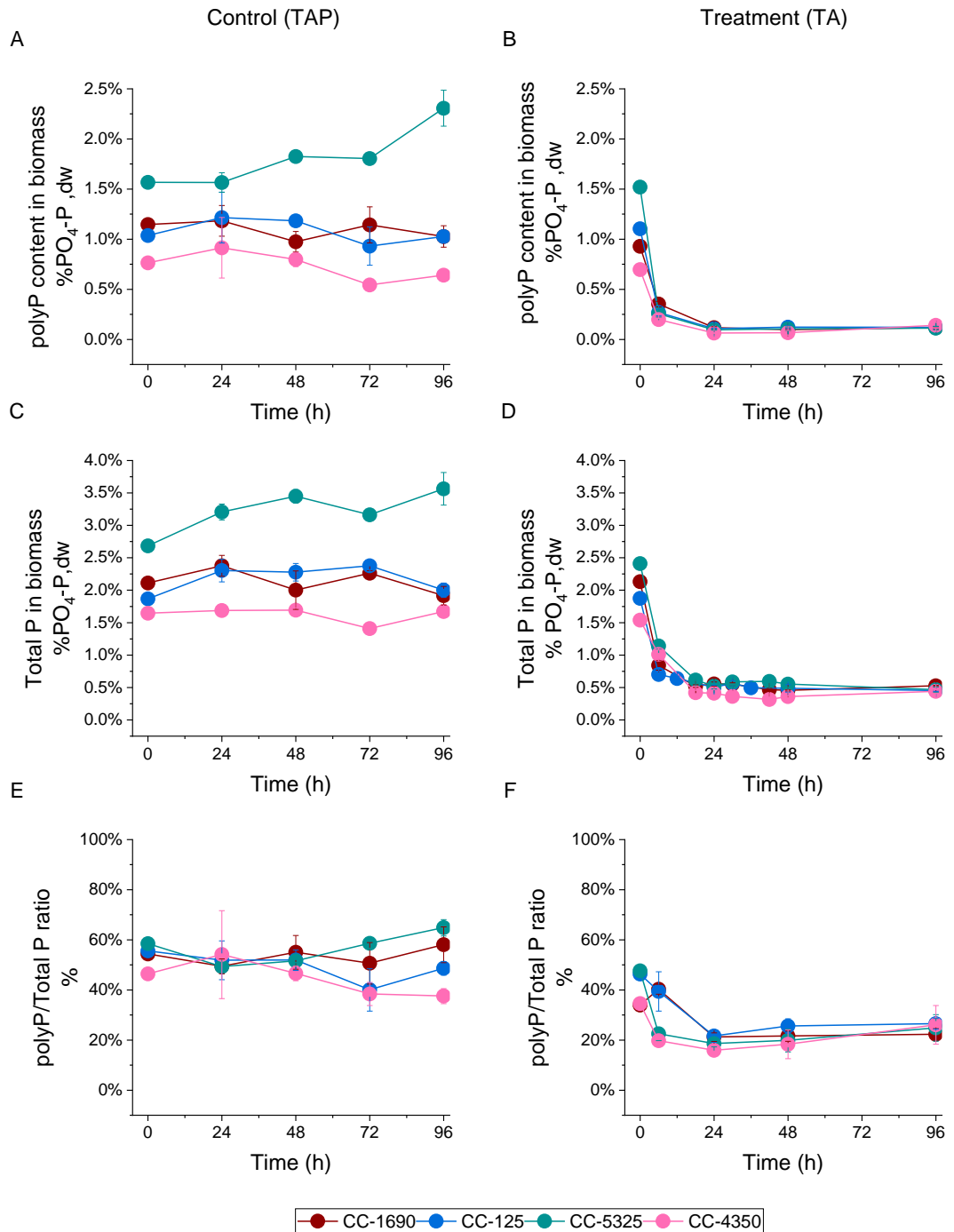


Figure 4.3 Phosphate accumulation of *C. reinhardtii* during the control and P-deprivation experiment. *C. reinhardtii* (CC-1690, CC-125, CC-5325 and CC-4350) mid-exponential cells were resuspended in TAP media (Control) or TA media (Treatment). A-B polyP content in biomass (% PO₄-P,dw), C-D Total P in biomass (% PO₄-P,dw) and E-F polyP/Total P mass ratio (% w/w).

As any living organism, *C. reinhardtii* is constituted of both inorganic (e.g. polyP, free phosphate) and organic (e.g. RNA/DNA, ATP, phospholipids, etc.) forms of phosphate. To measure the total content of phosphate in the biomass (organic and inorganic), I used an oxidating reagent composed of potassium persulfate and sulphuric acid to completely digest dry biomass samples, hence releasing all phosphate present in the biomass (**Figure 4.3C-D**). Released P was quantified using the ascorbic acid blue assay and further confirmed by IC-MS (see **Chapter 3** Material and Methods section **3.5.2** and **3.5.3**). In both the control and treatment experiments, the total P content in the biomass (%PO₄-P, dw¹) follows the same pattern as that of polyP (**Figure 4.3A-B**). After 24 h of P deprivation, all strains of *C. reinhardtii* reach their lowest content of both polyP (approx. 0.1%PO₄-P, dw) and total P (approx. 0.5%PO₄-P, dw) in biomass. This corresponds to growth cessation after resuspension in TA media (see **Figure 4.1B, D and F**). The ability to specifically quantify polyP in *C. reinhardtii* for the first time demonstrates that polyP reserves are not completely degraded upon P deprivation. P deprivation led to a decreased polyP/total P mass ratio of 20% (**Figure 4.3F**), compared to the constant ~50% observed in the control experiment (**Figure 4.3E**).

The quantification of polyP in **Figure 4.3A** and **B** was accompanied by the detection of polyP by polyacrylamide gel electrophoresis (PAGE) shown in **Figure 4.4**. PAGE was used to detect the polyP chain length distribution. polyP is a highly polyanionic polymer and thus, migrates down the vertically placed gel with the current and voltage applied, according to its molecular weight (Christ et al., 2020b). PAGE gives a qualitative perspective of polyP upon visualisation with toluidine blue O stain. RNA samples for PAGE analysis were normalised by dry mass. The equivalent to 20 µg RNA for mid-exponential cells (before TAP or TA resuspension) was approx. 500 µg dw. In the control experiment, no changes were observed in the intensity of the polyP smear over time (**Figure 4.4A and B**), except for CC-5325, for which the intensity appears to increase consistently with **Figure 4.3A**. The PAGE in **Figure 4.4A and B** also show that in the first 24 h, when growth was observed, the polyP pool is mostly composed of long/medium chain length polymers. As cells enter the stationary phase, polyP starts to be mobilised into medium and shorter-chain polyP. **Figure 4.4C and D** shows that PAGE polyP detection matched the pattern observed in **Figure 4.3B** for P-deprived cultures.

¹ Please note that units for polyP and total P content in biomass are the same but represent different quantities. polyP units represent phosphate degraded from the polyP chain after Ppx1 treatment. Total P accounts for all phosphate released from the dry biomass after acid digestion.

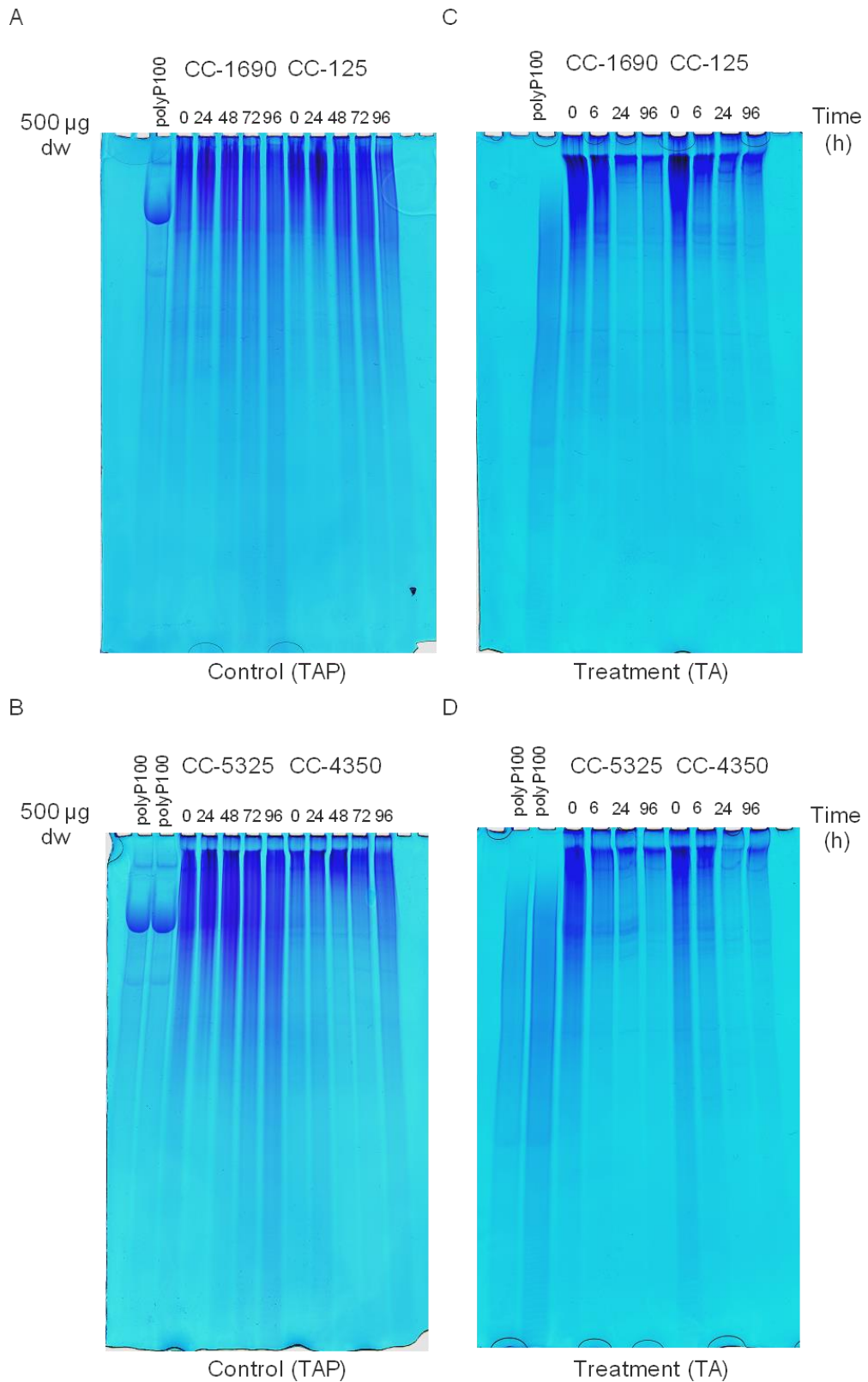


Figure 4.4 PAGE polyP visualisation with equal loading of dry biomass from control and P-deprivation experiment. Equivalent loading of dry mass on 20% PAGE provides accurate qualitative detection of polyP. *C. reinhardtii* CC-1690, CC-125, CC-5325 and CC-4350 mid-exponential cells were resuspended in TAP (Control) or TA media (Treatment) and monitored for 96 h. The equivalent of 500 μ g dw was loaded on each sample well. polyP100 is a standard for medium to short-chain polyphosphate. PAGE was stained with toluidine blue. Each time point corresponds to the first biological replicate (out of three), for each experiment (TAP vs TA).

4.3.3 RNA, the second largest pool of P in *C. reinhardtii* is degraded upon longer P deprivation

In photosynthetic microorganisms like microalgae, polyP and RNA are considered the largest pools of P (Raven, 2013, Rees and Raven, 2021). Thus, I also monitored the variation of the RNA content of *C. reinhardtii* during P-deprivation (**Figure 4.5**). In both the control and the treatment, I observed that the content of RNA decreased as the cells of the four strains entered the stationary growth phase. For the P-deprivation cultures, the RNA levels did not fall below approx. 2% RNA,dw for all the strains even after 96 h following resuspension in TA media (**Figure 4.5B**). These results indicate that the inorganic reserves of P (polyP) were used in the first 24 h after resuspension in TA media. After this period, *C. reinhardtii* cells seemed to use organic forms of P as an alternative source, which are presumably mostly obtained from the degradation of ribosomal RNA which accounts for 98% of total cellular RNA (Raven, 2013).

The results indicate that growth cessation and lowest inorganic (polyP) reserves of P concurred 24 h after P deprivation, whereas the lowest RNA content (organic pool of P) was reached later after 96 h of P deprivation. Therefore, it was decided to test the effect of reaching the lowest polyP (24 h) and lowest RNA (96 h) content, upon P deprivation, on the ability of the cells to exhibit P overplus.

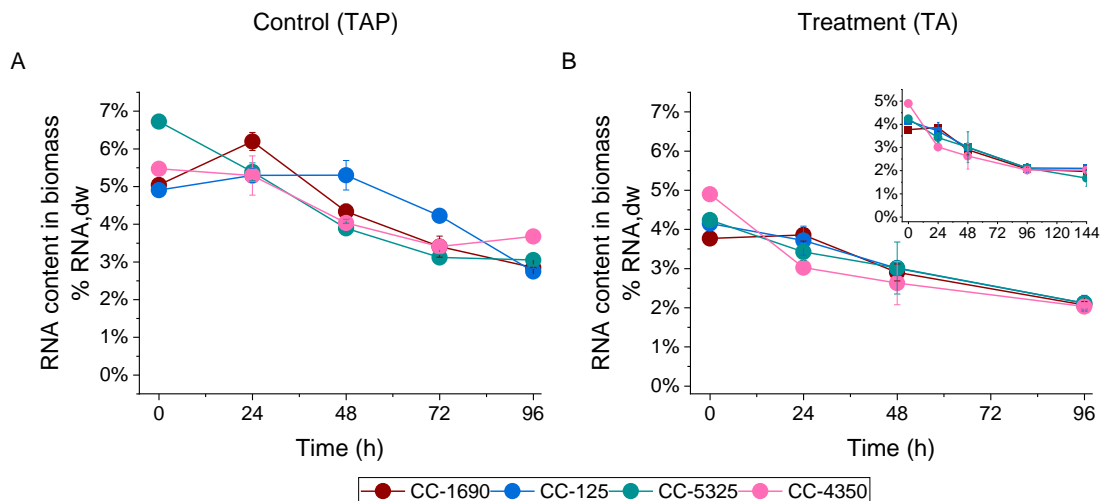


Figure 4.5 RNA content in the biomass variation during the P-deprivation experiment in *C. reinhardtii*. CC-1690, CC-125, CC-5325 and CC-4350 mid-exponential cells were resuspended in TAP (Control) or TA (Treatment) media. A-B RNA content in biomass (%RNA,dw). The inset in diagram B shows RNA variation with the addition of the 144 h time point.

4.3.4 Ammonium and sulphate removal from the media is not affected by P deprivation in *C. reinhardtii*

To measure the rate of P removal from the media and confirm the mass balance of P, I measured the phosphate concentration in the filtered supernatant (see **Chapter 3** Material and Methods section **3.5.3**), as mentioned above. TAP media contains Tris buffer and thus the culture pH never goes above the precipitation index (pH=8.5) for phosphorus as calcium phosphate. Therefore, it may be assumed that phosphate was present either in the media or in the biomass. **Figure 4.6A** shows the concentration of phosphate in the media and the biomass for the control experiment. As expected, the high content of phosphate in the biomass of strain CC-5325 (**Figure 4.3C**) was consistent with a higher removal of phosphate from the media (87% P removed), compared to the other strains. Since the values of P removed matched those of P accumulated in the biomass, it can be said that the mass balance of P for the four strains after resuspension in TAP media fits appropriately, which validates the techniques used for P analysis. Furthermore, the removal of P from the media in the control experiment evidences that under no P deprivation conditions, *C. reinhardtii* does not use its internal reserves of P as it occurred in P-deprived cultures (**Figure 4.6B**).

Furthermore, I was also interested in determining whether P deprivation could affect biomass composition. Elemental analysis (CHNS) was used to obtain the content of carbon, nitrogen and sulphur in dry biomass samples collected for both control and treatment experiments (see **Chapter 3** Material and Methods section **3.6.3**). However, I did not observe any significant differences (p-value=0.74) in the biomass composition of carbon of *C. reinhardtii* after 24 h of resuspension in either TAP or TA media (**Table 4.2**). The nitrogen concentration in the biomass for both the control and treatment obtained from CHNS analysis was plotted together with the media concentration of ammonium (mg NH₄-N/L), which is the only source of nitrogen in the media (**Figure 4.6C-D**). The ammonium and sulphate concentrations in the media were obtained from the IC-MS results.

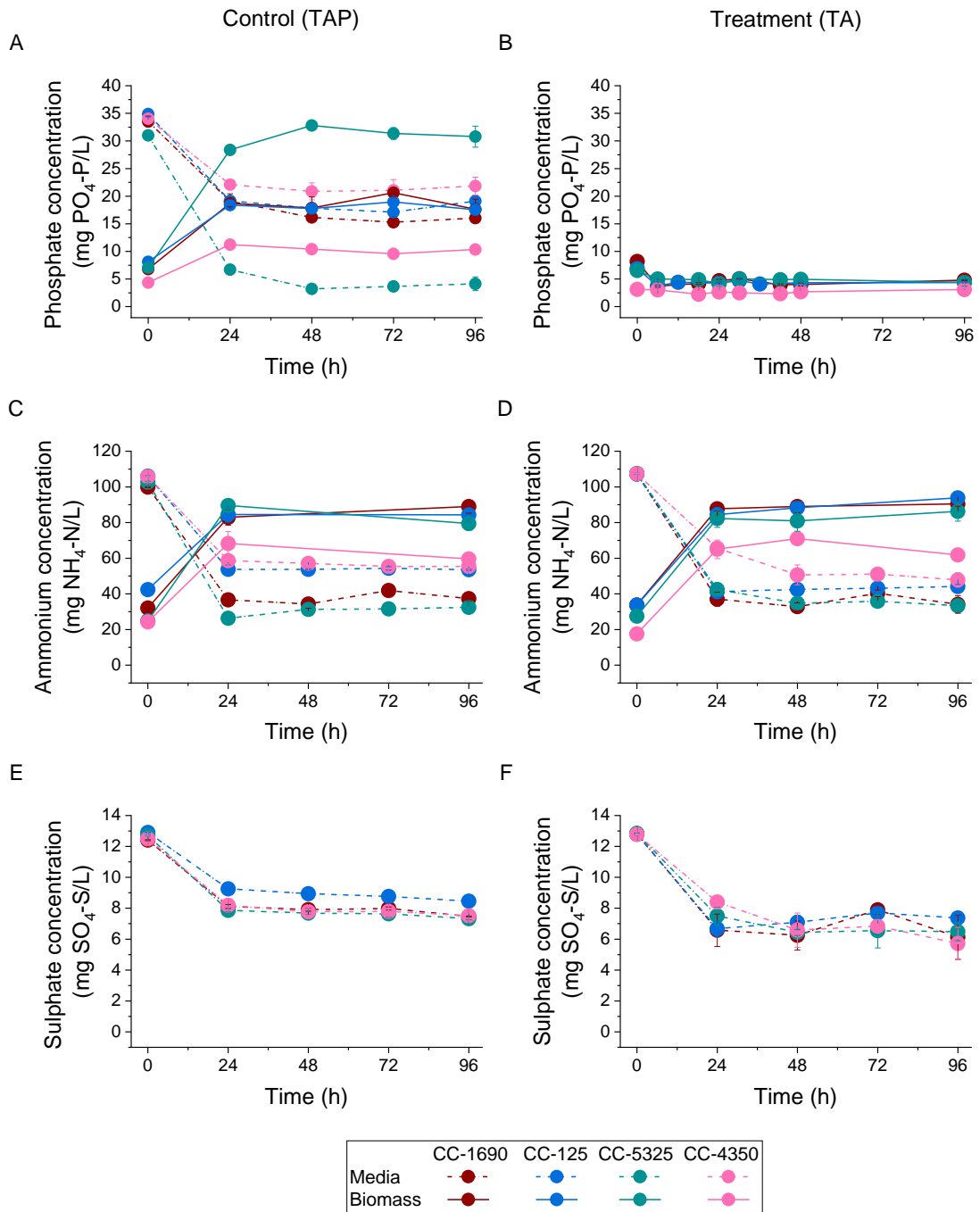


Figure 4.6 Nutrient removal from the media during the control and P-deprivation experiment. CC-1690, CC-125, CC-5235 and CC-4350 mid-exponential cells were resuspended in TAP (Control) or TA (Treatment) media. Nutrient concentration in the media (dash-dotted line) and in the biomass (solid lines) of A-B Phosphate (mg PO₄-P/L), C-D Ammonium (mg NH₄-N/L) and E-F Sulphate (mg SO₄-S/L)

No differences in the accumulation of nitrogen were observed according to the availability of P in the media. To note, biomass nitrogen concentration (mg N/L) accounts for all forms of nitrogen within the cell (not only ammonium), but the scale is the same as that for medium concentration. In the case of sulphur, unfortunately, biomass concentration data (mg SO₄-S/L) did not close the mass

balance. I believe this is because of its very low content in biomass in comparison with carbon and nitrogen. The biomass composition of *C. reinhardtii* is approx. 50% C,dw, 8-10% N,dw, and 0.5% S,dw. Thus, the S content may be under the limit of detection of the elemental analyser. Overall, the data suggests that P deprivation did not affect the removal of ammonium and sulphate from the media, under the experimental conditions tested².

Table 4.2 Biomass carbon and nitrogen composition in control and P-deprivation experiment. Mid-exponential cells of CC-1690, CC-125, CC-5325 and CC-4350 were resuspended in either TAP (Control) or TA (Treatment) media. Values represent the average of three biological replicates \pm SE at the 24 and 96 h time point

A				
%C,dw				
Strain	Control (TAP)		Treatment (TA)	
	24 h	96 h	24 h	96 h
CC-1690	49.6 \pm 0.3	50.0 \pm 0.3	50.1 \pm 0.3	50.6 \pm 0.1
CC-125	49.2 \pm 0.7	50.4 \pm 0.2	49.0 \pm 0.3	50.2 \pm 0.1
CC-5325	48.7 \pm 0.2	48.0 \pm 0.1	49.3 \pm 0.2	50.0 \pm 0.1
CC-4350	50.1 \pm 0.5	51.0 \pm 0.3	48.8 \pm 0.1	49.7 \pm 0.1
Average	49.4 \pm 0.3	49.8 \pm 0.2	49.3 \pm 0.2	50.1 \pm 0.1

B				
%N,dw				
Strain	Control (TAP)		Treatment (TA)	
	24 h	96 h	24 h	96 h
CC-1690	10.5 \pm 0.1	9.7 \pm 0.2	10.4 \pm 0.1	9.7 \pm 0.1
CC-125	10.5 \pm 0.1	9.6 \pm 0.1	9.9 \pm 0.1	9.3 \pm 0.1
CC-5325	10.1 \pm 0.1	9.2 \pm 0.1	10.3 \pm 0.2	9.2 \pm 0.1
CC-4350	10.2 \pm 0.1	9.6 \pm 0.1	10.0 \pm 0.1	9.5 \pm 0.1
Average	10.3 \pm 0.1	9.5 \pm 0.1	10.1 \pm 0.1	9.4 \pm 0.1

² The IC results also provided data for the concentration of any detectable anions or cations in the media over 1 mg/L, like magnesium and calcium which are relevant in the study of polyP, but the results were not consistent with the concentration of these cations in TAP media and thus, were not analysed

4.4 The study of P overplus in *C. reinhardtii*

4.4.1 P deprivation and subsequent resupply as KPO_4 does not affect biomass growth in *C. reinhardtii*

At the time following P deprivation when the lowest polyP (24 h) or RNA (96 h) levels were observed, the cultures of *C. reinhardtii* were supplied with 1 mM P with a KPO_4 solution (see **Chapter 3** Material and Methods section **3.3.5**) to trigger a P overplus response. A concentration of 1 mM P was chosen to match that of TAP media. To determine whether this response affected growth, I monitored biomass concentration (g dw/L), cell count (10^6 cells/mL) and optical density (Absorbance 750nm) (**Figure 4.7**). After KPO_4 repletion, I observed a subtle increase in growth in the 24 h P-deprived cultures of the four strains. For the 24 h P-deprived cultures indeed the growth rates were significantly higher than those of 96 h P-deprived cultures (p-value=0.001) (**Table 4.3**).

Nonetheless, the growth rates (h^{-1}) and biomass productivity ($\text{g dw L}^{-1} \text{h}^{-1}$) were negligible for all the strains (values below 0.005 h^{-1} or $\text{g dw L}^{-1} \text{h}^{-1}$) and no cell division was observed. This indicates that cells did not grow when supplied with KPO_4 after either P-deprivation until the lowest polyP (24 h) or lowest RNA (96 h).

Repletion after P deprivation

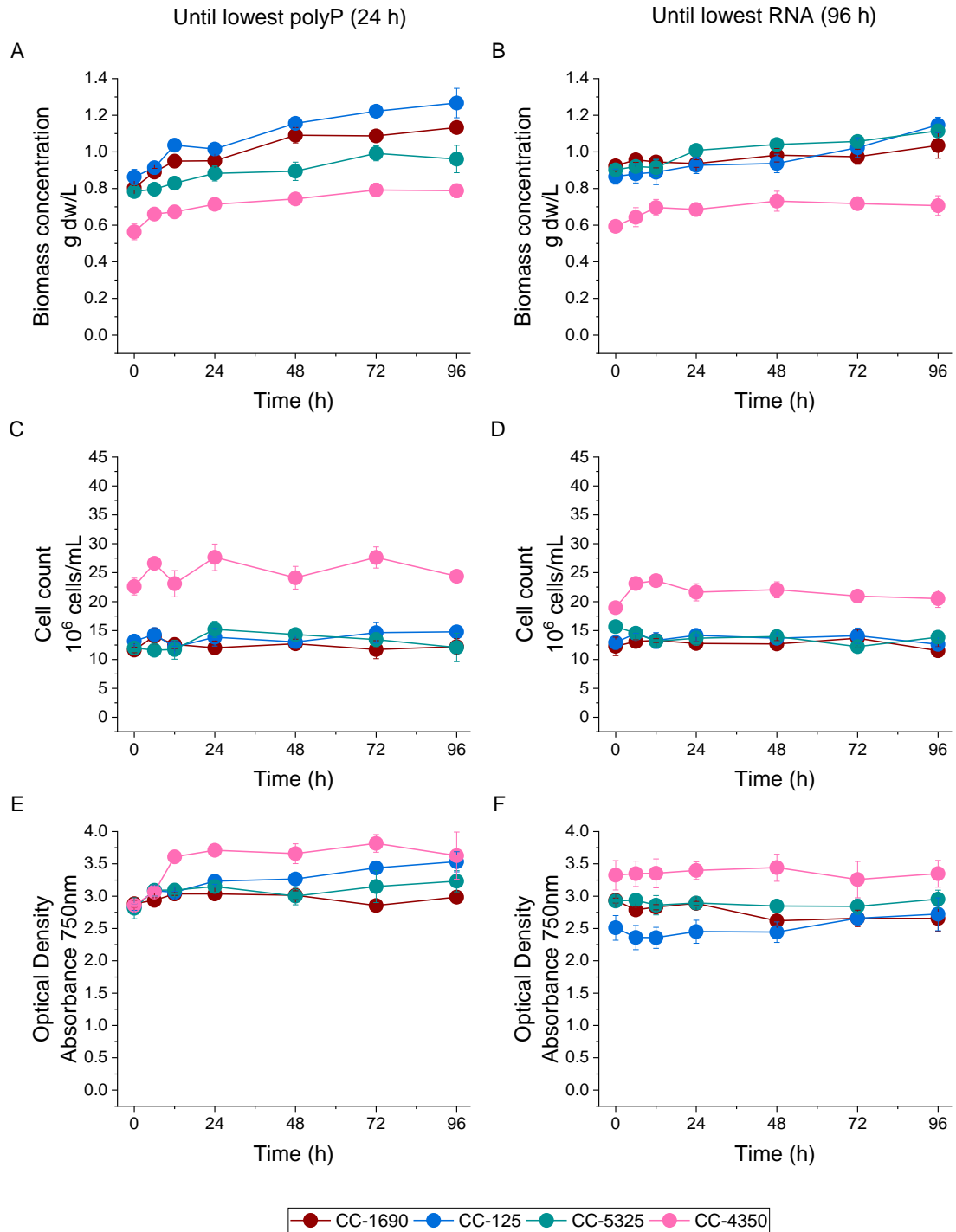


Figure 4.7 *C. reinhardtii* biomass growth during P overplus upon KPO₄ repletion. KPO₄ repletion did not affect P-deprived *C. reinhardtii* (CC-1690, CC-125, CC-5325 and CC-4350) growth. Mid-exponential cells were harvested and resuspended in TA media for 24 h (left) or 96 h (right) and then supplied with 1 mM P with a KPO₄ solution. A-B Biomass concentration (g dw/L), C-D Cell count (10⁶ cells/mL) and E-F Optical density (Absorbance 750nm).

Table 4.3 Growth parameters of P-deprived *C. reinhardtii* after KPO₄ repletion. Values were calculated after P-deprived cells of CC-1690, CC-125, CC5325 and CC-4350 were supplied with 1 mM P with a KPO₄ solution. Values show the average of three biological replicates \pm SE calculated during the whole monitoring period after P repletion

A		Specific growth rate	
KPO ₄ repletion after P-deprivation		(h⁻¹)	
Strain		Until min polyP (24 h)	Until min RNA (96 h)
CC-1690		0.003 \pm 0.001	0.001 \pm 0.001
CC-125		0.004 \pm 0.001	0.003 \pm 0.001
CC-5325		0.003 \pm 0.001	0.002 \pm 0.001
CC-4350		0.003 \pm 0.001	0.002 \pm 0.001

B		Biomass productivity	
KPO ₄ repletion after P-deprivation		(g dw L⁻¹ h⁻¹)	
Strain		Until min polyP (24 h)	Until min RNA (96 h)
CC-1690		0.003 \pm 0.001	0.001 \pm 0.001
CC-125		0.004 \pm 0.001	0.003 \pm 0.001
CC-5325		0.002 \pm 0.001	0.002 \pm 0.001
CC-4350		0.003 \pm 0.001	0.002 \pm 0.001

4.4.2 Longer P-deprivation does not always mean bigger P overplus in *C. reinhardtii*

As mentioned in section 4.3.3 I found three physiological parameters which reached a plateau upon P deprivation at different times: Growth cessation lowest polyP content (24 h) and lowest RNA content (96 h). I tested the effect of both P deprivation periods on P overplus to detect which one triggered the highest polyP accumulation. This is under the hypothesis that a longer P deprivation period should trigger the bigger P overplus as it has been commonly assumed in the literature.

Repletion after P deprivation

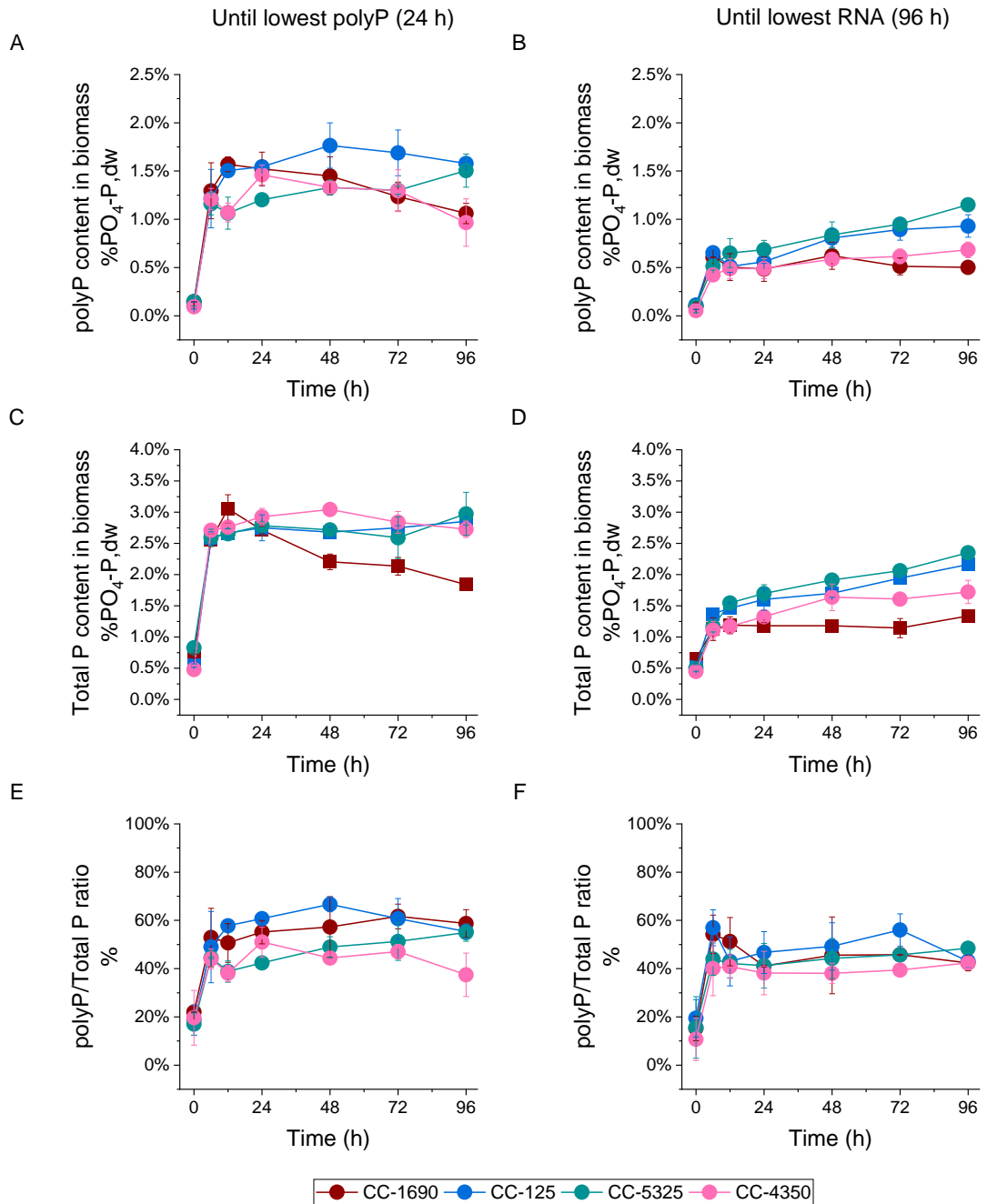


Figure 4.8 Phosphate accumulation of *C. reinhardtii* during P overplus upon KPO₄ repletion.

Bigger P overplus observed in *C. reinhardtii* cells P-deprived until the lowest polyP was observed (24 h) and supplied of 1 mM P. Mid-exponential cells of strains CC-1690, CC-125, CC-5325 and CC-4350 were resuspended in TA media for 24 h (left) or 96 h (Jonkman et al.) and then supplied of 1 mM P with a KPO₄ solution. A-B polyP content in biomass (%PO₄-P, dw), C-D Total phosphate (P) content in biomass (%PO₄-P, dw) and E-F polyP to Total P mass ratio (%w, w)

Contrary to this hypothesis, I found that 24 h P-deprived *C. reinhardtii* cells accumulated more polyP than 96 h P-deprived cultures upon P repletion with KPO₄ (Figure 4.8A and B). Figure 4.8A shows that all 24 h P-deprived strains had a 15-fold increase in their polyP content (going from 0.09% to 1.40%PO₄-P, dw), after only 6 h following P resupply. In contrast, 96 h P-deprived cultures

only exhibited a 6-fold increase in polyP content after 6 h of P addition (**Figure 4.8B**). Total P content in the biomass consistently followed the same pattern as that of polyP (**Figure 4.8C and D**). Interestingly, after the 6 h content peak, polyP or total P levels in 24 h P-deprived cultures did not decrease, but remained stable for the rest of the experiment, except for the strain CC-1690, for which polyP and total P levels decreased by approximately 30% and 40%, respectively. For the strain CC-4350 the polyP levels decreased 30% after the 24 h of KPO₄ repletion but not for total P. For 96 h P-deprived *C. reinhardtii*, polyP and total P accumulation increased after 6 h of P repletion and slowly increased further to reach its maximum value at the end of the experiment for strains CC-125 and CC-5325. Whereas for 96 h P-deprived CC-1690 and CC-4350, polyP and total P content remained stable after the 6 h peak. Overall, the P overplus response was consistent but the slight variation in the P accumulation dynamics may be attributed to differences between strains. The polyP/total P mass ratio (**Figure 4.8E and F**) during P overplus for both P deprivation periods tested, went back up to approximately 50% (w/w). However, the polyP/total P ratio after P repletion was significantly higher in 24 h P-deprived *C. reinhardtii* than in 96 h P-deprived cells (p-value=0.014).

Why a longer period of P deprivation did not trigger a higher polyP accumulation in this experiment? The data indicate that after 96 h of P-deprivation, the organic pools of P (e.g. RNA) were altered, hence counteracting P overplus. **Figure 4.9A** indicates that P-deprivation until the lowest polyP was observed, did not alter the RNA dynamics observed under no P-deprivation conditions (**Figure 4.5A**). Whereas, a longer period of P deprivation until the lowest RNA content (96 h) was reached (**Figure 4.9B**), triggered a completely different pattern in RNA content. Under these conditions, *C. reinhardtii* cells had no variation in the RNA content during the experiment, and P overplus was at least partially inhibited (**Figure 4.8B**). Thus, the observation that RNA was not recovered after P resupply may be a consequence of 1) the state of the cells at the point of repletion (late stationary growth) or 2) that reduced RNA content in biomass upon P deprivation, may have triggered a dormant state in the cells (probably quiescence).

This unique dynamic between polyP and RNA uncovered during this P overplus experiment in *C. reinhardtii* challenges the assumption that the longer the P deprivation, the bigger the P overplus in microalgae. Based on the previous studies mentioned in the introduction of this chapter (section 4.1) and my data, it may be said that this notion is probably valid until the lowest inorganic P levels (polyP) are reached within the cells. My data suggest that interfering with organic pools of P (i.e. RNA, ATP) upon P deprivation has a negative effect on

P overplus. Thus, *C. reinhardtii* cells, P-deprived for 96 h, possibly do not count with the energy (ATP) required to perform an optimum P overplus or to recover their RNA pool.

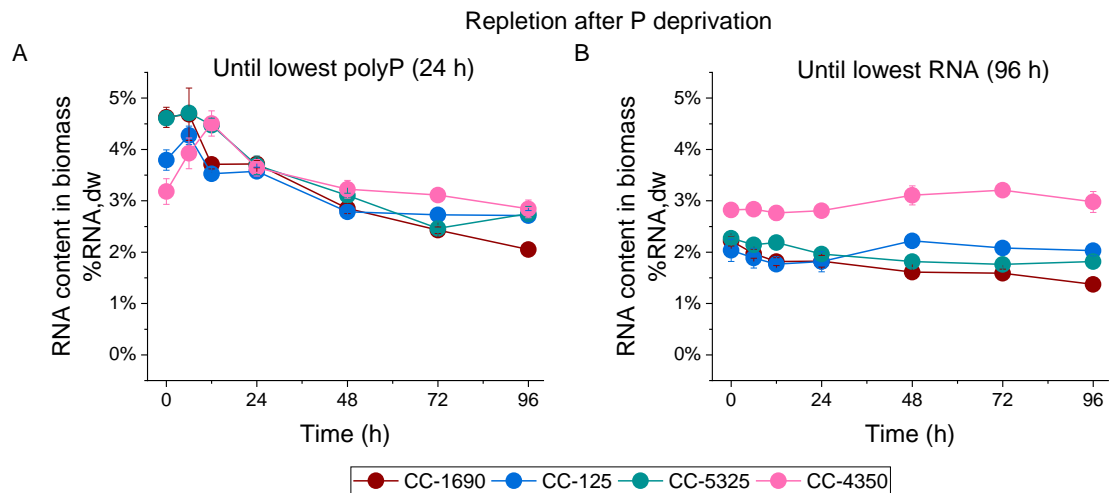


Figure 4.9 RNA content in biomass of P-deprived and KPO_4 repleted *C. reinhardtii* during P overplus. P deprivation until the lowest RNA content was observed (96 h), altered RNA dynamics. Mid-exponential cells of strains CC-1690, CC-125, CC-5325 and CC-4350 were resuspended in TA media for A 24 h or B 96 h and then supplied of 1 mM P with a KPO_4 solution

4.4.3 Unique polyP dynamics are shown for *C. reinhardtii* during phosphate overplus

PAGE was used to determine the pattern in the polyP chain length in *C. reinhardtii* under P overplus after P deprivation for either 24 h or 96 h (**Figure 4.10**). During P deprivation, the polyP size distribution is consistent with PAGE shown in **Figure 4.4C** for the strain CC-1690, showing decreased polyP smear as cells experience P deprivation. This same strain was used in **Figure 4.10** as a representative of the four strains used in this study. When KPO_4 was supplied to P-deprived cells (P repletion), P overplus in the form of polyP over accumulation generated mostly high molecular weight polyP, concentrated at the top of the gel in the first 6 h after repletion. After this time point, polyP is mobilised and degraded into medium and short chain lengths. The pattern in P overplus observed in these gels is consistent for the other three strains CC-125, CC-5325 and CC-4350 (see **Figure A 3** and **Figure A 4**). The pattern in polyP accumulation was very similar for both periods of P deprivation tested. Although lower intensity in the polyP smear was detected in P overplus on 96 h P-deprived CC-1690, as expected, given that this period of resuspension in TA media triggered less polyP accumulation after P addition (**Figure 4.3B**).

Why is polyP mobilised after the 6 h peak, even if cells are in the stationary phase? polyP turnover allows housekeeping of the biomass, even during

stationary growth, where phosphate is needed for the synthesis of organic molecules (DNA/RNA, ATP, phospholipids, etc.). Otherwise, it could also be that an increase in short-chain polyP at later stages of P overplus (after 24 h of P addition) could also allow readily available P to be used in the scenario of resumed growth under low P availability in the environment.

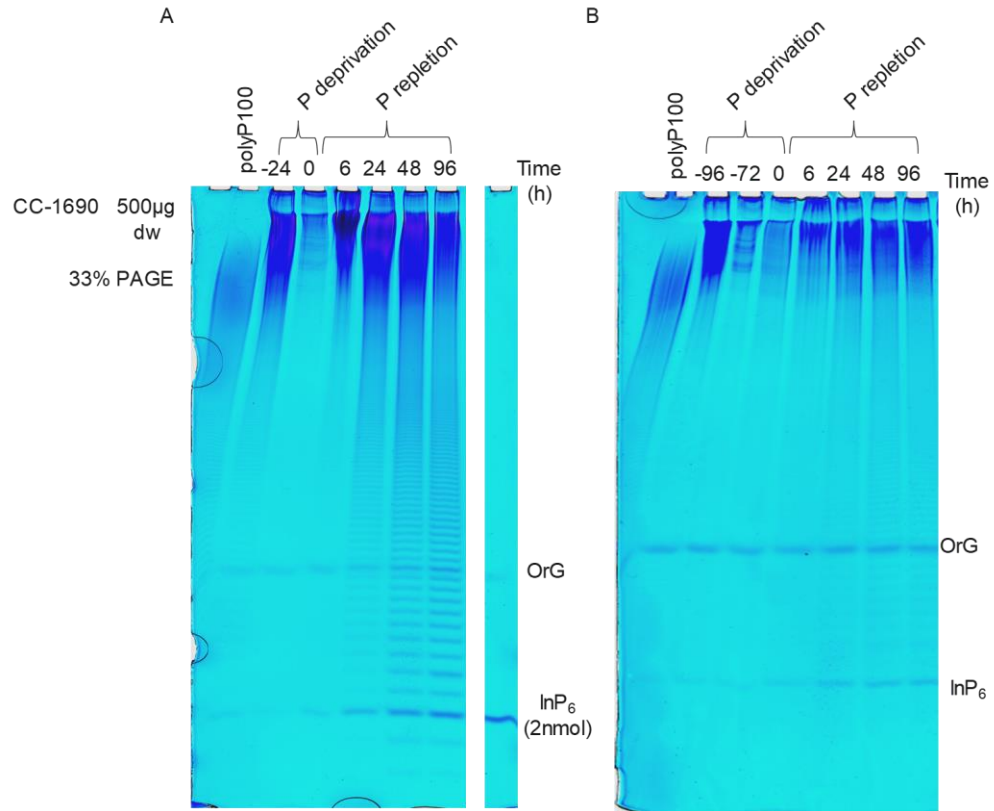


Figure 4.10 PAGE with polyP migration during P-deprivation and P repletion as KPO_4 . 33% PAGE shows polyP migration of strain CC-1690 mid-exponential cells (-24 h and -96 h time point) resuspended in TA media (P deprivation) for A 24 h or B 96 h (-72 h sample is equivalent to 24 h after P deprivation) and supplied of 1 mM P with a KPO_4 solution (P repletion). An equivalent of 500 μ g dw per well was loaded. polyP100 was used as a standard (left side of both PAGES). OrG indicates Orange G dye migration. IP_6 2 nmol standard confirmed the presence of IP_6 . Gel was cut to show only the relevant samples (Uncut gel shown in **Figure 4.3**, in **Chapter 4**). PAGE for strains CC-125, CC-5325 and CC-4350 are shown in **Figure A 3** and **Figure A 4**.

4.4.4 Phosphate overplus was accompanied by an unexpected IP_6 surplus pattern

As mentioned in the section **above**, phosphate repletion led to a rapid polyP accumulation in high polymeric species as observed by PAGE (**Figure 4.10**). PolyP was later mobilised into medium and short chain length forms. This observation is interesting given that the quantification of polyP measured remained overall stable after the 6 h peak (**Figure 4.8A** and **B**). The use of different methodologies for polyP analysis gives a more complete picture of

polyP dynamics as a combination of both quantitative and qualitative approaches.

For instance, by increasing the acrylamide concentration to 33.3% in PAGE, the presence of inositol hexakisphosphate (IP₆), a molecule which can also be stained with toluidine blue dye, was detected in RNA samples extracted at different time points during the P overplus experiment (**Figure 4.10**).

Surprisingly, IP₆ exhibits a completely different overplus pattern compared to polyP. A faint IP₆ signal could be observed 6 h after P repletion. This signal increased in its intensity and reached its maxima at the end of the experiment (96 h). The IP₆ surplus pattern was observed in all four strains of *C. reinhardtii* for both P-deprivation periods (see **Figure A 3** and **Figure A 4**).

4.4.5 *C. reinhardtii* phosphate overplus did not affect the removal of ammonium or sulphate from the media

As a result of the rapid polyP accumulation at the repletion stage of previously P-deprived *C. reinhardtii*, phosphate is removed from the media. **Figure 4.11A** and **B**, show the removal of P for both 24 h and 96 h P-deprived cultures.

Consistently with P accumulation in the biomass (**Figure 4.8C-D**), cells deprived of P until reaching the lowest polyP levels (24 h) achieved a higher P removal efficiency compared to 96 h P-deprived cultures (p-value=5.74x10⁻⁵). Interestingly, for the cultures that were deprived of P for 96 h, I observed significant differences in the percentage of P removal across the strains (p-value=3.23x10⁻⁵), with the strains CC-1690 and CC-5325 achieving the lowest (20%) and highest (63%) removal of phosphate by the end of the monitoring period (96 h), respectively. In contrast, all 24 h P-deprived strains removed 60% of phosphate from the media (p-value=0.25). As a comparison, Plouviez et al. reported the complete removal of P from the media in their experiments after 0.33 mM P supply as KPO₄, in 24 h (Plouviez et al., 2021). Although their initial biomass concentration was approx. half of the one I measured in this experiment (Table S1 in (Plouviez et al., 2021)), they also reported a very low increase in biomass concentration after P supply consistently with **Figure 4.7**.

Furthermore, as in section **4.3.4**, I monitored the concentration of ammonium and sulphate in the media to assess whether P overplus responses affect the removal of other nutrients apart from phosphate. I also wanted to determine if the removal of these nutrients was different between the two P-deprivation periods tested. **Figure 4.11C-F** shows that P overplus did not affect the removal of these nutrients, and neither did the previous P deprivation for 24 or 96 h. For both ammonium and sulphate, there was a low removal rate throughout the experiment and a 30% removal was achieved for the four strains (**Figure 4.11E-**

F). This indicates, under the cultures conditions I tested, that the P overplus phenomena is strictly related to P homeostasis within the cells, and the removal of other nutrients was not necessary to support this response. Probably, given that there was no biomass growth observed (**Figure 4.7**). Lastly, I did not observe any significant differences in the carbon or nitrogen content 24 h after P repletion in either of the P-deprived periods tested in **Table 4.4** (p-value=0.072 and p-value=0.059, respectively).

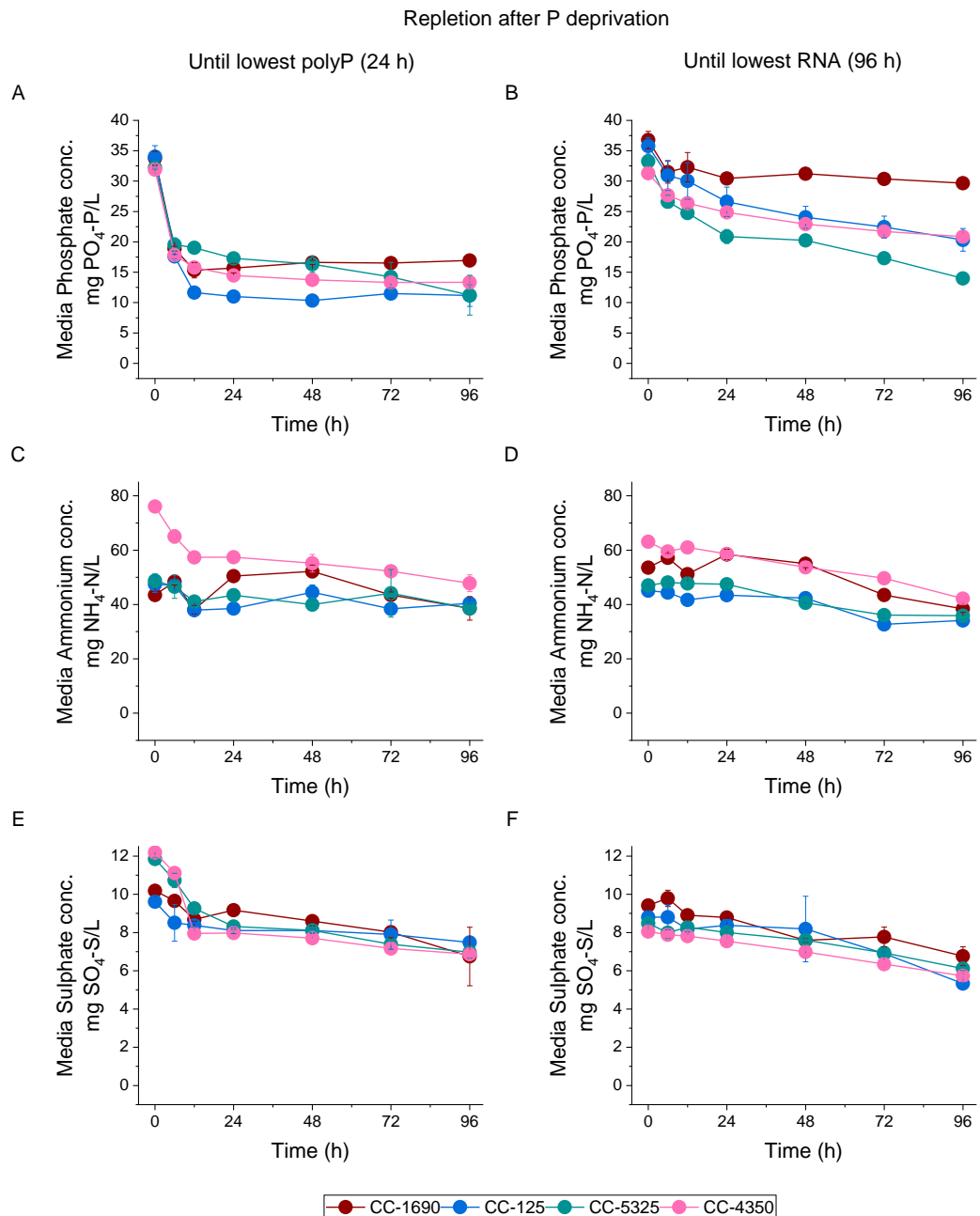


Figure 4.11 Nutrient removal from the media during P overplus upon KPO₄ repletion. Consistent higher phosphate removal was achieved after 24 h P-deprived *C. reinhardtii* was supplied with 1 mM P. Mid-exponential cells of strains CC-1690, CC-125, CC-5325 and CC-4350 were resuspended in TA media for 24 h (left) or 96 h (Jonkman et al.) and then supplied of 1 mM P with a KPO₄ solution. A-B Phosphate concentration in the media (mg PO₄-P/L), C-D Ammonium concentration in the media (mg NH₄-N/L) and E-F Sulphate concentration in the media (mg SO₄-S/L).

Table 4.4 Biomass carbon and nitrogen content during P overplus upon KPO₄ repletion. P-deprivation and repletion did not affect major components of biomass. A Carbon content in biomass (%C,dw) and B Nitrogen content in biomass (%N, dw). Values show carbon and nitrogen contents after (24 h) of KPO₄ repletion for *C. reinhardtii* cells P-deprived for 24 h and 96 h. Average of three biological replicates is shown \pm SE for strains CC-1690, CC-125, CC-5325 and CC-4350

A

KPO ₄ repletion after P deprivation:	%C,dw	
	Until min polyP	Until min RNA
	Strain (24 h)	(96 h)
CC-1690	51.3 \pm 0.2	50.3 \pm 0.4
CC-125	50.3 \pm 0.9	49.2 \pm 0.3
CC-5325	49.5 \pm 0.3	50.7 \pm 0.1
CC-4350	47.9 \pm 0.7	51.3 \pm 0.4
Average	49.8\pm0.7	50.4\pm0.4

B

KPO ₄ repletion after P deprivation:	%N,dw	
	Until min polyP	Until min RNA
	Strain (24 h)	(96 h)
CC-1690	8.8 \pm 0.1	9.4 \pm 0.1
CC-125	9.0 \pm 0.6	9.2 \pm 0.1
CC-5325	9.9 \pm 0.1	9.1 \pm 0.1
CC-4350	9.2 \pm 0.5	9.1 \pm 0.1
Average	9.2\pm0.2	9.2\pm0.1

4.5 Results summary and discussion

In this work, I demonstrate the successful application of polyP quantitative and qualitative analysis methods taken from *S. cerevisiae*, to the green microalgae *C. reinhardtii*. In the *S. cerevisiae* field, quantification of polyP is expressed relative to RNA content (Lonetti et al., 2011). However, for *C. reinhardtii* RNA is the second largest pool of phosphate and therefore is subjected to change during P-limiting conditions. Hence, in the appendix **Figure A 1** and **Figure A 2**, I show that both in quantitative and qualitative methods for polyP analysis under P deprivation polyP content relative to RNA decreases in the first 24 h of resuspension in TA media, but increases later at the 96 h time point. This observation could suggest that polyP was resynthesized using the phosphate released from RNA degradation observed upon P-deprivation (**Figure 4.5B**). Otherwise, polyP levels (relative to RNA content) could have increased solely because RNA content in the biomass decreased after growth terminated. The latter was confirmed by normalising polyP by dry biomass. The pattern in the biomass concentration under P-deprivation shows little change over time after reaching stationary growth and was no different in the control experiment (**Figure 4.1**). Thus, an increase in polyP relative to dry biomass, at the same time point, would lead to arguing whether P is mobilised from RNA to polyP under P deprivation conditions. However, as shown in **Figure 4.3B** and **Figure 4.4C-D**, no increase was observed in polyP content in proportion to the dry biomass of *C. reinhardtii* after 96 h. Overall, these results indicate that polyP quantification relative to RNA is not suitable for the study of P metabolism in *C. reinhardtii*. This is due to its RNA dynamics as a major pool of P (Raven, 2013). Doing so could lead to misinterpretations of the data. Therefore, I chose to express polyP quantification relative to the dry biomass (dw) because it is a more stable parameter and allows a more robust perspective of polyP dynamics in *C. reinhardtii*, using both quantitative and qualitative tools for the study of polyP accumulation during phosphate deprivation and overplus.

The standardisation of these methods highlighted the importance of choosing the appropriate normalisation parameter for polyP analysis. The methods of polyP quantification via Ppx1 treatment and its visualisation through PAGE allowed in-depth monitoring of the physiological behaviour of polyP accumulation during P-deprivation and P overplus. Interestingly, I observed that the variation in the total pool of phosphate in the biomass of *C. reinhardtii* (%PO₄-P,dw) followed the same trend as that of polyP (**Figure 4.3A-D** and **Figure 4.8A-D**). In this project, the development of a quantitative method for polyP allows its comparisons with the total pool of P within the cells. The values I observed for polyP, fall within the spectra reported in Rees et al. study of the

maximum growth hypothesis in photosynthetic organisms that accumulate polyP (Rees and Raven, 2021). In their study, polyP accounts for approximately 42% (w/w) of the total pool of phosphate, which is close to the 50% observed in the P overplus experiment after P repletion (**Figure 4.8E-F**). This value (50% polyP/total P) was also observed in the control experiment in **Figure 4.3E** (no P deprivation), which can be seen as a response to P homeostasis within the cells.

Moreover, the reliability of the polyP method led to the observation in the control experiment (no P-deprivation) that the strain CC-5325 has an enhanced capacity to accumulate polyP (**Figure 4.3A**) and remove phosphate from the media, compared to the other strains (**Figure 4.6A**). To the best of my knowledge, this phenotype is described for the first time on this strain and the genetic basis of it is yet to be uncovered.

The time period of P deprivation has been highlighted in previous literature for its effects on P overplus, but under different experimental conditions and with different species/strains, the physiological status of the cells may be very different (Solovchenko et al., 2019b, Aitchison and Butt, 1973, Plouviez et al., 2023b, Lavrinovičs et al., 2020, Lavrinovičs et al., 2021). The study of P deprivation in four independent strains of *C. reinhardtii* was designed to determine the physiological parameter of P deprivation triggering the biggest P overplus response. My data led to the careful observation that mid-exponential cultures ceased growth (**Figure 4.1**) simultaneously whilst reaching their lowest polyP content (**Figure 4.3B**), which under the culture conditions used, occurred 24 h after resuspension in TA media. These results are consistent with Aitchison and Butt, who reported that growth cessation was not due to exhaustion of nutrients in the media (including phosphate) in non-P-deprived cells. They observed that *C. vulgaris* P-deprived cells continued cell division at about the same rate as non-P-deprived cells, and this coincided with the use of internal reserves of P in the absence of P from the culture media (Aitchison and Butt, 1973). The observation that polyP was never completely depleted, reinforces its other roles apart from P storage (see **Chapter 2** Literature Review section **2.3.1**). Moreover, the finding that RNA content in biomass reached its lowest value further after 96 h of P-deprivation (**Figure 4.5D**) raised the question of whether there was a different effect of P-deprivation until the lowest inorganic or lowest organic P levels were reached, on P overplus. I found that P-deprivation until the lowest inorganic levels of P are reached (polyP), triggered a higher polyP accumulation than when P was deprived until lowest RNA content was reached (**Figure 4.8A**). This result challenges the long-term assumption that longer P deprivation triggers a bigger P overplus. Based on my

findings, we propose a new model for P overplus dynamics (**Figure 4.12**). In this model, 'optimum' P overplus is achieved when P is supplied just after the lowest inorganic P level is reached. Longer P deprivation is thought to interfere with the organic pool of P and negatively affect the state of the cells and their ability to respond to P resupply. This was reflected in lower polyP accumulation and led to a different pattern in RNA content in biomass in this experiment (**Figure 4.8B** and **Figure 4.9B**, respectively). Further research is needed to unveil the mechanism behind these dynamics.

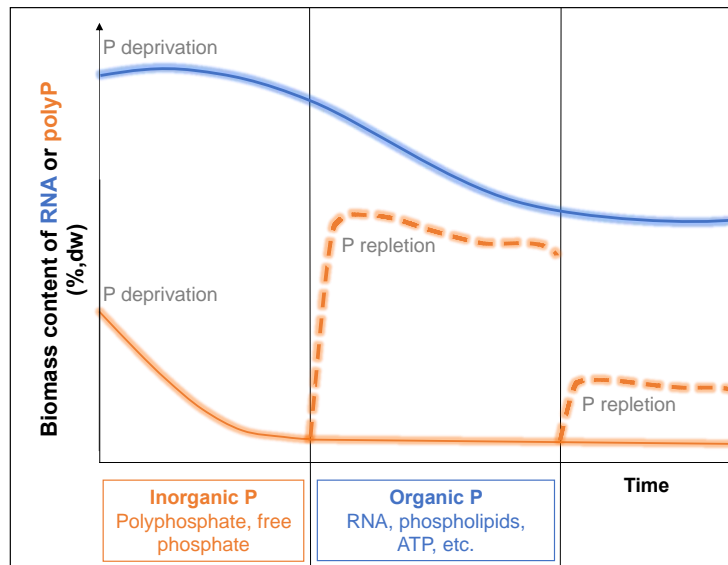


Figure 4.12 A suggested model on the effect of the P deprivation length on microalgal P overplus. Upon P-deprivation (solid lines), microalgae use inorganic P resources first and polyP (orange) reaches its lowest level (not fully degraded). Organic sources of P, like RNA (blue), are consumed after. A longer P deprivation period improves P overplus until the lowest inorganic pool of P content is reached. If P-deprivation conditions run for longer, a negative effect on P overplus will be prompted due to the mobilisation of organic pools of P. This will be reflected in a lower polyP accumulation (weaker P overplus). Dashed strains represent polyP accumulation after P.

Intriguingly, it seems that the original publication from which the assumption that longer P deprivation was better for P overplus goes back to 1973. In this study, Aitchison and Butt showed increased P accumulation when early-stationary *Chlorella vulgaris* cells were P-deprived for at least 24 h (Aitchison and Butt, 1973). Solovchenko et al. P deprivation period tested of **three consecutive days after growth cessation** was detected, coincides with the P deprivation period of 96 h I used in this experiment (Solovchenko et al., 2019b). In their study, they supplied 0.4 mM P to P-deprived *C. vulgaris* CCALA 256 cells and observed a polyP peak of approx. 4% (w/w) after 8 h of P repletion. However, the peak later decreased until reaching initial values before P addition. One explanation for the difference in the pattern of polyP accumulation may be the initial biomass concentration or growth phase at the P repletion stage. For

instance, Solovchenko et al. repleted P-deprived *C. vulgaris* cultures at an optical density at 680nm of absorbance of approx. 0.3 (assuming that cells were in the early exponential phase), and it can be observed how the polyP peak is quickly followed by a sudden decrease as biomass experiences exponential growth (Solovchenko et al., 2019b). Regardless, these last two studies mentioned were performed with another species and the divergent patterns of polyP accumulation during P overplus could be species-dependent.

Even so, the observation in my experiment that polyP levels remained stable after the 6 h peak, contrasts with the results reported in previous P overplus studies where the polyP peak is followed by a decreasing pattern (Solovchenko et al., 2019b, Aitchison and Butt, 1973, Sforza et al., 2018). In these studies, other methods to estimate polyP accumulation are used (e.g. Raman microscopy, DAPI, Total P content in dry biomass). Since different methods have a set of limitations and advantages, there is the question of how comparable these methods may be, as highlighted in Christ et al. review of polyP analysis tools in life sciences (Christ et al., 2020b). Also, Plouviez et al. showed that increased initial biomass concentration before P supply is related to lower total P accumulation during overplus (Plouviez et al., 2023b). Hence, it is not clear whether the inconsistency in the results of the polyP accumulation pattern is due to the use of alternative polyP analysis techniques, microalgae species, or different states of cells at the time of P repletion (lag, exponential, stationary phase). This highlights 1) the gap in standardising methodologies for consistent polyP analysis and P overplus in microalgae and 2) the importance of appropriately reporting on the state of the biomass (growth phase) and its initial concentration at each stage (P deprivation or P repletion).

In terms of polyP accumulation performance, the highest polyP (and total P) for both P deprivation periods at the 6 h peak are comparable with previous P overplus studies on *C. reinhardtii* (Plouviez et al., 2021). Although Plouviez et al. kept the culture in 'low P' for **5 days** and considered it P depleted, it is uncertain whether the state of their culture at the moment of P supply is comparable to one of the P deprivation periods I tested (Plouviez et al., 2021). In a later study, Plouviez et al. tested the effect of P deprivation length on P overplus in *C. reinhardtii* and found an increased rate of P accumulation in biomass with longer P deprivation periods (Plouviez et al., 2023b). When cells were P-deprived for **24 h** and supplied with 0.33 mM P (10 mg PO₄-P /L), P accumulation after 5 h is slightly lower (2.05% PO₄-P,dw) than the one I observed for the same P deprivation period but after 1 mM P supply (31 mg PO₄-P/L). Conversely, when their cultures were P-deprived for **96 h**, P accumulation after 5 h was higher (2.28% PO₄-P,dw) than the one we

observed. The main reason for this is that only after 96 h of P deprivation, the biomass reached its lowest total P content ($\sim 0.5\%$ $\text{PO}_4\text{-P}$, dw) (Plouviez et al., 2023b). In this study, we reached the lowest total P content at approx. 24 h when transferring mid-exponential cells ($\text{OD}_{750\text{nm}}=1.0$) to TA media. After 24 h P deprivation, biomass concentration had increased by 50% (compared to pre-deprivation values) and cells reached the early stationary phase. At 96 h of P deprivation, the second period tested for P overplus, cells were in a late stationary phase. Goodenough et al. showed in their study that *C. reinhardtii* cells in the stationary phase retain more polyP than log phase cells (Goodenough et al., 2019). Also, early stationary cells have been found to accumulate more polyP upon P re-supply (after P starvation) than exponential growth cells of *C. vulgaris* (Aitchison and Butt, 1973). It appears more effective to use microalgal cultures at this growth stage, to obtain higher accumulation of polyP.

Furthermore, I show that *C. reinhardtii* P overplus response generated mostly long-chain polyP in the first 6 h (**Figure 4.10**), confirming for the first time that this process of accumulation occurs likewise in yeast (Gerasimaitė et al., 2014, Gerasimaitė and Mayer, 2016). This observation was accompanied by the fact that long-chain polyP was later mobilised into shorter chain lengths. Even though there was no biomass growth observed, which would require the use of internal sources of P (**Figure 4.7**). Solovchenko et al. hypothesized the biological need for microalgae to accumulate polyP in this long-chain fashion, in their literature review and later studies (Solovchenko et al., 2019a, Lobakova et al., 2023, Solovchenko et al., 2019b). Nascent short-chain polyP may be simultaneously translocated to the acidocalcisomes by the VTC complex and elongated into long-chain polyP, to avoid polyP toxicity when located in the cytosol (Li et al., 2018). Solovchenko et al. postulated that one of the possible reasons for polyP toxicity in the cytosol is related to its uncovered role as a stabilising scaffold for protein folding intermediates in yeast (Solovchenko et al., 2019a, Xie and Jakob, 2019). Xie and Jakob et al. showed in their review that bacterial long-chain polyP can help to prevent protein aggregation to keep proteins soluble under stress conditions. Even though this role for polyP has not been uncovered in microalgae, the fact that the polyP length pattern matches that observed in yeast reinforces this hypothesis. However, further research is needed to confirm or validate this theory in microalgae.

My data also revealed the divergent pattern of IP_6 /polyP accumulation during P overplus (**Figure 4.10**) which challenges the presumption about the role of the IP_6 /PP-IPs pathway in polyP synthesis via the SPX domain of the VTC complex. This opens the possibility of IP_6 /PP-IPs role in polyP mobilisation or turnover

which is yet to be assessed. (Solovchenko et al., 2019a). During P overplus, the observation of IP₆ accumulating, even after reaching a polyP peak (6 h) was unexpected. *C. reinhardtii* and other species (Cliff et al., 2023) harbour a VTC complex with an SPX domain, similar to that of *Saccharomyces cerevisiae*, which is stimulated by the IP₆-derived inositol pyrophosphates (PP-IPs) (Wilson et al., 2013, Azevedo and Saiardi, 2017). The synthesis of IP₆/PP-IPs senses the ATP level (as a P donor for polyP synthesis) (Aksoy et al., 2014) and basic metabolism processes regulated by phosphate availability (Wang et al., 2021). Thus, it is hypothesized that the polyP synthesis mechanism in *C. reinhardtii* is also catalysed by an SPX-containing VTC complex, via the binding of inositol pyrophosphate 7 (IP₇) to the SPX domain (Wild et al., 2016). IP₆ is a precursor of IP₇ synthesis, via the IP₆ kinase KCS1 (Saiardi et al., 1999, Draškovič et al., 2008) or VIP1 (Lee et al., 2007, Onnebo and Saiardi, 2007), the latter with a homolog identified in *C. reinhardtii* (Couso et al., 2016). Hence, the presence and quantity of IP₆ suggests the presence of IP₇ or other PP-IPs. Furthermore, Plouviez et al. use neomycin treatment to confirm the role of IPs in polyphosphate synthesis (Plouviez et al., 2021). Neomycin is an aminoglycoside antibiotic which binds to the precursor of IPs and thus is considered to inhibit IPs synthesis. In their study, they observed approximately 80% less phosphate accumulation in cultures treated with neomycin than in the control, which suggests that IPs play an expected role in polyP synthesis. However, this study does not report the state of the biomass before and after the treatment, and whether the use of the antibiotic could have a toxic effect on *C. reinhardtii*, which could affect growth and hence phosphate accumulation.

In my experiment, the fact that IP₆ accumulation occurred later after polyP concentration reached its highest value, suggests that the IP₆/PP-IPs signalling pathway is unlikely the one activating polyP synthesis by the VTC complex. The question may be whether another role of IP₆ is involved in polyP mobilisation since the accumulation of IP₆ is accompanied by the degradation of long-chain polyP peak into medium and short-chain polyP in *C. reinhardtii* P overplus. Further research is needed to understand the polyphosphate synthesis mechanism and regulation in *C. reinhardtii* and other microalgae.

Lastly, higher polyP accumulation was observed together with enhanced phosphate removal from the media (**Figure 4.11A**). However, phosphate was not close to being completely depleted from the media. Additionally, I confirmed that P overplus did not enhance the removal of ammonium or sulphate (**Figure 4.11C-F**) nor it changed the biomass composition of carbon or nitrogen (**Table 4.4**)

Chapter 5 The effect of nutrients other than P on *Chlamydomonas reinhardtii* phosphate overplus response

5.1 Introduction

The phosphate overplus response is composed of two stages: P-deprivation and P-repletion. In **Chapter 4**, I focused mainly on the effect of P-deprivation on P overplus. In this present chapter, I focused on the effect of P repletion on P overplus. In the literature, P-deprived cultures are subjected to P-repleted conditions with either chemical addition of phosphate (as potassium or sodium phosphate) or resuspension in fresh media (or wastewater) (Plouviez et al., 2021, Solovchenko et al., 2019b, Lavrinovičs et al., 2020). The fact that the latter replenishes P-deprived cells with other nutrients as well as P, generated the question of whether the addition of other nutrients at the time of P repletion could affect *C. reinhardtii* P overplus response. Here, I assess this hypothesis by 1) modifying the standard experimental design of the P overplus experiment in **Chapter 4**, by supplying P as fresh TAP media containing all nutrients, and 2) comparing monitored parameters of biomass growth, P accumulation and nutrient removal from the media against those observed in KPO₄ repleted cultures from the previous chapter.

One question arising from the methodology used above to supply all nutrients (biomass harvesting and resuspension in TAP media), is how the different treatment of the biomass (the transfer from P-deprived to P-replete conditions) could affect the results. In the previous P overplus experiment, TAP repletion involved a centrifugation step, where the old culture media is discarded and microalgal cells are resuspended in fresh TAP media to trigger P overplus. In contrast, for P repletion, a volume of a KPO₄ solution was added to the P-deprived culture. In another experiment (referred to as the second P overplus experiment) I used two strains of *C. reinhardtii* (CC-1690 and CC-125) to test a different methodology. In the second section of this chapter, I avoided the factor of either centrifugation of biomass or discarding old media, to test whether these factors had an effect on P overplus, microalgal growth and nutrient removal from the media. The strains were P-deprived for 24 h and 96 h following the same protocol as in the first P overplus experiment. P-deprived cultures were both supplied with 1 mM P with a KPO₄ solution. To test the effect of nutrient addition apart from P, one group of cultures was supplied with a 5xTA (Tris-Acetate) solution (see **Chapter 3** Material and Methods section **3.3.5**) (1/5 v/v) and the same volume of sterile ddH₂O was added to the second group. To note, this experimental design, adds another factor to the analysis.

The group where ddH₂O was added is diluting the existing nutrients in the media used for P-deprivation (TA), whereas the group where 5xTA was added confers nutrients in excess to the ones existing in the P-deprived media.

To the best of my knowledge, the role of additional nutrients and the interdependence between nutrients has been poorly examined and represents an important research gap in the understanding of microalgal P overplus in more realistic scenarios where phosphate is often present with other nutrients (e.g. waste stabilisation ponds, wastewater treatment plants, etc).

5.2 Objective

To assess the role of nutrient availability, other than P, on P overplus at the P repletion stage using *C. reinhardtii*

5.3 First P overplus experiment

5.3.1 P repletion together with all other nutrients triggered biomass growth

P-deprived *C. reinhardtii* cells that reached minimum polyP (24 h) or RNA (96 h), were harvested and resuspended in fresh TAP media, to assess whether P repletion together with other nutrients (TAP media) affected microalgal growth during P overplus. Microalgal growth was monitored with the following parameters (**Figure 5.1**): biomass concentration (g dw/L), cell count (10⁶ cells/mL) and optical density (Absorbance 750nm). All strains of *C. reinhardtii* exhibited biomass growth when repleted with all nutrients in contrast with KPO₄ (P) repletion¹. This is unsurprising since TAP media provided both macro and micronutrients for P-deprived *C. reinhardtii* to resume growth. **Figure 5.1A, C** and **E** show biomass growth during the first 12 h after TAP repletion of 24 h P-deprived cells, which led to an average biomass productivity of 0.026 g L⁻¹ h⁻¹ for all the strains (**Table 5.1C**). Furthermore, no difference was observed (p-value=0.42) in the specific growth rates of the four strains (24 h P-deprived **Table 5.1A**). A similar biomass productivity was observed when cells that had been P-deprived for 96 h were resuspended in TAP media (0.025 g L⁻¹ h⁻¹). However, the average specific growth rate for all the strains, in this case, was significantly lower in 96 h P-deprived cultures repleted with TAP than in 24 h P-deprived cultures (p-value=0.03). This was mainly due to the strain CC-125

¹ To facilitate the clarity of the analysis, I have added the error bars shown in Chapter 4 corresponding to KPO₄ repletion analysis parameters as shaded segments in Figures 5.1, 5.2, 5.4 and 5.5.

which exhibited a considerably lower specific growth rate when P-deprived for 96 h and resuspended in TAP, which suggests that this strain has more sensitivity to P-deprivation. As reported in **Chapter 4**, differences in the doubling times of the strain CC-4350 are due to the characteristic cell size of this strain (**Figure 4.2**). The results show unsurprisingly that P supply together with other nutrients promoted an average 76% increase in biomass growth for both 24 and 96 h P-deprived cells. This is in contrast to the results in **Chapter 4** where identical cultures were resupplied with 'KPO₄' P only (**Figure 4.7**)

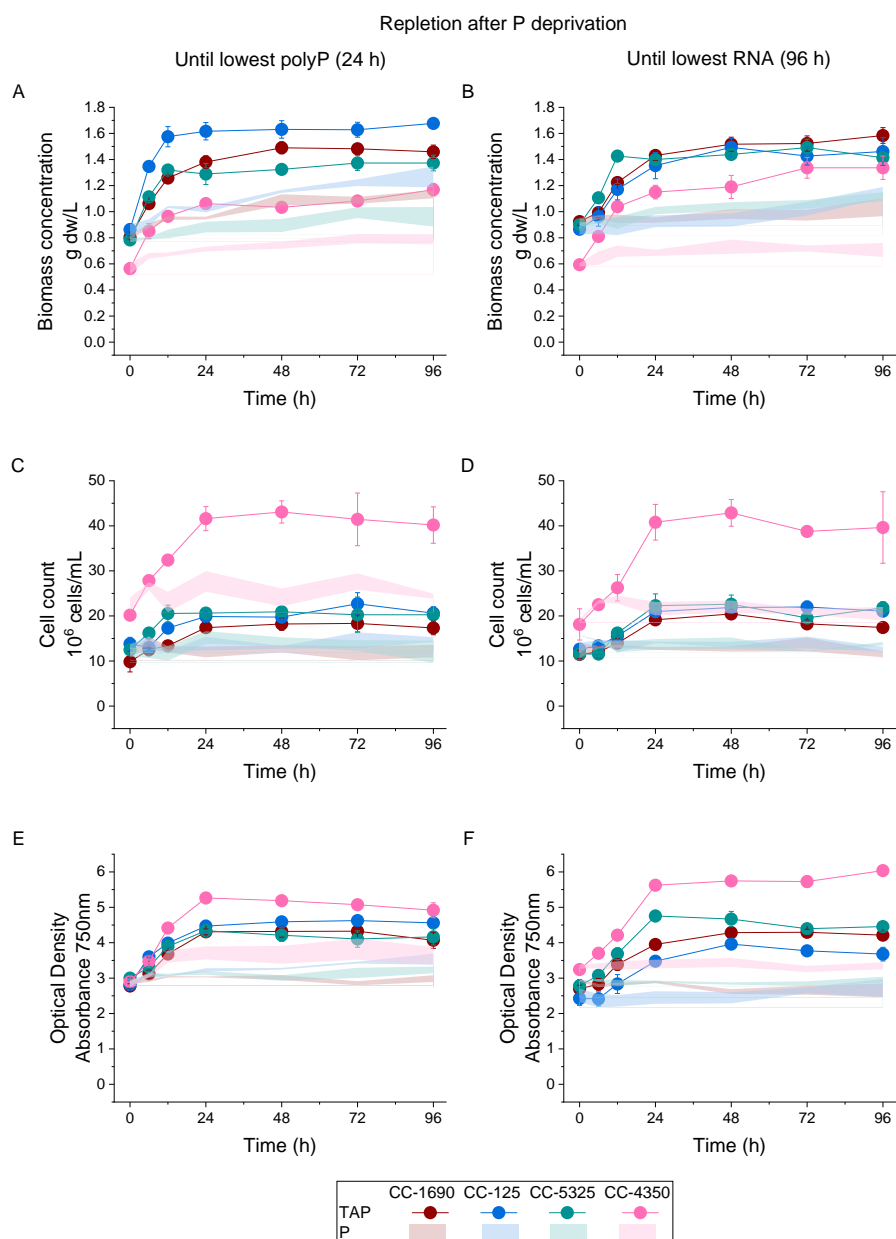


Figure 5.1 *C. reinhardtii* biomass growth during P overplus after resuspension in TAP media. Mid-exponential cells (strains CC-1690, CC-125, CC-5325 and CC-4350) were resuspended in TA media for 24 h (left) or 96 h (right) and then resuspended in fresh TAP media (1 mM P). A-B Biomass concentration (g dw/L), C-D Cell count (10⁶ cells/mL) and E-F Optical density (Absorbance 750nm). Shaded segments show the area covered by the error bars from parameters observed during KPO₄ (P) repletion from **Chapter 4** for reference (**Figure 4.7**).

Table 5.1 Growth parameters of TAP repleted *C. reinhardtii* during P overplus. P-deprived cells were resuspended in fresh TAP media. Values show the average ($n=3$) \pm SE calculated for the exponential growth phase after P repletion (see Chapter 3 Materials and Methods section 3.7.1)

A		Specific growth rate	
TAP repletion after	(h⁻¹)		
P-deprivation	until min	until min	
Strain	polyP (24 h)	RNA (96 h)	
CC-1690	0.034 \pm 0.006	0.024 \pm 0.001	
CC-125	0.050 \pm 0.007	0.019 \pm 0.003	
CC-5325	0.036 \pm 0.006	0.038 \pm 0.002	
CC-4350	0.035 \pm 0.011	0.034 \pm 0.006	
Average	0.039 \pm 0.004	0.029 \pm 0.005	
B		Doubling time	
TAP repletion after	(h)		
P-deprivation	until min	until min	
Strain	polyP (24 h)	RNA (96 h)	
CC-1690	39.3 \pm 4.4	33.8 \pm 3.5	
CC-125	40.6 \pm 12.2	34.9 \pm 8.3	
CC-5325	33.1 \pm 1.2	28.3 \pm 5.8	
CC-4350	14.1 \pm 0.9	22.5 \pm 0.9	
Average	31.8 \pm 6.1	29.9 \pm 2.8	
C		Biomass productivity	
TAP repletion after	(g dw L⁻¹ h⁻¹)		
P-deprivation	until min	until min	
Strain	polyP (24 h)	RNA (96 h)	
CC-1690	0.024 \pm 0.002	0.026 \pm 0.001	
CC-125	0.039 \pm 0.006	0.020 \pm 0.003	
CC-5325	0.021 \pm 0.004	0.030 \pm 0.002	
CC-4350	0.021 \pm 0.002	0.023 \pm 0.003	
Average	0.026 \pm 0.004	0.025 \pm 0.002	

5.3.2 PolyP accumulation during P overplus is not influenced by the availability of other nutrients apart from P

To assess the effect of nutrient availability on phosphate overplus I monitored polyP and total P accumulation in the biomass (**Figure 5.2A-D**) after P-deprived *C. reinhardtii* cultures were resuspended in fresh TAP media. The comparison between these results with those reported in the KPO₄ repletion experiment from **Chapter 4** (from **Figure 4.8**) and represented by the shaded segments, shows that the availability of other nutrients did not affect polyP accumulation during P overplus (**Figure 5.2A-B**). This observation was independent of the P deprivation state (lowest polyP or RNA) (p-value=0.45 at 6 h time point). On the contrary, total P accumulation in biomass after 6 h of P resupply (**Figure 5.2C-D**) was significantly higher (p-value=6.99x10⁻⁵) in cultures resuspended in TAP media compared to KPO₄ repleted cultures (**Figure 4.8C-D** in **Chapter 4**). Probably this is due to the increase in biomass growth (**Figure 5.1**) which generates a higher demand for key organic molecules containing phosphate (DNA/RNA, ATP, phospholipids, etc.). Consistently, the polyP to total P mass ratio is no different according to repletion as KPO₄ or TAP (**Figure 5.2E-F**). Interestingly, after 96 h of P-deprivation and P repletion with all nutrients, one of the strains (CC-5325) exhibited a clear increase in both polyP and total P accumulation compared to the other strains. However only total P content was significantly higher (p-value=0.0047 at 24 h time point) compared to the other strains (CC-1690, CC-125 and CC-4350). This observed phenotype adds to the one observed in **Figure 4.3A-C** from **Chapter 4**, where without P deprivation, the strain CC-5325 accumulated a higher polyP and total P content compared to the other strains.

Furthermore, the observation that polyP accumulation is independent of the availability of other nutrients (**Figure 5.2**), led to question whether biomass growth demand for phosphate, observed under TAP repletion, could affect polyP chain length dynamics observed in **Chapter 4**. PAGE was used to visualise polyP accumulation for both periods of P deprivation and P repletion types. **Figure 5.3** shows PAGE with polyP migration during its accumulation in the phosphate overplus experiment. No differences in the pattern of polyP chain length were observed after P or TAP repletion. PolyP was accumulated in the first hours as long chains and later mobilised into medium and shorter chain lengths. Consistently, more polyP was accumulated in 24 h P-deprived cultures than in the 96 h P-deprived group, as discussed in section **4.4.2** of **Chapter 4**. This finding further rejects the hypothesis that nutrient availability during P overplus affects biomass phosphate (especially polyP) accumulation. In this

same trend, the IP_6 surplus pattern observed remained unaltered according to the P repletion type and still diverted from that of polyP accumulation.

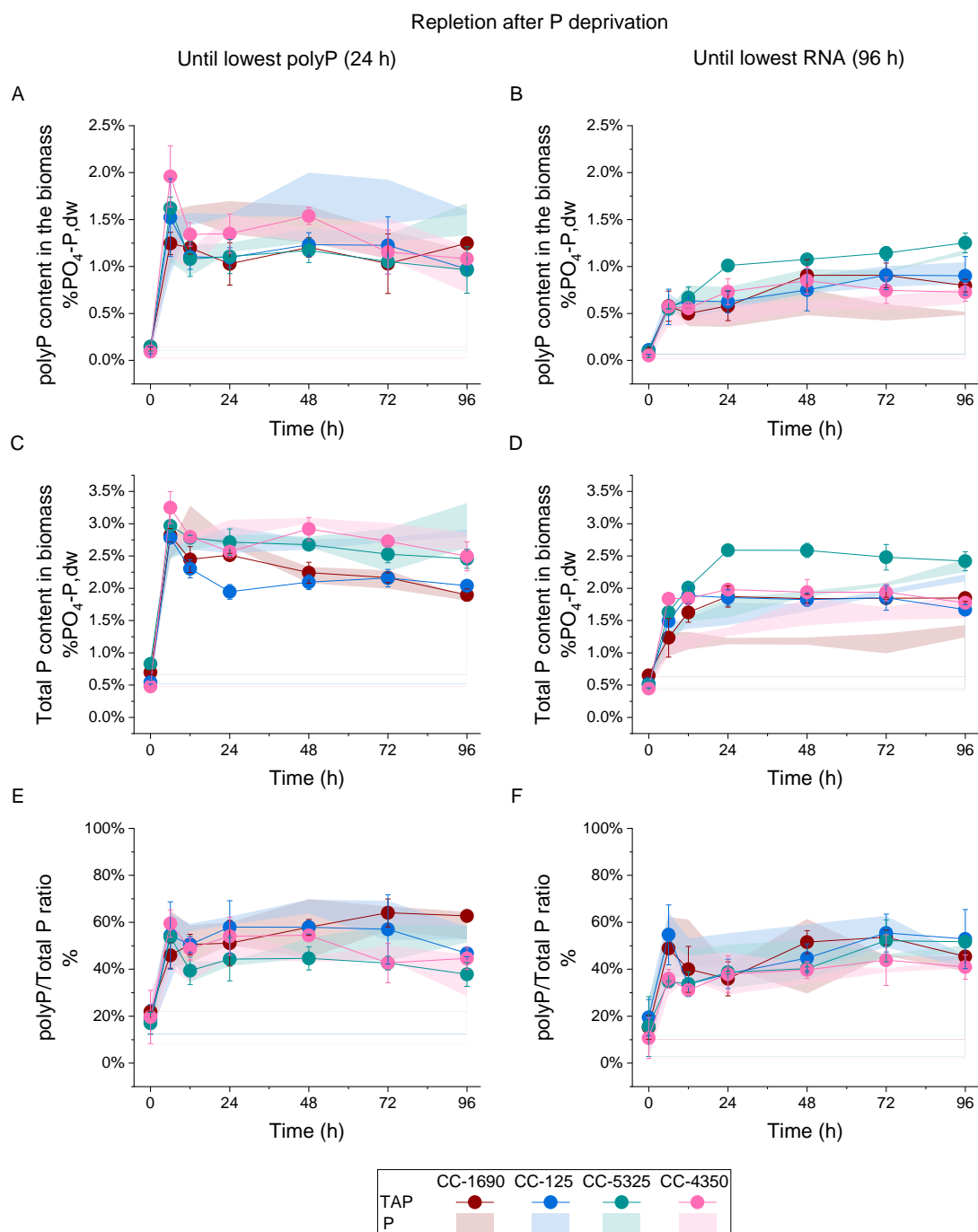


Figure 5.2 Phosphate accumulation of *C. reinhardtii* during P overplus upon TAP repletion. Repletion with all nutrients does not affect P overplus. Mid-exponential cells (strains CC-1690, CC-125, CC-5325 and CC-4350) were resuspended in TA media for 24 h (left) or 96 h (right) and then resuspended in fresh TAP media (1 mM P). A-B polyP content in biomass (% PO_4 -P,dw), C-D Total P content in biomass (% PO_4 -P,dw) and E-F polyP to total P mass ratio (% w/w). Shaded segments show the area covered by the error bars from the same parameters observed during KPO_4 repletion from **Chapter 4** for reference (**Figure 4.8**)

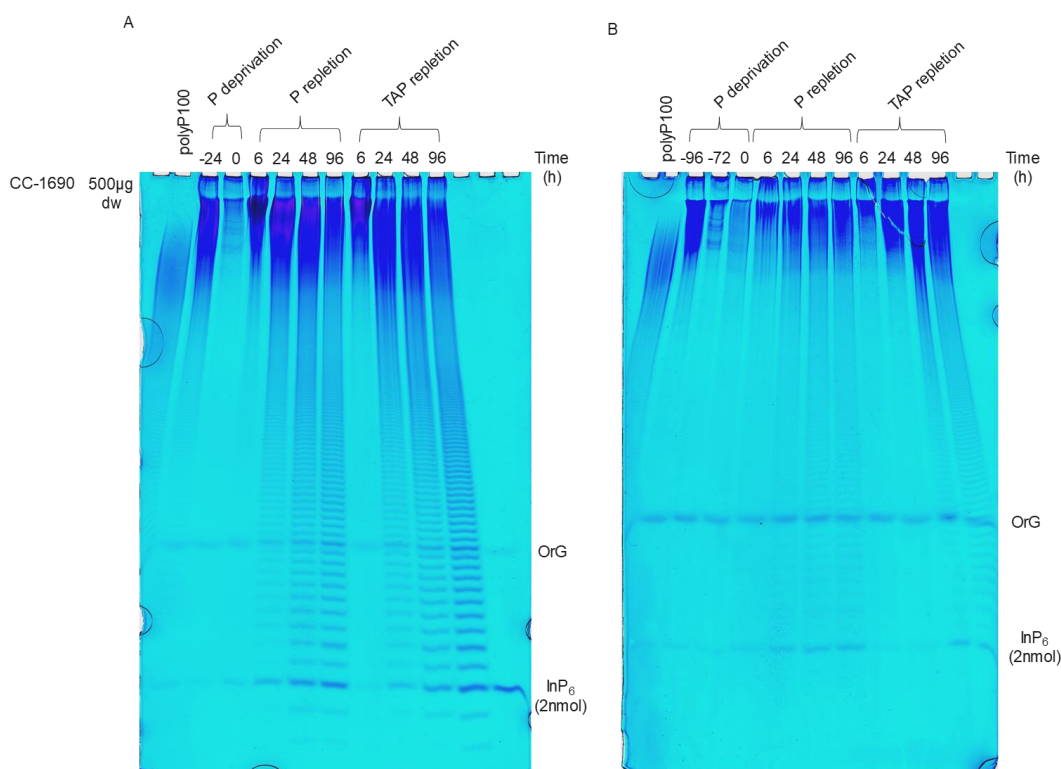


Figure 5.3 PAGE with polyP migration during P deprivation and P repletion as KPO_4 or TAP media. P repletion as TAP does not affect polyP or IP_6 dynamics of P overplus. 33% PAGE shows polyP migration of strain CC-1690 mid-exponential cells (-24 h and -96 h time point) resuspended in TA media (P deprivation) for A 24 h or B 96 h (-72 h sample is equivalent to 24 h after P deprivation) and supplied of 1 mM P with either a KPO_4 solution (P repletion) or resuspended in fresh TAP media (TAP repletion) and monitored for 96 h. An equivalent of 500 μg dw per well was loaded. polyP100 was used as a standard (left side of both PAGES). OrG indicates Orange G dye migration. IP_6 2 nmol standard confirmed the presence of IP_6 . PAGE images for the strains CC-125, CC-5325 and CC-4350 are shown in **Figure A 3** and **Figure A 4**.

5.3.3 RNA recovery occurs only upon P repletion together with all nutrients in 96 h P-deprived cultures

As mentioned in section 4.4.2 of **Chapter 4**, a period of 96 h of P deprivation resulted in reduced P overplus. Under this condition, a strong reduction of RNA content was observed compared to the control (no P deprivation) and 24 h P-deprived cultures. Since RNA is an organic molecule containing carbon, nitrogen and phosphorus (Geider and Roche, 2002), the hypothesis is that P repletion with all nutrients, after 96 h of P-deprivation, could trigger an RNA recovery response, in contrast with KPO_4 repleted cultures (**Figure 4.9A**).

Figure 5.4 shows RNA content in the biomass for both P deprivation periods and repletion types (the P-only data from the **Figure 4.9** in **Chapter 4** is shown by shading for comparison). P repletion type after a P deprivation until minimum polyP content (24 h) was reached, did not affect RNA content (**Figure 5.4A**). On the contrary, for 96 h P-deprived cells, the P repletion type (KPO_4 /TAP) affected

RNA content. Reduced RNA content in biomass upon 96 h P-deprivation (**Figure 4.5B** in **Chapter 4**), seemed to induce a quiescent state in the cells. After 96 h of P deprivation, at the P depletion stage, RNA recovery was observed if P was supplied together with all other nutrients in TAP media (**Figure 5.4B**). This observation together with lower polyP accumulation indicates a switch in the metabolism towards RNA recovery rather than polyP accumulation.

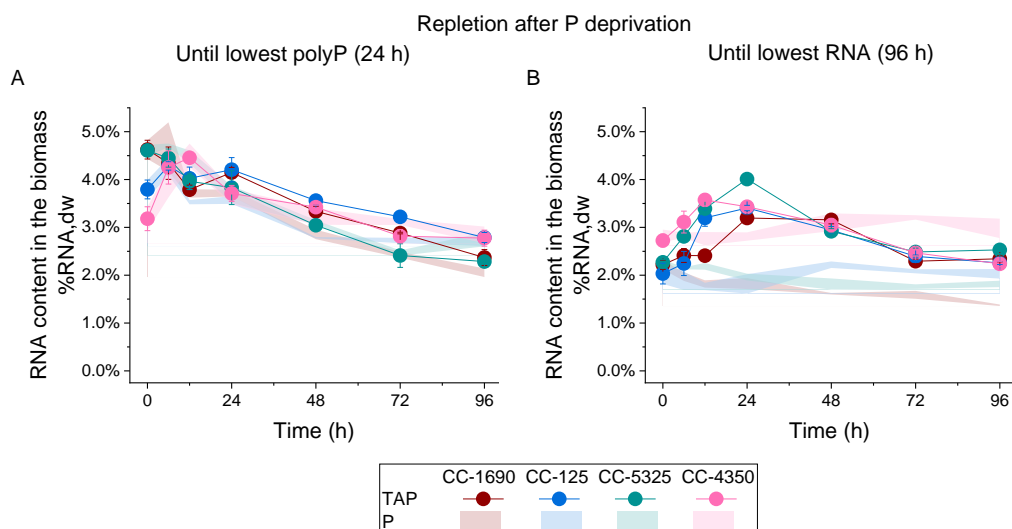


Figure 5.4 RNA content in biomass of 24 h and 96 h P-deprived *C. reinhardtii* during P overplus. RNA is recovered in 96 h P-deprived cells only if P is replenished with all other nutrients (TAP media). Mid-exponential cells (strains CC-1690, CC-125, CC-5325 and CC-4350) were resuspended in TA media for A 24 h or B 96 h and then resuspended in fresh TAP media (1 mM P). Shaded segments show the area covered by the error bars from parameters observed during KPO_4 depletion from **Chapter 4** for reference (**Figure 4.9**).

5.3.4 Biomass growth upon TAP repletion resulted in enhanced nutrient removal

While nutrient availability did not affect P overplus, I observed that P supply together with other nutrients enhanced P removal by promoting biomass growth. **Table 5.2** shows the P removal performance of the four strains after both P-deprivation periods tested and repletion as 'P' only (KPO_4) or all nutrients (TAP). A period of 24 h of P deprivation followed by a supply of all nutrients (**Figure 5.5A**) led to the complete removal of P from the media in only 12 h, in contrast with the average 60% of P removal obtained in KPO_4 repleted cultures (see **Figure 4.11A Chapter 4**). *C. reinhardtii* cells P-deprived until the lowest RNA content was observed (96 h), removed P more slowly and less extensively than cells that had been P-deprived until the lowest polyP was detected. Nonetheless, the difference between P only and complete nutrient repletion was retained for all strains (**Figure 5.5B**).

Of note is the behaviour of strain CC-5325. This line removed 65% and 63% of P by the end of the experiment after both 24 h and 96 h P deprivation periods and repletion with KPO_4 , at the end of the experiment (see **Figure 4.11A** and **B Chapter 4**). Meanwhile in the cultures repleted with TAP, the strain CC-5325 (24 and 96 h P deprived) was the only one to remove all P from the media. Otherwise, a period of 96 h of P deprivation followed by TAP repletion, let the other strains remove P from the media up to a minimum value ranging between 7-10 mg PO_4 -P/L. Overall, enhanced P removal occurred upon P repletion as resuspension in fresh TAP media, coinciding with biomass growth (**Figure 5.1**).

Table 5.2 Phosphate removal performance according during the P overplus experiment according to P-deprivation and P repletion type.

Values represent the average ($n=3$) \pm SE. The percentage value was calculated with the initial and last concentration of phosphate in the media according to each P-deprivation period and P-repletion type.

Repletion after P-deprivation	% P removal from the media			
	until min polyP (24 h)		until min RNA (96 h)	
	Strain	KPO_4	TAP	KPO_4
CC-1690	52% \pm 2	100%	19% \pm 3	71% \pm 5
CC-125	66% \pm 3	100%	53% \pm 4	64% \pm 10
CC-5325	65% \pm 10	100%	63% \pm 3	100%
CC-4350	58% \pm 1	100%	33% \pm 3	82% \pm 4
Average	60% \pm 4	100%	42% \pm 3	79% \pm 5

Furthermore, phosphate was not the only nutrient with an improved removal rate and efficiency. **Figure 5.5C-F** show the media concentration of ammonium and sulphate at the P repletion stage. In comparison with KPO_4 repleted cultures (shaded segments), TAP repletion improved the removal of these nutrients. It is important to remember that during the P-deprivation experiment from the previous chapter, mid-exponential cultures kept growing at the same rate as the control experiment (**Figure 4.1** in **Chapter 4**). This caused further depletion of other nutrients needed for biomass generation, like ammonium and sulphate (**Figure 4.6D** and **F**, respectively in **Chapter 4**). Therefore, the concentration of these nutrients in KPO_4 repleted cultures did not change over time, because there was no growth. Repletion with all nutrients increased the ammonium and sulphate concentration to the levels expected in TAP media (~110 mg NH_4 -N/L and ~13 mg SO_4 -S/L, respectively). Provision of these

nutrients, assisted microalgal cells to resume growth, which was reflected in the removal of these nutrients from the media, alongside phosphate.

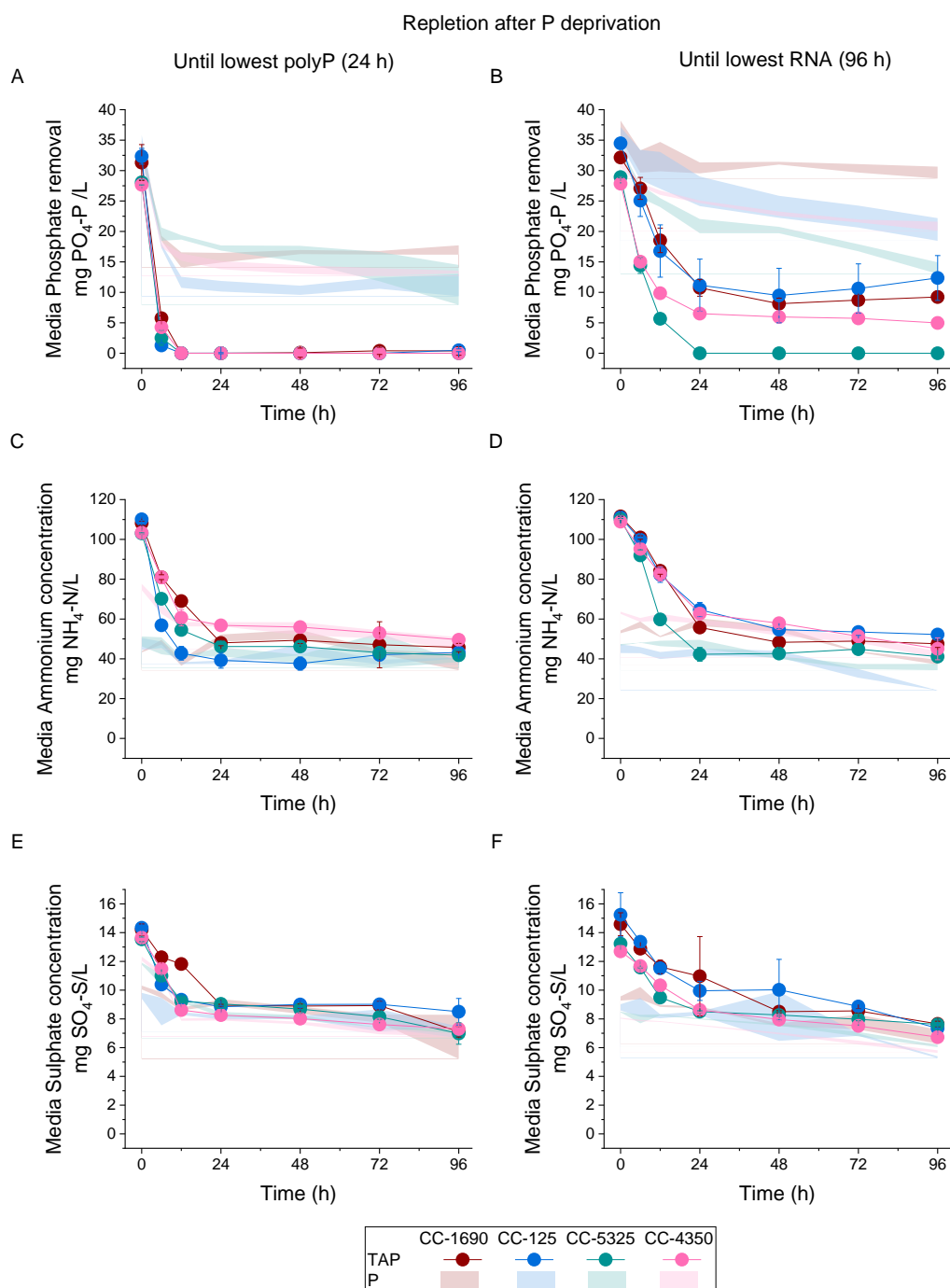


Figure 5.5 Phosphate, ammonium and sulphate concentration in the media during P overplus of 24 h and 96 h P-deprived cultures. Provision of all nutrients apart from P after P deprivation, enhanced nutrient removal. Mid-exponential cells of strains CC-1690, CC-125, CC-5325 and CC-4350 were resuspended in TA media for 24 h (left) or 96 h (right) and then resuspended in fresh TAP media. A-B Phosphate concentration in the media (mg PO₄-P/L), C-D Ammonium concentration in the media (mg NH₄-N/L) and E-F Sulphate concentration in the media (mg SO₄-S/L). Shaded segments show the area covered by the error bars from parameters observed during KPO₄ repletion from **Chapter 4** for reference (**Figure 4.11**).

All the strains followed a very similar trend in the removal of both nutrients during the period of growth and reached a plateau at the level of approximately 40 mg NH₄-N/L and 8 mg SO₄-S/L, approximately. At the end of the growth period (between 12 h-24 h), the cultures might have become stationary due to light limitation (as the biomass concentration was high and self-shading could occur due to culture density), or due to nutrient availability at the balance required by *Chlamydomonas*. The strain CC-5325 depleted ammonium from the media at a faster rate, although not significantly (**Figure 5.5D**). Interestingly, this observation appears to coincide with the enhanced phosphate removal observed in 96 h P-deprived cells of CC-5325, repleted with TAP (**Figure 5.5B**).

Moreover, I calculated the phosphate (PO₄-P), ammonium (NH₄-N) and sulphate (SO₄-S) uptake rates (**Table 5.3**) during the first 24 h after P repletion (P-only and TAP) for the average values of four strains of *C. reinhardtii* (see **Chapter 3** Materials and Methods section **3.7.1**). The values were calculated in the segments of 0-6 h, 6-12 h and 12-24 h when the most rapid changes were observed during the experiment. Except for ammonium in the group of 96 h P-deprived cells repleted with TAP, the highest nutrient uptake rates were observed during the first 6 h, which coincides with the polyP accumulation peak observed in **Figure C-D**. In the first 6 h segment, the highest nutrient uptake rates were obtained in the cultures deprived of P until the lowest polyP (24 h) and repleted with TAP media (highlighted in **bold** in **Table 5.3**). In contrast, the lowest nutrient uptake rates were observed for 96 h P-deprived cultures, repleted with KPO₄. Since the analysis of the nutrient uptake rates over time and according to the P-deprivation state and P repletion type can be complex due to the number of variables, I decided to use principal component analysis (PCA) (see **Chapter 3** Materials and Methods section **3.7.3**). This tool provides a multivariable evaluation of these factors to enable a compiled perspective of how nutrients affect P overplus in *C. reinhardtii* under my experimental conditions (**Figure 5.6**).

Table 5.3 Nutrient uptake rates of *C. reinhardtii* cells during P overplus according to P-deprivation state and P repletion type. Average values (n=3) for the four strains were used \pm SE. nn corresponds to values below 0.1 mg g dw⁻¹ h⁻¹

A				
P deprivation	Repletion type	Phosphate uptake rate		
		(mg PO ₄ -P g dw ⁻¹ h ⁻¹)		
	P/TAP	0-6 h	6-12 h	12-24 h
Until min	P	3.31 ± 0.24	0.72 ± 0.13	nn
polyP (24 h)	TAP	5.94 ± 0.28	0.57 ± 0.11	nn
Until min	P	1.03 ± 0.07	0.23 ± 0.05	0.27 ± 0.04
RNA (96 h)	TAP	2.25 ± 0.33	1.31 ± 0.08	0.38 ± 0.03
B				
P deprivation	Repletion type	Ammonium uptake rate		
		(mg NH ₄ -N g dw ⁻¹ h ⁻¹)		
	P/TAP	0-6 h	6-12 h	12-24 h
Until min	P	1.64 ± 0.39	1.94 ± 0.26	nn
polyP (24 h)	TAP	7.41 ± 0.57	2.50 ± 0.42	0.60 ± 0.18
Until min	P	0.40 ± 0.21	0.53 ± 0.14	0.44 ± 0.06
RNA (96 h)	TAP	2.81 ± 0.33	3.38 ± 0.40	1.42 ± 0.13
C				
P deprivation	Repletion type	Sulphate uptake rate		
		(mg SO ₄ -S g dw ⁻¹ h ⁻¹)		
	P/TAP	0-6 h	6-12 h	12-24 h
Until min	P	0.22 ± 0.05	0.15 ± 0.04	nn
polyP (24 h)	TAP	0.59 ± 0.05	0.26 ± 0.06	nn
Until min	P	nn	nn	nn
RNA (96 h)	TAP	0.33 ± 0.07	0.28 ± 0.03	nn

PCA reduces the dimensionality of all the variables under different treatments and allows the integration of all the factors into principal components that explain the variance across treatments. In this case, the first two principal components (PC1 and PC2) in **Figure 5.6** accounted for 91.9% of the variance across the data. PC1 (representing 71.48% of the correlation), explains the effect of the addition of nutrients apart from P on the nutrient uptake rates. PC2 (representing 18.41% of the correlation) accounts for the effect of P addition only. The loading vectors (blue lines) show that the initial concentration of ammonium and sulphate in the media are positively correlated with PC1 and with all three nutrient uptake rates, whereas only initial P concentration in the media and P uptake rate had a positive correlation with PC2. The principal component scores (dots) represent the P repletion time segments (0-6 h, 6-12 h and 12-24 h) for 24 and 96 h P-deprived *Chlamydomonas*, repleted with P only or complete nutrients (TAP). The score's position according to the direction of a particular loading vector indicates the strength of the correlation towards a specific variable. For instance, we can say that in the first 6 h of P supply, the phosphate uptake rates of KPO_4 repleted cultures are strictly correlated with P addition only. On the other side, all three nutrient uptake rates in TAP-repleted cultures are strongly correlated with nutrient availability in the media. As time passed (6-12 h and 12-24 h), the strength of correlation to each component weakens. It is interesting, given that for both periods of P deprivation, polyP accumulation was no different if P was supplied together with all other nutrients (**Figure 5.2**). P uptake rate is positively correlated with both PC1 and PC2. However, when P-deprived cells were supplied with all nutrients in TAP, more P was taken up together with other nutrients supplied, to sustain biomass growth (**Figure 5.1**). The dynamic observed in the PCA analysis (**Figure 5.6**) together with the biomass concentration data (**Figure 5.1**) shows that nutrient uptake drives biomass growth and vice versa.

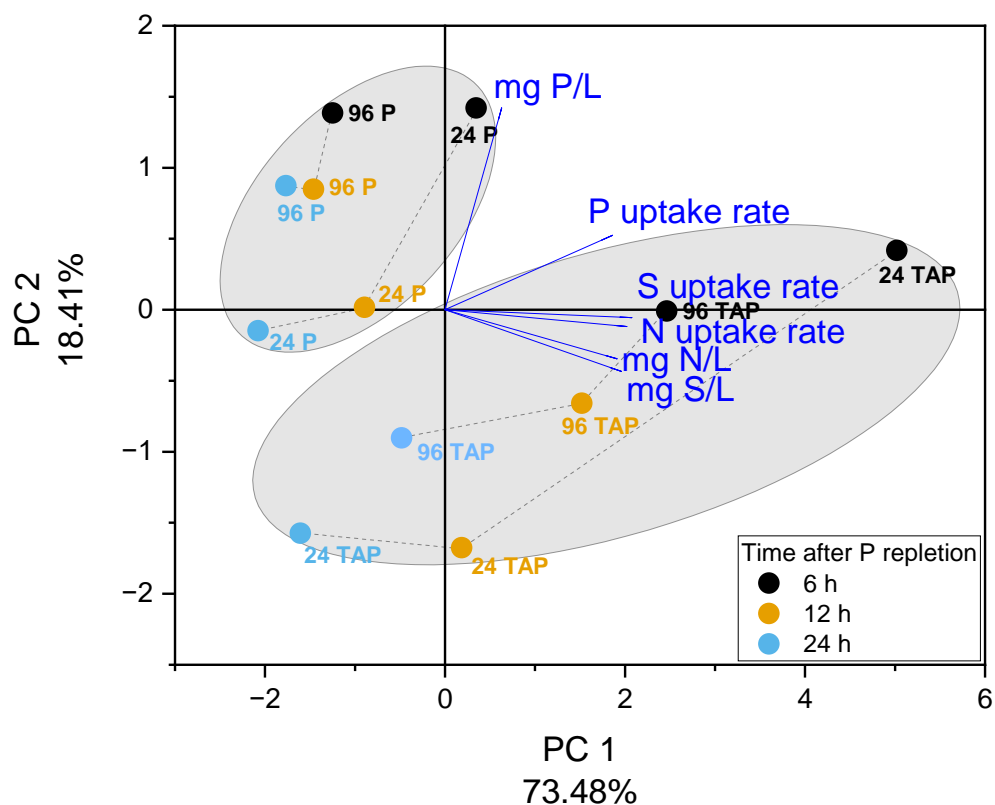


Figure 5.6 PCA analysis of the effect of P-deprivation and nutrient availability on P overplus in *C. reinhardtii*. For the average of four strains (CC-1690, CC-125, CC-5325 and CC-4350) the biplot shows the principal component 1 (x-axis) explaining 73.48% and principal component 2 (y-axis) explaining 18.41% of the correlation of the nutrient uptake rates with the initial nutrient concentration in the media (PO₄-P, NH₄-N, SO₄-S in mg/L). The loading vectors close together indicate the parameters with more similar variance. The dots show the values calculated for each of the six parameters (loading vectors), 6, 12 and 24 h after repletion of 1 mM P with either P (KPO₄ solution) or resuspended in fresh TAP media, of 24 or 96 h P-deprived cells. Ellipses group the dots and loading vectors according to P repletion type.

Lastly, since the uptake of nutrients in **Table 5.3** varied according to P-deprivation state and P repletion type, I wanted to evaluate whether the biomass composition would change depending on nutrient availability. To do so, I used the data from the biomass composition of KPO₄ repleted cultures from the previous chapter (**Table 4.4**) and the carbon and nitrogen biomass content of cultures resuspended in TAP media, shown in **Table 5.4**. Statistical analysis showed that neither the P-deprivation state nor the P repletion type affected carbon content in biomass (p-value=0.18). Otherwise, nitrogen content in the biomass was affected by the P-deprivation period (p-value=1.12x10⁻⁶), but not by nutrient availability at the repletion stage (p-value=0.41). Higher N content in the biomass was observed in cultures P-deprived until the lowest RNA was observed (96 h) and repleted with TAP than in 24 h P-deprived cultures repleted with TAP. This observation indicates that a higher demand for nitrogen was required to recover the RNA pool.

Table 5.4 Biomass composition of *C. reinhardtii* 24 h after resuspension in TAP media during P overplus. A Carbon content in biomass (%C,dw) and B Nitrogen content in biomass (%N, dw). Values show carbon and nitrogen contents 24 h after resuspension in TAP for *C. reinhardtii* cells P-deprived for 24 h and 96 h. Average of three biological replicates is shown \pm SE for strains CC-1690, CC-125, CC-5325 and CC-4350

A		%C,dw	
TAP repletion after P deprivation:		until min	until min
Strain		polyP (24 h)	RNA (96 h)
CC-1690		51.4 \pm 0.2	48.4 \pm 0.5
CC-125		51.6 \pm 0.1	48.3 \pm 0.2
CC-5325		47.3 \pm 0.2	49.3 \pm 0.1
CC-4350		46.9 \pm 0.3	49.5 \pm 0.2
Total average		49.3\pm1.3	48.9\pm0.3
B		%N,dw	
TAP repletion after P deprivation:		until min	until min
Strain		polyP (24 h)	RNA (96 h)
CC-1690		7.1 \pm 0.1	9.8 \pm 0.1
CC-125		7.7 \pm 0.3	9.6 \pm 0.1
CC-5325		8.4 \pm 0.2	9.9 \pm 0.1
CC-4350		9.0 \pm 0.1	9.5 \pm 0.1
Total average		8.1\pm0.4	9.7\pm0.1

5.4 Second P overplus experiment

5.4.1 Reduced biomass growth observed in P-deprived cultures supplied of P with excess nutrients

In this section, I wanted to evaluate the effect of nutrient availability on P overplus using a methodology that avoids centrifugation and discarding of old media (second P overplus experiment). In the first P overplus experiment (section **above**), I compared the two most common methodologies to test P overplus, which is by adding a volume of a KPO_4 solution to the P-deprived cultures versus harvesting of P-deprived biomass by centrifugation and resuspension in fresh media. Since the treatment of the P-deprived biomass before P repletion was not exactly the same, I wanted to assess if the centrifugation step could have affected negatively the P overplus performance or the growth of *C. reinhardtii*. One group of P-deprived cultures were supplied with nutrients other than P with a 5xTA solution (1/5 v/v), whereas for the second group, an equal volume of ddH₂O was added (Excess vs. Diluted nutrients compared to TAP media). For both groups, 1mM P was supplied with a KPO_4 solution. Biomass concentration (g dw/L) was monitored from the beginning of phosphate repletion. The variation of biomass growth was compared to the results obtained in the previous P overplus experiment, reflected by the shaded segments², for the strains CC-1690 and CC-125 (**Figure 5.7**). To note, the initial biomass concentration after P repletion in the second P overplus experiment is lower than that of the first experiment, due to the volume addition of either 5xTA or ddH₂O.

Interestingly, the biomass concentration pattern in the second P overplus experiment (**Figure 5.7**) was similar to that of the first P overplus experiment (**Figure 5.1**), for both experiments for both repletion types (P/TAP, ddH₂O+P/5xTA+P) and P-deprivation periods (24 h and 96 h). Phosphate repletion together with all nutrients stimulated biomass growth in contrast with KPO_4 (P) repleted cultures.

² To facilitate the clarity of the analysis, I have added the error bars calculated for the monitor parameters during the P overplus experiment A (strains CC-1690 and CC-125) as shaded segments from **Figure 5.7-Figure 5.10**

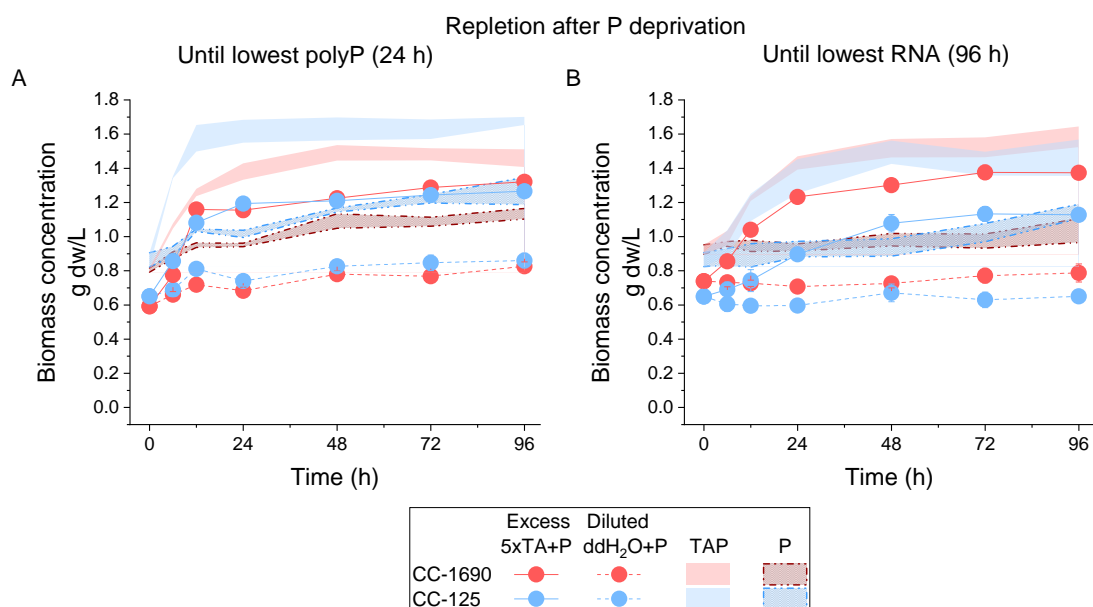


Figure 5.7 *C. reinhardtii* biomass growth after P supply in the second P overplus experiment. Mid-exponential cells (strains CC-1690 and CC-125) were resuspended in TA media for A 24 h or B 96 h and then supplied with 1 mM P with a KPO₄ solution. Nutrients were supplied to one group of cultures, with a 5xTA solution (1/5 v/v) and the same volume of sterile ddH₂O was added to the other group. Graphs show biomass concentration (g dw/L). Shaded segments show the area covered by the error bars from parameters observed in the P overplus experiment, where P was supplied as either KPO₄ (P) or TAP (**Figure 5.1A** and B).

For the 24 h P-deprived cultures, no significant differences were observed in the specific growth rates (p -value=0.96), and biomass productivity (p -value=0.38) between the first (**Table 5.1**) and second (**Table 5.5**) P overplus experiments (TAP vs. 5xTA+P). Interestingly, for the 24 h P-deprived cultures, I observed an opposite pattern in the specific growth rates of the strain CC-1690 and CC-125. The strain CC-1690 exhibited a higher specific growth rate in the first P overplus experiment (TAP) than in the second (5xTA+P), whereas CC-125 had a lower specific growth rate in the second P overplus experiment (5xTA+P) than in the first (TAP). This observation suggests that there are differences in the response to different nutrient levels that may be strain-dependent. Otherwise, in the 96 h P-deprived cultures, I observed lower specific growth rates and biomass productivity when P repletion was done with excess nutrients (5xTA+P) than by resuspension in fresh TAP media (p -value=0.01). No differences were observed in the growth parameters of diluted P-repleted and P-repleted cultures that were P-deprived for 96 h (p -value=0.93), as these were negligible (barely detected or undetected) in both groups. The strain CC-125 appeared to be more sensitive to the 5xTA+P repletion after a 96 h period of P-deprivation than the strain CC-1690, as it exhibited half the specific growth rate and biomass productivity than CC-1690.

Table 5.5 Growth parameters during *C. reinhardtii* P overplus after P supply in the second P overplus experiment. P-deprived cells of CC-1690 and CC-125 were supplied 1 mM P with a KPO₄ solution. Excess nutrients were supplied with a 5xTA solution (1/5 v/v) and the same volume was added in sterile ddH₂O to dilute existing nutrients in the other group. Values show the average of three biological replicates \pm SE calculated for each strain during the period that fitted an exponential growth model after P repletion (see **Chapter 3** Materials and methods **3.7.1**). ud accounts for ‘undetected’

A		Specific growth rate (h ⁻¹)			
		until min polyP (24 h)		until min RNA (96 h)	
Repletion after P deprivation	Strain	ddH ₂ O+P	5xTA+P	ddH ₂ O+P	5xTA+P
	CC1690	0.003 \pm 0.001	0.048 \pm 0.003	0.001 \pm 0.001	0.021 \pm 0.002
	CC125	0.003 \pm 0.001	0.037 \pm 0.005	ud	0.010 \pm 0.001

B		Biomass productivity (g dw L ⁻¹ h ⁻¹)			
		until min polyP (24 h)		until min RNA (96 h)	
Repletion after P deprivation	Strain	ddH ₂ O+P	5xTA+P	ddH ₂ O+P	5xTA+P
	CC1690	0.002 \pm 0.001	0.041 \pm 0.007	0.001 \pm 0.001	0.022 \pm 0.002
	CC125	0.002 \pm 0.001	0.032 \pm 0.004	ud	0.009 \pm 0.001

5.4.2 PolyP accumulation pattern altered in P-deprived cells supplied with P with both excess and diluted nutrients

The finding in section **5.3.2** that P overplus was not affected by nutrient availability was determined by supplying P to P-deprived cells with either KPO₄ or as a resuspension in TAP media in the first P overplus experiment (**Figure 5.2**). Since the treatment of the P-deprived cells at the moment of P repletion was not the same, I wanted to determine whether the effect of centrifugation, used to replace P-deprivation media with fresh TAP media could have influenced the results observed in **Figure 5.2**. To do so, I monitored polyP and total P content in the biomass after P-deprived cells of *C. reinhardtii* were supplied with 1 mM P with either KPO₄ (P)+ddH₂O or 5xTA+P (**Figure 5.8**).

The effect of P repletion type on P overplus was noticeable during the second experiment in 24 h P-deprived cultures (**Figure 5.8A**). After the first 6 h of P repletion, a higher polyP accumulation was observed in cultures repleted of P with diluted nutrients (ddH₂O+P) than with excess nutrients (5xTA+P) until the end of the monitoring period. This observation was also consistent with the pattern of total P accumulation for the same P-deprivation period (**Figure 5.8C**). The biomass P accumulation observed in the second P overplus experiment for the 24 h P-deprived cultures, diverges from the first P overplus experiment where no differences were observed between KPO₄ repletion or resuspension in resuspension in TAP media (shaded segments). Overall, the effect of 5xTA+P repletion against resuspension in TAP media was greater than that of ddH₂O+P and P repletion, in terms of polyP accumulation: After 24 h of P-deprivation, polyP accumulation after 'P' only repletion, was only statistically different at the 24 h timepoint (p-value=0.003 P vs. ddH₂O+P). Whereas for cultures repleted with all nutrients polyP accumulation was lower in cultures supplied with 5xTA+P at all time points except for the first 6 h of repletion (p-value at 6, 24 and 96 h time points: 0.21, 0.03 and 0.04 in **Figure 5.8A**).

For the cultures that had been deprived of P for 96 h, ddH₂O+P repleted cultures appear to have an overall higher polyP accumulation than that of 5xTA+P repleted cultures, which was significant at the 6 h and 96 h timepoint (p-value=0.027 and 0.003, respectively). The polyP content of the cultures was not significantly different between TAP and 5xTA+P repleted cultures at the 24 h timepoint (p-value=0.12). However, cultures resuspended in TAP media exhibited a steady increase in polyP accumulation in contrast with 5xTA+P repleted cultures where a 24 h peak was followed by a steady decrease (**Figure 5.8B**). This difference is more evident for total P accumulation (**Figure 5.8D**). Thus, in comparison with the first P overplus experiment, the polyP accumulation pattern may differ especially when changing the method of nutrient supply, or due to the nutrient balance (resuspension in TAP media vs. 5xTA+P addition).

As in the first P overplus experiment (**Figure 5.2**) and the data reported in **Chapter 4 (Figure 4.8)**, a bigger P overplus was observed after P-deprivation had just reached the lowest polyP content, compared to a longer period of P-deprivation which disturbs the organic pools of P. Finally, I did not observe a different polyP to total P mass ratio for both periods of P-deprivation between the first and second P overplus experiments (**Figure 5.8E-F**).

Repletion after P deprivation

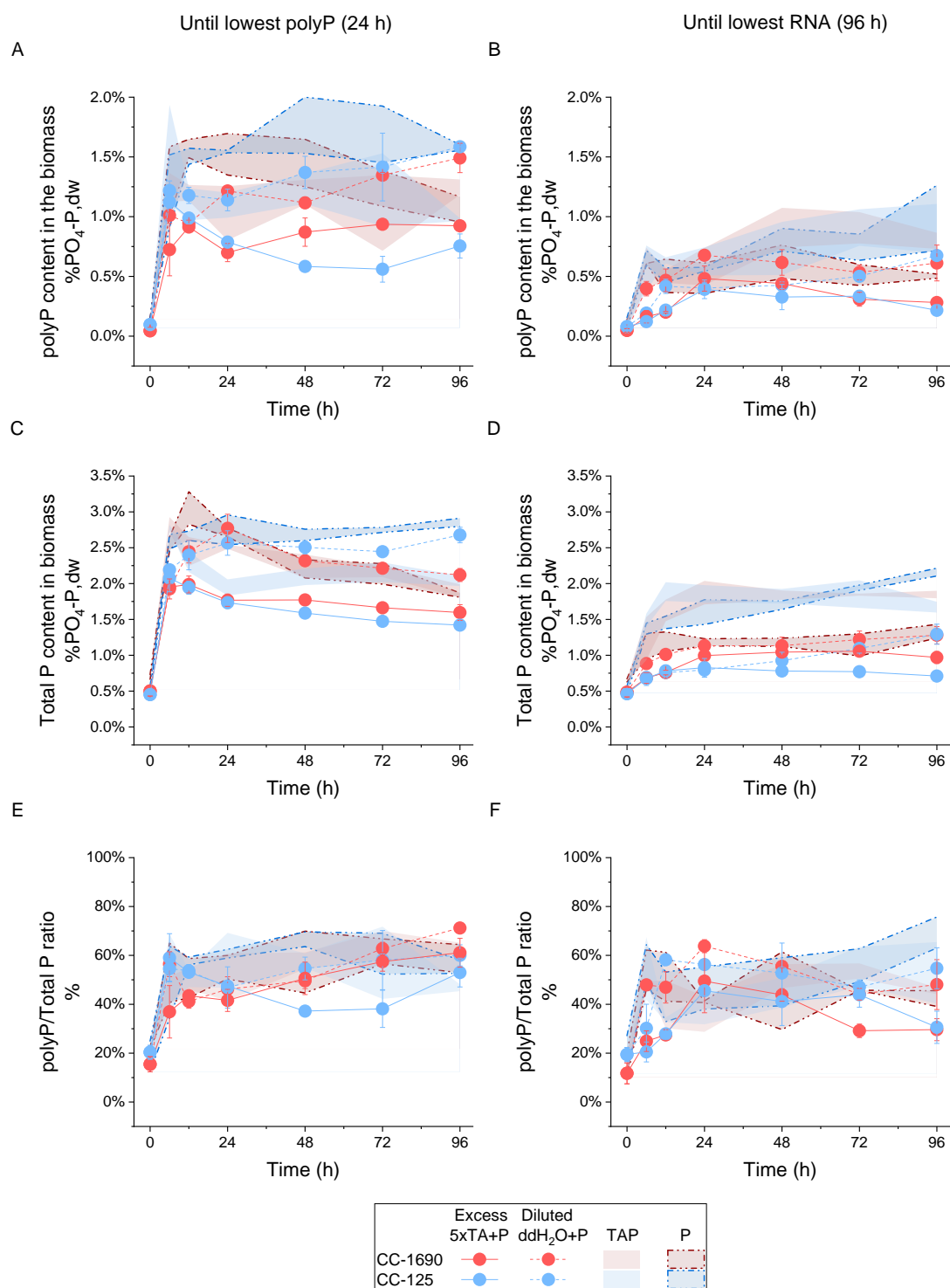


Figure 5.8 *C. reinhardtii* P overplus response after P supply in the second P overplus experiment. Mid-exponential cells (strains CC-1690 and CC-125) were resuspended in TA media for 24 h (left) or 96 h (right) and then supplied with 1 mM P with a KPO₄ solution. Excess nutrients were supplied with a 5xTA solution (1/5 v/v) and the same volume was added in sterile ddH₂O to dilute existing nutrients in the other group. A-B, PolyP content in biomass (% PO₄-P, dw), C-D Total phosphate in the biomass (% PO₄-P, dw) and E-F PolyP to total P mass ratio (% mg/mg). Shaded segments show the area covered by the error bars from parameters observed in the P overplus experiment, where P was supplied as either KPO₄ (P) or TAP (**Figure 5.2**).

5.4.3 RNA recovery was still dependent on nutrient availability in the second P overplus experiment

From **Figure 4.5B** in **Chapter 4**, I observed that 96 h P-deprived cultures had reached their lowest RNA content in the P-deprivation experiment. Then in the first P overplus experiment, 96 h P-deprived cells exhibited RNA recovery only upon P repletion together with all nutrients (**Figure 5.4B**). It became interesting to assess how RNA recovery could be affected by the effect of adding extra nutrients with the 5xTA solution. **Figure 5.9** shows the RNA content (%RNA,dw) of the strains CC-1690 and CC-125 after both periods of P-deprivation and supply of ddH₂O+P or 5xTA+P. For cultures deprived until the lowest polyP was observed, the RNA content in the biomass exhibited no differences throughout the whole monitoring period across strains (CC-1690 vs. CC-125), nutrient availability (P vs. TAP) and experiment (first vs. second) (**Figure 5.9A**). RNA content consistently decreases as biomass enters the stationary growth phase (**Figure 5.7A**). On the other side, when cells were P-deprived until the lowest RNA content was reached (96 h), then supplied with P with all nutrients using a 5xTA solution, a lower RNA recovery was observed, in comparison with cultures resuspended in TAP media (**Figure 5.9B**).

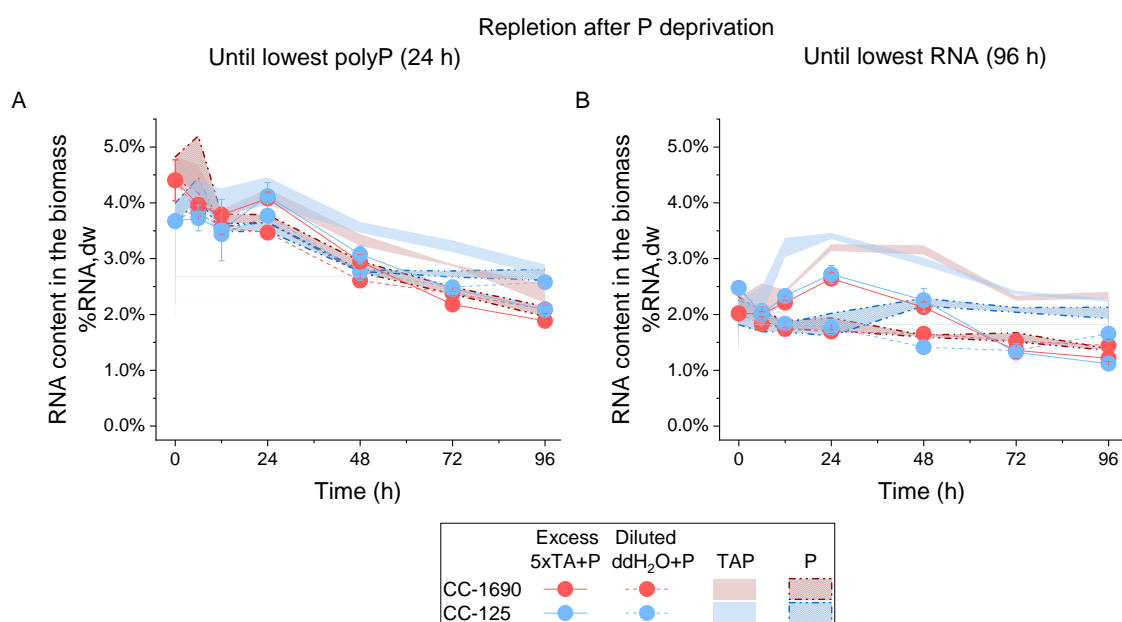


Figure 5.9 RNA content in *C. reinhardtii* biomass during P overplus after P supply in the second P overplus experiment. Mid-exponential cells (strains CC-1690 and CC-125) were resuspended in TA media for A 24 h or B 96 h and then supplied with 1 mM P with a KPO₄ solution. Excess nutrients were supplied with a 5xTA solution (1/5 v/v) and the same volume was added in sterile ddH₂O to dilute existing nutrients in the other group. Graphs show RNA content in the biomass (% RNA,dw). Shaded segments show the area covered by the error bars from parameters observed in the P overplus experiment, where P was supplied as either KPO₄ (P) or TAP (**Figure 5.4**).

5.4.4 Reduced phosphate removal observed in the second P overplus experiment

To assess the effect of nutrient supply with 5xTA+P in contrast with resuspension in TAP media on nutrient removal, I monitored phosphate, ammonium and sulphate concentration in the media throughout the second experiment (**Figure 5.10**). **Figure 5.10A** shows no differences in phosphate removal when 24 h P-deprived cultures were supplied of P as KPO_4 on its own or with added water (ddH_2O+P). However, when nutrients were supplied with a 5xTA solution, only 55% of phosphate was removed in contrast with cultures resuspended in TAP media (first P overplus experiment), where I observed a 100% phosphate removal. In the cultures that were P-deprived for 96 h (**Figure 5.10B**), the decrease in the percentage of P removal was also observed when changing the method to supply all nutrients (39% for 5xTA+P vs. 68% for resuspension in TAP media). Overall this observation matches the mass balance of phosphate during the second experiment since a lower polyP and total P accumulation was observed in 5xTA+P repleted cultures compared to cultures resuspended in TAP media (**Figure 5.8**).

In the case of ammonium and sulphate removal, I observed a higher initial concentration of these nutrients in the cultures that were supplied of P with the 5xTA solution, in comparison with cultures resuspended in TAP media from the first P overplus experiment (shaded segments in **Figure 5.10C-F**). This observation evidences that 5xTA added nutrients in excess to the ones in the media used for P-deprivation. To determine if there were any differences in ammonium or sulphate removal according to the nutrient addition method, I calculated the nutrient uptake rates of phosphate, ammonium and sulphate (**Table 5.6**). The phosphate uptake rate was more rapid during the first 6 h after P repletion. Within the first 6 h, the highest P uptake rate was detected on 24 h P-deprived cultures repleted with 5xTA+P (**Table 5.6A**). These results are consistent with the first P overplus experiment (**Table 5.3A**). However, for both ammonium and sulphate, I observed that the highest uptake rate was observed in the 6 h period for 96 h P-deprived cultures supplied with 5xTA+P (highlighted in bold in **Table 5.6B-C**). Conversely, in the first P overplus experiment, all three nutrients had their highest uptake rates after 24 h of P deprivation and resuspension in TAP media (**Table 5.3B-C**).

Once again, I used PCA analysis to reduce the multidimensionality across the P-deprivation treatments and nutrient availability in the second P-overplus experiment. **Figure 5.11** shows the PCA biplot for the second P overplus experiment. With a more integrated perspective of how these factors are

correlated together, I observed that similarly to **Figure 5.6**, PC1 represented the effect of P addition only, whereas PC2 represented the effect of the addition of other nutrients (represented here by ammonium and sulphate).

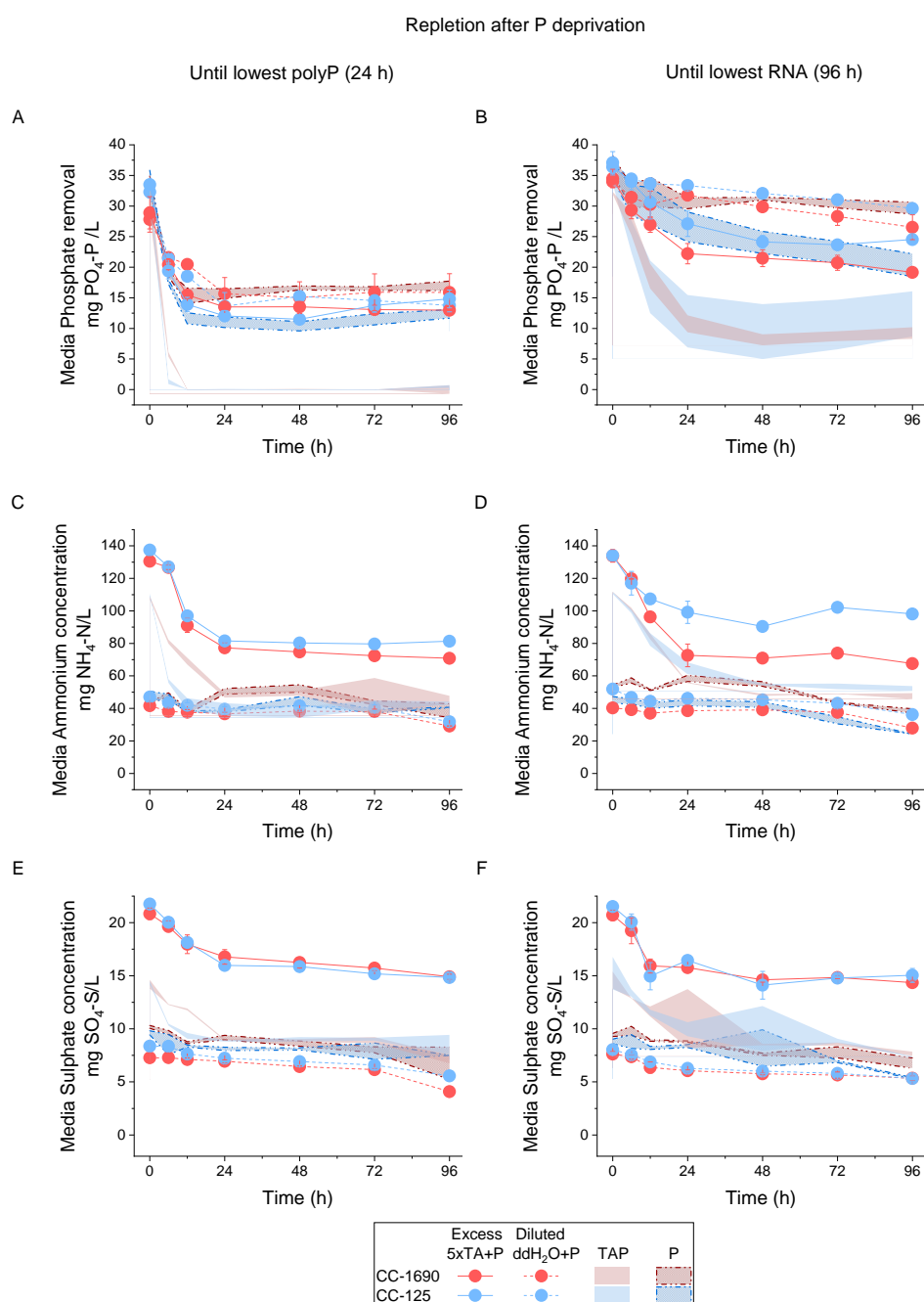


Figure 5.10 Phosphate, ammonium and sulphate removal from the media by *C. reinhardtii* after P supply in the second P overplus experiment. Mid-exponential cells (strains CC-1690 and CC-125) were resuspended in TA media for 24 h (left) or 96 h (right) and then supplied with 1 mM P with a KPO₄ solution. Excess nutrients were supplied with a 5xTA solution (1/5 v/v) and the same volume was added in sterile ddH₂O to dilute existing nutrients in the other group. Graphs show media concentration of A-B Phosphate (mg PO₄-P/L), C-D Ammonium (mg NH₄-N/L) and E-F (mg SO₄-S/L). Shaded segments show the area covered by the error bars from parameters observed in the P overplus experiment, where P was supplied as either KPO₄ (P) or TAP (**Figure 5.5**).

Table 5.6 Nutrient uptake rates of *C. reinhardtii* cells observed in the second P overplus experiment. Average values, according to P-deprivation state and P repletion type, for the four strains were used \pm SE. nn corresponds to values below $0.1 \text{ mg g dw}^{-1} \text{ h}^{-1}$.

A				
P-deprivation	Repletion	Phosphate uptake rate		
	type	(mg PO ₄ -P g dw h)		
	P/TAP	0-6 h	6-12 h	12-24 h
Until min polyP (24 h)	ddH ₂ O+P	2.23 ± 0.36	0.5 ± 0.14	0.54 ± 0.19
	5xTA+P	2.98 ± 0.55	1.05 ± 0.20	0.14 ± 0.02
Until min RNA (96 h)	ddH ₂ O+P	0.66 ± 0.19	0.31 ± 0.20	nn
	5xTA+P	0.95 ± 0.42	0.64 ± 0.23	0.39 ± 0.14
B				
P-deprivation	Repletion	Ammonium uptake rate		
	type	(mg NH ₄ -N g dw h)		
	P/TAP	0-6 h	6-12 h	12-24 h
Until min polyP (24 h)	ddH ₂ O+P	0.97±0.16	0.26±0.08	0.19±0.06
	5xTA+P	2.16±0.46	6.76±0.51	1.09±0.08
Until min RNA (96 h)	ddH ₂ O+P	0.98±0.32	0.44±0.28	nn
	5xTA+P	4.67±1.23	3.3±1.35	2.04±0.68
C				
P-deprivation	Repletion	Sulphate uptake rate		
	type	(mg SO ₄ -S g dw h)		
	P/TAP	0-6 h	6-12 h	12-24 h
Until min polyP (24 h)	ddH ₂ O+P	nn	0.11±0.04	nn
	5xTA+P	0.39±0.04	0.37±0.03	0.13±0.02
Until min RNA (96 h)	ddH ₂ O+P	nn	0.20±0.07	nn
	5xTA+P	0.57±0.24	1.00±0.30	nn

PC1 in the second P overplus experiment accounted for 57.07% of the overall correlation. In the second experiment, the effect of nutrient supply was lower than that observed in the first experiment, which accounted for 73.48% of the overall correlation. PC2 accounted for 19.67% of the correlation trend, which is nearly the same as in PC2 from **Figure 5.6** (18.41%). This is unsurprising since the P addition itself was not the second factor between both experiments. In total, PC1 and PC2 in **Figure 5.11** can explain 76.59% of the variance observed in the nutrient uptake rates according to different P-deprivation periods and nutrient availability. In contrast PC1 and PC2 in **Figure 5.6** account for 91.89% of the variance according to the different treatments. This raises the question about what factor(s) the 15.30% left ($91.89\% - 76.59\% = 15.30\%$) represent. That 15.30% left would explain the differences observed so far in terms of biomass growth, polyP accumulation and nutrient removal between the two experiments.

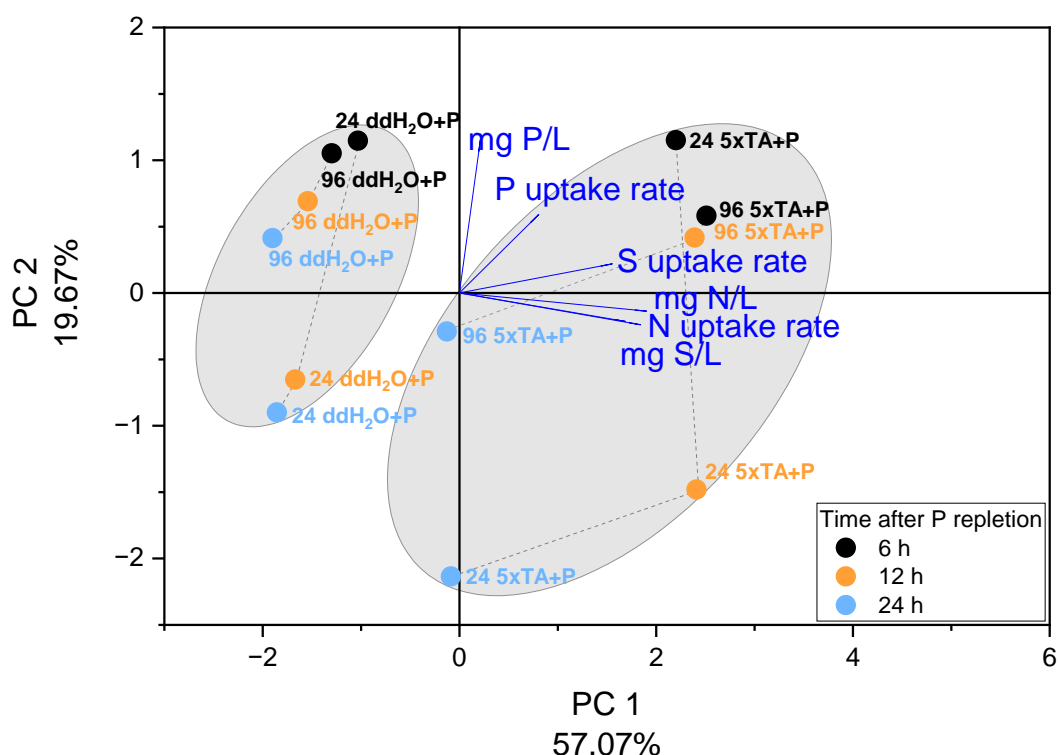


Figure 5.11 PCA analysis of the effect of P-deprivation and nutrient availability during the second P overplus experiment in *C. reinhardtii*. For the average of two strains (CC-1690 and CC-125), the biplot shows the principal component 1 (x-axis) explaining 57.82% and principal component 2 (y-axis) explaining 19.25% of the correlation of the nutrient uptake rates with the initial nutrient concentration in the media ($\text{PO}_4\text{-P}$, $\text{NH}_4\text{-N}$, $\text{SO}_4\text{-S}$ in mg/L). The loading vectors close together indicate the parameters with more similar variance. The dots show the values calculated for each of the six parameters (loading vectors), 6, 12 and 24 h after repletion of 1 mM P with either ddH₂O+P or 5xTA+P, of 24 or 96 h P-deprived cells. Ellipses group the dots and loading vectors according to P repletion type.

Furthermore, the location of the score in the biplot, which represents both P-deprivation periods and P repletion types matches the pattern observed in the first P overplus experiment (**Figure 5.6**). The strongest positive correlation towards PC1 or PC2 was detected in the first 6 h of P repletion. As time passed the correlation weakens, and in some cases is inverted towards PC1 or PC2, depending on the treatment. This observation means that changing the method of nutrient supply in the second experiment did not change the fact that 1) P-deprivation until minimum polyP was reached, was better for P overplus, and 2) P repletion together with all nutrients is better for biomass growth, which promotes nutrient removal. Moreover, I could observe that some loading vectors in the PCA biplot from **Figure 5.11** seemed shorter, compared to **Figure 5.6**. However, after calculating the length of the vector according to the coordinates of PC1 and PC2, I found that only two variables exhibited a weaker correlation with PC1 and PC2: 1) Initial phosphate concentration (mg P/L) and 2) P uptake rate. This indicates that the strength of the correlation between initial phosphate concentration and phosphate uptake rate in **Figure 5.11** was weaker than that observed in **Figure 5.6** according to the principal components that explain most of the variance. Hence, this confirms that the P overplus response in the second experiment was weaker, as we can observe in **Figure 5.10A-B**.

5.4.5 Negative effect on P overplus observed in second P overplus experiment with excess nutrient supply

In the second P overplus experiment, the addition of 5xTA+P supplied extra nutrients to the ones still available after each P-deprivation period tested (24 h or 96 h), whereas the addition of P+ddH₂O, diluted these nutrients one in five to match the volume of 5xTA added, as mentioned above. Thus, in the second experiment, there is a wider range of nutrient concentrations other than P than in the first experiment. To further examine the effect of this wider range of nutrient concentrations on *C. reinhardtii* P overplus I plotted the average polyP fold increase (FI) at the 6 h timepoint in both P overplus experiments (**Figure 5.2A-B**, **Figure 5.8A-B**), together with the percentage of P removal from the media by the end of both experiments (**Figure 5.5A-B** and **Figure 5.10A-B**). Both the polyP FI and %P removal were plotted as a function of the nitrogen to phosphorus (N:P) and sulphur to phosphorus (S:P) molar ratios (**Figure 5.12**). In this figure, I observed that the polyP FI was only affected significantly when 96 h P-deprived cultures in the second P overplus experiment, where nutrients were diluted (ddH₂O+P), in comparison to the first experiment (P only 'KPO₄' repletion) (p-value= 0.24 24 h P-deprived, p-value= 0.007 96 h P-deprived). The :P and S:P ratios were lower in ddH₂O+P repleted cultures than in the 'P' only

repleted cultures but this was only significant for the S:P ratio (p-value=0.61, N:P and p-value=8.3x10⁻⁴, S:P). Moreover, I observed that 5xTA+P repletion negatively affected the polyP FI during P overplus of *C. reinhardtii* in both P-deprivation periods but was only significant for 96 h P-deprived cultures (p-value=0.062 24 h P-deprived, p-value= 0.016 96 h P-deprived), compared to resuspension in TAP media in the first experiment. Higher N:P and S:P ratios were observed in the 5xTA+P repleted cultures than in TAP repletion (p-value= 3.2x10⁻⁴, N:P and p-value < 1x10⁻⁴, S:P). Therefore, it is possible that *C. reinhardtii* P overplus may be affected by divergent nutrient/P ratios (P is kept constant at 1 mM), to those of the widely used TAP media, which was designed to provide an adequate nutrient balance for the study of *C. reinhardtii* (Kropat et al., 2011). However, 5xTA+P supply affected 96 h P-deprived cultures the most (compared to TAP repletion). It means that other factor(s) could also explain such differences, which is also reinforced by the bars corresponding to P removal from the media. The fact that the polyP FI bar height compared to that of the %P removal from the media inverted in the 96 h P deprived cultures indicates that a higher proportion of the P that was removed went to the recovery of organic P compounds that were lost during 96 h of P-deprivation.

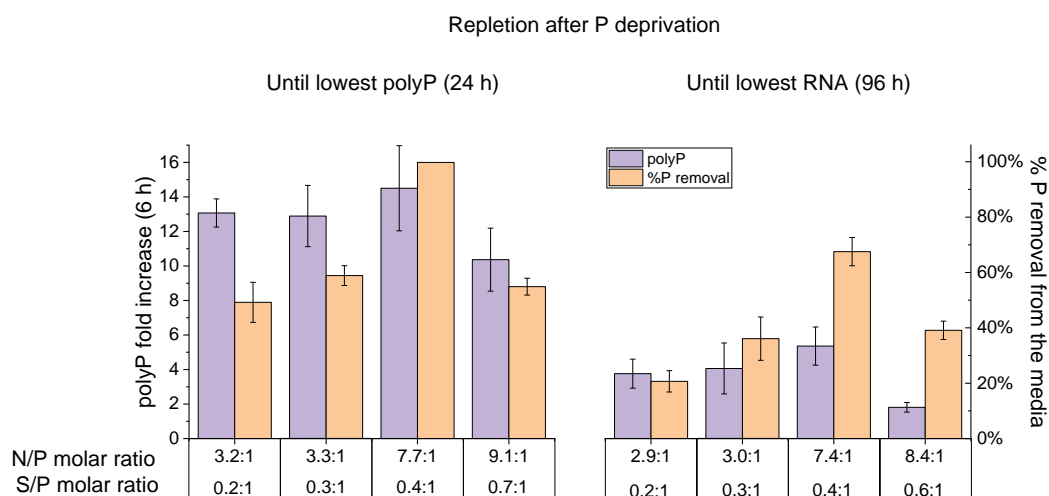


Figure 5.12 Effect of N:P and S:P ratio on polyP fold increase in P overplus experiments. Mid-exponential cells (strains CC-1690 and CC-125) were resuspended in TA media for 24 h (left) or 96 h (right) and in the first P overplus experiment were supplied with 1 mM P with a KPO₄ solution or all nutrients by harvesting and resuspension in TAP media. In the second P overplus experiment, P-deprived cultures were both supplied with 1 mM P with a KPO₄ solution. Excess nutrients were supplied with a 5xTA solution (1/5 v/v) and the same volume was added in sterile ddH₂O to dilute existing nutrients in the other group. Bars show polyP fold increase after 6 h of P repletion (purple), and %P removal from the media at the end of the experiment (orange). The N:P molar ratio and S:P molar ratio for different repletion types (P, ddH₂O+P, TAP, 5xTA+P) are shown at the bottom. Data of polyP FI and %P removal from the media from 'P' only (KPO₄) repletion after 24 h or 96 h P-deprivation belongs to the **Chapter 4** of this thesis (**Figure 4.8A-B**, and **Figure 4.11A-B**).

5.5 Results summary and discussion

In this chapter, the objective was to evaluate how other nutrients apart from P influence *C. reinhardtii* P overplus response. To do so, I resupplied P-depleted *Chlamydomonas* with KPO_4 or by harvesting and resuspending biomass in fresh TAP media, following the experimental methodologies of previous studies (Plouviez et al., 2021, Solovchenko et al., 2019b). My findings show that nutrient availability did not influence polyP accumulation (**Figure 5.2**) or chain length pattern (**Figure 5.3**), but did promote biomass growth (**Figure 5.1**) which resulted in enhanced nutrient removal from the media (**Figure 5.5** and **Figure 5.6**). These results imply that the P overplus response of *C. reinhardtii* is not dependent on biomass growth or affected by the lack of it. Microalgal growth was resumed due to nutrient resupply which increased the uptake of phosphate from the media with a high demand for phosphate-containing organic molecules (DNA/RNA, ATP, etc.) to sustain cell division. This explains why the polyP chain length pattern remained unchanged when repletion occurred with all nutrients, compared to KPO_4 repletion (**Figure 5.3**). This suggests that any additional phosphate that was removed by supplying all nutrients went directly to the synthesis or organic P compounds.

The best results (in terms of biomass growth, P removal and polyP accumulation) were observed for P-depleted cells that had just reached minimum polyP levels and were harvested and resuspended in fresh TAP media: under these conditions, I observed a 15-fold increase in polyP content, a 6-fold increase in total P content, and a 76% increase in biomass concentration which in 12 h removed all phosphate from the media. Furthermore, I found that nutrient availability after P repletion was key for RNA recovery in the cultures that were P-depleted until reaching their minimum RNA content (**Figure 5.4**). This result is consistent with Plouviez et al. proteome data of P overplus in *C. reinhardtii*, where they found an increase in proteins related to RNA biosynthesis, although phosphate was supplied as KPO_4 in their experiment (Plouviez et al., 2023a). Probably other factors like nitrogen availability in the media at the moment of P repletion could play a role in the ability of *C. reinhardtii* to restore its RNA pool. However, physiological parameters of RNA content, or nutrient removal from the media were not reported in that study.

Also, the observation that RNA was recovered upon repletion with all nutrients led to examine whether the maximum growth hypothesis (see **Chapter 2** Literature Review section **2.3.1**) was valid for the period of biomass growth observed upon TAP repletion (12 – 24 h). However, the RNA contribution to total P in this present P overplus experiment did not amount to the 25% range

indicated by Rees and Raven for eukaryotic photosynthetic organisms, as it did in the control experiment (**Figure 4.5A in Chapter 4**) (Rees and Raven, 2021). To elaborate, if RNA contains an average of 9.1% P as suggested in previous literature (Geider and Roche, 2002, Raven, 2013), then RNA contributed to 12.5% of total P in biomass, in P overplus after P was supplied as resuspension in TAP media. Meaning that the biomass growth observed in **Figure 5.1** did not match the maximum growth rates expected under exponential growth. Possibly, the rest of the P accumulated goes into ATP which is the P-donor for polyP, or phospholipids (Sanz-Luque et al., 2020). ATP together with other P-esters and phospholipids usually account for around 10% and 14% of total P, respectively (Rees and Raven, 2021).

The strain CC-5325 accumulated more polyP and total P than the other strains when P-deprived for 96 h and resuspended in TAP media (**Figure 5.2B and D**). By the end of the monitoring period, this strain had accumulated the same amount of polyP and total P when it was P-deprived for 24 h and supplied of P (P or TAP) (**Figure 5.2A and C**). This behaviour allowed this strain to remove all phosphate from the media in contrast with the other strains (**Figure 5.5B**). This phenotype adds to the one described in section **4.5 in Chapter 4**. This new phenotype is surprising given that CC-5325 (also known as CC-4533) is the background of the CliP mutant library and is derived from commonly used laboratory strains. Li et al. found three variations in its genome, with the potential to disrupt gene function (Li et al., 2016). From these variations, one could potentially be behind the observed phenotype in phosphate accumulation. A single nucleotide polymorphism potentially interferes with a gene encoding a Histone deacetylase (HDAC). HDACs help to restore compact chromatin structure, restricting access to RNA polymerase which negatively regulates gene expression, and may prevent transcription factors from accessing promoters (Park and Kim, 2020, Neupert et al., 2020). Phosphate metabolism is regulated by the PSR1 transcription factor in *C. reinhardtii* (Shimogawara et al., 1999). PSR1 is upregulated under low or no P conditions and downregulated under P-replete conditions (Moseley et al., 2006, Plouviez et al., 2021). Many genes and pathways are transcriptionally regulated by PSR1 (see **Chapter 2 Literature Review section 2.4.1**), including phosphate transport. Thus, CC-5325 could hypothetically have an abnormal regulation of PSR1 leading to the phenotypes observed during this study: 1) Higher polyP and total P accumulation under no P-deprivation conditions and 2) what seems to be a higher resistance or abnormal response to P-deprivation, giving that it accumulates almost the same amount of phosphate in both P deprivations periods tested (24 and 96 h). Since this strain is the background of the Clip

mutant library, there is relevance in uncovering the genotype behind the observed behaviour, which to the best of my knowledge has not yet been described.

To benchmark the performance of *C. reinhardtii* under the P overplus experimental conditions tested, it is necessary to compare these results (complete removal of 1 mM P in 12 h) with previous reports. Plouviez et al. reported complete removal of P from the media after 5 d P depleted *C. reinhardtii* was supplied with 0.33 mM P with KPO₄, in 24 h (Plouviez et al., 2021). Although their initial biomass concentration was approximately half of the one observed in this present experiment (Table S1 in Plouviez et al.), they also reported a very low increase in biomass concentration after P supply, consistently with the biomass concentration pattern observed in KPO₄ repleted cultures (**Figure 4.1**). In a later report, Plouviez et al. showed that increasing the P dose and initial biomass concentration at the P repletion stage had a positive effect on P removal from the media (Plouviez et al., 2023b). In this chapter, I observed that the high performance in P removal of 24 h P-deprived cells repleted with TAP, may be attributed not only to the high initial P and biomass concentration but also to the supply of all nutrients in TAP media. Solovchenko et al. obtained a complete removal of P from the media in 40 h when resuspending 0.4 g dw/L of *Chlorella vulgaris* in fresh BG-11 medium (0.4 mM P), after approximately 3-5 d of P deprivation (Solovchenko et al., 2019b). The slower removal of P, in this case, could be due to the longer period of P-deprivation, lower dose of P and lower initial biomass concentration. The comparison of my results with other studies begins to undam the interplay of different factors in microalgal P overplus, like initial phosphate and biomass concentration, the limits of P deprivation and nutrient availability.

To the best of my knowledge, the effect of other nutrients apart from P on biomass growth during phosphate overplus has not been specifically explored before. Indirectly, Lavrinovičs et al. tested the effect of other nutrients at the P repletion stage when resuspending 7 and 14 days P-deprived cells from *Desmodesmus communis*, *Tetradesmus obliquus* and *Chlorella protothecoides*, in primary or secondary effluent from a municipal wastewater treatment facility (Lavrinovičs et al., 2020). Primary wastewater treatment effluents are richer in nutrients than secondary effluents (Cabanelas et al., 2013). In Lavrinovičs et al. study, higher biomass concentration was observed when resuspending biomass in primary effluent in non-P-deprived and 14 days P-deprived *Chlorella protothecoides*, but not for the other species. The differences in the experimental setup and design do not allow a direct comparison of their results with the ones observed in **Figure 5.1** in this present study. Firstly, the initial

biomass concentration at the repletion stage is lower in their case (0.05 g dw/L) than the 0.6-0.9 g dw/L used here. Secondly, the pH in their experiment was not controlled or buffered and reached alkaline levels (pH > 9.0) which may also affect microalgal growth in a species-dependent manner (Hansen, 2002, Berge et al., 2012). Growth inhibition under high pH could be partly due to the deprotonation of ammonium (NH₄) to ammonia (NH₃) (Bowmer and Muirhead, 1987, Källqvist and Svenson, 2003). In this experiment, *C. reinhardtii* is grown in TAP or TA media, which is buffered with Tris pH 8.5 (see **Chapter 3 Materials and Methods 3.2**). Thirdly, the characterisation of primary and secondary effluent does not report the presence and concentrations of other macronutrients apart from nitrogen and micronutrients (e.g. magnesium, calcium, zinc, etc.) which also play a role in biomass growth. However, it would be interesting to assess in the future whether the observation of enhanced biomass growth during phosphate overplus showed in this experiment for *C. reinhardtii*, would be significantly different when using more realistic (less controlled) conditions (e.g. wastewater treatment effluent).

By comparing the results of this P overplus experiment to previous reports (Lavrinovičs et al., 2022, Plouviez et al., 2021, Plouviez et al., 2023b, Solovchenko et al., 2019b, Aitchison and Butt, 1973), I found that the results are variable in terms of phosphate removal performance, biomass growth and polyP or total P accumulation. However, these differences highlight the importance of the following parameters: 1) initial biomass concentration, 2) initial P concentration, 3) P deprivation indicators and 4) nutrient availability. The last two, are the centre of my research in these last two chapters. Standardising the interplay of these four parameters will help to deliver a more robust model of the phosphate overplus response in microalgae.

A second P overplus experiment was designed to avoid the centrifugation of biomass before resuspension in TAP media, by adding a 5xTA+P solution to P-deprived cultures. I found that biomass growth was still promoted by supplying nutrients in this way (**Figure 5.7**). Although, significantly lower biomass productivity was observed only for 96 h P-deprived cultures (see **Table 5.1C** and **Table 5.5B**, CC-1690 and CC-125)). Furthermore, I observed that the dynamic of P overplus in 5xTA+P repleted cultures was different (**Figure 5.8**). 24 h P-deprived cultures exhibited the same peak of polyP after 6 h of 5xTA+P repletion, although this was followed by a steady decreased content. This pattern contrasted with TAP repleted cultures from the first experiment, where the peak remained more or less stable throughout the monitoring period.

Table 5.7 Differences between P overplus response in first and second experiments. Values represent the average of the strains CC-1690 and CC-125 (n=3). Phosphate, ammonium and sulphate removal (%) was calculated with the initial and final value of the media concentration (mg/L). Asterisks represent the parameter with significant differences (*, **, *** for p-value≤0.05, 0.01 and 0.001, respectively), which are shaded in red. uc accounts for 'unchanged'.

Experiment	First	Second	First	Second
P deprivation	Until minimum polyP (24 h)		Until minimum RNA (96 h)	
P repletion type	TAP	5xTA+P	TAP	5xTA+P
Biomass Centrifugation	Yes	No	Yes	No
New/Old media	New	Old	New	Old
Nutrients	Unaltered	Excess	Unaltered	Excess
Biomass productivity (g L⁻¹ h⁻¹)	0.041	0.034	0.023	0.015*
PolyP fold increase (%PO₄-P,dw) (6 h)	14.5	10.4	4.8	2.5*
Total P fold increase (%PO₄-P,dw) (6 h)	5.1	4.2*	2.4	1.4*
RNA fold increase (%RNA,dw) (24 h)	uc	uc	1.6	1.2*
Media P removal at the end of the experiment (%)	100%	55%***	68%	39%***
Media N removal at the end of the experiment (%)	59%	44%*	55%	44%*
Media S removal at the end of the experiment (%)	42%	30%*	48%	30%*

A longer period of P-deprivation (96 h) caused *C. reinhardtii* to accumulate less polyP, even at the 6 h time point, if the strains were repleted with 5xTA+P, instead of resuspended in TAP media. No differences were detected in polyP accumulation of ddH₂O+P repleted cultures compared to P repleted cultures (**Figure 5.8A-B**). Hence, for the cultures deprived of P until reaching the lowest polyP content (24 h), ddH₂O+P cultures exhibited a significantly bigger P overplus than 5xTA+P repleted cultures. Otherwise, the effect of P deprivation until reaching the lowest polyP or lowest RNA content on P overplus remained similar between the two experiments, hence more polyP was accumulated for the 24 h P-deprived cultures. Moreover, for the cultures deprived of P until the lowest RNA content was reached, the effect of nutrients on RNA recovery was significantly lower in the second experiment than in the first experiment (**Figure 5.9B**).

Furthermore, the lower total P accumulation observed in cultures that were repleted with 5xTA+P was reflected in a lower phosphate removal from the media than that observed for cultures resuspended in TAP media in the first experiment (**Figure 5.10A-B**). Other than phosphate, I observed that ammonium and sulphate removal was less efficient in 5xTA+P repleted cultures than in resuspension in TAP media, independently of the P-deprivation period (**Figure 5.10C-F**). This is consistent with the observation of lower biomass productivity which translated into a lesser need for nutrients from the environment, due to possible factors partially inhibiting growth

Up to this point, we observed the differences in the effect of supplying nutrients as resuspension in TAP media or 5xTA+P addition on P overplus, which are summarised in **Table 5.7**. The scope of the second experiment was to test the hypothesis that the step of centrifugation before resuspension in TAP media could affect negatively *C. reinhardtii* biomass and hence its P overplus response. Yet, the results showed that in the second experiment, the P overplus response did not improve, nor did the nutrient availability affect biomass growth and nutrient removal, which were observed in the first experiment. On the contrary, I observed that repletion as 5xTA+P addition affected negatively some of the monitored parameters in comparison with resuspension in TAP media, especially for 96 h P-deprived cultures as shown red shaded in **Table 5.7**. This is supported by **Figure 5.12** which shows that different nutrient to phosphorus molar ratios to those in TAP media, could affect the polyP FI upon repletion, but those effects were more adverse in the longer P-deprived cultures. These results raise further questions which require further research and will be discussed in the general discussion chapter of this thesis.

Chapter 6 PSR1 is a key component of polyphosphate synthesis during the phosphate overplus response in *Chlamydomonas reinhardtii*

6.1 Introduction

This chapter aims to explore the role of PSR1 in the phosphate overplus response of *C. reinhardtii*. The PSR1 transcription factor has been widely described in the last two decades for its role in the response to P deprivation (Shimogawara et al., 1999, Wykoff et al., 1999). This response includes the upregulation of high-affinity low-rate phosphate transporters and alkaline phosphatases, which assist in the scavenging of P (Moseley et al., 2006). PSR1 also acts as a regulator of in-cell P recycling via the downregulation of the Chloroplast ribonuclease polynucleotide phosphorylase (PNPase) and increasing polyphosphate synthesis through the upregulation of components of the VTC complex (Yehudai-Resheff et al., 2007, Moseley et al., 2006, Cliff et al., 2023). These mechanisms were uncovered by studying the abnormal behaviour of the *psr1-1* mutant under 'low P' levels, compared to its background strain, CC-125 (see **Chapter 2 Literature review**) (Shimogawara et al., 1999, Wykoff et al., 1999, Moseley et al., 2006). As PSR1 expression is triggered by low P, separating PSR1-specific responses from other responses to P deprivation is complicated. To gain insight into this, PSR1 was over-expressed in *C. reinhardtii* under the control of a light-regulated promoter, which regulation should be independent of the level of external P. These strains were produced by Dr. Lili Chu and are described in our recent publication (Slocombe et al., 2023). Three independent transgenic strains were grown on TAP media and samples were collected for physiological, and confocal analysis, transgene protein expression (analysed by me) and RNA sequencing (analysed by Dr. Slocombe), as the strains gradually depleted P and other nutrients from the media. This led to the conclusion that overexpression of PSR1 was sufficient to induce a luxury P uptake/P overplus response (Slocombe et al. and below).

I then addressed the question of whether PSR1 overexpression was additive with P deprivation in inducing phosphate overplus of *C. reinhardtii* and how this compared with the non-transgenic strains used in Chapters 4 and 5 of this thesis (CC-1690, CC-125, CC-5325 and CC-4350). With these strains, I observed that the best phosphate overplus response was obtained after P-deprivation until the lowest polyP level was observed and biomass was harvested and resuspended in fresh TAP media. Thus, I wanted to test, under the same conditions, the phosphate overplus performance of our strongest

PSR1 overexpression strain (8-27) in contrast with its background UVM4. The background of UVM4 is the strain CC-4350, which was used in Chapters 4 and 5 of this thesis (Neupert et al., 2009). Furthermore, the fact that PSR1 overexpression enhanced phosphate accumulation in the biomass of *C. reinhardtii* without P-deprivation (Slocombe et al., 2023, Bajhaiya et al., 2016, Wang et al., 2023), may suggest that PSR1 not only controls the response to P-deprivation but also potentially intervenes at the repletion stage during P overplus. Thus, I decided to add the *psr1-1* mutant strain to the P overplus experiment with the stronger PSR1 overexpression strain from our paper and its background, UVM4. The hypothesis is that an abnormal response to P depletion and repletion will be observed due to the loss of function or overexpression of PSR1 in the *psr1-1* and the 8-27 strains, respectively. The *psr1-1* mutant background is the strain CC-125. This strain was used in the P overplus experiment in section 5.3 of **Chapter 5** of this thesis¹.

6.2 Objective

To evaluate the role of the PSR1 transcription factor on the phosphate overplus response of *C. reinhardtii*.

6.3 Overexpression of PSR1 induces luxury phosphate uptake in *C. reinhardtii*

6.3.1 Non-native PSR1 was successfully detected in transgenic strains

The design of the PSR1 overexpression construct includes 1) a light-sensitive promoter of the ferredoxin-binding protein of the photosystem I (PSAD) gene, 2) an RBCS2 intron, 3) the PSR1 gene with an inserted 3xHA-tag, 4) the Venus YFP and 5) the terminator of the gene PSAD (Slocombe et al., 2023). The construct was inserted in the genome of the background strain UVM4. The Venus tag included in the construct allows for the detection of the transgene PSR1 via western blotting, which was completed after the strains 8-27, 8-42 and 8-2 were generated. I confirmed the presence of the transgene PSR1 for the strains 8-27 and 8-42 as shown in **Figure 6.1**. In this figure, the band corresponding to the PSR1-YFP protein is located at an approximate molecular weight of 140 kDa, whereas no band is observed in the background strain

¹ To facilitate the comparison with *psr1-1* in section 6.4, I show the behaviour of the strain CC-125 shown as a shaded segment of the error bars from that experiment (section 5.3 of **Chapter 5**).

UVM4. Although, the predicted size of the construct is 109.4 kDa, the protein characteristics might be affecting its migration through the SDS-PAGE gel.

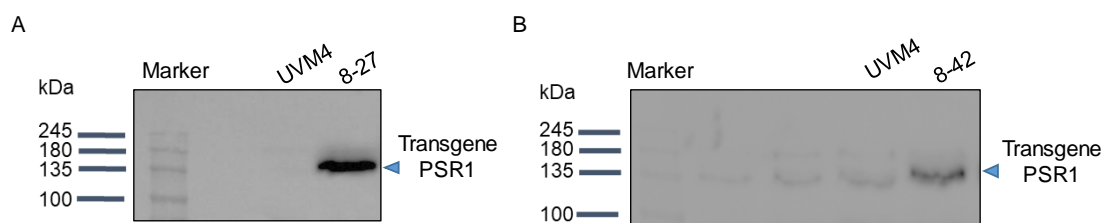


Figure 6.1 Transgene PSR1 was still detected in PSR1 overexpression strains 8-27 and 8-42. Precultures were inoculated in TAP media and protein samples were collected after 72 h for PSR1-Venus protein detection via Western Blotting for PSR1 overexpression strains A 8-27 and B 8-42. The non-transformed control (UVM4) shown in both A and B shows no detection. The bars on the left indicate the molecular weight of each band of the marker (kDa). 10 μ g of chlorophyll loaded per lane. 1 min exposure time was used for both blots.

6.3.2 Overexpression of the PSR1 transcription factor does not alter the growth and viability of *C. reinhardtii*

Since PSR1 has been reported to be involved in many different processes in the cell, growth must be a key parameter to be monitored as it provides evidence of the viability of the *C. reinhardtii* cells overexpressing PSR1. pH is another critical parameter to be monitored as phosphate precipitates strongly as calcium phosphate at pH above 8.5, making it non-bioavailable to microalgae (Crimp, 2015). Therefore, after monitoring growth during 168 h of cultivation, it was observed that all the strains exhibited a classic sigmoidal growth model, starting with a lag phase of 24 h, followed by an exponential phase from 24 h - 96 h and finally reaching a stationary phase until the end of the monitoring period (168 h). Among the three growth parameters measured (**Figure 6.2A** Optical density, **B** Biomass concentration and **C** Chlorophyll a+b concentration), together with the pH in the media (**Figure 6.2D**), no differences were observed between the transgenic strains and the non-transformed control, UVM4.

A linear regression allowed the determination of the exponential growth phase between 24 h - 96 h, for which growth rates were calculated (**Table 6.1**). These rates were consistent with **Figure 6.1** and showed no differences in the rate of growth and the doubling time. During the log phase, the cells divided approximately every 12 h, and throughout the exponential growth phase (24 h – 96 h) produced between 0.7-0.8 grams of dry biomass per litre of culture. Overall, these results indicate that the manipulation of the transgenic strains to overexpress the transcription factor PSR1 did not alter the growth and the pH in the media.

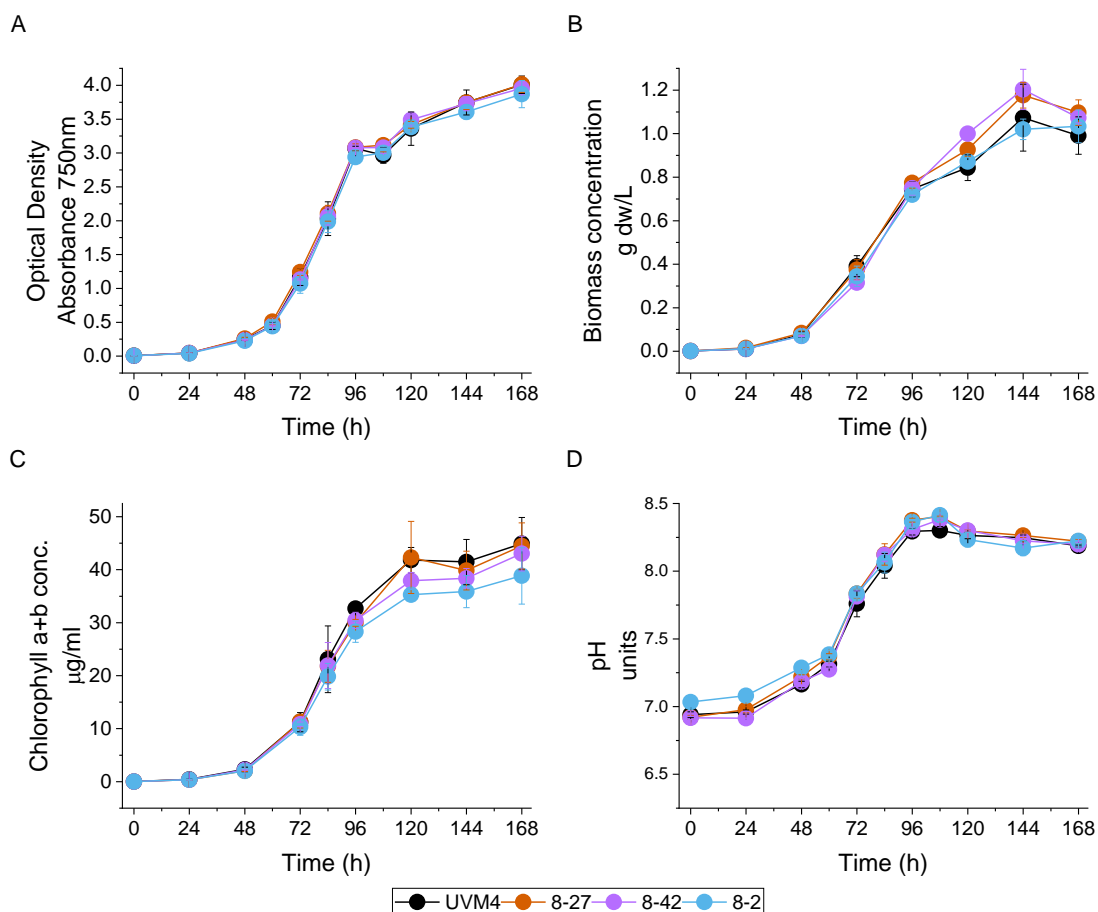


Figure 6.2 *C. reinhardtii* growth not affected by PSR1 overexpression.

Precultures of the non-transformant control UVM4 and the three PSR1 overexpression strains 8-27, 8-42 and 8-2 were inoculated in TAP media to an initial OD_{750nm} 0.005 and monitored during 168 h. A. Optical Density (Absorbance 750nm), B. Biomass concentration (g dw/L), C. Chlorophyll concentration (µg/mL) and D. pH in the media. Each data point represents the mean (n=3) and error bars show the standard error of the mean value.

Table 6.1 Growth rates estimated for the PSR1 overexpression strains and the non-transformant control. The values were calculated for the exponential phase (24 h – 96 h) as per linear regression showed for the specific growth rate, doubling time and biomass productivity. Each value represents the mean (n=3) and error bars show the standard error of the mean value.

Strain	Specific growth rate (h ⁻¹)	Doubling time (h)	Biomass productivity (g dw L ⁻¹ h ⁻¹)
UVM4	0.060 ± 0.003	11.5 ± 0.6	0.010 ± 0.001
8-27	0.055 ± 0.002	12.5 ± 0.4	0.011 ± <0.001
8-42	0.059 ± <0.001	11.7 ± 0.1	0.010 ± <0.001
8-2	0.059 ± 0.002	11.7 ± 0.3	0.010 ± <0.001
Average	0.058 ± 0.001	11.8 ± 0.2	0.010 ± <0.001

6.3.3 Levels of biomass phosphate follow transgene PSR1 protein expression pattern, leading to enhanced P accumulation

To determine the effect of PSR1 overexpression on *C. reinhardtii* P uptake I monitored phosphate accumulation relative to the dry biomass (**Figure 6.3A**). The pattern over the time course shows great differences between the three transgenic strains. The strain 8-27, displayed a peak of phosphate content in its biomass between 24 h and 96 h, reaching a maximum after 48 h with 7.5% PO₄-P,dw. After day 3, though, there is a strong decrease in the phosphate content, which stabilises to approximately 3.0% PO₄-P,dw. For the other transgenic strains, 8-42 and 8-2, the content of phosphate in the biomass increased gradually day by day and reached its highest value (8-42= 3.1% PO₄-P,dw and 8-2= 4.1% PO₄-P,dw) after 168 h and 120 h, respectively. The non-transformed control UVM4, on the other hand, had an average content of phosphate of 2.0% PO₄-P,dw throughout the 168 h of cultivation. Nonetheless, it is important to note that the initial content of phosphate in the biomass of strain 8-27, was approximately twice as much as that of the other strains, UVM4, 8-42 and 8-2, which once more reveals interesting differences between the control and the PSR1 overexpression strains but also between the transgenic strains

Consequently, to link the differences in the biomass phosphate content as one of the effects of overexpressing the transcription factor PSR1, I also monitored the PSR1-YFP fusion protein expressed from the transgene using antibodies against GFP which cross-react with YFP (**Figure 6.3B**). The blot revealed a protein expression pattern that fits nicely with that of the biomass phosphate concentration and leads to the observation that the phosphate content in the biomass follows the pattern of expression of the PSR1-YFP in the transgenic strains. The strain 8-27, consistently, exhibited the most intense protein bands, whereas the strain 8-42 showed a much weaker abundance of the protein (although still present), which serves as a possible explanation for the differences in the phosphate accumulation patterns between these two strains. The blot on the bottom shows the immunoblot corresponding to the non-transformed control UVM4, showing the non-specific antibody background. The pattern of expression of the PSR1-YFP protein exhibited an upregulation between 24 h - 96 h in all strains, followed unexpectedly by a downregulation after 120 h and 144 h of cultivation, despite cultivation under continuous light. This observation is interesting given that the PSR1 overexpression construct harbours the constitutive promoter of the ferredoxin-binding protein of the photosystem I (PSAD) gene, and thus, it is considered a light-regulated promoter (Crozet et al., 2018).

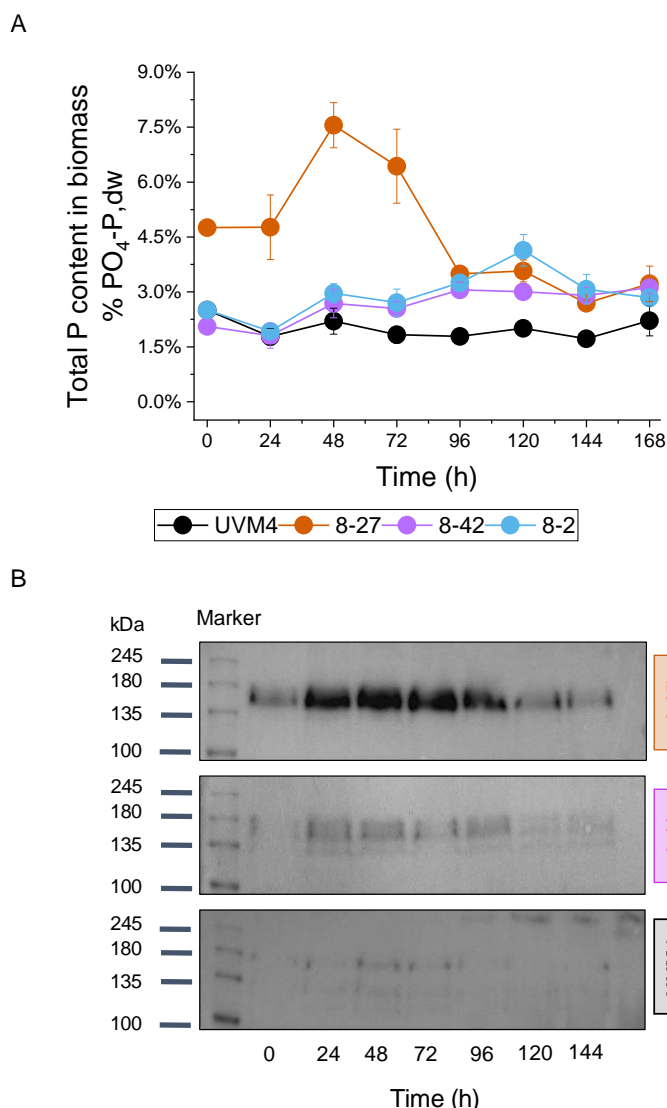


Figure 6.3 PSR1 overexpression enhanced total phosphate accumulation in *C. reinhardtii*.

Precultures of the non-transformant control UVM4 and the PSR1 overexpression strains 8-27, 8-42 and 8-2 were inoculated in TAP media and monitored for 168 h. A Total phosphate content in the biomass (%PO₄-P/dw) B Transgene PSR1 protein detection via Western Blotting with anti-GFP antibody for PSR1-YFP in strains (8-27 and 8-42). No detection was observed in the non-transformed control (UVM4). The bars on the left indicate the molecular weight of each band of the marker (kDa). 10µg of chlorophyll loaded per lane. 1.5 min exposure time was used for all blots.

6.3.4 Enhanced phosphate removal is achieved under nitrogen-replete conditions via PSR1 overexpression

TAP media contains all nutrient requirements for optimal growth of *C. reinhardtii*, therefore this media is ideal for testing the effect of PSR1 overexpression on nutrient removal under 'optimal' conditions. **Figure 6.4** shows the variation in the concentration of six of the nutrients contained in TAP media during 168 h of cultivation. The removal of these nutrients, except for potassium, seemed to follow the sigmoidal growth observed in **Figure 6.2A-C**. Media phosphate concentration (**Figure 6.4A**) varied significantly between the transgenic strains and the control when the exponential growth phase started. The control, UVM4, displayed a high uptake rate of phosphate during the exponential phase, and then it reached a plateau during the stationary phase. This strain ultimately removed approximately 70% of all phosphate from the media by the end of the monitoring period. Conversely, all the PSR1

overexpression strains (8-27, 8-42 and 8-2) depleted all phosphate from the media (under the limit of detection for blue molybdate method ~ 0.04 mg PO₄-P/L), but at different rates. The transgenic strain 8-27 exhibited the highest removal rate (P depleted after 84 h), followed by 8-2 (108 h) and 8-42 (between 120 h - 144 h). Interestingly, the highest and lowest phosphate removal rates observed for strains 8-27 and 8-42 respectively also coincide with a higher and lower level of the transgene PSR1 detected in **Figure 6.3B**.

Moreover, I observed that the removal of magnesium was different between the transgenic strains and the control (**Figure 6.4C**). Whilst a complete depletion of this nutrient was not achieved as with phosphate, the transgenic strains removed two times more magnesium than the control. The removal pattern during the exponential phase seemed to follow that of phosphate. The strain 8-27 started to remove magnesium sooner than the control after 48 h and reached the plateau at the 84 h time point. This pattern was also observed for the other transgenic strains 8-2 (start – 72 h, plateau – 120 h) and 8-42 (start – 84 h, plateau – 120 h).

Otherwise, in the case of sulphate, ammonium, calcium and potassium concentration in the media (**Figure 6.4B, D, E, F**), no differences in the pattern of removal were observed. All the strains removed about 50%, 70%, 5% and 0%, respectively, of these nutrients from the media by the end of the experiment. I calculated the maximum uptake rate for the nutrients shown in **Figure 6.4**. The maximum uptake rates for phosphate, magnesium, ammonium and sulphate occur simultaneously between 48 h – 72 h of cultivation for all the strains, including the control (**Table 6.2**). However, statistical differences between the strains were only observed for phosphate and magnesium. This observation suggests that there is a potential link between phosphate and magnesium, which was visible due to the overexpression of PSR1 in the transgenic strains 8-27, 8-42 and 8-2. Calcium and potassium uptake rates were negligible and thus, are not shown.

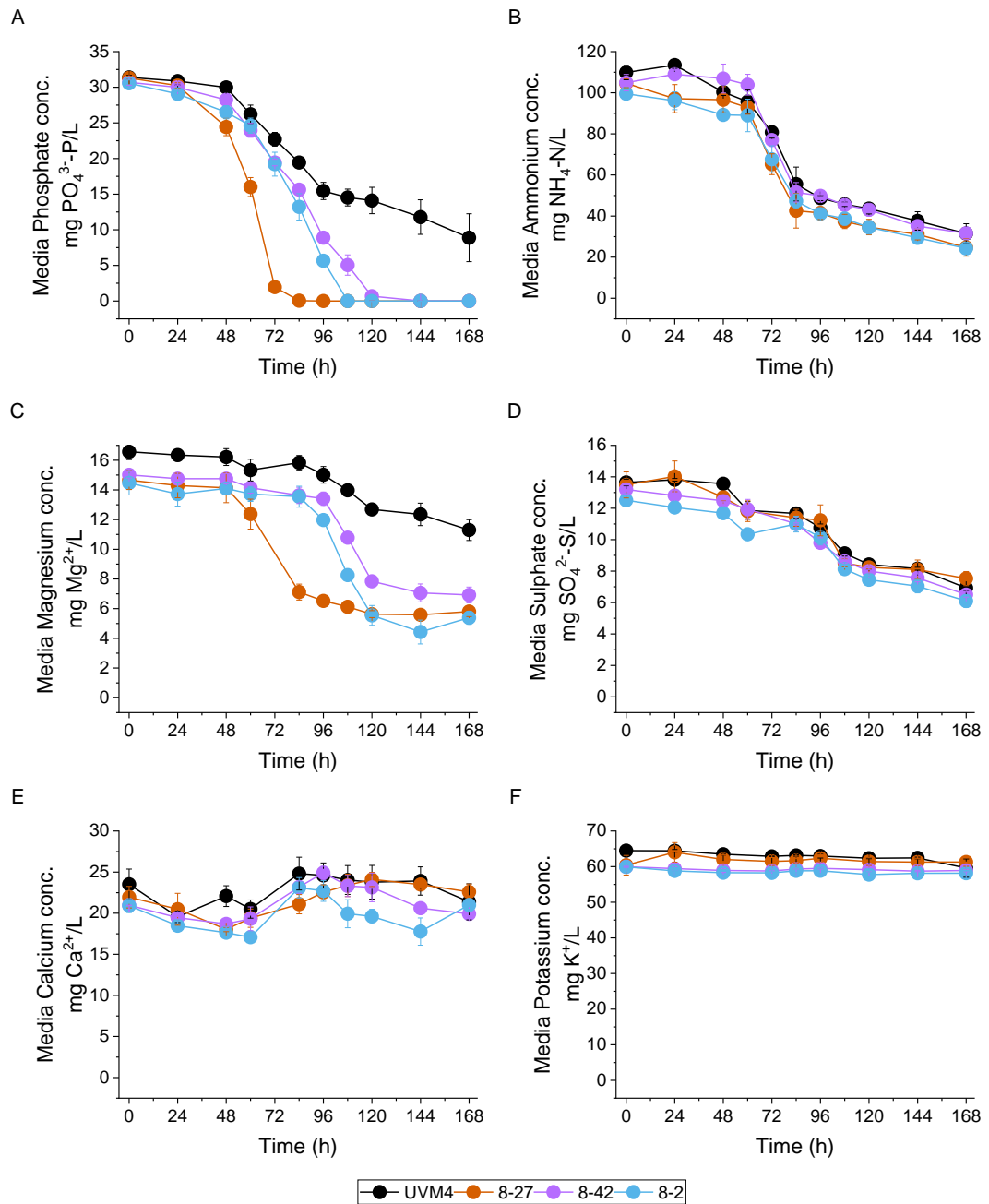


Figure 6.4 Nutrient removal from the media of PSR1 overexpression strains (8-27, 8-42 and 8-2) and the non-transformed control (UVM4). A Phosphate (mg PO₄³⁻-P/L), B Ammonium (mg NH₄⁻-N/L), C Magnesium (mg Mg²⁺/L), D Sulphate (mg SO₄²⁻-S/L), E Calcium (mg Ca²⁺/L), and F Potassium (mg K⁺/L). Each data point represents the mean (n=3) and error bars show the standard error of the mean value.

Table 6.2 Maximum nutrient uptakes observed in the non-transformant control and the PSR1 overexpression strains. Precultures of the strains UVM4, 8-27, 8-42 and 8-2 were inoculated in TAP media and monitored over 168 h. The maximum nutrient uptake rates of phosphate (mg PO₄-P g dw⁻¹ h⁻¹), magnesium (mg Mg²⁺ g dw⁻¹ h⁻¹), ammonium (mg NH₄-N g dw⁻¹ h⁻¹), and sulphate (mg SO₄-S g dw⁻¹ h⁻¹) were observed between 48 h – 72 h for all strains. Values represent the average of three biological replicates ±SE (ns, *, ** and *** represent OneWay ANOVA p-values = > 0.05, ≤ 0.05, ≤ 0.01 and ≤ 0.001). Letters a and b correspond to statistical differences across strains via Tukey HSD.

(48 - 72 h)	Maximum nutrient uptake rate (mg g dw ⁻¹ h ⁻¹)			
	Phosphate PO ₄ -P	Magnesium Mg ²⁺	Ammonium NH ₄ -N	Sulphate SO ₄ -S
UVM4	5.01 ± 0.46 (b)	0.26 ± 0.08 (b)	13.49 ± 3.09	1.31 ± 0.14
8-27	15.5 ± 0.37 (a)	4.84 ± 0.66 (a)	21.64 ± 3.04	1.19 ± 0.01
8-42	6.07 ± 0.32 (b)	1.12 ± 0.65 (b)	20.66 ± 3.13	1.01 ± 0.01
8-2	5.03 ± 1.11 (b)	1.06 ± 0.23 (b)	14.89 ± 5.53	1.08 ± 0.40
Statistical significance	***	**	ns	ns

6.3.5 Polyphosphate dynamics under PSR1 overexpression reveal insights into P-recycling processes within the cells

Figure 6.3A showed a peak of total phosphate concentration in the biomass, which can be assumed to be due to accumulation (as polyP), rather than growth, as there were no differences in biomass observed in **Figure 6.2B**. This result led to conjecture about the formation of polyP granules, its variation over time and the difference between strains, as an effect of the PSR1 overexpression. Thus, 4',6-diamidino-2-phenylindole (DAPI) staining, which is commonly used for the staining of DNA but also polyP, was used to image polyP granules within the microalgal cells (see section 2.3.3 in **Chapter 2 Literature Review**). DNA has an emission maxima at 461 nm and polyphosphate at 525 nm when using DAPI (Aschar-Sobbi et al., 2008a). Thus, DNA signal (stained in blue) can be differed from polyP signal (stained in yellow), with the appropriate confocal microscopy setting, as we showed in our research paper (Figure 1 in Slocombe et al., 2023).

Samples were stained with DAPI and preserved for confocal imaging, for one replicate of the non-transformed strain UVM4 and the transgenic strain 8-27, respectively. The images were processed as a projection of six to twelve z-stacks, to ensure that the full z-axis of the cell was covered. Ten representative images (from 30-50 pictures taken) from each line and each day, are shown in

the appendix **Figures A5-7**. Images of polyP granules (yellow channel, bottom row) are shown together with the brightfield channel (grey, top row), for the 48 h, 72 h and 144 h time points, which are relevant in terms of growth, and phosphate accumulation in biomass. A summary composite figure of the DAPI-stained cells is shown in **Figure 6.5**.

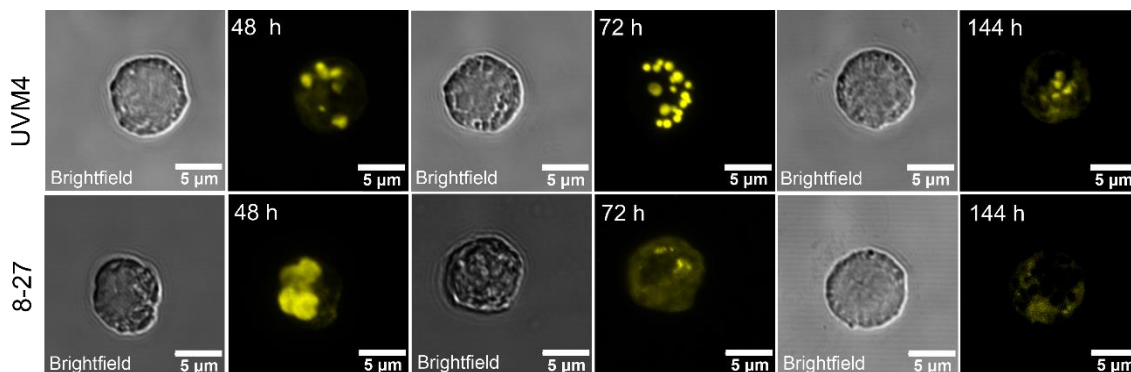


Figure 6.5 DAPI-polyP timeline of PSR1-OE and its background UVM4. 24 h, 72 h and 144 h time points of confocal images of DAPI stained cells (one representative image from the appendix **Figures A5-7**)

The images of the non-transformed control UVM4, showed a formation of round-shaped polyP granules at the 48 h time point (early exponential growth phase) followed by what appears to be a great condensation of the granules and an increase in their number within each cell, after 72 h. Finally, as the levels of media phosphate decreased and cells reached the stationary phase, the images showed ‘diffuse’ granules, which might be due to the degradation of polyP for further use of these phosphate reserves. For the transgenic strain 8-27, the timeline seemed accelerated and divergent in the sense that 48 h polyP granules looked substantially bigger than those of the control, for what appears to be an expedited formation and condensation of the granules. After 72 h, when the cells are dividing at the fastest rate and the phosphate in the media is almost depleted, the granules look less intense and ‘diffuse’ within the cells. Finally, after 144 h, with no phosphate availability in the media, the granules in the transgenic strain 8-27 looked more ‘diffuse’ compared to the 72 h time point. This suggests that polyP was mobilised to sustain the demand for organic molecules containing P (e.g. DNA/RNA, ATP, etc.).

Table 6.3 Summary of observations of polyP dynamics from composite Figure 6.5. DAPI-polyP is linked to the time of cultivation, growth phase, media phosphate concentration and characteristics of the polyP granules as per the confocal analysis of DAPI stained cells, for the non-transformed control UVM4 and the PSR1 overexpression line 8-27.

Time (h)	Growth phase	UVM4		8-27	
		Media Phosphate	polyP state	Media Phosphate	polyP state
48	Early exponential	High ~30 mg PO ₄ -P/L	Formation of small granules	High ~24 mg PO ₄ -P /L	Formation of larger condensed granules
72	Mid exponential	High ~23 mg PO ₄ -P /L	Condensation	Low ~2 mg PO ₄ -P /L	Mobilisation
144	Stationary	Low ~9 mg PO ₄ -P /L	Mobilisation	Depleted Undetected	Mobilisation

A description of the main observations is displayed in **Table 6.3** for better illustration. After 48 h, both strains are entering the early exponential phase, and the phosphate concentration in the media is still high (>25 mg PO₄-P/L). The formation of polyP granules expected during non-limiting P conditions occurs in both strains, although for 8-27, the granules appear to cover a significantly higher proportion of the cell. At the 72 h time point corresponding to the mid-exponential growth phase, the strain UVM4 seemed to go through a process of condensation of the granules and an increase in their number, and the concentration of phosphate in the media still high (>20 mg PO₄-P/L). On the contrary, strain 8-27, with a low media phosphate concentration (<2 mg PO₄-P/L), showed a marked transient peak which is likely due to degradation of the polyP polymer. After 144 h, mid-stationary phase, UVM4 cultures had an average phosphate concentration in the media of 10 mg PO₄-P/L and seemed to start degrading the polyP at this point. In contrast, the transgenic strain 8-27, with no detectable phosphate in the media, has presumably utilised all the P arising from poly P granule degradation, thus, explaining the disappearance of the polyP granules (**Figure 6.5**).

6.3.6 Assessing the potential effect of PSR1 overexpression on cell volume under phosphate non-limiting conditions

Since PSR1 is a transcription factor upregulated by phosphate limitation, the overexpression of PSR1 could hypothetically mimic a phosphate stress response, even when there is no P deprivation. One of these responses is the increase in cell size as an effect of lipid or starch accumulation. Therefore, cell volumes were calculated from the confocal images (**Figure 6.6**). At the early stages of growth and under continuous light cultivation, it is expected to observe unsynchronised cell cycles leading to greater variations in the cell volumes. This means that the cell cycles are not as synchronised as they can be when photoperiods of 16 h:8 h or 12 h:12 h (light: dark) are used (Zones et al., 2015).

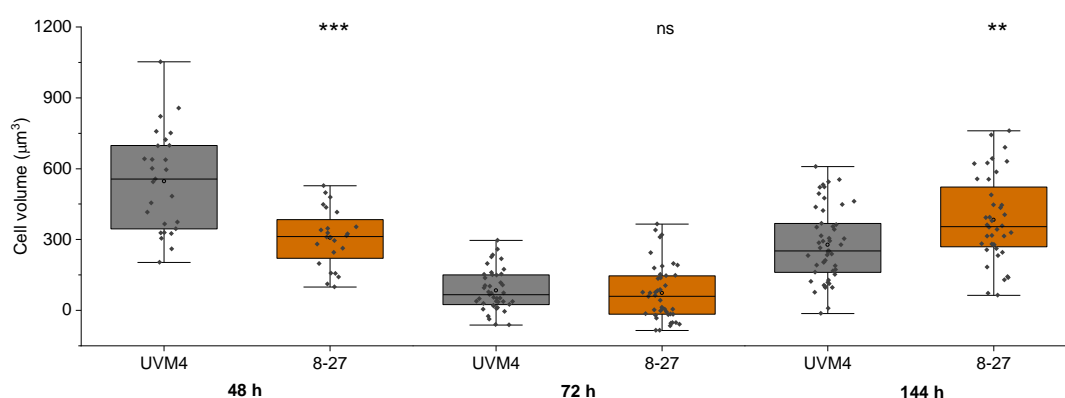


Figure 6.6 Distribution of cell volumes of the non-transformant control UVM4 and the PSR1 overexpression strain 8-27 over time. Cell volumes (μm^3) were estimated from confocal images after 48 h, 72 h and 144 h of cultivation. Asterisks represent the statistical significance of the results compared to the control (ns - not significant, * - p -value <0.05 , ** - p -value <0.01). Data is representative of one of the triplicates of the non-transformed control UVM4 and the PSR1 overexpression 8-27.

Nevertheless, at the 48 h time point, the cells of the transgenic strain 8-27 were significantly smaller than those from the control. Interestingly, the 8-27 cultures at this time point had smaller cells (average $307 \mu\text{m}^3$) with a total phosphate content of 7.5% $\text{PO}_4\text{-P}$, dw. In contrast, UVM4 cultures had larger cells (average $571 \mu\text{m}^3$) but exhibited a four times lower total phosphate content of 2.0% $\text{PO}_4\text{-P}$, dw (**Figure 6.3A**). After 72 h, there were no differences in the cell sizes, although at this time point, the cells were overall smaller than at the 48 h time point. After 144 h, there was an increase in the average cell size for both strains, but 8-27 cells were significantly bigger.

6.3.7 Magnesium, rather than calcium, is the potential counterion, assisting PSR1 overexpression strains with increased uptake of phosphate

Polyphosphate is a chain of more than three phosphate ions joined by phosphoanhydride bonds and hence, is a highly anionic biopolymer (Albi and Serrano, 2016). Therefore, when polyP is accumulated within the cells, a counterion is required to balance the charge of the molecule. In the case of *C. reinhardtii*, calcium (Ca^{2+}) has been mentioned as the most common counterion for polyphosphate (Siderius et al., 1996). Thus, considering the substantial increase in the P accumulation in the biomass (**Figure 6.3A**) and characteristic polyP accumulation (**Figure 6.5**) of the PSR1 overexpression strains, a hypothesis was formulated about the potential responses assisting the cells to cope with the increased P uptake rates. Ergo, the presumption was that a higher uptake of calcium as a response to the increase of polyP accumulation, was a possible coping mechanism. Nonetheless, **Figure 6.4E** showed that there were no differences in the removal pattern of calcium from the media. Instead, the PSR1 overexpression strains seemed to have preferred magnesium as a possible counterion (**Figure 6.4C**). This observation is confirmed by the higher uptake rates of magnesium observed in the PSR1-OE strains, given that their pattern of removal followed that of phosphate (**Table 6.2**).

6.4 Assessing the effect of PSR1 on *C. reinhardtii* P overplus

6.4.1 *C. reinhardtii* growth abnormal in *psr1-1* mutant but not affected by PSR1 overexpression during P overplus

To determine the effect of PSR1 knockout or overexpression on *C. reinhardtii* growth during phosphate overplus, I harvested and washed mid-exponential cultures of the strains UVM4, 8-27 and *psr1-1* and resuspended them in phosphate-free media (TA) for 24 h. This was followed by harvesting the P-deprived biomass and resuspension in fresh TAP media to trigger a phosphate overplus response. A sample was collected before (-24 h), after P-deprivation (0 h) and then for 96 h after TAP repletion, to monitor biomass concentration, cell counts and optical density (**Figure 6.7**).

During P-deprivation (grey box in **Figure 6.7**), I observed no differences in the growth pattern of the strains UVM4 and 8-27, compared to CC-125 (shaded segment representing data from **Figure 5.1A** in **Chapter 5**). This suggests that mid-exponential cells of these strains were able to mobilise internal reserves of

P to sustain growth when P was not available in the media. In contrast, the *psr1-1* mutant exhibited a significantly lower increase in biomass concentration after 24 h of resuspension in TA media (**Table 6.4**). This was expected due to the PSR1 gene knockout of this mutant, which is precisely involved in the response to phosphate stress. However, this observation may also suggest that PSR1 is potentially involved in assisting or regulating P mobilisation.

As expected, I observed that resuspension in TAP media of P-deprived cells promoted biomass growth for all the strains. However, the *psr1-1* mutant lagged in terms of growth rate, doubling time and biomass productivity as shown in **Table 6.5**. This observation could suggest that 1) PSR1 possible role in the response to the resupply of phosphate with other nutrients to P-deprived cells was affected by the knockout in this mutant or more likely that 2) the abnormal response to P-deprivation caused a lag in the growth response after upon TAP supply. Although, compared to its background (CC-125), *psr1-1* divided significantly faster after resuspension in TAP media (see **Table 5.1B** in **Chapter 5**, p-value=0.037). This could be due to the cw15 background of the original *psr1-1* mutant, which was later backcrossed with CC-125 (at least four times) (Shimogawara et al., 1999).

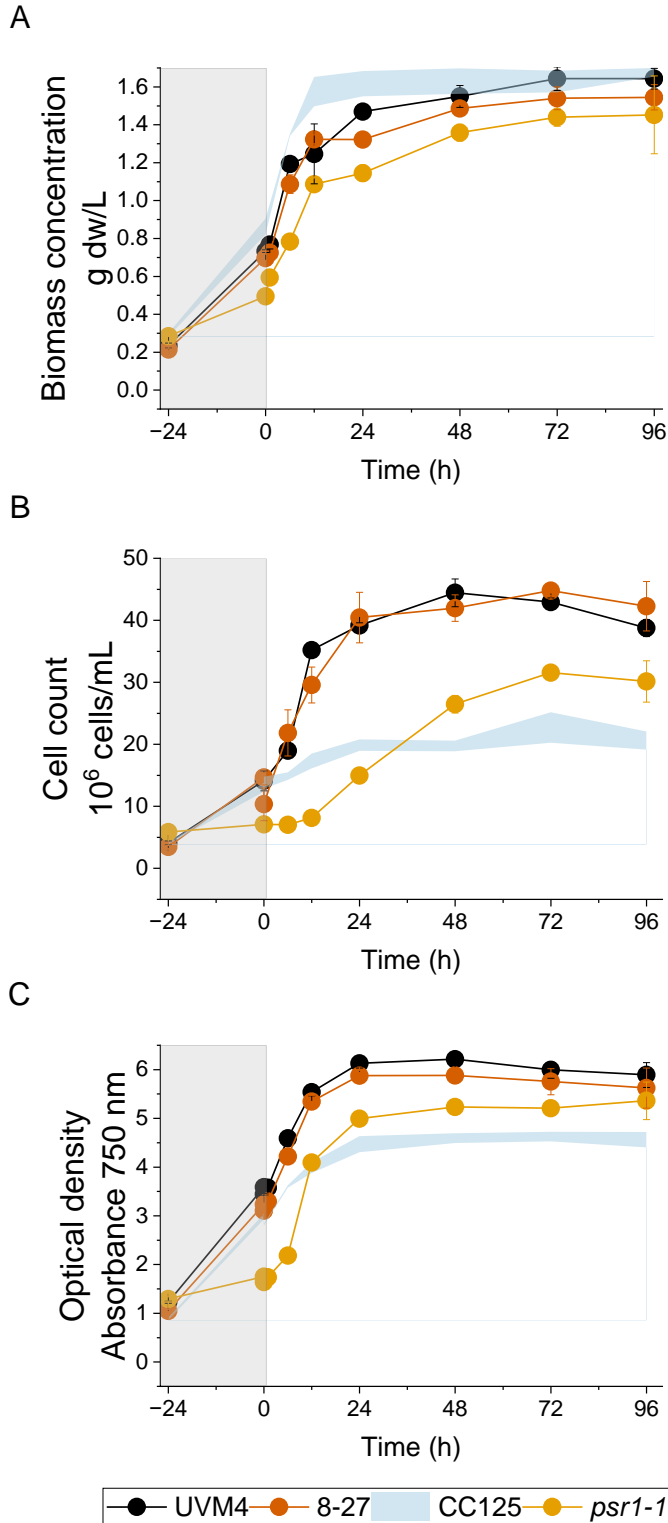


Figure 6.7 Effect of PSR1 knockout or overexpression on *C. reinhardtii* growth during P-deprivation and repletion. Mid-exponential cells of the strains UVM4, PSR1 overexpression 8-27 and *psr1-1* mutant were resuspended in TA media for 24 h (grey box) and then resuspended in fresh TAP media. A Biomass concentration (g dw/L), B Cell count (10^6 cells/mL) and C Optical density (Absorbance 750nm). Shaded segments show the area covered by the error bars from parameters observed for the strain CC-125 from **Chapter 5** for reference (**Figure 5.1B, D, and F**).

Table 6.4 Increase of biomass concentration after P-deprivation of PSR1 overexpression and *psr1-1* mutant. Values correspond to the average difference between biomass concentrations of mid-exponential cultures before and after 24 h of resuspension in TA media \pm SE (Statistical significance of *** corresponds to p-value \leq 0.001).

Increase in biomass concentration (g dw/L) after 24 h of P deprivation	
Strain	% \pm SE
UVM4	67 \pm 1
8--27	70 \pm 1
CC125	66 \pm 2
<i>psr1-1</i>	43 \pm 4
Statistical significance	***

Unsurprisingly, the PSR1 overexpression strain 8-27 had similar biomass productivity after resuspension in TAP media to its background (UVM4). Nonetheless, the transgenic strain 8-27 exhibited a higher specific growth rate (p-value = 0.023) and divided faster (although not significantly, p-value = 0.051) than the non-transformant control UVM4 (**Table 6.5**). In comparison with the experiment in section 6.3, UVM4 exhibited a lower specific growth rate and higher doubling time during P overplus, but with a higher biomass productivity. 8-27, exhibited a very similar specific growth rate and doubling time to that of the previous experiment, and a higher biomass productivity. A higher increase in biomass concentration occurred due to a higher initial biomass concentration before resuspension in TAP media (average of UVM4 and 8-27 = 0.715 g dw/L) compared to the previous experiment in section 6.3 (0.013 g dw/L).

Table 6.5 Growth parameters of PSR1 overexpression strain and *psr1-1* mutant after P repletion. Values represent the average (n=3) \pm SE after resuspension in TAP media of 24 h P-deprived cells of UVM4, 8-27 and *psr1-1* (ns, *, **, and *** represent OneWay ANOVA p-values > 0.05, \leq 0.05, \leq 0.01 and \leq 0.001)

Strain	Specific growth rate (h ⁻¹)	Doubling time (h)	Biomass productivity (g dw L ⁻¹ h ⁻¹)
UVM4	0.044 \pm 0.004	16.1 \pm 1.5	0.026 \pm 0.004
8-27	0.061 \pm 0.007	11.4 \pm 2.3	0.026 \pm 0.001
<i>psr1-1</i>	0.023 \pm 0.001	30.3 \pm 1.0	0.012 \pm 0.001
Statistical significance	**	***	**

6.4.2 P overplus response was also observed when PSR1 is overexpressed in *C. reinhardtii*

To assess the effect of PSR1 overexpression or knockout on phosphate overplus, I monitored polyP accumulation and total phosphate content in the biomass throughout both stages of P overplus (P-deprivation and repletion). **Figure 6.8A** shows that before P-deprivation, mid-exponential cultures of the PSR1 overexpression strain 8-27 had four times more polyP than its background, UVM4, and the wild-type CC-125. Then, during P deprivation the strain 8-27 exhibited a lower biomass P depletion rate compared to its background and the wild-type CC-125 (**Table 6.6**), and reached an average polyP content of 1.5% PO₄-P,dw (from a starting polyP content of 4.5% PO₄-P,dw) in contrast with the 0.1% PO₄-P,dw observed in UVM4 and CC-125 (from a starting polyP content of 0.5% PO₄-P,dw). After resuspension in TAP media, 8-27 still exhibited a P overplus response in a 6 h period and reached a polyP content of 2.4% PO₄-P,dw, which is not near the level observed before P-deprivation. After this period, the polyP content of this strain decreased and remained stable at the level reached after P-deprivation (1.5% PO₄-P,dw). The strain UVM4, had a very similar pattern in the polyP content at all stages (mid-exponential, P-deprivation and resuspension in TAP media), to that observed for the wild-type strain CC-125 (**Figure 5.2A** in **Chapter 5**). Surprisingly, I could not detect polyphosphate in the *psr1-1* mutant at any stage of the experiment. This phenotype to the best of my knowledge has not been described before for this mutant.

Table 6.6 Fold change of polyP content after P-deprivation affected in PSR1-OE strain. Values correspond to the average (n=3) difference in the polyP content of mid-exponential cultures before and after 24 h of resuspension in TA media ±SE (Statistical significance of * corresponds to p-value ≤0.05). nd = not detected

PolyP fold decrease after 24 h of P-deprivation (% PO ₄ -P,dw)	
Strain	FC±SE
UVM4	6.7 ±0.2
8--27	2.7 ±0.1
CC-125	5.1 ±0.6
<i>psr1-1</i>	nd
Statistical significance	*

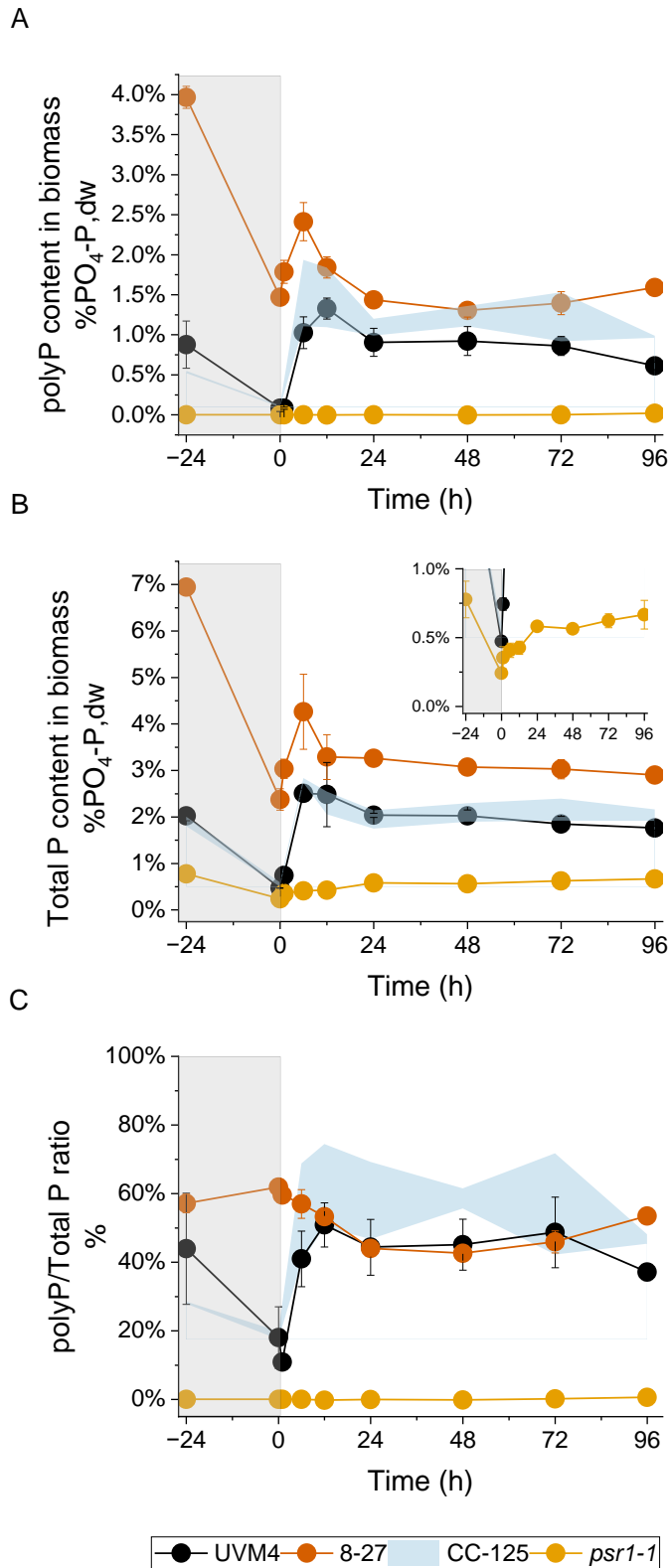


Figure 6.8 Phosphate accumulation of PSR1 overexpression strain and *psr1-1* mutant during P-deprivation and repletion. Mid-exponential cells of the strains UVM4, PSR1 overexpression 8-27 and *psr1-1* mutant were resuspended in TA media for 24 h (grey box) and then resuspended in fresh TAP media. A polyP content in biomass (% PO₄-P, dw), B Total P content in biomass (% PO₄-P, dw) and C polyP to total P mass ratio (% w/w). Shaded segments show the area covered by the error bars from parameters observed for the strain CC-125 from **Chapter 5** for reference (**Figure 5.2**).

Consistent with the P overplus experiment in section 5.3 in **Chapter 5 (Figure 5.2C)**, the pattern of the total P content in the biomass followed that of polyP for all strains, except for the *psr1-1* mutant **Figure 6.8B**. This strain has a lower total P content than its background, CC-125, at all stages of the experiment. Mid-exponential cultures of *psr1-1* had a total P content of 0.78%PO₄-P,dw and reached 0.24%PO₄-P,dw after 24 h of P-deprivation. After 96 h of resuspension in TAP media, *psr1-1* recovered most of its initial level before P-deprivation (see inset diagram in **Figure 6.8B**). Finally, **Figure 6.8C** shows the polyP to total P mass ratio at each stage of the experiment. UVM4, as expected followed a similar trend compared to that described for CC-125 in **Figure 5.2E in Chapter 5**. Interestingly, I could observe that the PSR1 overexpression strain 8-27 maintained its polyP to total P mass ratio, unlike its background UVM4 and the wild type CC-125. 8-27 kept a constant ratio of approximately 60% (w,w) after 24 h P-deprivation. After resuspension in TAP media, 8-27 exhibited a slight decrease in the polyP to total P mass ratio and matched that of UVM4 until the end of the experiment.

6.4.3 RNA content pattern not affected by PSR1 overexpression during P overplus

The observation that the *psr1-1* mutant did not contain polyP at any point of the experiment (**Figure 6.8A**) but was still able to increase its biomass concentration after P-deprivation (**Table 6.4**), raised the question about the alternative phosphate source this mutant used to sustain growth. **Figure 6.9** shows the RNA content in the biomass before and after 24 h of P-deprivation and after resuspension in TAP media. I observed that before P-deprivation, the mid-exponential cultures of the *psr1-1* mutant and the PSR1 overexpression strain 8-27 had the highest and lowest RNA content compared to the background strains CC-125 and UVM4, respectively. After 24 h of P-deprivation, the *psr1-1* mutant exhibited a considerable decrease in its RNA content, in contrast to the other strains (**Table 6.7**). This observation suggests that RNA may be the alternative source of P that the *psr1-1* uses to sustain growth under P deprivation.

Table 6.7 Difference in RNA content of PSR1 overexpression and *psr1-1* mutant during P-deprivation. Values correspond to the average (n=3) percentage difference between the RNA content of mid-exponential cultures before and after 24 h of resuspension in TA media \pm SE (Statistical significance of ** corresponds to p-value \leq 0.01). Positive and negative values represent an increase or decrease, respectively.

Change in RNA content in biomass (%RNA,dw) after 24 h of P deprivation	
Strain	% \pmSE
UVM4	- 17 \pm 1
8--27	+ 10 \pm 2
CC125	- 13 \pm 5
<i>psr1-1</i>	- 66 \pm 13
Statistical significance	**

After resuspension in TAP media, I observed no changes in the RNA content pattern between the PSR1 overexpression strain 8-27 and its background UVM4. For the *psr1-1* mutant, RNA recovery was observed in the first 24 h after resuspension TAP but did not reach its initial level of RNA before P-deprivation. The RNA pattern after resuspension in TAP media in the *psr1-1* mutant was similar to its background CC-125. Although, the RNA content decreased after the recovery peak (24 h), in contrast with CC-125.

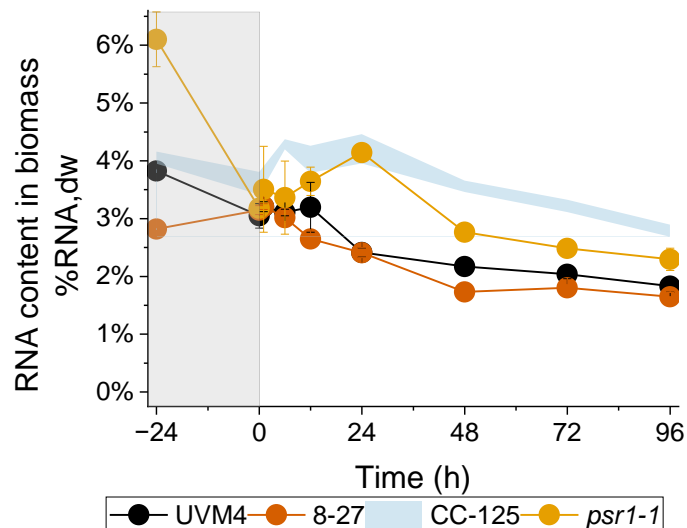


Figure 6.9 RNA variation in biomass of PSR1 overexpression strain and *psr1-1* mutant during P-deprivation and repletion. Mid-exponential cells of the strains UVM4, PSR1 overexpression 8-27 and *psr1-1* mutant were resuspended in TA media for 24 h (grey box) and then were resuspended in fresh TAP media. Shaded segments show the area covered by the error bars from parameters observed for the strain CC-125 from **Chapter 5** for reference (**Figure 5.4**).

6.4.4 PSR1 overexpression enhanced phosphate removal efficiency during P overplus

To evaluate the effect of PSR1 knockout or overexpression on nutrient removal during P overplus, I monitored the concentration of phosphate, ammonium and sulphate during the experiment (**Figure 6.10**). Consistently with the phosphate accumulation in the biomass (**Figure 6.8B**), I observed that the *psr1-1* mutant was the only one that did not remove all phosphate from the media after resuspension in TAP media (**Figure 6.10A**). This strain only removed 40% of phosphate from the media by the end of the monitoring period. The other strains (UVM4 and 8-27) removed all phosphate from the media in 12 h, which is consistent with the previous P overplus experiment discussed in **Chapter 5** (**Figure 5.5**).

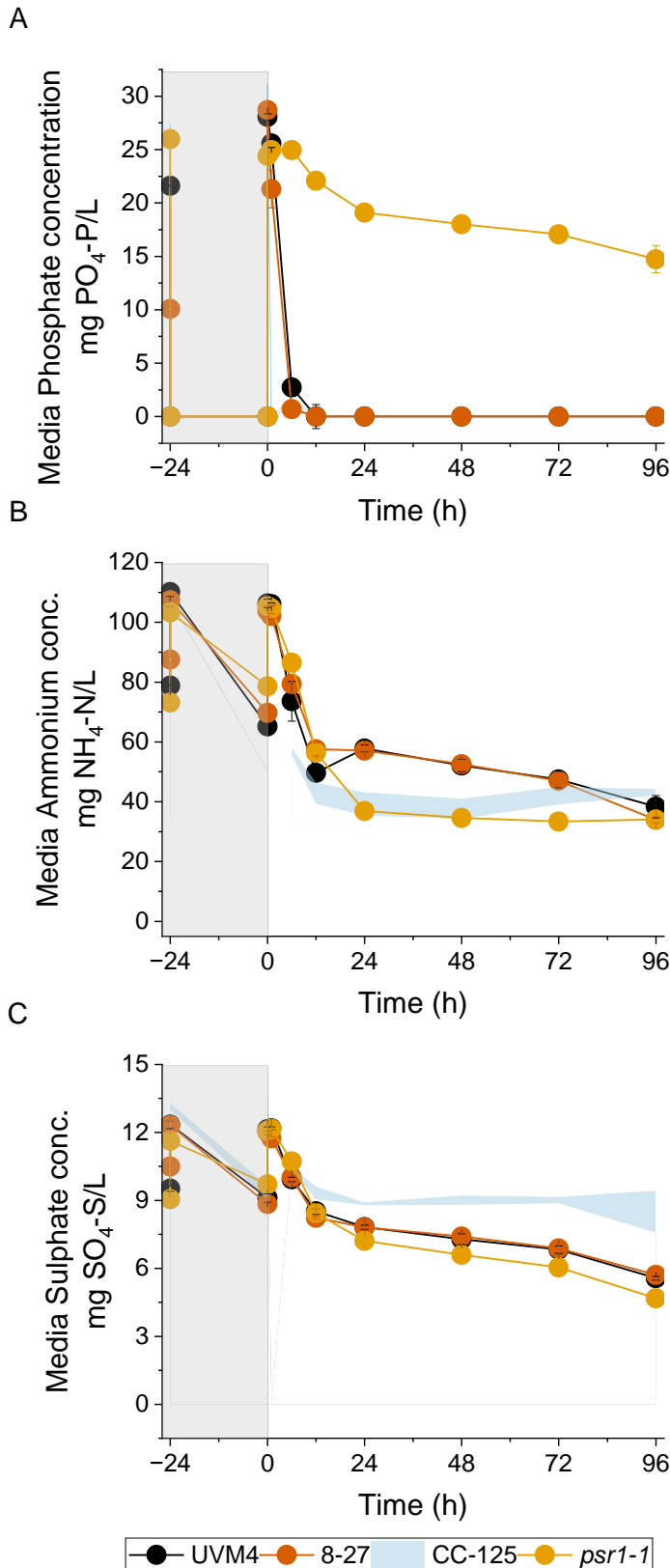


Figure 6.10 Nutrient removal from the media by the PSR1 overexpression strain and *psr1-1* mutant, during P-deprivation and repletion. Mid-exponential cells of the strains UVM4, PSR1 overexpression 8-27 and *psr1-1* mutant were resuspended in TA media for 24 h (grey box) and then resuspended in fresh TAP media. A-B Phosphate concentration in the media (mg PO₄-P/L), C-D Ammonium concentration in the media (mg NH₄-N/L) and E-F Sulphate concentration in the media (mg SO₄-S/L). Shaded segments show the area covered by the error bars from parameters observed for the strain CC-125 from **Chapter 5** for reference (**Figure 5.5**).

In the case of ammonium, I observed that *psr1-1* exhibited a higher removal efficiency compared to UVM4 and 8-27, but no different to that of its background, CC-125 (**Figure 6.10B**). Finally, no differences were observed in the removal of sulphate for the strains UVM4, 8-27 and *psr1-1* (**Figure 6.10C**). The shaded segment corresponding to CC-125 shows a higher concentration of sulphate in the media (**Figure 5.5E in Chapter 5**). However, the initial concentration of sulphate of CC-125 after resuspension in TAP media was higher than for the other strains (UVM4, 8-27 and *psr1-1*), which could be due to TAP media preparation for each experiment. To eliminate any differences in TAP media preparation, I calculated the nutrient uptake rates for phosphate, ammonium and sulphate for the first 24 h after resuspension in TAP media. The nutrient uptake rates were calculated for each sampling time point (0-1, 1-6 h, 6-12 h, 12-24 h) for the strains UVM4, 8-27 and *psr1-1* and are shown in the appendix **Table A 1**. This table shows that the PSR1-OE strain 8-27 exhibited a more immediate response to nutrient resupply than its background UVM4, where higher nutrient uptake rates were observed in the first hour after nutrient supply. However, to compare with the 'wild type' strain CC-125 I calculated the nutrient uptake rates for the time segments where data was available for (0-6 h, 6-12 h, 12-24 h) (**Table 6.8**). Comparisons were made between 8-27 and *psr1-1* with their corresponding backgrounds UVM4 and CC-125, respectively. The nutrient uptake rates of strain CC-125 correspond to the experiment shown in section 5.3 of **Chapter 5**, calculated from **Figure 5.5**.

I observed that PSR1 overexpression caused a more rapid uptake of phosphate in the first 6 h and then in the 6-12 h period, compared to UVM4. Thus, 8-27 may have depleted all phosphate from the media sooner than UVM4 before the 12 h time point (**Table 6.8A**). In contrast, no differences were observed in the uptake rate of ammonium between UVM4 and 8-27, except for the 12-24 h segment (**Table 6.8B**). Finally, the effect of PSR1 overexpression on the sulphate uptake rate was only significant in the 6-12 h period (**Table 6.8C**).

The *psr1-1* mutant exhibited a considerably lower uptake rate of phosphate at all time points compared to its background, CC-125 (**Table 6.8A**). Interestingly, in the case of both ammonium and sulphate, I observed that *psr1-1* exhibited a significantly lower nutrient uptake rate in the first 6 h which was followed by a significantly higher nutrient uptake rate during the 6-12 h period, compared to CC-125 (**Table 6.8B-C**). The delay in the uptake of these nutrients was reflected in the slower growth rate of this mutant upon resuspension in TAP (**Table 6.5**).

Table 6.8 Changes in nutrient uptake rates by PSR1 overexpression strain and *psr1-1* mutant, compared to the control. Average values (n=3) for the four strains were used \pm SE. nn corresponds to values below 0.1 mg g dw⁻¹ h⁻¹. Statistical significance was tested for 8-27 and *psr1-1* compared exclusively to their background strains, UVM4 and CC-125 (*, **, *** for p-value \leq 0.05, 0.01 and 0.001, respectively).

A		Phosphate uptake rate		
		mg PO₄-P g dw⁻¹ h⁻¹		
Strain	0-6	6-12	12-24	
UVM4	6.02 \pm 0.15	0.31 \pm 0.11	nn	
8-27	6.76 \pm 0.19 *	nn	*	nn
CC-125	6.04 \pm 0.50	0.15 \pm 0.04	nn	
<i>psr1-1</i>	0.63 \pm 0.33 ***	0.61 \pm 0.08 **	0.22 \pm 0.04 **	
B		Ammonium uptake rate		
		mg NH₄-N g dw⁻¹ h⁻¹		
Strain	0-6	6-12	12-24	
UVM4	7.47 \pm 1.27	2.67 \pm 0.95	0.55 \pm 0.05	
8-27	5.87 \pm 0.51 ns	3.35 \pm 0.31 ns	0.13 \pm 0.06 *	
CC-125	10.31 \pm 0.32	1.74 \pm 0.57	0.19 \pm 0.02	
<i>psr1-1</i>	6.38 \pm 0.78 **	6.70 \pm 0.29 **	1.35 \pm 0.26 **	
C		Sulphate uptake rate		
		mg SO₄-S g dw⁻¹ h⁻¹		
Strain	0-6	6-12	12-24	
UVM4	0.50 \pm 0.10	0.20 \pm 0.10	nn	
8-27	0.48 \pm 0.03 ns	0.28 \pm 0.02 **	nn	
CC-125	0.77 \pm 0.04	0.13 \pm 0.04	nn	
<i>psr1-1</i>	0.45 \pm 0.03 **	0.49 \pm 0.01 ***	nn	

6.5 Results summary and discussion

1. PSR1-YFP construct is expressed in the transgenic strains

In the first section of this chapter, I showed my contribution to the paper “Overexpression of PSR1 in *Chlamydomonas reinhardtii* induces luxury phosphate uptake” (Slocombe et al., 2023). The hypothesis that we formulated was that PSR1 overexpression would trigger a luxury phosphate uptake response, without previous P-deprivation conditions. P-deprivation (or deprivation of other nutrients) is typically needed to activate this phenomenon in microalgae (Aksoy et al., 2014, Chu et al., 2020a, Solovchenko et al., 2019b). While PSR1 overexpression was used in previous studies, their focus was to unveil the role of this transcription factor on lipid and starch accumulation and its connection to nutrient stress (Ngan et al., 2015, Bajhaiya et al., 2016).

By western blotting, I confirmed that the PSR1-OE construct was still present in strains 8-27 and 8-42 (**Figure 6.1**). *C. reinhardtii* harbours a transcriptional gene silencing pathway that affects foreign DNA integration into the genome (Neupert et al., 2020). Although the background strain UVM4 was modified to provide long-term stability and high transgene expression, it still expresses the gene silencing pathway, and thus, could potentially affect the expression of the PSR1 overexpression construct over time (Neupert et al., 2009). The PSR1 transgenic strains are maintained in TAP agar supplied with paromomycin but in liquid cultures, only TAP media is used to avoid any effect of the antibiotic on transgenic *C. reinhardtii* growth.

2. Growth not affected by PSR1-OE, consistent with previous PSR1-OE studies

To test the hypothesis that PSR1-OE induces luxury P uptake without previous P-deprivation, I tested the performance of three PSR1 overexpression strains of *C. reinhardtii* (8-27, 8-42 and 8-2) with differing levels of expression of PSR1 and a non-transformed background (UVM4), in terms of growth, phosphate accumulation in the biomass and nutrient removal from the media. All the strains showed similar changes over time in the biomass and chlorophyll a+b concentration, and optical density, which was consistent with no statistical differences in the specific growth rates and doubling times (**Figure 6.2** and **Table 6.1**). The strains divided approximately every 12 h during the exponential growth phase, which is within the range expected for *C. reinhardtii*, under similar culture conditions (Boyle and Morgan, 2009, Ramos-Martinez et al., 2017, Barolo et al., 2022). This demonstrates that PSR1 transgenic strains show no growth penalty compared to the non-transformed control under the tested conditions. This outcome was not necessarily expected since PSR1 is a

transcription factor involved in many processes other than phosphate metabolism (Ngan et al., 2015), and hence its overexpression could have affected the growth of these strains. My results were consistent with Bajhaiya et al., who also found no differences in the growth rates of PSR1 overexpression strains and their background strain CC-4351 (Bajhaiya et al., 2016). The chlorophyll content, on the other hand, was significantly higher on their PSR1 overexpression strains under 'high P' conditions (Bajhaiya et al., 2016), which is contrary to our results (**Figure 6.2C**). These differences could be due to the distinctive design of both constructs. The PSR1 overexpression strains in the Bajhaiya et al. study were generated from the auxotrophic strain CC-4351, and PSR1 is under the control of the promoter of the heat shock protein HSP70A (Bajhaiya et al., 2016). In our study, the PSR1 overexpression strains come from a high transgene expression background (UVM4) and the PSR1 transgene is under the control of the light-regulated promoter of a ferredoxin-binding protein of photosystem I, PSAD (Fischer and Rochaix, 2001). Moreover, in Bajhaiya et al., a photoperiod of 16:8 h light: dark was used while in our experiment we cultivated all strains under continuous illumination. All of the factors mentioned above could affect in a different way parameters like the chlorophyll concentration in the cells.

Moreover, in our experiment, I observed that the biomass concentration for all the strains reached a maximum of approximately one gram of dry biomass per litre between the 120-144 h time point (**Figure 6.2B**), which corresponds with optimal growth and high biomass productivity for *C. reinhardtii* cultivation standards (Anam et al., 2021, Moon et al., 2013). The cessation of growth occurred simultaneously with a plateau in the pH of the media at a value of approximately 8.5, which was expected since TAP media is buffered with Tris (**Figure 6.2D**). This also prevented the precipitation of phosphorus as calcium phosphate and was useful to track phosphate removal as biomass uptake only.

3. PSR1-OE triggered luxury P uptake and led to the highest P content reported in the literature

I monitored the accumulation of total P in the biomass and found that one of the PSR1-OE, 8-27, exhibited a massive peak of approximately 7.5% PO₄-P,dw after 48 h of cultivation. This was almost four times higher than that observed in the non-transformant control, UVM4 (**Figure 6.3A**). The other PSR1-OE strains 8-42 and 8-2, exhibited a lower performance in biomass total P accumulation than 8-27, although still higher than the control, UVM4. Such a high total P content in the biomass (~7% PO₄-P,dw) was also achieved by Wang et al., using PSR1 overexpression strains of *C. reinhardtii* and by increasing the initial phosphate concentration to three times that of TAP media (30.97 mg PO₄-P/L),

to reach this high total P content (Wang et al., 2023). Although in their study they implemented PSR1 overexpression in a *ptc1* mutant background (Wang et al., 2023). In a previous study, Wang et al. showed that PTC1 has a role in P recycling as it catalyses phosphate transport outside of acidocalcisomes, which suggests that PTC1 is involved in polyP metabolism and P starvation-dependent signalling (Wang et al., 2021). Once more, any differences between different PSR1-OE strains may be attributed to the design of the constructs, the background strains used and cultivation conditions. In their study, Wang et al. also used the HSP70A promoter and cultivated the strains under continuous illumination in TAP media.

Therefore, to the best of my knowledge, a total P content in the biomass of this magnitude (~7.0% PO₄-P,dw), reported in this thesis is among the highest ever reported for microalgae (Powell et al., 2008, Powell et al., 2009, Solovchenko et al., 2019b, Plouviez et al., 2021, Slocombe et al., 2023, Wang et al., 2023). The PSR1 overexpression strains are programmed to express PSR1 as if they were experiencing P limitation in the media. However, these strains were inoculated in P-replete media and thus, P was rapidly taken up and stored in the form of polyP, a response that is typical when luxury P uptake or P overplus take place (Aitchison and Butt, 1973). Consistently with the increase in biomass P accumulation, I observed that PSR1-OE enhanced P removal from the media under nutrient-replete conditions. In fact, a 100% phosphate removal efficiency was achieved, in a time lapse of 84-144 h (under the limit of detection of the ascorbic acid method (<0.01 mg P/L) - EPA Method 365.3), in contrast with the non-transformant control (**Figure 6.4A**). Ammonium, which is the source of nitrogen in TAP media was not removed from the media differently by the PSR1-OE strains, compared to UVM4. This macronutrient has been found to influence phosphate removal which depends on the nitrogen to phosphorus ratio (N:P), although the 'optimum' range is wide (7-42 N:P molar ratio) (Beuckels et al., 2015). TAP media provides a molar N:P ratio of approximately 7:1, which leads to the observation that PSR1 overexpression strains P removal efficiency occurred under nitrogen-replete conditions (**Figure 6.4B**).

4. PSR1-OE accelerates the formation, condensation and mobilisation of polyP

From another perspective, the DAPI-stained cells imaged by confocal microscopy revealed a polyP recycling response (**Figure 6.5**). I observed that both the control and the transgenic lines exhibited three polyphosphate states: 1. Formation, 2. Condensation and 3. Mobilisation (**Table 6.3**). The first occurs when microalgae sense high P levels in the environment. The second is a result of luxury P uptake, resulting in the accumulation of dense polyP granules. The

third shows the degradation of polyP as a response to the depleted P or reduced concentration of P in the media. The transgenic strains, differ only by accelerating these polyP states, leading to the conjugation of formation and condensation of the larger granules (after 48 h), which was followed by the degradation and mobilisation of P reserves (after 72 h). This acceleration, in my view, assisted the transgenic strains in achieving the same biomass productivity as the control. The PSR1-OE strain 8-27 had almost depleted all P from the media after 72 h (**Figure 6.4A**) when the cultures were still in the middle of the exponential phase (**Figure 6.2**). This strain was able to rapidly mobilise its P reserves to sustain growth at the same rate as the control UVM4, which was reflected in a rapid decline in the total P content after day 3 in **Figure 6.3A**, until matching UVM4 levels. From the DAPI images, I could also observe that PSR1 overexpression generated bigger cell volumes after 144 h of cultivation, compared to the control (**Figure 6.6**). At this point, the strain 8-27 had experienced P-deprivation for almost 72 h. Bajhaiya et al. also observed larger cell volumes when cultivating their PSR1-OE strains for 7 days in 'low P' (Bajhaiya et al., 2016).

5. Magnesium is likely the preferred counterion in PSR1-OE strains

Finally, an interesting observation linked to the divergent polyphosphate accumulation pattern, between the PSR1-OE strains and the control, was the enhanced removal of magnesium from the media (**Figure 6.4C**). Magnesium is likely acting as the preferred counterion, instead of calcium, assisting in the stabilisation of the additional load of phosphate taken up by the cells at such rates (**Table 6.2**). From a biological perspective, it makes more sense to switch to a cation other than calcium, which would not interfere with the sensitive signalling pathways where calcium is involved (Pivato and Ballottari, 2021). At the cellular level, calcium needs to be maintained at a very low concentration and its level is tightly regulated as it is an important second messenger in many signalling pathways (e.g. abiotic stress) (Dodd et al., 2010). Moseley et al. found that PSR1 regulates the putative H^+/Ca^{2+} antiporter, a protein that may regulate intracellular calcium levels and its distribution after release from polyphosphate during P deprivation. Although, it has been suggested that released Ca^{2+} , provides the internal signal of P-deprivation that ends up activating PSR1 itself (Moseley and Grossman, 2009). Magnesium, on the contrary, is located in the cytosol as a core component of the chloroplast and participates in various enzymatic processes (Sarma et al., 2014).

6. Transcriptional and post-transcriptional responses observed in PSR1-OE strains

After inoculation of the PSR1 overexpression strains 8-27, 8-42 and 8-2 and the background, UVM4 in TAP media, samples were collected for RNA sequencing after 48 h, 72 h and 144 h. RNA was prepared for sequencing and raw data was analysed and processed by Dr. Slocombe (Slocombe et al., 2023). From his analysis, a list of phosphate metabolism genes were identified and classified according to their role in P transport, salvage/sparing, homeostasis, polyP synthesis and cation transport, which pattern of expression was different for the PSR1-OE strains compared to the background (Table 2 in Slocombe et al., 2023). I used this list to calculate the z-scores of the RPKM (reads per kilobase per million) for each gene at the 48 h, 72 h and 144 h time points in the PSR1 overexpression strains 8-27 and 8-42 and their background UVM4, and generated a heatmap of gene expression (**Figure 6.11**). The figure shows how the strain 8-27 upregulated the expression of these genes considerably compared to the background but also to the other PSR1 overexpression strains 8-42. This may explain, at the transcriptional level, some of the differences observed between both PSR1-OE strains in terms of phosphate accumulation in the biomass and removal from the media (**Figure 6.3A** and **Figure 6.4A**).

During the experiment, it can be observed how the strain 8-27 exhibited an upregulation of genes involved in the transport of phosphate either early after 48 h of cultivation, from the 72 h timepoint onwards or at the end of the experiment (144 h). This followed the model that Dr. Slocombe proposed of a feedforward response due to 1) the high levels of P in the media at the beginning of the experiment and the overexpression of PSR1 induced luxury uptake of phosphate and high polyP accumulation, 2) the fast removal of phosphate from the media after 72 h of cultivation, triggered the upregulation of genes involved in the response 'low P' and P salvage, sparing mechanisms.

In this sense, after 48 h of cultivation of the strain 8-27, we observed a strong upregulation of 1) the PTA1, PTA3 and PTA4 genes, which are likely involved in low-affinity transport of phosphate under P-replete conditions (Moseley et al., 2006), 2) PTB6, a high-affinity P transporter presumably operating at 'low P' conditions (Wang et al., 2020). Other transporters were upregulated on the three time points (48 h, 72 h and 144 h), and peaked either at 72 h (a putative phosphate binding component of ABC transporter - PSTS, and high-affinity uptake system under 'low P' - PTB12, PTB4 and PTB2) or after 144 h (high-affinity uptake system under 'low P' - PTB5, PTB3) when the levels of P in the media were almost or completely exhausted.

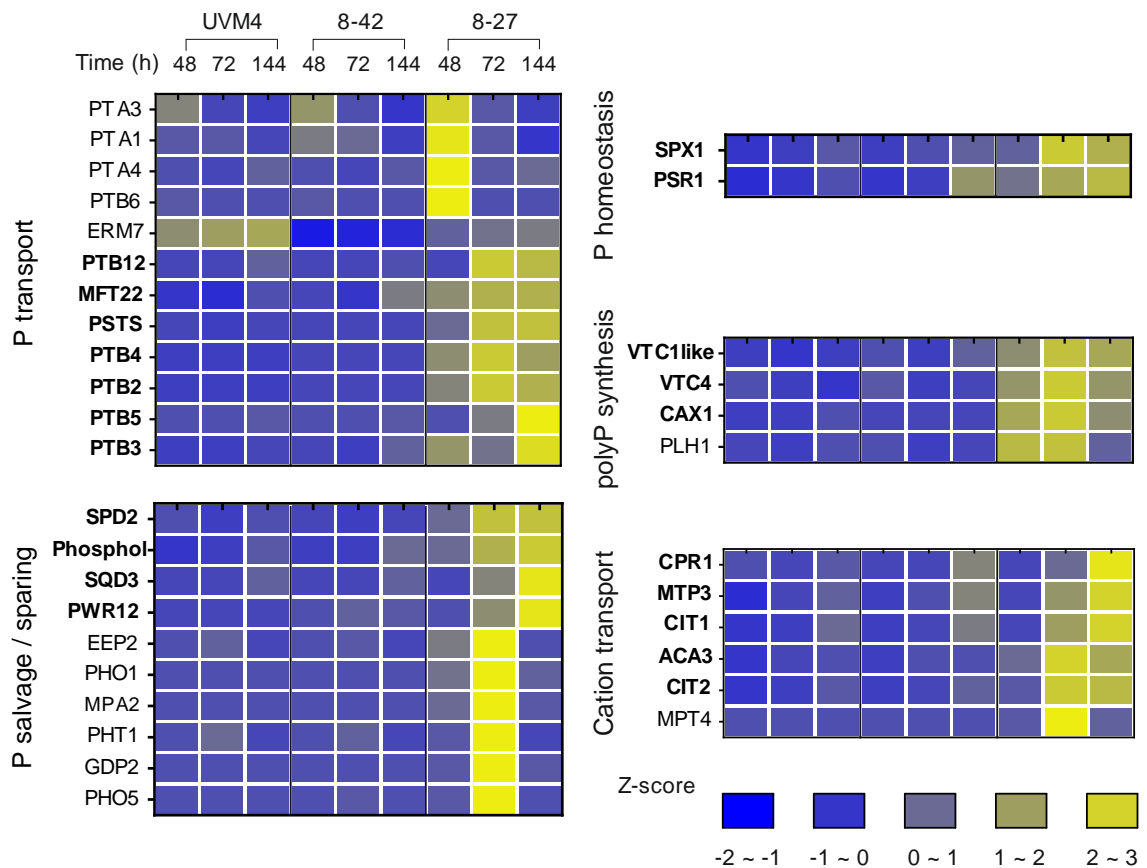


Figure 6.11 Heatmap of key genes involved in P metabolism differentially expressed in PSR1-OE strains. Precultures of the PSR1-OE strains and the non-transformant control UVM4 were inoculated in fresh TAP media and samples were collected after 48 h, 72 h and 144 h of cultivation for RNA sequencing. RPKM values from the RNAseq dataset were transformed into Z-scores. For UVM4, only endogenous levels of PSR1 are present, whereas, for 8-27 and 8-42, both endogenous and transgene levels are shown. Genes in bold exhibited a positive Pearson's correlation index with PSR1 as shown in Table 2 of (Slocombe et al., 2023)

The genes involved in P salvage or sparing by degrading organic molecules that contain P (The exophosphatases PHO1 and PHO5, phosphodiesterase GDP2, the metallo phosphatase MPA2, the phytase PHT1, and the nuclease phosphatase EEP2), were mostly upregulated in the strain 8-27 at the 72 h time point, whereas the phosphodiesterase SPD2, the nuclease PWR12 and phospholipid phosphatase Phospho1 were upregulated at both the 72 h and 144 h time points. In the meantime, PSR1 was upregulated in both PSR1-OE strains with the difference that for 8-27, it exhibited an 11-fold increase after 48 h and 72 h of cultivation in contrast with a 3-fold increase of the strain 8-42, compared to UVM4 (Table 2 in Slocombe et al. 2023). This is the reason why, in the heatmap, 8-42 appears as if the upregulation of PSR1 occurs only after 144 h. To note, RNA sequencing analysis can only provide information about the variation in the transcript abundance across the samples and time points. Transcript abundance data provides valuable information about the gene expression patterns, but it does not always relate to protein abundance, due to

post-transcriptional regulation mechanisms. Also, in the case of PSR1, the transcript abundance observed across the PSR1-OE strains and the control UVM4 at each time point corresponds to both the endogenous and transgene PSR1. On the other hand, western blotting provides information on the protein abundance patterns and allows to distinguish between the transgene and endogenous PSR1, as only the transgene PSR1 has the YFP tag (see **Figure 3.1, Chapter 3 Materials and Methods**).

To link the increase in biomass P accumulation with the overexpression of PSR1, I used western blotting to detect the transgene PSR1 protein and observed a similar expression pattern for both transgenic strains, although considerably stronger in the strain 8-27, compared to 8-42 (**Figure 6.3B**). These differences could be due to the random positioning of the PSR1 overexpression construct within the genome of each strain, as well as, a different (unknown) number of extra copies of the transgene PSR1 in the genome of these strains, which is yet to be determined. Over the monitoring period, the pattern of biomass total P content (**Figure 6.3A**) seemed to follow the transgene PSR1 protein expression, which was upregulated between the 24 and 96 h time points and was followed by a downregulation after 120 h of cultivation, coinciding with a lower total content of P. A lower transgene PSR1 protein expression (PSR1-YFP), despite being controlled by the light-driven PSAD promoter indicates possible post-transcriptional or post-translational regulation of PSR1, triggered by the signal of phosphate depletion from the media. This conjecture is consistent with the observation of Dr. Slocombe that the PSAD transcript levels were reduced a 40% by the end of the experiment.

The gene SPX1, involved in P signalling and response to P availability via the SPX-IP pathway in yeast and high plants (Jia et al., 2023, Secco et al., 2012, Yao et al., 2014, Wang et al., 2021), was upregulated in 8-27 after 72 h. At this time point, P was almost completely depleted from the media by 8-27 (**Figure 6.4A**). The binding of inositol pyrophosphate to SPX, assist in the repression of the AtPHR1 (the transcription factor involved in P deprivation response of *A. thaliana*) under P sufficient conditions (Dong et al., 2019, Puga et al., 2014). Therefore, an upregulation of SPX1 observed in our PSR1-OE strains could be due to the intracellular signal of inositol pyrophosphate, as a response to high P accumulation. This observation coincides with Yao et al. who observed upregulation of SPX1 by overexpressing PHR1 in the bean plant *Phaseolus vulgaris* L. (Yao et al., 2014). Interestingly, in this present study, the upregulation of SPX1 coincides with the downregulation of the transgene PSR1 protein after 72 h of cultivation, observed by western blotting (**Figure 6.3**). Although, there is no direct evidence that this mechanism works in the same

way in *C. reinhardtii* as it does in *A. thaliana* or *P. vulgaris*, there is a clear pattern suggesting that it could be at least similar.

Finally, upregulation of polyP metabolism genes was also observed in the strain 8-27 compared to the background UVM4: members of the VTC complex VTC1like and VTC4, the calcium antiporter CAX1 and a putative triphosphate hydrolase, PLH1, which also clustered with these group of genes. These genes may have promoted the high polyP accumulation observed for this strain at the 48 h and 72 h time points (**Figure 6.3A**). Also, the upregulation of genes with a cation transport function was detected in 8-27 in contrast with UVM4. We believed that these genes assisted the increase in magnesium transport observed in the PSR1-OE strains (**Figure 6.4C**).

Given the extraordinary results of our PSR1-OE strains demonstrating their capacity for luxury P uptake, I wanted to test their phosphate overplus performance. To do so, 24 hours of P-deprivation was used, followed by biomass harvesting and resuspension in TAP media. These conditions proved to be the most efficient in **Chapter 5**, for non-transgenic strains of *C. reinhardtii*, in terms of biomass productivity, P overplus and nutrient removal from the media. I added the *psr1-1* mutant (CC-4267), to determine the effect of PSR1 knockout vs. PSR1 overexpression, compared to their corresponding background strains.

I observed that the *psr1-1* mutant exhibited reduced biomass productivity and growth rates compared to its background, CC-125, and the other strains, UVM4 and 8-27 (**Table 6.5**). These results are consistent with those of previous studies and represent one of the manifestations of the abnormal response to P-deprivation in this mutant (Wykoff et al., 1999, Bajhaiya et al., 2016, Ngan et al., 2015, Shimogawara et al., 1999). Then after resuspension in TAP media, the growth of *psr1-1* was first characterised by a lag phase followed by sustained growth, which contrasted the immediate rapid growth observed in its background CC-125 (**Figure 6.7B**). The differences in growth between *psr1-1* and CC-125 after nutrient repletion were also reflected in the ammonium and sulphate uptake rates which were higher for *psr1-1* after the first 6 h, than for CC-125 which had an immediate response to nutrient resupply (**Table 6.8B-C**). Ngan et al. reported no differences in growth between *psr1-1* and CC-125 when cultivated under P-replete conditions (Ngan et al., 2015). Therefore, the lag phase observed in *psr1-1* cultures could be interpreted as an effect of the previous 24 h period of P-deprivation.

A surprising result was the inability to detect polyphosphate at any stage of the experiment in the *psr1-1* mutant (**Figure 6.8A**). To the best of my knowledge, this phenotype is described for the first time in this mutant. In *C. reinhardtii*, polyP synthesis is assumed to be similar to *S. cerevisiae*. In *S. cerevisiae*, polyP synthesis is mediated by the binding of inositol pyrophosphates (IP₇/IP₈) to the SPX domain of the VTC complex, with ATP as the P-donor (Gerasimaite et al., 2017). Homologs of the VTC complex have been found in the *C. reinhardtii* genome (Aksoy et al., 2014, Cliff et al., 2023). The generation of a *vtc1-1* and *vtc4-1* mutant in *C. reinhardtii* that were unable to produce polyP, suggested that the VTC complex of *C. reinhardtii* has a similar role in polyP synthesis to that in yeast (Aksoy et al., 2014, Sanz-Luque et al., 2020). The transcription and translation of the components of the VTC complex, VTC4, and VTC1, were found to increase upon P-deprivation (Plouviez et al., 2021, Plouviez et al., 2023a, Bajhaiya et al., 2016). It is believed that the availability of these proteins upon transfer to P-replete conditions assists in the rapid synthesis of polyP during the P overplus response (Plouviez et al., 2023a). Moseley et al. showed that VTC1 was not upregulated in the *psr1-1* mutant upon P-deprivation (Moseley et al., 2006). This was confirmed by Bajhaiya et al., who also observed the aberrant response of the *psr1-1* mutant to P-deprivation leading to the inability to upregulate both VTC1 and VTC4, compared to its background CC-125 (Bajhaiya et al., 2016). Therefore, the lack of polyphosphate observed in the *psr1-1* mutant in my experiment could be related, at least partially, to the link between PSR1 and the regulation of the VTC complex during P-deprivation. However, no polyP was detected before P deprivation or after P repletion, either. This suggests that another factor (e.g. a polyphosphate kinase) potentially controlled or regulated by PSR1, could explain the role of this transcription factor in polyP synthesis, which is yet to be uncovered. Since polyP was not present in the *psr1-1* mutant, the total P content observed was considerably lower at all stages of the experiment compared to the background CC-125 (**Figure 6.8B**). This was reflected in a much lower efficiency of phosphate removal from the media (**Figure 6.10A** and **Table 6.8A**). The inability of the *psr1-1* mutant to accumulate or synthesise polyP, suggests that almost all P contained in the *psr1-1* mutant biomass corresponds to organic forms of phosphate.

The *psr1-1* mutant had twice the content of RNA of its background before P-deprivation and before resuspension in TAP media, the RNA content was reduced to approximately 33% of the initial value (**Table 6.7**). As mentioned *psr1-1* mutant was still able to grow under P-deprivation, although at a significantly slower rate (**Table 6.5**). This suggests that, in the absence of

polyP, *psr1-1* uses RNA as an alternative source of P under P deprivation. A response that has been also described in previous studies for 'wild type' strains for longer periods of P-deprivation (Plouviez et al., 2023a, Couso et al., 2017), and is also consistent with my findings in **Chapter 4**, where a 96 h P-deprivation period triggered RNA degradation (**Figure 4.5C** in **Chapter 4**). In their proteomic study, Plouviez et al. observed an increase in the structural constituents of the ribosome, proteins involved in ribosome synthesis and translation after P was resupplied to P-depleted wild-type *C. reinhardtii* (Plouviez et al., 2023a). After resuspension in TAP media, I observed that the *psr1-1* mutant, exhibited a 24 h period of RNA recovery, followed by a decrease as the cultures reached the stationary phase, which was similar to its background CC-125 (**Figure 6.9**). This suggests that the processes behind RNA-P mobilisation may not be regulated by PSR1. Although, there seems to be a link with chloroplast DNA degradation. Yehuda et al. observed increase levels of chloroplast RNA and decreased levels of chloroplast DNA under P limitation of *C. reinhardtii* cells (Yehudai-Resheff et al., 2007). This response appeared to be mediated by PSR1, to control P recycling mechanisms, and its key for *C. reinhardtii* survival to P-deprivation.

In contrast with the *psr1-1* mutant, the PSR1-OE strain 8-27 did not have a different growth pattern under either P-deprivation or resuspension in TAP media compared to its background, UVM4 (**Figure 6.7**). Previous studies consistently observed no differences in growth between their PSR1-OE strains and their background or wild-type strains, under 'low P' or 'high P' conditions, including our recent paper (Bajhaiya et al., 2016, Ngan et al., 2015, Slocombe et al., 2023).

An interesting finding was that 8-27, with an initial total P content of approximately 7.0% PO₄-P,dw, before P deprivation, rapidly mobilised its P reserves after 24 h of resuspension in TA media. This observation is consistent with our previous experiment in **Figure 6.3**, where I detected a transient level of total P in the biomass of 8-27 after P was almost completely depleted from the media after 72 h (**Figure 6.4A**). However, after 24 h of P deprivation, this strain only reached its lowest at a value of 2.4% PO₄-P,dw, before P resupply as TAP (**Figure 6.8B**). The background UVM4 reached its lowest value of 0.5% PO₄-P,dw, which is consistent with my previous P-deprivation experiment with non-transgenic strains of *C. reinhardtii* (**Figure 4.3D** in **Chapter 4**), and with Bajhaiya et al., who observed higher P content in their PSR1-OE strains under 'low P', compared to the control (Bajhaiya et al., 2016). The polyphosphate content followed the pattern of total P content in the biomass, which led to the observation that the polyP to total P mass ratio did not vary after P-deprivation

and kept a constant value of 60% (w,w). In contrast, its background (UVM4) consistently lowered its polyP to total P mass ratio to approximately 20%, as observed in my P-deprivation experiment (**Figure 4.3F** in **Chapter 4**).

Interestingly, Wang et al. PSR1-OE strains exhibited a clear polyP decline (4.6-folds decrease after 24 h of P deprivation), whereas I observed a 2.6 fold-decrease in the polyP content of the strain 8-27 in this study (after 24 h of P deprivation) (Wang et al., 2023). Once again, this can be attributed to the construct design, background strain chosen, etc.

After resuspension in TAP media, I observed that both polyP and total P content of 8-27 peaked after 6 h but did not get close to the pre-deprivation levels (**Figure 6.8A-B**). Probably this observation could be explained by two different reasons. 1) In my previous P overplus experiment shown in **Chapter 4**, I showed that P-deprivation until reaching the lowest polyP content was optimum for P overplus, which in the case of this experiment occurred after 24 h of resuspension in TA media (**Figure 4.8A** in **Chapter 4**). The model proposed suggests that the assumption that a longer period of P-deprivation correlates with a bigger P overplus may be true until the lowest polyP content is reached (**Figure 4.11** in **Chapter 4**). In this experiment, the PSR1-OE strain 8-27 had a 17-fold higher polyP content than its background before resuspension in TAP media. Thus, it is possible that a high internal P signal counteracted the P overplus response of this strain. As reported in our recent study, the transcript of polyP synthesis genes correlated with internal phosphate levels (Slocombe et al., 2023). 2) PSR1 transcripts are upregulated during P-deprivation and downregulated during 'High P' conditions (Moseley et al., 2006, Bajhaiya et al., 2016). Plouviez et al. found that PSR1 transcript levels are also downregulated during P overplus at the repletion stage (Plouviez et al., 2021). Therefore, we cannot rule out a possible post-transcriptional or post-translational regulation of the transgene PSR1 during my experiment after resuspension in TAP media, which could reduce the biomass accumulation of phosphate by 8-27. As shown in **Figure 6.3B**, from the previous experiment, the transgene PSR1 levels decreased even under the control of the PSAD promoter under continuous light, which means that other factors can indeed influence PSR1 transgene expression. Nevertheless, both polyP and total P content of the strain 8-27 were at all times higher than those of the background strains, which is expected in PSR1-OE strains of *C. reinhardtii* (Slocombe et al., 2023, Wang et al., 2023, Bajhaiya et al., 2016).

Such high initial reserves of polyP in the 8-27 strain, were consistent with the observation of no alteration of RNA reserves during P-deprivation, consistent with the background strains **Figure 6.9**. After resuspension in TAP media, no

differences were observed in the content of RNA of this strain and the background UVM4. An observation that further reinforces the hypothesis that PSR1 does not regulate the mobilisation of P reserves coming from RNA.

Finally, the observation that 8-27 did not reach its initial phosphate content (pre-deprivation) after resuspension in TAP media, was not reflected in a lower removal of phosphate from the media. This strain removed all phosphate from the media likewise its background, UVM4 and the wild type CC-125, in the first 12 h after resuspension in TAP media (**Figure 6.10**). However, 8-27 exhibited a significantly higher P uptake rate than its background, UVM4 in the first 6 h after P depletion and had an almost negligible uptake rate in the 6-12 h segment, which indicates that a 100% removal of phosphate may have been achieved soon after the 6 h period, earlier than for UVM4 (**Table 6.8A**). A 100% removal of phosphate by the strain 8-27 in the time interval of 6-12 h improves considerably the result obtained in the previous experiment. For instance, in the experiment from section **6.3** in this chapter, 8-27 was inoculated in TAP media without previous P-deprivation and removed all phosphate from the media in 84 h (**Figure 6.4A**). However, the initial biomass concentration in the previous experiment was 210-fold lower (0.001 g dw/L, **Figure 6.2B**) than in this last experiment (0.21 g dw/L, **Figure 6.7A**). The initial biomass concentration is a factor that strongly influences phosphate removal (Plouviez et al., 2023b). Nonetheless, the P removal efficiency of 8-27 during P overplus only reduced the time of complete P removal by a few hours (< 6 h), compared to the non-transgenic strains under the same conditions, for which 100% P removal was obtained in 12 h after resuspension in TAP media (**Figure 4.5A in Chapter 5**). A higher initial biomass concentration, is equal to having more transport proteins a, which increases the capacity for P uptake. If PSR1 overexpression is added to the equation, we have upregulation of both high and low affinity phosphate transporters, as seen in **Figure 6.11**. This means that phosphate can be more rapidly removed to very low levels by PSR1-OE strains. Lastly, PSR1 overexpression did not affect the removal of ammonium or sulphate from the media (**Figure 6.10C-D**).

The interesting dichotomy of the PSR1-OE strain and the *psr1-1* mutant highlights the role of PSR1 not only as a transcription factor that activates responses to P deprivation but also as a crucial constituent of P storage in the form of polyphosphate. Therefore, without PSR1, no P overplus responses can be activated in the green microalgae *C. reinhardtii*.

Chapter 7 General Discussion and Conclusions

Phosphate overplus response and luxury P uptake phenomena in microalgae have generally been described as a period of high accumulation of phosphate in the form of polyphosphate granules, following a period of nutrient stress or deprivation (i.e., deprived access to P, N, S, etc.) (Chu et al., 2020a, Aksoy et al., 2014, Aitchison and Butt, 1973). Whether microalgae P overplus and luxury P uptake phenomena are the same remains unknown. Therefore, this research project was conducted to contribute uncovering the particularities or similarities in the biology of P overplus and luxury P uptake in microalgae. So far it appears that P overplus is exclusively related to the polyP accumulation response to P-deprived cells exposed to P-replete conditions. One of the main gaps is the fact that polyP analysis tools in microalgae are not as well established as in yeast (Christ and Blank, 2018, Christ et al., 2020b). This is a major obstacle to enabling a better understanding of P overplus in microalgae. Unfortunately, current evidence of microalgae polyP accumulation, biomass growth and nutrient removal, is far from being able to show the real potential of P overplus for P recovery. This chapter summarises new evidence found as part of the research work undertaken in this thesis, which will contribute to improving our understanding of how P deprivation, nutrient availability and the role of the transcription factor PSR1, affect the phosphate overplus response of *C. reinhardtii*.

7.1 The use of reliable qualitative and quantitative polyP analysis tools in microalgae

Polyphosphate is the main form of cellular phosphate storage during the P overplus response in microalgae and other microorganisms. This polymer allows microalgae, yeast and bacteria to store more phosphate than is needed to sustain cell division and chain lengths of linear polyP can extend between two and a thousand phosphate units (Harold, 1966). In microalgae, the P overplus response has been studied for approximately six decades and yet, accurate polyP quantitative tools have only recently become available and have not been adapted for use in all microorganisms of interest. This has also led to a lack of standardised methods for polyP analysis that give the most robust results in microalgae. This represents a major gap in the progress towards uncovering microalgae P metabolism processes and potential future use in real-life applications.

The quantification of polyphosphate in the study of P overplus is key to increasing our understanding of this phenomenon in microalgae. Aitchison and Butt used trichloroacetic acid and KOH to extract soluble and insoluble polyphosphate from *Chlorella vulgaris*, respectively. Samples were treated with concentrated sulphuric acid and 60% perchloric acid for the release of orthophosphate which can be determined by using spectrophotometric methods (aka, colourimetry) (Aitchison and Butt, 1973). Moudříková et al. standardised a method to quantify polyphosphate from *Chlorella vulgaris* using 2D Raman microscopy, a method which does not require a previous extraction step and describes the interaction between light a matter, and polyP of any chain length may be detected from a range of peaks and observed at specific wavelengths (Christ et al., 2020b, Moudříková et al., 2017). In the Moudříková et al. study, the results of the 2D Raman microscopy method were highly correlated to those obtained using the phenol/chloroform extraction of polyP, followed by enzymatic digestion of polyP with the recombinant *S. cerevisiae* exopolyphosphatase Ppx1, which releases orthophosphate that can be further quantified colourimetrically (Werner et al., 2005, Moudříková et al., 2017). Also, in their study, phenol/chloroform extraction of polyP was highlighted as the method with the highest extraction efficiency compared to other tested methods. However, polyP analysis by Raman microscopy requires expensive specialist equipment, and appropriate training which prevents a wide application of this method in different research contexts (e.g. research groups with fewer resources in developing countries). Solovchenko et al. also used the 2D Raman microscopy method developed by Moudříková et al., to quantify polyP in *Chlorella vulgaris* performing P overplus (Solovchenko et al., 2019b).

Other methods used to quantify polyP include, as Sforza et al. showed, the staining of fresh cell samples of *Nannochloropsis salina* with a solution containing Tris-HCl pH 7.0 and DAPI. They measured its fluorescence to report polyP quantification relative to DAPI fluorescence, against the autofluorescence of algal cells (Sforza et al., 2018). Moreover, Lavrinovičs et al. extracted polyP from *Desmodesmus communis*, *Tetradesmus obliquus*, *Chlorella photothecoides*, *Tetradesmus obliquus*, *Botryococcus braunii*, *Chlorella vulgaris*, and *Ankistrodesmus falcatus* with sonication, followed by a two-hour water bath, mixture with a chloroform /isoamyl alcohol solution and finally staining of the remaining supernatant with toluidine blue in acetic acid for colourimetry assay against a commercial standard of sodium phosphate glass Type-45 (Lavrinovičs et al., 2020, Lavrinovičs et al., 2021, Lavrinovičs

et al., 2022). Sanz-Luque et al. extracted polyphosphate from *Chlamydomonas reinhardtii*, using the phenol/chloroform protocol and used a commercial MicroMolar Polyphosphate Assay Kit (ProFoldin, PPD1000), which can estimate polyphosphate relative to the fluorescence of a polyphosphate dye that binds to polyP and is calibrated with an of sodium phosphate glass Type-45 standard (Sanz-Luque et al., 2020).

From these methodologies used in microalgae, it appears that 2D Raman microscopy and biochemical assay (Phenol/chloroform, Ppx1 treatment and colourimetry) are the most robust so far for the quantification of polyphosphate. Both methodologies have been compared previously by Moudříková et al., with similar results. However, they highlighted the possible drawbacks of either method: For 2D Raman microscopy an average of 50 cell images can be taken in 3 h. In this method, it is necessary to set assumptions regarding the shape of the cells, the distribution and shape of cellular compartments and the heterogeneity of the cultures, among others. The assumption of homogeneity of the microalgal culture is problematic for the research of nutrient deprivation responses in microalgae, which cause several effects on the cells, including at the physiological transcriptional and post-transcriptional levels as much as the morphological and structural level. 3D Raman microscopy is recommended for improved quality but is considered 'extremely time-consuming' (Moudříková et al., 2017). On the other hand, the biochemical assay has the issue of involving the manipulation of such a toxic compound as phenol, which requires appropriate health and safety training and the use of the necessary personal protection elements (PPE). Also, this assay includes multiple steps which are sensitive to human errors. For one to approximately twenty 96-well plates would take approximately 1.5 days to process, which means that real-time analysis is not possible during time-course experiments.

The qualitative analysis of polyP provides a complementary set of information that the quantitative analysis tools cannot deliver. Qualitative analysis of polyP is often accompanied by a visual perspective of polyphosphate granules or a distribution of polyP chain length and involves the use of metachromatic dyes. In microalgae and cyanobacteria, the most widely used polyphosphate dye is DAPI (4',6-diamidino-2-phenylindole). DAPI was first developed for the staining of DNA but was later highlighted for its ability to stain polyphosphate as well, by changing the emission maxima from 461 nm to 525 nm, respectively (Christ et al., 2020b). The use of DAPI to visualise polyP using confocal microscopy can be used to produce interesting insights into polyP accumulation patterns in microalgae. For instance, the work

presented in this thesis, included a time-line of polyP accumulation of a PSR1 overexpression strain of *C. reinhardtii*, compared to its non-transformed background (Slocombe et al., 2023). In this work, the observed DAPI-stained polyphosphate granules revealed the ability of PSR1 overexpression *C. reinhardtii* to form larger polyP granules. It appeared that *C. reinhardtii* generated large polyP granules to accommodate the high amount of P removed from the media at considerably high rates. This observation, which was in contrast with the control, allowed us to link the PSR1 transcription factor to polyP dynamics in an unprecedented way.

A major drawback of DAPI is that nucleic acids like RNA and P-rich molecules like inositol polyphosphates may interfere with the signal of DAPI-polyP due to their similar highly anionic characteristic, which can be especially challenging when polyP concentrations are low within the cells (Martin and Mooy, 2013, Kolozsvari et al., 2014). Moreover, as a light-sensitive dye, confocal images of DAPI-stained samples require a standard procedure that accounts for the effect of photo-sensitivity on the fluorescence intensity (Sanz-Luque et al., 2020). Thus, DAPI may not be the most reliable method if used as a quantitative assay of microalgal polyP, as the signal can fade in minutes. In this work, I observed that for the same cell, two confocal microscope images taken within a time range of ten minutes would look considerably different in terms of the DAPI-polyP fluorescence intensity (unpublished work). Hence, a standard methodology for the collection of confocal images was key and required the pictures for each cell to be collected as soon as the focus of the lens had the desired level of resolution.

DAPI and Toluidine blue, a far more traditional metachromatic dye, have been widely used in yeast research, to visualise polyphosphate in polyacrylamide gels (PAGE) (Smith and Morrissey, 2007, Losito et al., 2009). This technique allows for qualitative detection of the distribution of polyphosphate chain lengths and the presence of inositol polyphosphates in a sample. In microalgae, this technique has been used on a few occasions (Sanz-Luque et al., 2020, Yi-Hsuan et al., 2023). Sanz-Luque et al. used DAPI stained PAGE to visualise the absence of polyP in the *vtc4-1* mutants of *C. reinhardtii* (gene with polyphosphate kinase activity), in contrast with the WT and the VTC4 complemented strains generated in this study (Sanz-Luque et al., 2020). Yi-Hsuan et al. recently used Toluidine Blue stained PAGE to visualise the wide distribution of polyphosphate chain length in the green microalgae *Chlorella vulgaris* (Yi-Hsuan et al., 2023).

In my thesis, I used the biochemical assay to quantify polyP in *Chlamydomonas reinhardtii* (see **Chapter 3** Materials and Methods section

3.6.4). This method allows to monitor the polyP dynamics of this microalgae during P-deprivation conditions (and control non-P-deprivation conditions), as well as during P overplus. To the best of my knowledge, it is the very first time that a biochemical assay like this has been used in *C. reinhardtii* (or indeed in any other alga species) to monitor a time-course experiment at such a level of detail. The results obtained followed the same pattern as that of the biomass total phosphate content (see **Chapter 3** Materials and Methods section **3.6.2**), which allows to confirm that the quality of the polyP data was in agreement with previous studies of P overplus in *C. reinhardtii* (Plouviez et al., 2023b). However, it is important to note that this result might be specific for *C. reinhardtii* and thus, total P content in biomass should not be used as a surrogate for polyP quantification. PolyP analysis and quantification is the unequivocal evidence to directly assess P overplus. It is worth mentioning that although total P content in biomass samples helped to detect P accumulation patterns in *C. reinhardtii* during P overplus, this pattern can change for other species. The quality of the polyP data obtained in this thesis, was consistent with the estimated polyP content of photosynthetic eukaryotic microorganisms that accumulate polyP, when growing at their maximum rate (Rees and Raven, 2021).

The quantification of polyP in my project was accompanied by its qualitative detection via PAGE. The high-quality imaging of toluidine blue O staining of PAGE allowed the visualisation of the polyphosphate chain pattern of *C. reinhardtii* during its response to P-deprivation and P repletion. Uncovering this dynamic in microalgae is unprecedented and provides valuable new evidence on P overplus response in *C. reinhardtii*. For instance, polyphosphate is a molecule with high relevance in medical and agricultural fields (Kulakovskaya et al., 2012). Recent studies have dedicated efforts to purifying polyP of different chain lengths from microalgae (Yi-Hsuan et al., 2023). The findings in this work show that longer chains of polyP are available at the earliest stage of P overplus whereas a more heterogeneous mixture is obtained after the highest peak of polyP is observed. These results provide information that could be used to determine the time of extraction of polyP, according to the desired chain length. Furthermore, the striking observation made of PAGE detection of IP₆ pattern during *C. reinhardtii* P overplus challenges the assumed mechanism of polyP synthesis, believed to follow that of the yeast model *S. cerevisiae* via the binding of inositol pyrophosphates (IP₇/IP₈) to the SPX domain of the VTC complex, which activates polyP synthesis (Gerasimaite et al., 2017, Wild et al., 2016). This finding will not only lead to encourage the application of well-established

polyP analysis tools from yeast and bacteria to microalgae but also to the future design of new experimental strategies to answer unknown polyphosphate synthesis and mobilisation processes in *C. reinhardtii* and other microalgae.

7.2 What physiological parameter of P deprivation is better for studying P overplus?

Before this study, it was asserted that a longer time period of P deprivation was correlated with an improved P overplus response. This assumption appears to have arisen from Aitchison and Butt's report (Aitchison and Butt, 1973). They tested the polyphosphate accumulation of *Chlorella vulgaris* that had been P-depleted for 0, 4, 8, 12, 24 and 36 h, after resuspension in fresh media. A higher polyP accumulation was observed in the longest periods of P deprivation (24 h and 36 h). After this study, Lavrinovičs et al. studies tested the difference in the effect of 7 and 14 days of P-deprivation on polyP accumulation of three different species (*Desmodesmus communis*, *Tetradismus obliquus* and *Chlorella photothecoides*) (Lavrinovičs et al., 2020). They observed very high variability in the polyP accumulation pattern according to the tested P-deprivation periods and species, which further highlights the gap mentioned above in terms of the applicability of P overplus in real-life processes for P recovery. Time is not a reliable parameter of P deprivation because the underlying physiological responses may not take place at the same rate or may have different sensitivity to, for example, external P levels. Subsequently, Lavrinovičs reported different responses to 3 and 5 days of P-deprivation followed by resuspension in municipal wastewater, by *Chlorella vulgaris*, *Botryococcus braunii*, *Tetradismus obliquus* and *Ankistrodesmus falcatus*. *C. vulgaris* showed the best performance after 3 days of P-deprivation (Lavrinovičs et al., 2021). In a later study, Lavrinovičs chose *C. vulgaris* to further optimise the conditions leading this species to accumulate more polyP and tried different periods of P deprivation (0 - 10 days) before P repletion. They reported that a period of 10 days of P-deprivation, exhibited a higher polyP production rate, however, in their supplementary data, there is no clear trend suggesting that a longer period of P-deprivation led to a higher polyP accumulation (Lavrinovičs et al., 2022). Finally, Plouviez et al. tested a set of periods of P-deprivation (1 hour, 1, 2 and 4 days), and observed a higher accumulation of total phosphate content in the biomass of *C. reinhardtii* after 4 days of P-deprivation (Plouviez et al., 2023b). All the results from the studies mentioned above appear to agree to some degree, with the affirmation that the longest period of P

deprivation tested by them, resulted in a bigger P overplus response in microalgae. However, from these reports, it is unclear why the P deprivation periods tested were chosen to test microalgae P overplus performance. Time is a parameter that does not offer information about the biological state of the microalgal biomass due to the effect of a P deprivation treatment. Therefore, a fixed period of P deprivation cannot be used as a guideline for different experimental scenarios, let alone, should it be used as a design parameter in a real-life application of microalgal P overplus. Also, the time period that was effective for one particular experiment or case scenario can vary depending on the type of microalgal species, the environmental and cultivation conditions, etc.

Additionally, the difference between the concepts of phosphate deprivation, depletion, stress and starvation, which in the context of P overplus are often mixed, has led to misinterpretations of the effect of P-deprivation on P overplus: (1) Phosphate deprivation is the action of removing phosphate from the media as a treatment, (2) Phosphate depletion is the action of complete phosphate removal by microalgae from the media/environment, and (3) Phosphate stress and/or starvation occur after a signal of 'low' or no phosphate activates a response within the microalgal cells.

For instance, Solovchenko et al. tested the performance of *C. vulgaris* P overplus response and defined the period of 'P deprivation' as 3 consecutive days after microalgal growth ceased after resuspension in P-free media (Solovchenko et al., 2019b). Moreover, in Plouviez et al. work on *C. reinhardtii* P overplus, cultures were cultivated in 'low P' media (1 mg PO₄-P/L) for 5 days. These cultures were considered 'P-depleted' as all phosphate had been removed from the media after this period (Plouviez et al., 2021). Even though these two previous studies intended to relate the period of P deprivation to another parameter (Growth cessation or phosphate removal from the media), they still used time (days) as a reference. Also, the mix of the concepts of deprivation, stress, depletion and deprivation of phosphate in the field, affects the reproducibility of the results reported previously. From the experimental perspective, P deprivation is the only action that we can control, whereas P stress, P depletion and P starvation, will depend on the microalgal species, the cultivation conditions, etc.

In this project (Chapter 4), I tackled the issues above by:

1. Designing a P deprivation experiment to understand how this treatment affected the physiological state of the *C. reinhardtii* cells. First, I used four independent strains of *C. reinhardtii* at the same growth phase (mid-

exponential). Second, I provided information about the state of the biomass and the cultivation media, before the resuspension in P-free media with the following parameters: biomass concentration; in-cell total P, polyP and RNA content; and nutrient removal from the media. Third, I used those parameters as the point of comparison with those monitored during P deprivation. From this experimental approach, I found that mid-exponential cultures took 24 h to reach the lowest content of in-cell polyP and total P content, which also coincided with growth cessation. Hence, growth cessation depended on the availability of P reserves. RNA reached its lowest level after 96 h and thus, I tested whether either the lowest polyP or RNA (inorganic P pool vs. organic P pool) would trigger the bigger P overplus.

2. Subsequently, I used these two parameters of P deprivation, in a P overplus experiment where P-deprived *C. reinhardtii* was supplemented with a KPO_4 solution up to 1 mM P. After P repletion, I monitored the same parameters as in the preculture and P deprivation stages to enable the determination of the P deprivation parameter that would trigger the best performance.

My experiments provide unequivocal evidence that the lowest in-cell polyP content is the parameter to monitor before resupplying P to P-deprived microalgae, to obtain a higher P overplus response. A parameter that can be reproduced in other cultivation scenarios. The extent of this period will depend on the algae species, the initial biomass concentration before P deprivation and the initial polyP content in the biomass. To conclude, my data shows that a longer period of P deprivation triggers a bigger P overplus only until the lowest polyP content is reached. From this point onwards, depriving P for a longer time counteracts P overplus as it disturbs the organic P reserves in the cells.

7.3 What is the importance of nutrients other than P in the P overplus response?

In the literature on microalgal P overplus, I found that P repletion was done as either KPO_4 supplementation (Plouviez et al., 2021) to P-deprived cultures or biomass harvesting and resuspension in fresh culture media (Solovchenko et al., 2019b). Within those reports, the results of polyP or total P accumulation and P removal from the media were compared with previous studies. Such comparisons did not take into account the method of P repletion in their discussion. In my view, this overgeneralises the P overplus response as if the presence of nutrients other than P was irrelevant. Thus, I

tested in the same experiment, the difference between P repletion as KPO_4 addition or resuspension in fresh media (**Chapter 5**). My findings show that nutrient availability did not affect P overplus, as I did not observe different trends for either the lowest polyP or lowest RNA levels in P-deprived cultures upon resuspension in fresh TAP media, under the conditions tested. However, the repletion of phosphate together with other nutrients in TAP media promoted biomass growth which consequently, enhanced nutrient removal from the media. Moreover, if P-deprived cultures had interfered with their RNA reserves, P repletion with all nutrients in TAP would promote the recovery of RNA content to match the demand of this nucleic acid to resume biomass growth.

These results are relevant to the context of the potential application of microalgal P overplus for P control and recovery at WWTWs, where the objective is to cost-effectively meet the strict P discharge limits whilst producing P-rich biomass that enables the return of phosphate to land. In WWTWs that use microalgae, one possible challenge is the trade-off of polyP versus biomass growth versus phosphate removal. Aitchison and Butt, observed a big drop in the polyP levels of *Chlorella vulgaris*, during the exponential growth phase (Aitchison and Butt, 1973). Solovchenko et al. also observed a high peak in polyP accumulation, followed by a sharp decrease during the exponential growth of *C. vulgaris* during P overplus, when P was almost completely depleted from the media (Solovchenko et al., 2019b). In this present work (see **Chapter 6**), our PSR1-OE strain 8-27 also exhibited a very similar pattern of polyP accumulation, biomass growth and P removal from the media, as mentioned above (Slocombe et al., 2023). Hence, the interplay between these three parameters needs to be taken into account for the use of microalgae in WWTWs for P control and recovery. The results in the reports mentioned suggest that the window for biomass harvesting (at the highest in-cell P content) would be very narrow, which operationally speaking may be challenging.

In this thesis, this trade-off was overcome by tuning these three parameters at the 'right' level in my P overplus experiments. First, the use of mid-exponential precultures for the P-deprivation, allowed me to shorten the time at which polyP (or total P) levels would reach their lowest value to 24 hours only, in contrast with other studies (Plouviez et al., 2023b). The precultures, which reached the stationary phase after P-deprivation, rapidly accumulated polyP, within six hours after KPO_4 addition or resuspension in TAP media. The level of polyP remained stable until the end of the monitoring period (96 h). This confirms that biomass that is in the stationary growth phase can

indeed maintain excess polyP accumulated during P overplus for at least four days. Second, nutrient provision with phosphate allowed biomass growth without altering polyP levels as has been observed in previous studies (Aitchison and Butt, 1973, Lavrinovičs et al., 2020, Solovchenko et al., 2019b). Since all P was removed from the media, this suggests that microalgal P metabolism was diverted from using accumulated polyP to remove more P from the media to produce more biomass. This observation highlights the importance of nutrient availability to achieve simultaneous biomass growth, polyphosphate accumulation and enhanced nutrient removal, under tested conditions.

Furthermore, nutrient availability has been shown to affect nutrient uptake by microalgae, especially in the case of nitrogen and phosphorus (Beuckels et al., 2015). Nitrogen and phosphorus are two of the three main components of microalgal biomass, apart from carbon. The proportion of nutrient composition in microalgae was defined by the known Redfield ratio 'C₁₀₆H₁₈₁N₁₆P' (Redfield, 1960). From that study, the nitrogen to phosphorus molar ratio in algal biomass of 16:1 (7:1, N:P mass ratio) has been assumed to provide optimal conditions to sustain microalgal growth and consequently nutrient uptake. However, a later review of studies in phytoplankton under nutrient-replete conditions established a revisited range of molar N:P ratios between 5-19, that increased up to 34 if nutrient limiting conditions were added to the analysis (Redfield ratio) (Geider and Roche, 2002). Such variation may be due to the species (microalgae/cyanobacteria) and different environmental conditions affecting nutrient uptake ratios. Therefore, optimum N:P ratios should be determined according to the specific questions to be answered under relevant experimental scenarios. In fact, common commercial nutrient solutions for microalgal cultivation, fall below the Redfield ratio. One example is TAP media, which I have used throughout my experimental work (including some variations). TAP media has a molar N:P ratio of 7:1 and has been designed to provide suitable conditions for *C. reinhardtii* cultivation (Gorman and Levine, 1965, Kropat et al., 2011). Beuckels et al. reported that phosphate removal, more than nitrogen removal, is sensitive to the N:P ratio, with optimal values found in the range of 7 to 42 N:P; during their experiment, *Chlorella vulgaris* and *Scenedesmus obliquus* were cultivated in a WC medium with varying N:P ratios (Beuckels et al., 2015). In this present work, the N:P ratio increased to approximately 9:1 when P was supplied as 5xTA+P in the second P overplus experiment. While it is possible that the change in the nutrient composition of the repletion media in the second P overplus experiment, affected P removal from the

media, the literature suggests that a 9:1 N:P ratio is far from the critical point where N:P may affect P removal.

In the first P overplus experiment, the treatment of the microalgal biomass before P repletion was different because the aim was to test the common ways that P is added to trigger P overplus in the literature. I wanted to determine whether the centrifugation and resuspension of biomass in fresh media would affect P overplus, in contrast with the KPO_4 addition to the culture. Centrifugation of liquid cultures can trigger mechanical stress, and it is unclear how this could influence *C. reinhardtii* P overplus response (Scarsella et al., 2012). Another P overplus experiment was designed to take the factor of centrifugation out, by adding a solution containing all nutrients except for phosphate (5xTA) plus the KPO_4 solution. The objective was to treat both P repletion types in the same way. However, this added an excess/diluted nutrient factor to take into account. The results showed that in the second experiment, the P overplus response did not improve, nor did the effect of nutrient availability on biomass growth and nutrient removal, as observed in the first P overplus experiment. On the contrary, I observed that repletion as 5xTA+P addition negatively affected some of the monitored parameters in comparison with TAP resuspension. One possibility could be the added excess of nutrients compared to the nutrient-balanced TAP media (Kropat et al., 2011). However, as mentioned above, the N:P ratio of 5xTA+P repleted cultures does not exceed the considerably wide range of N:P ratio suitable for biomass growth and nutrient uptake (Geider and Roche, 2002).

Another thought is that the adverse effects on P overplus and nutrient removal from the media were more noticeable if the cultures were P-deprived for a longer period (lowest RNA level observed). Microalgae can release extracellular polymeric substances (EPS) for different reasons which include the onset of nutrient stress (Garza-Rodríguez et al., 2022, Reignier et al., 2023). This possibility could be behind the differences observed between both experiments. In the first P overplus experiment, the old media was discarded and biomass was resuspended in fresh TAP media, eliminating any substances produced by the cells. On the contrary, in the second P overplus experiment, the P deprivation media was kept and nutrients were added. Assuming that a longer period of P deprivation triggers a further release of exopolymeric substances (EPS), would explain the bigger adverse effect of EPS observed in 96 h P-deprived cultures. In cyanobacteria and microalgae, EPS are released under nutrient deprivation or salinity stress conditions (Reignier et al., 2023). For both, EPS are mainly composed of proteins and polysaccharides. The presence of polysaccharides released by

microalgae has been linked to enhanced auto-flocculation processes in the presence of phosphate and calcium (Rashid et al., 2019, Tang et al., 2021). A possibility is that during P-deprivation, polyP rapid degradation assisted the generation of polysaccharide-rich EPS, which were released by *C. reinhardtii*. Assuming that the longer P-deprivation of 96 h (until the lowest RNA was observed) was correlated with a higher production of EPS where more P could have been provided by the degradation of in-cell organic P compounds. At the moment of repletion as 5xTA+P, since the putative EPS-rich media was not discarded, the response might have been to encourage the mass transfer of EPS-bound phosphate first and then remove the supplied phosphate in the 5xTA+P solution. Mass transfer of phosphate contained in microalgal-released EPS has been highlighted before as another biologically driven process of microalgal removal of phosphate via surface adsorption (Wu et al., 2021, Xu et al., 2020, Yao et al., 2011). This could explain the reduced phosphate removal observed in 5xTA+P repleted cultures observed in **Chapter 5** (see **Figure 5.10A-B**).

Further research is needed to bring some clarity about the possible effect of any extracellular substances that *C. reinhardtii* may release to the media whilst undergoing P-deprivation and how these substances could affect P overplus, algal growth and nutrient removal performance. From the engineering application perspective, unveiling the effect of EPS on P overplus and nutrient removal in WWTWs using microalgae is necessary. In a real-life process of P recovery using microalgal P overplus, the presence of EPS triggered by either nutrient stress or the presence of other components in wastewater is very likely. To the best of my knowledge, the influence of EPS on P overplus and P removal from media has not been explored yet. Therefore, exploring how these substances may affect the performance of a system using microalgal P overplus response would bring the application of this process one step closer to reality.

Finally, other than nitrogen and phosphorus, this present work highlights the role of magnesium as a preferred counterion assisting in the enhanced polyphosphate accumulation observed in the PSR1 overexpression strains of *C. reinhardtii* developed by our research group (Slocombe et al., 2023). This result was surprising as calcium has been widely mentioned as the potential preferred counterion for polyphosphate. As mentioned in the results summary and discussion section of **Chapter 6**, the selection of magnesium over calcium makes sense from the biological point of view that calcium levels require far stricter regulation due to its role as a signalling molecule. For instance, calcium released to the cytosol from polyP mobilisation under P-

deprivation could act as a signal to activate the phosphate starvation response (PSR1) (Moseley and Grossman, 2009).

Magnesium association with polyP is not uncommon (Komine et al., 2000, Ruiz et al., 2001). Within the context of WWTWs, this result highlights, once more, the importance of counter ions in biological phosphorus removal systems. For instance, Schönborn et al. achieved enhanced biological phosphorus removal when increasing the concentration of magnesium in wastewater, by polyphosphate accumulating organisms (PAOs) (Schönborn et al., 2001). Therefore, it is possible that a similar effect could be observed in a wastewater treatment process using microalgal P overplus to recover P. This, also requires further research.

7.4 PSR1 and P overplus in *C. reinhardtii*

To bring microalgal P overplus closer to a level of application in P recovery systems at WWTWs, we need to examine the physiological changes of microalgae according to the P deprivation and P repletion conditions. However, the physiological changes that we observe in microalgae are controlled by the expression and regulation of phosphate metabolism and regulatory genes which coordinate the changes observed in terms of polyphosphate accumulation and biomass growth. Hence, there is relevance in understanding the transcriptional and post-transcriptional processes behind the physiological parameters. In the case of *Chlamydomonas reinhardtii* the transcription factor PSR1 has a key role in the regulation of phosphate metabolism. PSR1 has been mostly highlighted for its function in activating the response to P deprivation/stress (Wykoff et al., 1999, Shimogawara et al., 1999, Moseley et al., 2006), and its manipulation (overexpression) has been linked to the metabolism of lipids and starch, as a means to increase the potential for biofuel production (Bajhaiya et al., 2016, Ngan et al., 2015). The work of Bajhaiya et al. on PSR1 overexpression strains of *C. reinhardtii* unveiled the potential of this genetic manipulation to procure an outstanding accumulation of phosphate (Bajhaiya et al., 2016). In our recent work, we found that PSR1 overexpression enhanced P accumulation and hence P removal, by promoting a feedforward response in P metabolism. Genes that were first upregulated by PSR1 overexpression under P-repleted conditions led to a reduction of external P concentration. A second set of genes was activated in response to the low-to-depleted P levels in the media and the increase in in-cell P accumulation. As internal P increased downregulation of the transgene PSR1 protein levels occurred (Slocombe et al., 2023). These results highlight PSR1 in its role in both

luxury P uptake and P overplus responses. Nonetheless, from our results, it cannot be assumed that the overexpression of PSR1 activated one process or the other. In our published review, the difference between these two phenomena was explained as either the enhanced polyP accumulation triggered by P stress (P overplus response) or other nutrient stress (luxury P uptake) (Slocombe et al., 2020). It is still unclear whether the response of polyP accumulation in both processes is activated by the same set of transcriptional responses. Plouviez et al. RNA sequencing analysis of *C. reinhardtii* during P overplus revealed that PSR1 transcriptional levels were downregulated upon P depletion (Plouviez et al., 2021). Whereas in the RNA sequencing analysis of PSR1 overexpression strains from our study, endogenous and transgenic PSR1 levels were upregulated after 48 h of inoculation in P-replete media, when phosphate concentration in the media was still high, and no other nutrient was depleted (Slocombe et al., 2023). This suggests that the transgene PSR1 switches on the expression of the endogenous PSR1, which led to conclude that PSR1 autoregulates itself (see Figure 2G-H in Slocombe et al., 2023). To note, the endogenous PSR1 in *C. reinhardtii* is under the control of its own promoter but the transgene PSR1 (from our study) is under the control of the light-regulated promoter PSAD. Therefore, it is possible that PSR1 overexpression triggered a luxury P uptake response rather than a P overplus response. Moreover, the accumulation of P (approximately 8%, dry biomass weight - dw), by the PSR1 overexpression strain 8-27 is impressive given the average 1-2%P dw, that is expected in microalgal biomass. The observation that the peak of P accumulation was transient after P was depleted from the media, raises the question about the maximum capacity of P accumulation that this strain may have. Would this strain accumulate more than 8%P dw, if cultivated under a continuous flow system, that maintains phosphate concentration in the media at a specific level?

Nonetheless, the results presented in this research work show undoubtedly, that PSR1 is a key component of the P overplus response of *C. reinhardtii*. My data shows PSR1 overexpression induces P overplus or luxury P uptake without previous nutrient deprivation, whereas the inactivation of PSR1 (knockout) inhibits completely the P overplus response due to the inability to synthesize or accumulate polyphosphate (see **Chapter 6**).

Many other microalgal species harbour a homolog of the transcription factor PSR1 (Kumar Sharma et al., 2020). Thus, there is relevance in understanding how the manipulation of PSR1 not only improves biomass phosphate accumulation but is vital to trigger a P overplus response in

microalgae, due to its newly uncovered role in polyP synthesis. However, other relevant species in MBWT research like *C. vulgaris* and *S. obliquus*, do not harbour a homolog of PSR1, thus it is also important to understand how these species regulate their responses to P deprivation and subsequent resupply, at the transcriptional and translational level.

While the application of transgenic organisms in real-life applications is limited due to the regulation of the use of genetically modified organisms in some areas, like agriculture or wastewater treatment, there is value in using this methodology for the study of P metabolism in microalgae. One example of this is the finding of new phenotypes in the strain CC-5325 of *C. reinhardtii* which appears to coincide (at least partly) with the behaviour observed in our best PSR1 overexpression strain 8-27. CC-5325 exhibited more resistance to longer P-deprivation, high accumulation of polyphosphate and consequently, high phosphate removal efficiency, compared to other strains tested in this present study (see **Chapter 4** and **Chapter 5**). In fact, the knowledge obtained from RNA sequencing analysis from our previously published work, provides relevant information about the possible genetic processes behind this background, as discussed in Chapter 4 (Slocombe et al., 2023). Therefore, the genetic manipulation of the components of P metabolism in a model like *C. reinhardtii* can help to deliver guidance for the selection of phosphate hyperaccumulating strains, even with other microalgal species, to be used in MBWT systems for P recovery.

7.5 Conclusions and Recommendations

The research work undertaken in this project has achieved the aim and objectives presented in **Chapter 1** Introduction (section **1.4**). This section underlines the main conclusions from this project in line with the initially proposed research objectives, and reports recommendations for further research.

7.5.1 Conclusions

Polyphosphate is the direct measurement of the phosphate overplus response in microalgae. So far, the methodologies to analyse polyphosphate accumulation in microalgae provided inconsistent results that do not allow a comparison of polyP accumulation patterns between species or different cultivation conditions. Also, the specificity of commonly used techniques like DAPI staining has been questioned due to the shared biophysical properties of polyP with other molecules like RNA and inositol polyphosphates. The biochemical assay for polyP quantification and the qualitative detection of

polyP via toluidine blue-stained PAGE allow a reproducible and specific analysis of polyphosphate dynamics in *C. reinhardtii* and potentially other microalgae.

Minimum polyphosphate content of mid-exponential cultures (as it is not completely depleted), undergoing P-deprivation is the physiological parameter to monitor before P re-supply, to trigger maximum polyP accumulation in *C. reinhardtii*. To enhance phosphate removal, P repletion with all nutrients is required as a means to promote biomass growth and hence an increased demand for organic P compounds as well as inorganic polyP accumulation. Further P-deprivation will promote the use of organic P reserves principally (RNA and presumably also phospholipids although these were not measured), which will switch microalgal metabolism to prioritise the re-synthesis of these organic P compounds over polyP accumulation after P resupply. Since phospholipids are mobilised and replaced by sulpholipids during P-deprivation, it would have been interesting to monitor the phospholipid content of *C. reinhardtii* during my experiments (Moseley et al., 2009a, Sanz-Luque and Grossman, 2023). This would have allowed me to determine whether phospholipid intracellular consumption matches that of RNA, during P deprivation. Further research is needed to confirm this, although the conclusion remains that inorganic reserves of P are consumed before organic P reserves during P-deprivation. In this study, I focused on the two largest pools of P in microalgae: polyP and RNA.

The biomass growth phase plays an important role in the storage of polyphosphate in microalgae. The fact that P-deprivation of mid-exponential cultures did not impede biomass growth, meant that P overplus took place at a point when the biomass was in the early stationary phase. Accumulation of polyP was not immediately used to sustain biomass growth as it occurred in other studies with exponential growth cultures. Instead, polyP content was maintained for at least four days, which is practical from the application perspective. The window to harvest polyP-rich biomass for valorisation would be wider, hence reducing the operation complexity of the P recovery system.

Nonetheless, polyphosphate accumulation during P overplus occurs as a long-chain polymer that is mobilised into medium and short-chain polyP to support microalgal activity. From the industrial or agricultural application context, long and medium-chain polyP is used for different commercial processes. Therefore, biomass harvesting can be optimised to reach a higher content of long polyP at the early stage of P overplus if desired. Otherwise, a heterogeneous mixture of long, medium and short-chain polyP will be obtained at the latter stage of P overplus. Furthermore, the finding that IP_6

does not follow the pattern of polyP accumulation during P overplus, should encourage a rethink of the regulation of polyphosphate synthesis and degradation in microalgae rather than the assumption that it is the same as in *S. cerevisiae*.

That PSR1 overexpression enhanced the accumulation of phosphate and its removal from the media, without a previous step of preparation of the biomass (e.g. with nutrient deprivation), is an outstanding finding in the field. SPX1 upregulation by PSR1 overexpression suggests that the suppression mechanism of PSR1 under intracellular P sufficient levels may be similar to that of *A. thaliana*. Further research is required to test this hypothesis.

Nevertheless, the even more unprecedented observation is the fact that the absence of PSR1 expression inhibits P overplus due to its essential role in polyphosphate synthesis or accumulation. This finding will drive the development of new research strategies to unveil the regulation of polyphosphate synthesis and degradation in *C. reinhardtii* and other microalgae. Probably the focus should not only take into account the similarities of microalgae with yeast and land plants P metabolism but also consider the possible 'unique' characteristics of P metabolism machinery in microalgae.

Overall, this study has developed a reliable experimental protocol for studying the P overplus response in *C. reinhardtii* with potential application to other algal species. This methodology provides a focus on the direct measurement of P overplus, polyphosphate. The results obtained from this work represent a major contribution to our understanding of this phenomenon and its implications for maximum polyP accumulation, biomass production and enhanced nutrient removal. The manipulation of the physiological parameters of P deprivation and nutrient availability at the repletion stage provides new design criteria with potential application in WWTWs using microalgae P overplus to recover P in bioavailable ways and help to close the broken phosphorus cycle.

7.5.2 Recommendations and further research

The advantage of P overplus over luxury P uptake is that microalgae can still grow during P-deprivation, in contrast with N deprivation, which has been shown to inhibit microalgal growth in previous studies (Msanne et al., 2012, Chu et al., 2020a). Since biomass growth was the factor which enhanced P removal from the media in my P overplus experiment, upon resuspension in fresh media with all nutrients, we may think that is more convenient to make use of P overplus for nutrient control in wastewater. In WWTWs, the P

overplus response of microalgae could be adapted since both 'low P' and 'high P' conditions can be found at different stages of the treatment process (e.g. tertiary effluent – low P, digestate effluent – high P as shown in **Figure 2.3** in **Chapter 2** Literature Review) (**Figure 7.1**). Although, further research is needed to provide the optimal design parameters for this process to work.

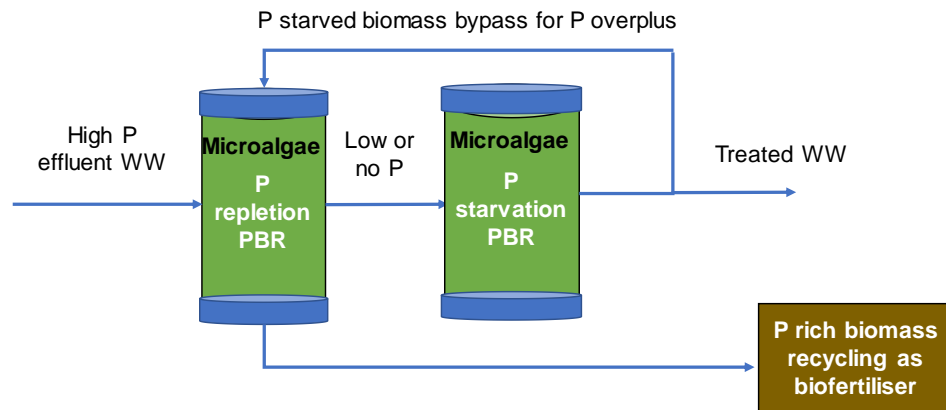


Figure 7.1 A vision of P-deprivation and P repletion steps in P recovery from wastewater using microalgae P overplus response.

In the last P overplus experiment shown in this thesis (section 6.4 in **Chapter 6**), the PSR1-OE strain 8-27 was P-deprived until it exhibited its lowest polyP content and then resuspended in fresh TAP media. The resulting media from this experiment would meet P discharge limits in the UK (<0.1 mg P/L), set by the Water Framework Directive after only 6 h-12 h (Pratt et al., 2012, Leaf, 2018). The total nitrogen discharge limits in the UK (<10 mg N/L for a population >100.000) mean that due to the minimum average limit, WWTWs need to procure to comply with a much lower discharge concentration (approximately 3 mg NH₄-N/L). Therefore, for nitrogen, the resulting media from this last experiment (and all of the experiments in this thesis) would not meet the N discharge limit (UK-Environment-Agency, 2019, Marsden et al., 2012). However, within a WWTW context, nitrogen removal has the advantage of including a gaseous phase of nitrogen, unlike phosphorus, thus allowing its removal via nitrification/denitrification mechanisms in bacteria, among other processes (Von Sperling, 2007, Camargo Valero et al., 2010).

Therefore, it is important to assess the P overplus performance of microalgae under more realistic conditions closer to the wastewater treatment context. First, this could be evaluated using synthetic or real wastewater instead of artificial culture media (e.g. TAP). The availability and concentration of nutrients (especially micronutrients) in wastewater, may be different to the 'optimal' conditions provided by artificial TAP media. This may affect the efficiency of biomass growth and thus, P removal during P overplus. Second, by studying the influence of the naturally occurring symbiotic relationship

between bacteria and microalgae in both cost-effective (WSPs) and sophisticated wastewater treatment systems, on the response to P-deprivation and P overplus performance. Third, the fact that phosphate removal efficiency during P overplus decreased possibly due to the presence of the P-deprivation media, suggests that EPS would play a definitive role in the robustness of P recovery processes using microalgae P overplus phenomenon. Integrating tools for the analysis of P removal by microalgae, either by intracellular P uptake or adsorption in EPS, under P-deprived and P-replete conditions is necessary. Lastly, my experiments were conducted under continuous illumination, and 25°C of temperature. More realistic conditions would involve the use of light/dark regimes and wider ranges of temperature. However, the phosphate metabolism of microalgae in the dark has been a rather unexplored field. Even though, it has been shown that microalgae like *C. reinhardtii* can produce polyP during P overplus under dark conditions (Plouviez et al., 2022). Further research is required to determine whether polyphosphate metabolism is linked to the cell cycle of microalgae. This would require the use of synchronised cultures growing under light/dark regimes (e.g. 12 h/ 12 h). A detailed characterisation of polyP dynamics during each phase of the cell cycle, under these conditions, would help to uncover a potential role of darkness versus light on microalgal P metabolism.

References

- ABDULSADA, Z. K. 2014. *Evaluation of Microalgae for Secondary and Tertiary Wastewater Treatment*. Master in Applied Science in Environmental Engineering, Carleton University.
- ABIS, K. L. & MARA, D. D. 2003. Research on waste stabilisation ponds in the United Kingdom - initial results from pilot-scale facultative ponds. *Water Science and Technology*, 48, 1-7.
- ABREU, A. P., MORAIS, R. C., TEIXEIRA, J. A. & NUNES, J. 2022. A comparison between microalgal autotrophic growth and metabolite accumulation with heterotrophic, mixotrophic and photoheterotrophic cultivation modes. *Renewable and Sustainable Energy Reviews*, 159, 112247.
- ACHBERGEROVÁ, L. & NAHÁLKA, J. 2011. Polyphosphate - an ancient energy source and active metabolic regulator. *Microbial Cell Factories*, 10, 63.
- ACIÉN FERNÁNDEZ, F. G., GÓMEZ-SERRANO, C. & FERNÁNDEZ-SEVILLA, J. M. 2018. Recovery of Nutrients From Wastewaters Using Microalgae. *Frontiers in Sustainable Food Systems*, 2.
- ACIÉN, F. G., MOLINA, E., REIS, A., TORZILLO, G., ZITTELLI, G. C., SEPÚLVEDA, C. & MASOJÍDEK, J. 2017. 1 - Photobioreactors for the production of microalgae. In: GONZALEZ-FERNANDEZ, C. & MUÑOZ, R. (eds.) *Microalgae-Based Biofuels and Bioproducts*. Woodhead Publishing.
- AITCHISON, P. A. & BUTT, V. S. 1973. The Relation between the Synthesis of Inorganic Polyphosphate and Phosphate Uptake by *Chlorella vulgaris*. *Journal of Experimental Botany*, 24, 497-510.
- AKSOY, M., POOTAKHAM, W. & GROSSMAN, A. R. 2014. Critical function of a *Chlamydomonas reinhardtii* putative polyphosphate polymerase subunit during nutrient deprivation.(Report). 26, 4214.
- ALBI, T. & SERRANO, A. 2016. Inorganic polyphosphate in the microbial world. Emerging roles for a multifaceted biopolymer. *World Journal of Microbiology and Biotechnology*, 32, 1-12.
- ALLEN, A. P. & GILLOOLY, J. F. 2009. Towards an integration of ecological stoichiometry and the metabolic theory of ecology to better understand nutrient cycling. *Ecology Letters*, 12, 369-384.
- ALOBWEDE, E., LEAKE, J. R. & PANDHAL, J. 2019. Circular economy fertilization: Testing micro and macro algal species as soil improvers and nutrient sources for crop production in greenhouse and field conditions. *Geoderma*, 334, 113-123.
- ANAM, K., RAHMAN, D. Y., HIDHAYATI, N., RACHMAYATI, R., SUSILANINGSIH, D., AGUSTINI, N. W. S., PRAHARYAWAN, S.,

- SUSANTI, H. & APRIASTINI, M. 2021. Lipid accumulation on optimized condition through biomass production in green algae. *IOP Conference Series: Earth and Environmental Science*, 762, 012075.
- ANDREEVA, N., RYAZANOVA, L., DMITRIEV, V., KULAKOVSKAYA, T. & KULAEV, I. 2014. Cytoplasmic inorganic polyphosphate participates in the heavy metal tolerance of *Cryptococcus humicola*. *Folia microbiologica*, 59, 381-389.
- ÁNGELES, R., RODERO, R., CARVAJAL, A., MUÑOZ, R. & LEBRERO, R. 2019. Potential of Microalgae for Wastewater Treatment and Its Valorization into Added Value Products. *In: GUPTA, S. K. & BUX, F. (eds.) Application of Microalgae in Wastewater Treatment: Volume 2: Biorefinery Approaches of Wastewater Treatment*. Cham: Springer International Publishing.
- APPLETON, J. & NOTHOLT, A. 2002. Local phosphate resources for sustainable development in Central and South America.(CR/02/122N).
- ARUMUGAM, M., AGARWAL, A., ARYA, M. C. & AHMED, Z. 2013. Influence of nitrogen sources on biomass productivity of microalgae *Scenedesmus bijugatus*. *Bioresource Technology*, 131, 246-249.
- ASCHAR-SOBBI, R., ABRAMOV, A., DIAO, C., KARGACIN, M., KARGACIN, G., FRENCH, R. & PAVLOV, E. 2008a. High Sensitivity, Quantitative Measurements of Polyphosphate Using a New DAPI-Based Approach. *Journal of Fluorescence*, 18, 859-866.
- ASCHAR-SOBBI, R., ABRAMOV, A. Y., DIAO, C., KARGACIN, M. E., KARGACIN, G. J., FRENCH, R. J. & PAVLOV, E. 2008b. High Sensitivity, Quantitative Measurements of Polyphosphate Using a New DAPI-Based Approach. *Journal of Fluorescence*, 18, 859-866.
- ASHLEY, K., CORDELL, D. & MAVINIC, D. 2011. A brief history of phosphorus: From the philosopher's stone to nutrient recovery and reuse. *Chemosphere*, 84, 737-746.
- AU - LOSS, O., AU - AZEVEDO, C., AU - SZIJGYARTO, Z., AU - BOSCH, D. & AU - SAIARDI, A. 2011. Preparation of Quality Inositol Pyrophosphates. *JoVE*, e3027.
- AUESUKAREE, C., HOMMA, T., KANEKO, Y. & HARASHIMA, S. 2003. Transcriptional regulation of phosphate-responsive genes in low-affinity phosphate-transporter-defective mutants in *Saccharomyces cerevisiae*. *Biochem Biophys Res Commun*, 306, 843-50.
- AZEVEDO, C. & SAIARDI, A. 2017. Eukaryotic Phosphate Homeostasis: The Inositol Pyrophosphate Perspective. *Trends Biochem Sci*, 42, 219-231.
- BAJHAIYA, A. K., DEAN, A. P., ZEEF, L. A. H., WEBSTER, R. E. & PITTMAN, J. K. 2016. PSR1 is a global transcriptional regulator of phosphorus deficiency responses and carbon storage metabolism in *Chlamydomonas reinhardtii*.(Report). 170, 1216.

- BAROLO, L., COMMAULT, A. S., ABBRIANO, R. M., PADULA, M. P., KIM, M., KUZHIUMPARAMBIL, U., RALPH, P. J. & PERNICE, M. 2022. Unassembled cell wall proteins form aggregates in the extracellular space of *Chlamydomonas reinhardtii* strain UVM4. *Applied Microbiology and Biotechnology*, 106, 4145-4156.
- BELKOURA, M., DAUTA, A. & BOUTERFAS, R. 2006. The effects of irradiance and photoperiod on the growth rate of three freshwater green algae isolated from a eutrophic lake. *Limnetica*, ISSN 0213-8409, Vol. 25, N^o. 3, 2006, pags. 647-656, 25.
- BERGE, T., DAUGBJERG, N. & HANSEN, P. J. 2012. Isolation and cultivation of microalgae select for low growth rate and tolerance to high pH. *Harmful Algae*, 20, 101-110.
- BEUCKELS, A., SMOLDERS, E. & MUYLAERT, K. 2015. Nitrogen availability influences phosphorus removal in microalgae-based wastewater treatment. *Water Research*, 77, 98-106.
- BOLIER, G., DE KONINGH, M. C. J., SCHMALE, J. C. & DONZE, M. 1992. Differential luxury phosphate response of planktonic algae to phosphorus removal. *Hydrobiologia*, 243, 113-118.
- BOROWITZKA, M. A. 2013. High-value products from microalgae—their development and commercialisation. *Journal of Applied Phycology*, 25, 743-756.
- BOWMER, K. H. & MUIRHEAD, W. 1987. Inhibition of algal photosynthesis to control pH and reduce ammonia volatilization from rice floodwater. *Fertilizer research*, 13, 13-29.
- BOYLE, N. R. & MORGAN, J. A. 2009. Flux balance analysis of primary metabolism in *Chlamydomonas reinhardtii*. *BMC Systems Biology*, 3, 4.
- BRU, S., JIMÉNEZ, J., CANADELL, D., ARIÑO, J. & CLOTET, J. 2017. Improvement of biochemical methods of polyP quantification. *Microbial Cell*, 4, 6.
- BUNCE, J. T., NDAM, E., OFITERU, I. D., MOORE, A. & GRAHAM, D. W. 2018. A Review of Phosphorus Removal Technologies and Their Applicability to Small-Scale Domestic Wastewater Treatment Systems. *Frontiers in Environmental Science*, 6.
- CABANELAS, I. T. D., RUIZ, J., ARBIB, Z., CHINALIA, F. A., GARRIDO-PÉREZ, C., ROGALLA, F., NASCIMENTO, I. A. & PERALES, J. A. 2013. Comparing the use of different domestic wastewaters for coupling microalgal production and nutrient removal. *Bioresource Technology*, 131, 429-436.
- CAMARGO VALERO, M. A., MARA, D. D. & NEWTON, R. J. 2010. Nitrogen removal in maturation waste stabilisation ponds via biological uptake and sedimentation of dead biomass. *Water Science and Technology*, 61, 1027-1034.

- CAMEJO, P. Y., OYSERMAN, B. O., MCMAHON, K. D. & NOGUERA, D. R. 2019. Integrated Omic Analyses Provide Evidence that a "Candidatus Accumulibacter phosphatis" Strain Performs Denitrification under Microaerobic Conditions. *mSystems*, 4, e00193-18.
- CARPENTER, S. R. 2008. Phosphorus control is critical to mitigating eutrophication. *Proceedings of the National Academy of Sciences*, 105, 11039-11040.
- CARTER, S. G. & KARL, D. W. 1982. Inorganic phosphate assay with malachite green: an improvement and evaluation. *Journal of biochemical and biophysical methods*, 7, 7-13.
- CHANG, C.-W., MOSELEY, J. L., WYKOFF, D. & GROSSMAN, A. R. 2005. The LPB1 gene is important for acclimation of chlamydomonas reinhardtii to phosphorus and sulfur deprivation (1) ([w]). *Plant Physiology*, 138, 319.
- CHEREGI, O., EKENDAHL, S., ENGELBREKTSSON, J., STRÖMBERG, N., GODHE, A. & SPETEA, C. 2019. Microalgae biotechnology in Nordic countries – the potential of local strains. *Physiologia Plantarum*, 166, 438-450.
- CHEVALIER, P. & DE LA NOÛE, J. 1985. Efficiency of immobilized hyperconcentrated algae for ammonium and orthophosphate removal from wastewaters. *Biotechnology Letters*, 7, 395-400.
- CHILDERS, D. L., CORMAN, J., EDWARDS, M. & ELSER, J. J. 2011. Sustainability Challenges of Phosphorus and Food: Solutions from Closing the Human Phosphorus Cycle. *BioScience*, 61, 117-124.
- CHOI, H. J. & LEE, S. M. 2015. Effect of the N/P ratio on biomass productivity and nutrient removal from municipal wastewater. *Bioprocess and Biosystems Engineering*, 38, 761-766.
- CHRISPIM, M. C., SCHOLZ, M. & NOLASCO, M. A. 2019. Phosphorus recovery from municipal wastewater treatment: Critical review of challenges and opportunities for developing countries. *Journal of Environmental Management*, 248, 109268.
- CHRIST, J. J. & BLANK, L. M. 2018. Analytical polyphosphate extraction from *Saccharomyces cerevisiae*. *Analytical Biochemistry*, 563, 71-78.
- CHRIST, J. J., SMITH, S. A., WILLBOLD, S., MORRISSEY, J. H. & BLANK, L. M. 2020a. Biotechnological synthesis of water-soluble food-grade polyphosphate with *Saccharomyces cerevisiae*. *Biotechnology and Bioengineering*, n/a.
- CHRIST, J. J., WILLBOLD, S. & BLANK, L. M. 2020b. Methods for the Analysis of Polyphosphate in the Life Sciences. *Analytical Chemistry*, 92, 4167-4176.

- CHU, F., CHENG, J., LI, K., WANG, Y., LI, X. & YANG, W. 2020a. Enhanced Lipid Accumulation through a Regulated Metabolic Pathway of Phosphorus Luxury Uptake in the Microalga *Chlorella vulgaris* under Nitrogen Starvation and Phosphorus Repletion. *ACS Sustainable Chemistry & Engineering*, 8, 8137-8147.
- CHU, Q., LYU, T., XUE, L., YANG, L., FENG, Y., SHA, Z., YUE, B., MORTIMER, R. J. G., COOPER, M. & PAN, G. 2020b. Hydrothermal carbonization of microalgae for phosphorus recycling from wastewater to crop-soil systems as slow-release fertilizers. *Journal of Cleaner Production*, 124627.
- CID, C. A., JASPER, J. T. & HOFFMANN, M. R. 2018. Phosphate Recovery from Human Waste via the Formation of Hydroxyapatite during Electrochemical Wastewater Treatment. *ACS Sustainable Chemistry & Engineering*, 6, 3135-3142.
- CLIFF, A., GUIEYSSE, B., BROWN, N., LOCKHART, P., DUBREUCQ, E. & PLOUVIEZ, M. 2023. Polyphosphate synthesis is an evolutionarily ancient phosphorus storage strategy in microalgae. *Algal Research*, 73, 103161.
- CONFRARIA, H., MIRA GODINHO, M. & WANG, L. 2017. Determinants of citation impact: A comparative analysis of the Global South versus the Global North. *Research Policy*, 46, 265-279.
- COOPER, J. & CARLIELL-MARQUET, C. 2013. A substance flow analysis of phosphorus in the UK food production and consumption system. *Resources, Conservation & Recycling*, 74, 82-100.
- COPPENS, J., GRUNERT, O., VAN DEN HENDE, S., VANHOUTTE, I., BOON, N., HAESAERT, G. & DE GELDER, L. 2016. The use of microalgae as a high-value organic slow-release fertilizer results in tomatoes with increased carotenoid and sugar levels. *Journal of Applied Phycology*, 28, 2367-2377.
- CORDELL, D., DRANGERT, J.-O. & WHITE, S. 2009. The story of phosphorus: Global food security and food for thought. *Global Environmental Change*, 19, 292-305.
- CORDELL, D., ROSEMARIN, A., SCHRÖDER, J. J. & SMIT, A. L. 2011. Towards global phosphorus security: A systems framework for phosphorus recovery and reuse options. *Chemosphere*, 84, 747-758.
- COUSO, I., EVANS, B. S., LI, J., LIU, Y., MA, F., DIAMOND, S., ALLEN, D. K. & UMEN, J. G. 2016. Synergism between Inositol Polyphosphates and TOR Kinase Signaling in Nutrient Sensing, Growth Control, and Lipid Metabolism in *Chlamydomonas*. *The Plant Cell*, 28, 2026-2042.
- COUSO, I., PÉREZ-PÉREZ, M. E., FORD, M. M., MARTÍNEZ-FORCE, E., HICKS, L. M., UMEN, J. G. & CRESPO, J. L. 2020. Phosphorus Availability Regulates TORC1 Signaling via LST8 in *Chlamydomonas*. *The Plant Cell*, 32, 69.

- COUSO, I., PÉREZ-PÉREZ, M. E., MARTÍNEZ-FORCE, E., KIM, H.-S., HE, Y., UMEN, J. G. & CRESPO, J. L. 2017. Autophagic flux is required for the synthesis of triacylglycerols and ribosomal protein turnover in *Chlamydomonas*. *Journal of Experimental Botany*, 69, 1355-1367.
- COUSO, I., SMYTHERS, A. L., FORD, M. M., UMEN, J. G., CRESPO, J. L. & HICKS, L. M. 2021. Inositol polyphosphates and target of rapamycin kinase signalling govern photosystem II protein phosphorylation and photosynthetic function under light stress in *Chlamydomonas*. *New Phytologist*, 232, 2011-2025.
- CRAIG, R. J., GALLAHER, S. D., SHU, S., SALOMÉ, P. A., JENKINS, J. W., BLABY-HAAS, C. E., PURVINE, S. O., O'DONNELL, S., BARRY, K., GRIMWOOD, J., STRENKERT, D., KROPAT, J., DAUM, C., YOSHINAGA, Y., GOODSTEIN, D. M., VALLON, O., SCHMUTZ, J. & MERCHANT, S. S. 2023. The *Chlamydomonas* Genome Project, version 6: Reference assemblies for mating-type plus and minus strains reveal extensive structural mutation in the laboratory. *Plant Cell*, 35, 644-672.
- CRAIGIE, R. A. & CAVALIER-SMITH, T. 1982. Cell volume and the control of the *Chlamydomonas* cell cycle. *Journal of Cell Science*, 54, 173-191.
- CRIMP, A., BROWN, N. & SHILTON, A. 2018. Microalgal luxury uptake of phosphorus in waste stabilization ponds - frequency of occurrence and high performing genera. *Water science and technology : a journal of the International Association on Water Pollution Research*, 78, 165-173.
- CRIMP, A. J. 2015. *Luxury uptake of phosphorus by microalgae in New Zealand waste stabilisation ponds : a thesis presented in partial fulfilment of the requirements for the degree of Masters in Engineering at Massey University, Manawatu, New Zealand*. Doctor of Philosophy (Ph.D.) Doctoral, Massey University.
- CROZET, P., NAVARRO, F., WILLMUND, F., MEHRSHAHI, P., BAKOWSKI, K., LAUERSEN, K., PÉREZ-PÉREZ, M., AUROY, P., GORCHS ROVIRA, A., SAURET-GUETO, S., NIEMEYER, J., SPANIOL, B., THEIS, J., TRÖSCH, R., WESTRICH, L., VAVITSAS, K., BAIER, T., HÜBNER, W., DE CARPENTIER, F. & LEMAIRE, S. 2018. Birth of a Photosynthetic Chassis: A MoClo Toolkit Enabling Synthetic Biology in the Microalga *Chlamydomonas reinhardtii*. *ACS Synthetic Biology*, 7.
- DAVIES, D. R. & PLASKITT, A. 1971. Genetical and structural analyses of cell-wall formation in *Chlamydomonas reinhardtii*. *Genetics Research*, 17, 33-43.
- DE SOUSA, R. T. X., KORNDÖRFER, G. H., BREM SOARES, R. A. & FONTOURA, P. R. 2015. Phosphate Fertilizers for Sugarcane Used at Pre-Planting (Phosphorus Fertilizer Application). *Journal of Plant Nutrition*, 38, 1444-1455.
- DEFRA-UK Observatory monitoring framework – indicator data sheet. OpenDataNI.

- DELGADILLO-MIRQUEZ, L., LOPES, F., TAIDI, B. & PAREAU, D. 2016. Nitrogen and phosphate removal from wastewater with a mixed microalgae and bacteria culture. *Biotechnology Reports*, 11, 18-26.
- DEMAY, J., RINGEVAL, B., PELLERIN, S. & NESME, T. 2023. Half of global agricultural soil phosphorus fertility derived from anthropogenic sources. *Nature Geoscience*, 16, 69-74.
- DI CAPUA, F., DE SARIO, S., FERRARO, A., PETRELLA, A., RACE, M., PIROZZI, F., FRATINO, U. & SPASIANO, D. 2022. Phosphorous removal and recovery from urban wastewater: Current practices and new directions. *Science of The Total Environment*, 823, 153750.
- DIAZ, J., INGALL, E., VOGT, S., DE JONGE, M. D., PATERSON, D., RAU, C. & BRANDES, J. A. 2009. Characterization of phosphorus, calcium, iron, and other elements in organisms at sub-micron resolution using X-ray fluorescence spectromicroscopy. *Limnology and Oceanography: Methods*, 7, 42-51.
- DINESHKUMAR, R., KUMARAVEL, R., GOPALSAMY, J., SIKDER, M. N. A. & SAMPATHKUMAR, P. 2018. Microalgae as Bio-fertilizers for Rice Growth and Seed Yield Productivity. *Waste and Biomass Valorization*, 9, 793-800.
- DODD, A. N., KUDLA, J. & SANDERS, D. 2010. The Language of Calcium Signaling. *Annual Review of Plant Biology*, 61, 593-620.
- DONG, J., MA, G., SUI, L., WEI, M., SATHEESH, V., ZHANG, R., GE, S., LI, J., ZHANG, T.-E. & WITTEWER, C. 2019. Inositol pyrophosphate InsP8 acts as an intracellular phosphate signal in Arabidopsis. *Molecular plant*, 12, 1463-1473.
- DRAŠKOVIČ, P., SAIARDI, A., BHANDARI, R., BURTON, A., ILC, G., KOVAČEVIČ, M., SNYDER, S. H. & PODOBNIK, M. 2008. Inositol hexakisphosphate kinase products contain diphosphate and triphosphate groups. *Chemistry & biology*, 15, 274-286.
- DU, H., YANG, L., WU, J., XIAO, L., WANG, X. & JIANG, L. 2012. Simultaneous removal of phosphorus and nitrogen in a sequencing batch biofilm reactor with transgenic bacteria expressing polyphosphate kinase. *Applied Microbiology and Biotechnology*, 96, 265-272.
- DUTCHER, S. K. & O'TOOLE, E. T. 2016. The basal bodies of *Chlamydomonas reinhardtii*. *Cilia*, 5, 18-18.
- DYHRMAN, S. T. 2016. Nutrients and Their Acquisition: Phosphorus Physiology in Microalgae. In: BOROWITZKA, M. A., BEARDALL, J. & RAVEN, J. A. (eds.) *The Physiology of Microalgae*. Cham: Springer International Publishing.
- DYHRMAN, S. T., JENKINS, B. D., RYNEARSON, T. A., SAITO, M. A., MERCIER, M. L., ALEXANDER, H., WHITNEY, L. P., DRZEWIANSKI, A., BULYGIN, V. V., BERTRAND, E. M., WU, Z.,

- BENITEZ-NELSON, C. & HEITHOFF, A. 2012. The Transcriptome and Proteome of the Diatom *Thalassiosira pseudonana* Reveal a Diverse Phosphorus Stress Response. *PLOS ONE*, 7, e33768.
- EIXLER, S., KARSTEN, U. & SELIG, U. 2006. Phosphorus storage in *Chlorella vulgaris* (Trebouxiophyceae, Chlorophyta) cells and its dependence on phosphate supply. *Phycologia*, 45, 53-60.
- EL WALI, M., GOLROUDBARY, S. R. & KRASLAWSKI, A. 2019. Impact of recycling improvement on the life cycle of phosphorus. *Chinese Journal of Chemical Engineering*, 27, 1219-1229.
- ELADEL, H., ABOMOHR, A. E.-F., BATTAH, M., MOHMMED, S., RADWAN, A. & ABDELRAHIM, H. 2019. Evaluation of *Chlorella sorokiniana* isolated from local municipal wastewater for dual application in nutrient removal and biodiesel production. *Bioprocess and Biosystems Engineering*, 42, 425-433.
- ELSER, J. & BENNETT, E. 2011. A broken biogeochemical cycle. *Nature*, 478, 29-31.
- ELSER, J. J. 2012. Phosphorus: a limiting nutrient for humanity? *Current Opinion in Biotechnology*, 23, 833-838.
- ELSER, J. J., ACHARYA, K., KYLE, M., COTNER, J., MAKINO, W., MARKOW, T., WATTS, T., HOBBIE, S., FAGAN, W., SCHADE, J., HOOD, J. & STERNER, R. W. 2003. Growth rate–stoichiometry couplings in diverse biota. *Ecology Letters*, 6, 936-943.
- ENGEL, B. D., SCHAFFER, M., KUHN CUELLAR, L., VILLA, E., PLITZKO, J. M. & BAUMEISTER, W. 2015. Native architecture of the *Chlamydomonas* chloroplast revealed by in situ cryo-electron tomography. *eLife*, 4, e04889.
- FAO 2019. World fertilizer trends and outlook to 2022. Rome.
- FAUSER, F., VILARRASA-BLASI, J., ONISHI, M., RAMUNDO, S., PATENA, W., MILLICAN, M., OSAKI, J., PHILP, C., NEMETH, M., SALOMÉ, P. A., LI, X., WAKAO, S., KIM, R. G., KAYE, Y., GROSSMAN, A. R., NIYOGI, K. K., MERCHANT, S. S., CUTLER, S. R., WALTER, P., DINNENY, J. R., JONIKAS, M. C. & JINKERSON, R. E. 2022. Systematic characterization of gene function in the photosynthetic alga *Chlamydomonas reinhardtii*. *Nature Genetics*, 54, 705-714.
- FERNÁNDEZ, E. & MATAGNE, R. F. 1984. Genetic analysis of nitrate reductase-deficient mutants in *Chlamydomonas reinhardtii*. *Curr Genet*, 8, 635-40.
- FISCHER, N. & ROCHAIX, J. D. 2001. The flanking regions of *PsaD* drive efficient gene expression in the nucleus of the green alga *Chlamydomonas reinhardtii*. *Molecular Genetics and Genomics*, 265, 888-894.

- FITZGERALD, G. P. & NELSON, T. C. 1975. EXTRACTIVE AND ENZYMATIC ANALYSES FOR LIMITING OR SURPLUS PHOSPHORUS IN ALGAE. *Journal of Phycology*, 11, 32-37.
- FLYNN, K. J., RAVEN, J. A., REES, T. A. V., FINKEL, Z., QUIGG, A. & BEARDALL, J. 2010. IS THE GROWTH RATE HYPOTHESIS APPLICABLE TO MICROALGAE?1. *Journal of Phycology*, 46, 1-12.
- FUKAMI, K., NISHIJIMA, T. & ISHIDA, Y. 1997. Stimulative and inhibitory effects of bacteria on the growth of microalgae. *Hydrobiologia*, 358, 185-191.
- GALLAHER, S. D., FITZ-GIBBON, S. T., GLAESNER, A. G., PELLEGRINI, M. & MERCHANT, S. S. 2015. Chlamydomonas Genome Resource for Laboratory Strains Reveals a Mosaic of Sequence Variation, Identifies True Strain Histories, and Enables Strain-Specific Studies. *The Plant cell*, 27, 2335-2352.
- GARSDIE, A., BELL, M., ROBOTHAM, B., MAGAREY, R. & STIRLING, G. 2005. Managing yield decline in sugarcane cropping systems. *International Sugar Journal*, 107, 16-26.
- GARZA-RODRÍGUEZ, Z. B., HERNÁNDEZ-PÉREZ, J., SANTACRUZ, A., JACOBO-VELÁZQUEZ, D. A. & BENAVIDES, J. 2022. Prospective on the application of abiotic stresses to enhance the industrial production of exopolysaccharides from microalgae. *Current Research in Biotechnology*, 4, 439-444.
- GEIDER, R. J. & ROCHE, J. L. 2002. Redfield revisited: variability of C[ratio]N[ratio]P in marine microalgae and its biochemical basis. *European Journal of Phycology*, 37, 1-17.
- GERASIMAITÉ, R. & MAYER, A. 2016. Enzymes of yeast polyphosphate metabolism: structure, enzymology and biological roles. *Biochemical Society Transactions*, 44, 234-239.
- GERASIMAITE, R., PAVLOVIC, I., CAPOLICCHIO, S., HOFER, A., SCHMIDT, A., JESSEN, H. J. & MAYER, A. 2017. Inositol Pyrophosphate Specificity of the SPX-Dependent Polyphosphate Polymerase VTC. *ACS Chemical Biology*, 12, 648-653.
- GERASIMAITÉ, R., SHARMA, S., DESFOUGÈRES, Y., SCHMIDT, A. & MAYER, A. 2014. Coupled synthesis and translocation restrains polyphosphate to acidocalcisome-like vacuoles and prevents its toxicity. *Journal of Cell Science*, 127, 5093.
- GONÇALVES, J., FREITAS, J., FERNANDES, I. & SILVA, P. 2023. Microalgae as Biofertilizers: A Sustainable Way to Improve Soil Fertility and Plant Growth. *Sustainability*, 15, 12413.
- GONZÁLEZ-CAMEJO, J., BARAT, R., PACHÉS, M., MURGUI, M., SECO, A. & FERRER, J. 2018. Wastewater nutrient removal in a mixed microalgae–

bacteria culture: effect of light and temperature on the microalgae–bacteria competition. *Environmental Technology*, 39, 503-515.

- GOODENOUGH, U., HEISS, A. A., ROTH, R., RUSCH, J. & LEE, J.-H. 2019. Acidocalcisomes: Ultrastructure, Biogenesis, and Distribution in Microbial Eukaryotes. *Protist*, 170, 287-313.
- GORMAN, D. S. & LEVINE, R. P. 1965. Cytochrome f and plastocyanin: their sequence in the photosynthetic electron transport chain of *Chlamydomonas reinhardtii*. *Proceedings of the National Academy of Sciences*, 54, 1665-1669.
- GROSSMAN, A. R. A. A., M. 2015. Algae in a phosphorus-limited landscape. *Annual Plant Reviews Volume 48*.
- GÜNTHER, S. 2011. *Population structure and dynamics of polyphosphate accumulating organisms in a communal wastewater treatment plant*. University of Dresden.
- GUTIÉRREZ, R., PASSOS, F., FERRER, I., UGGETTI, E. & GARCÍA, J. 2015. Harvesting microalgae from wastewater treatment systems with natural flocculants: Effect on biomass settling and biogas production. *Algal Research*, 9, 204-211.
- GUTMAN, B. L. & NIYOGI, K. K. 2004. *Chlamydomonas* and *Arabidopsis*. A Dynamic Duo. *Plant Physiology*, 135, 607-610.
- HALLEGRAEFF, G. M., ANDERSON, D. M., BELIN, C., BOTTEIN, M.-Y. D., BRESNAN, E., CHINAIN, M., ENEVOLDSEN, H., IWATAKI, M., KARLSON, B., MCKENZIE, C. H., SUNESEN, I., PITCHER, G. C., PROVOOST, P., RICHARDSON, A., SCHWEIBOLD, L., TESTER, P. A., TRAINER, V. L., YÑIGUEZ, A. T. & ZINGONE, A. 2021. Perceived global increase in algal blooms is attributable to intensified monitoring and emerging bloom impacts. *Communications Earth & Environment*, 2, 117.
- HAN, L., PEI, H., HU, W., HAN, F., SONG, M. & ZHANG, S. 2014. Nutrient removal and lipid accumulation properties of newly isolated microalgal strains. *Bioresource Technology*, 165, 38-41.
- HANSEN, P. J. 2002. Effect of high pH on the growth and survival of marine phytoplankton: implications for species succession. *Aquatic microbial ecology*, 28, 279-288.
- HAROLD, F. M. 1966. Inorganic polyphosphates in biology: structure, metabolism, and function. *Bacteriological Reviews*, 30, 772-794.
- HARRIS, E. H. 2001. CHLAMYDOMONAS AS A MODEL ORGANISM. *Annual Review of Plant Physiology and Plant Molecular Biology*, 52, 363-406.
- HART, M. R., QUIN, B. F. & NGUYEN, M. L. 2004. Phosphorus runoff from agricultural land and direct fertilizer effects: A review. *Journal of environmental quality*, 33, 1954-1972.

- HEBELER, M., HENTRICH, S., MAYER, A., LEIBFRITZ, D. & GRIMME, L. PHOSPHATE REGULATION AND COMPARTMENTATION IN CHLAMYDOMONAS-REINHARDTII STUDIED BY INVIVO P-31-NMR. *Photosynthesis research*, 1992. KLUWER ACADEMIC PUBL SPUIBOULEVARD 50, PO BOX 17, 3300 AA DORDRECHT, NETHERLANDS, 199-199.
- HELLEBUST, J. A. & AHMAD, I. 1989. Regulation of Nitrogen Assimilation in Green Microalgae. *Biological Oceanography*, 6, 241-255.
- HIDAYATI, N. A., YAMADA-OSHIMA, Y., IWAI, M., YAMANO, T., KAJIKAWA, M., SAKURAI, N., SUDA, K., SESOKO, K., HORI, K., OBAYASHI, T., SHIMOJIMA, M., FUKUZAWA, H. & OHTA, H. 2019. Lipid remodeling regulator 1 (LRL1) is differently involved in the phosphorus-depletion response from PSR1 in *Chlamydomonas reinhardtii*. *The Plant Journal*, 100, 610-626.
- HILLEBRAND, H., DÜRSELEN, C.-D., KIRSCHTEL, D., POLLINGHER, U. & ZOHARY, T. 1999. BIOVOLUME CALCULATION FOR PELAGIC AND BENTHIC MICROALGAE. *Journal of Phycology*, 35, 403-424.
- HOLFORD, I. 1997. Soil phosphorus: its measurement, and its uptake by plants. *Soil Research*, 35, 227-240.
- HU, Q., SOMMERFELD, M., JARVIS, E., GHIRARDI, M., POSEWITZ, M., SEIBERT, M. & DARZINS, A. 2008. Microalgal triacylglycerols as feedstocks for biofuel production: perspectives and advances. *The plant journal*, 54, 621-639.
- IZADI, P., IZADI, P. & ELDYASTI, A. 2021. A review of biochemical diversity and metabolic modeling of EBPR process under specific environmental conditions and carbon source availability. *Journal of Environmental Management*, 288, 112362.
- JARVIE, H. P., NEAL, C. & WITHERS, P. J. A. 2006. Sewage-effluent phosphorus: A greater risk to river eutrophication than agricultural phosphorus? *Science of The Total Environment*, 360, 246-253.
- JEYANAYAGAM, S. 2005. True confessions of the biological nutrient removal process. *Florida water resources journal*, 1, 37-46.
- JIA, X., WANG, L., NUSSAUME, L. & YI, K. 2023. Cracking the code of plant central phosphate signaling. *Trends in Plant Science*, 28, 267-270.
- JIANG, M., SUN, L., ISUPOV, M. N., LITTLECHILD, J. A., WU, X., WANG, Q., WANG, Q., YANG, W. & WU, Y. 2019. Structural basis for the Target DNA recognition and binding by the MYB domain of phosphate starvation response 1. *The FEBS Journal*, 286, 2809-2821.
- JOHNSON, M., CAMARGO VALERO, M. A. & MARA, D. D. 2007. Maturation ponds, rock filters and reedbeds in the UK: statistical analysis of winter performance. *Water Science and Technology*, 55, 135-142.

- JONKMAN, J., BROWN, C. M., WRIGHT, G. D., ANDERSON, K. I. & NORTH, A. J. 2020. Tutorial: guidance for quantitative confocal microscopy. *Nature Protocols*, 15, 1585-1611.
- KÄLLQVIST, T. & SVENSON, A. 2003. Assessment of ammonia toxicity in tests with the microalga, *Nephroselmis pyriformis*, Chlorophyta. *Water Research*, 37, 477-484.
- KAPUSCINSKI, J. 1995. DAPI: a DNA-specific fluorescent probe. *Biotechnic & histochemistry*, 70, 220-233.
- KAWAKOSHI, A., NAKAZAWA, H., FUKADA, J., SASAGAWA, M., KATANO, Y., NAKAMURA, S., HOSOYAMA, A., SASAKI, H., ICHIKAWA, N., HANADA, S., KAMAGATA, Y., NAKAMURA, K., YAMAZAKI, S. & FUJITA, N. 2012. Deciphering the genome of polyphosphate accumulating actinobacterium *Microlunatus phosphovorus*. *DNA research : an international journal for rapid publication of reports on genes and genomes*, 19, 383-394.
- KOISTINEN, J., SJÖBLOM, M. & SPILLING, K. 2020. Determining Inorganic and Organic Phosphorus. In: SPILLING, K. (ed.) *Biofuels from Algae: Methods and Protocols*. New York, NY: Springer New York.
- KOLOZSVARI, B., PARISI, F. & SAIARDI, A. 2014. Inositol phosphates induce DAPI fluorescence shift. *Biochemical Journal*, 460, 377-385.
- KOMINE, Y., EGGINK, L. L., PARK, H. & HOOBER, J. K. 2000. Vacuolar granules in *Chlamydomonas reinhardtii*: polyphosphate and a 70-kDa polypeptide as major components. *Planta*, 210, 897-905.
- KRIENITZ, L., HUSS, V. A. R. & BOCK, C. 2015. *Chlorella*: 125 years of the green survivalist. *Trends in Plant Science*, 20, 67-69.
- KROPAT, J., HONG-HERMESDORF, A., CASERO, D., ENT, P., CASTRUITA, M., PELLEGRINI, M., MERCHANT, S. S. & MALASARN, D. 2011. A revised mineral nutrient supplement increases biomass and growth rate in *Chlamydomonas reinhardtii*. *Plant J*, 66, 770-80.
- KRZEMIŃSKA, I., PAWLIK-SKOWROŃSKA, B., TRZCIŃSKA, M. & TYS, J. 2014. Influence of photoperiods on the growth rate and biomass productivity of green microalgae. *Bioprocess and biosystems engineering*, 37, 735-741.
- KUESEL, A. C., SIANOUDIS, J., LEIBFRITZ, D., GRIMME, L. H. & MAYER, A. 1989. P-31 in-vivo NMR investigation on the function of polyphosphates as phosphate-and energysource during the regreening of the green alga *Chlorella fusca*. *Archives of Microbiology*, 152, 167-171.
- KULAEV, I., KRASHENINNIKOV, I. & KOKURINA, N. 1966. On the localization of inorganic polyphosphates and nucleotides in *Neurospora crassa* mycelium. *Biokhimiia (Moscow, Russia)*, 31, 850-859.

- KULAEV, I. & KULAKOVSKAYA, T. 2000. Polyphosphate and Phosphate Pump. *Annual Review of Microbiology*, 54, 709-734.
- KULAEV, I. S., VAGABOV, V. M. & KULAKOVSKAYA, T. V. 2005. The Chemical Structures and Properties of Condensed Inorganic Phosphates. *The Biochemistry of Inorganic Polyphosphates*.
- KULAKOVSKAYA, T. V., VAGABOV, V. M. & KULAEV, I. S. 2012. Inorganic polyphosphate in industry, agriculture and medicine: Modern state and outlook. *Process Biochemistry*, 47, 1-10.
- KUMAR SHARMA, A., MÜHLROTH, A., JOUHET, J., MARÉCHAL, E., ALIPANAH, L., KISSEN, R., BREMBU, T., BONES, A. M. & WINGE, P. 2020. The Myb-like transcription factor phosphorus starvation response (PtPSR) controls conditional P acquisition and remodelling in marine microalgae. *New Phytologist*, 225, 2380-2395.
- LARSDOTTER, K., LA COUR JANSEN, J. & DALHAMMAR, G. 2010. Phosphorus removal from wastewater by microalgae in Sweden – a year-round perspective. *Environmental Technology*, 31, 117-123.
- LAVRINOVIČS, A., MEŽULE, L., CACIVKINS, P. & JUHNA, T. 2022. Optimizing phosphorus removal for municipal wastewater post-treatment with *Chlorella vulgaris*. *Journal of Environmental Management*, 324, 116313.
- LAVRINOVIČS, A., MEŽULE, L. & JUHNA, T. 2020. Microalgae starvation for enhanced phosphorus uptake from municipal wastewater. *Algal Research*, 52, 102090.
- LAVRINOVIČS, A., MURBY, F., ZĪVERTE, E., MEŽULE, L. & JUHNA, T. 2021. Increasing Phosphorus Uptake Efficiency by Phosphorus-Starved Microalgae for Municipal Wastewater Post-Treatment. *Microorganisms*, 9.
- LEAF, S. 2018. Taking the P out of pollution: an English perspective on phosphorus stewardship and the Water Framework Directive. *Water and Environment Journal*, 32, 4-8.
- LEE, C. S., LEE, S.-A., KO, S.-R., OH, H.-M. & AHN, C.-Y. 2015. Effects of photoperiod on nutrient removal, biomass production, and algal-bacterial population dynamics in lab-scale photobioreactors treating municipal wastewater. *Water Research*, 68, 680-691.
- LEE, Y. S., MULUGU, S., YORK, J. D. & O'SHEA, E. K. 2007. Regulation of a cyclin-CDK-CDK inhibitor complex by inositol pyrophosphates. *Science*, 316, 109-12.
- LI, C., CHEN, J., WANG, J., MA, Z., HAN, P., LUAN, Y. & LU, A. 2015. Occurrence of antibiotics in soils and manures from greenhouse vegetable production bases of Beijing, China and an associated risk assessment. *Science of The Total Environment*, 521-522, 101-107.

- LI, K., LIU, Q., FANG, F., LUO, R., LU, Q., ZHOU, W., HUO, S., CHENG, P., LIU, J., ADDY, M., CHEN, P., CHEN, D. & RUAN, R. 2019. Microalgae-based wastewater treatment for nutrients recovery: A review. *Bioresource Technology*, 291.
- LI, Q., FU, L., WANG, Y., ZHOU, D. & RITTMANN, B. E. 2018. Excessive phosphorus caused inhibition and cell damage during heterotrophic growth of *Chlorella regularis*. *Bioresource Technology*, 268, 266-270.
- LI, X., ZHANG, R., PATENA, W., GANG, S. S., BLUM, S. R., IVANOVA, N., YUE, R., ROBERTSON, J. M., LEFEBVRE, P. A., FITZ-GIBBON, S. T., GROSSMAN, A. R. & JONIKAS, M. C. 2016. An Indexed, Mapped Mutant Library Enables Reverse Genetics Studies of Biological Processes in *Chlamydomonas reinhardtii*. *Plant Cell*, 28, 367-87.
- LICHKO, L., KULAKOVSKAYA, T., PESTOV, N. & KULAEV, I. 2006. Inorganic polyphosphates and exopolyphosphatases in cell compartments of the yeast *Saccharomyces cerevisiae* under inactivation of PPX1 and PPN1 genes. *Biosci Rep*, 26, 45-54.
- LICHKO, L. P., KULAKOVSKAYA, T. V. & KULAEV, I. S. 2010. Properties of Partially Purified Endopolyphosphatase of the Yeast *Saccharomyces cerevisiae*. *Biochemistry (Moscow)*, 75, 1404-1407.
- LISS, E. & LANGEN, P. 1962. [Experiments on polyphosphate overcompensation in yeast cells after phosphate deficiency]. *Arch Mikrobiol*, 41, 383-92.
- LIU, B. & BENNING, C. 2013. Lipid metabolism in microalgae distinguishes itself. *Current opinion in biotechnology*, 24, 300-309.
- LIU, J., PEMBERTON, B., LEWIS, J., SCALES, P. J. & MARTIN, G. J. 2020a. Wastewater treatment using filamentous algae—a review. *Bioresource technology*, 298, 122556.
- LIU, X. L., WANG, L., WANG, X. W., YAN, Y., YANG, X. L., XIE, M. Y., HU, Z., SHEN, X., AI, H. & LIN, H. H. 2020b. Mutation of the chloroplast-localized phosphate transporter OsPHT2; 1 reduces flavonoid accumulation and UV tolerance in rice. *The Plant Journal*, 102, 53-67.
- LOBAKOVA, E., GORELOVA, O., SELYAKH, I., SEMENOVA, L., SCHERBAKOV, P., VASILIEVA, S., ZAYTSEV, P., SHIBZUKHOVA, K., CHIVKUNOVA, O., BAULINA, O. & SOLOVCHENKO, A. 2023. Failure of *Micractinium simplicissimum* Phosphate Resilience upon Abrupt Re-Feeding of Its Phosphorus-Starved Cultures. *International Journal of Molecular Sciences*, 24, 8484.
- LONETTI, A., SZIJGYARTO, Z., BOSCH, D., LOSS, O., AZEVEDO, C. & SAIARDI, A. 2011. Identification of an Evolutionarily Conserved Family of Inorganic Polyphosphate Endopolyphosphatases*. *Journal of Biological Chemistry*, 286, 31966-31974.

- LORENZO-ORTS, L., COUTO, D. & HOTHORN, M. 2020. Identity and functions of inorganic and inositol polyphosphates in plants. *New Phytol*, 225, 637-652.
- LOSITO, O., SZIJGYARTO, Z., RESNICK, A. C. & SAIARDI, A. 2009. Inositol Pyrophosphates and Their Unique Metabolic Complexity: Analysis by Gel Electrophoresis. *PLOS ONE*, 4, e5580.
- LUO, Y., LE-CLECH, P. & HENDERSON, R. K. 2018. Assessment of membrane photobioreactor (MPBR) performance parameters and operating conditions. *Water Research*, 138, 169-180.
- LYNCH, J. P. 2019. Root phenotypes for improved nutrient capture: an underexploited opportunity for global agriculture. *New Phytologist*, 223, 548-564.
- MACKINDER, L. C., MEYER, M. T., METTLER-ALTMANN, T., CHEN, V. K., MITCHELL, M. C., CASPARI, O., FREEMAN ROSENZWEIG, E. S., PALLESEN, L., REEVES, G., ITAKURA, A., ROTH, R., SOMMER, F., GEIMER, S., MÜHLHAUS, T., SCHRODA, M., GOODENOUGH, U., STITT, M., GRIFFITHS, H. & JONIKAS, M. C. 2016. A repeat protein links Rubisco to form the eukaryotic carbon-concentrating organelle. *Proc Natl Acad Sci U S A*, 113, 5958-63.
- MANISALI, A. Y., SUNOL, A. K. & PHILIPPIDIS, G. P. 2019. Effect of macronutrients on phospholipid production by the microalga *Nannochloropsis oculata* in a photobioreactor. *Algal Research*, 41, 101514.
- MARA, D. 2013. *Domestic wastewater treatment in developing countries*, Routledge.
- MARA, D. D. 2006. Constructed Wetlands and Waste Stabilization Ponds for Small Rural Communities in the United Kingdom: A Comparison of Land Area Requirements, Performance and Costs. *Environmental Technology*, 27, 753-757.
- MARSDEN, A., MANIDAKI, M. & MORT, S. 2012. Delivering the Esholt wastewater treatment works scheme, Bradford, UK. *Proceedings of the Institution of Civil Engineers - Waste and Resource Management*, 165, 79-92.
- MARTIN, P. & MOOY, B. A. S. V. 2013. Fluorometric Quantification of Polyphosphate in Environmental Plankton Samples: Extraction Protocols, Matrix Effects, and Nucleic Acid Interference. *Applied and Environmental Microbiology*, 79, 273-281.
- MARTÍNEZ LONDOÑO, E. A., CAÑÓN BARRIGA, J. E. & PALM, M. 2016. Solid biofuels production from energy crops in Colombia: challenges and opportunities. *Biofuels, Bioproducts and Biorefining*, 10, 359-368.
- MARTÍNEZ, M. E., SÁNCHEZ, S., JIMÉNEZ, J. M., EL YOUSFI, F. & MUÑOZ, L. 2000. Nitrogen and phosphorus removal from urban wastewater by the

- microalga *Scenedesmus obliquus*. *Bioresource Technology*, 73, 263-272.
- MBWELE, L. A. 2006. *Microbial Phosphorus Removal in Waste Stabilisation Pond Wastewater Treatment Systems*. Licentiate thesis, comprehensive summary, KTH.
- MEJBEL, H. S., IRWIN, C. L., DODSWORTH, W., HIGGINS, S. N., PATERSON, M. J. & PICK, F. R. 2023. Long-term cyanobacterial dynamics from lake sediment DNA in relation to experimental eutrophication, acidification and climate change. *Freshwater Biology*, n/a.
- MEKONNEN, M. M. & HOEKSTRA, A. Y. 2016. Four billion people facing severe water scarcity. *Science Advances*, 2, e1500323.
- MELIA, P. M., CUNDY, A. B., SOHI, S. P., HOODA, P. S. & BUSQUETS, R. 2017. Trends in the recovery of phosphorus in bioavailable forms from wastewater. *Chemosphere*, 186, 381-395.
- MIYACHI, S. & TAMIYA, H. 1961. DISTRIBUTION AND TURNOVER OF PHOSPHATE COMPOUNDS IN GROWING CHLORELLA CELLS. *Plant and cell physiology*, 2, 405-414.
- MOLINA GRIMA, E., BELARBI, E. H., ACIÉN FERNÁNDEZ, F. G., ROBLES MEDINA, A. & CHISTI, Y. 2003. Recovery of microalgal biomass and metabolites: process options and economics. *Biotechnology Advances*, 20, 491-515.
- MONFET, E., AUBRY, G. & RAMIREZ, A. A. 2018. Nutrient removal and recovery from digestate: a review of the technology. *Biofuels: Biorefinery for fuels and platform chemicals*, 9, 247-262.
- MOON, M., KIM, C. W., PARK, W.-K., YOO, G., CHOI, Y.-E. & YANG, J.-W. 2013. Mixotrophic growth with acetate or volatile fatty acids maximizes growth and lipid production in *Chlamydomonas reinhardtii*. *Algal Research*, 2, 352-357.
- MORALES-PINEDA, M., GARCÍA-GÓMEZ, M. E., BEDERA-GARCÍA, R., GARCÍA-GONZÁLEZ, M. & COUSO, I. 2023. CO₂ Levels Modulate Carbon Utilization, Energy Levels and Inositol Polyphosphate Profile in *Chlorella*. *Plants*, 12, 129.
- MOSELEY, J., GONZALEZ-BALLESTER, D., POOTAKHAM, W., BAILEY, S. & GROSSMAN, A. 2009a. Genetic Interactions Between Regulators of *Chlamydomonas* Phosphorus and Sulfur Deprivation Responses. *Genetics*, 181, 889-905.
- MOSELEY, J. & GROSSMAN, A. R. 2009. Chapter 6 - Phosphate Metabolism and Responses to Phosphorus Deficiency. *In*: HARRIS, E. H., STERN, D. B. & WITMAN, G. B. (eds.) *The Chlamydomonas Sourcebook (Second Edition)*. London: Academic Press.

- MOSELEY, J. L., CHANG, C.-W. & GROSSMAN, A. R. 2006. Genome-Based Approaches to Understanding Phosphorus Deprivation Responses and PSR1 Control in *Chlamydomonas reinhardtii*. *Eukaryotic Cell*, 5, 26.
- MOSELEY, J. L., GONZALEZ-BALLESTER, D., POOTAKHAM, W., BAILEY, S. & GROSSMAN, A. R. 2009b. Genetic interactions between regulators of *Chlamydomonas phosphorus* and sulfur deprivation responses. *Genetics*, 181, 889-905.
- MOUDŘÍKOVÁ, Š., IVANOV, I. N., VÍTOVÁ, M., NEDBAL, L., ZACHLEDER, V., MOJZEŠ, P. & BIŠOVÁ, K. 2021. Comparing Biochemical and Raman Microscopy Analyses of Starch, Lipids, Polyphosphate, and Guanine Pools during the Cell Cycle of *Desmodesmus quadricauda*. *Cells*, 10.
- MOUDŘÍKOVÁ, Š., SADOWSKY, A., METZGER, S., NEDBAL, L., METTLER-ALTMANN, T. & MOJZEŠ, P. 2017. Quantification of Polyphosphate in Microalgae by Raman Microscopy and by a Reference Enzymatic Assay. *Analytical Chemistry*, 89, 12006-12013.
- MSANNE, J., XU, D., KONDA, A. R., CASAS-MOLLANO, J. A., AWADA, T., CAHOON, E. B. & CERUTTI, H. 2012. Metabolic and gene expression changes triggered by nitrogen deprivation in the photoautotrophically grown microalgae *Chlamydomonas reinhardtii* and *Coccomyxa* sp. C-169. *Phytochemistry*, 75, 50-59.
- MÜHLROTH, A., WINGE, P., EL ASSIMI, A., JOUHET, J., MARÉCHAL, E., HOHMANN-MARRIOTT, M. F., VADSTEIN, O. & BONES, A. M. 2017. Mechanisms of Phosphorus Acquisition and Lipid Class Remodeling under P Limitation in a Marine Microalga. *Plant Physiology*, 175, 1543-1559.
- MULBRY, W., KONDRAD, S. & PIZARRO, C. 2007. Biofertilizers from Algal Treatment of Dairy and Swine Manure Effluents. *Journal of Vegetable Science*, 12, 107-125.
- MULBRY, W., WESTHEAD, E. K., PIZARRO, C. & SIKORA, L. 2005. Recycling of manure nutrients: use of algal biomass from dairy manure treatment as a slow release fertilizer. *Bioresource Technology*, 96, 451-458.
- MURPHY, J. & RILEY, J. P. 1962. A modified single solution method for the determination of phosphate in natural waters. *Analytica Chimica Acta*, 27, 31-36.
- NASSEF, E. 2012. Removal of phosphates from industrial waste water by chemical precipitation. *Engineering Science and Technology: An International Journal*, 2, 409-413.
- NATRAH, F. M. I., BOSSIER, P., SORGELOOS, P., YUSOFF, F. M. & DEFOIRDT, T. 2014. Significance of microalgal-bacterial interactions for aquaculture. *Reviews in Aquaculture*, 6, 48-61.
- NÄTTORP, A., KABBE, C., MATSUBAE, K. & OHTAKE, H. 2019. Development of Phosphorus Recycling in Europe and Japan. *In: OHTAKE, H. &*

- TSUNEDA, S. (eds.) *Phosphorus Recovery and Recycling*. Singapore: Springer Singapore.
- NEEF, D. W. & KLADDE, M. P. 2003. Polyphosphate Loss Promotes SNF/SWI- and Gcn5-Dependent Mitotic Induction of PHO5. *Molecular and Cellular Biology*, 23, 3788-3797.
- NELSON, D. R., HAZZOURI, K. M., LAUERSEN, K. J., JAISWAL, A., CHAIBOONCHOE, A., MYSTIKOU, A., FU, W., DAAKOUR, S., DOHAI, B. & ALZAHMI, A. 2021. Large-scale genome sequencing reveals the driving forces of viruses in microalgal evolution. *Cell Host & Microbe*, 29, 250-266. e8.
- NEUPERT, J., GALLAHER, S. D., LU, Y., STRENKERT, D., SEGAL, N., BARAHIMIPOUR, R., FITZ-GIBBON, S. T., SCHRODA, M., MERCHANT, S. S. & BOCK, R. 2020. An epigenetic gene silencing pathway selectively acting on transgenic DNA in the green alga *Chlamydomonas*. *Nat Commun*, 11, 6269.
- NEUPERT, J., KARCHER, D. & BOCK, R. 2009. Generation of *Chlamydomonas* strains that efficiently express nuclear transgenes. *Plant Journal*, 57, 1140-1150.
- NGAN, C. Y., WONG, C.-H., CHOI, C., YOSHINAGA, Y., LOUIE, K., JIA, J., CHEN, C., BOWEN, B., CHENG, H., LEONELLI, L., KUO, R., BARAN, R., GARCÍA-CERDÁN, J. G., PRATAP, A., WANG, M., LIM, J., TICE, H., DAUM, C., XU, J., NORTHEN, T., VISEL, A., BRISTOW, J., NIYOGI, K. K. & WEI, C.-L. 2015. Lineage-specific chromatin signatures reveal a regulator of lipid metabolism in microalgae. *Nature Plants*, 1, 15107.
- NICHOLSON, F. A., GROVES, S. J. & CHAMBERS, B. J. 2005. Pathogen survival during livestock manure storage and following land application. *Bioresource Technology*, 96, 135-143.
- NYAMANGARA, J., KODZWA, J., MASVAYA, E. N. & SOROPA, G. 2020. Chapter 5 - The role of synthetic fertilizers in enhancing ecosystem services in crop production systems in developing countries. *In: RUSINAMHODZI, L. (ed.) The Role of Ecosystem Services in Sustainable Food Systems*. Academic Press.
- OHTAKE, H. & TSUNEDA, S. 2019. *Phosphorus recovery and recycling*, Springer.
- OKAZAKI, Y., SHIMOJIMA, M., SAWADA, Y., TOYOOKA, K., NARISAWA, T., MOCHIDA, K., TANAKA, H., MATSUDA, F., HIRAI, A. & HIRAI, M. Y. 2009. A chloroplastic UDP-glucose pyrophosphorylase from *Arabidopsis* is the committed enzyme for the first step of sulfolipid biosynthesis. *The Plant Cell*, 21, 892-909.
- ONG, Y. H., CHUA, A. S. M., HUANG, Y. T., NGOH, G. C. & YOU, S. J. 2016. The microbial community in a high-temperature enhanced biological phosphorus removal (EBPR) process. *Sustainable Environment Research*, 26, 14-19.

- ONNEBO, S. M. & SAIARDI, A. 2007. Inositol pyrophosphates get the vip1 treatment. *Cell*, 129, 647-9.
- OSUNDEKO, O., DAVIES, H. & PITTMAN, J. K. 2013. Oxidative stress-tolerant microalgae strains are highly efficient for biofuel feedstock production on wastewater. *Biomass and Bioenergy*, 56, 284-294.
- PARK, S.-Y. & KIM, J.-S. 2020. A short guide to histone deacetylases including recent progress on class II enzymes. *Experimental & Molecular Medicine*, 52, 204-212.
- PICOT, B., BAHLAOUI, A., MOERSIDIK, S., BALEUX, B. & BONTOUX, J. 1992. Comparison of the Purifying Efficiency of High Rate Algal Pond with Stabilization Pond. *Water Science and Technology*, 25, 197-206.
- PIERZYNSKI, G. M. 2000. Methods of phosphorus analysis for soils, sediments, residuals, and waters. North Carolina State University ISBN: 1581613962.
- PIVATO, M. & BALLOTTARI, M. 2021. Chlamydomonas reinhardtii cellular compartments and their contribution to intracellular calcium signalling. *J Exp Bot*, 72, 5312-5335.
- PŁACZEK, M., PATYNA, A. & WITCZAK, S. Technical evaluation of photobioreactors for microalgae cultivation. E3S web of conferences, 2017. EDP Sciences, 02032.
- PLOUVIEZ, M., ABYADEH, M., HASAN, M., MIRZAEI, M., PAULO, J. A. & GUIEYSSE, B. 2023a. The proteome of Chlamydomonas reinhardtii during phosphorus depletion and repletion. *Algal Research*, 71, 103037.
- PLOUVIEZ, M., BOLOT, P., SHILTON, A. & GUIEYSSE, B. 2023b. Phosphorus uptake and accumulation in Chlamydomonas reinhardtii: Influence of biomass concentration, phosphate concentration, phosphorus depletion time, and light supply. *Algal Research*, 71, 103085.
- PLOUVIEZ, M., FERNÁNDEZ, E., GROSSMAN, A. R., SANZ-LUQUE, E., SELLS, M., WHEELER, D. & GUIEYSSE, B. 2021. Responses of Chlamydomonas reinhardtii during the transition from P-deficient to P-sufficient growth (the P-overplus response): The roles of the vacuolar transport chaperones and polyphosphate synthesis. *Journal of Phycology*, 57, 988-1003.
- PLOUVIEZ, M., OLIVEIRA DA ROCHA, C. S. & GUIEYSSE, B. 2022. Intracellular polyphosphate is a P reserve in Chlamydomonas reinhardtii. *Algal Research*, 66, 102779.
- PODEVIN, M., DE FRANCISCI, D., HOLDT, S. L. & ANGELIDAKI, I. 2015. Effect of nitrogen source and acclimatization on specific growth rates of microalgae determined by a high-throughput in vivo microplate autofluorescence method. *Journal of Applied Phycology*, 27, 1415-1423.

- PORRA, R. J., THOMPSON, W. A. & KRIEDEMANN, P. E. 1989. Determination of accurate extinction coefficients and simultaneous equations for assaying chlorophylls a and b extracted with four different solvents: verification of the concentration of chlorophyll standards by atomic absorption spectroscopy. *Biochimica et Biophysica Acta (BBA) - Bioenergetics*, 975, 384-394.
- POWELL, N., SHILTON, A., CHISTI, Y. & PRATT, S. 2009. Towards a luxury uptake process via microalgae – Defining the polyphosphate dynamics. *Water Research*, 43, 4207-4213.
- POWELL, N., SHILTON, A., PRATT, S. & CHISTI, Y. 2011. Luxury uptake of phosphorus by microalgae in full-scale waste stabilisation ponds. *Water science and technology : a journal of the International Association on Water Pollution Research*, 63, 704-709.
- POWELL, N., SHILTON, A. N., PRATT, S. & CHISTI, Y. 2008. Factors influencing luxury uptake of phosphorus by microalgae in waste stabilization ponds. *Environmental science & technology*, 42, 5958-5962.
- PRATT, C., PARSONS, S. A., SOARES, A. & MARTIN, B. D. 2012. Biologically and chemically mediated adsorption and precipitation of phosphorus from wastewater. *Current Opinion in Biotechnology*, 23, 890-896.
- PRÖSCHOLD, T., HARRIS, E. H. & COLEMAN, A. W. 2005. Portrait of a Species: *Chlamydomonas reinhardtii*. *Genetics*, 170, 1601-1610.
- PUGA, M. I., MATEOS, I., CHARUKESI, R., WANG, Z., FRANCO-ZORRILLA, J. M., DE LORENZO, L., IRIGOYEN, M. L., MASIERO, S., BUSTOS, R., RODRÍGUEZ, J., LEYVA, A., RUBIO, V., SOMMER, H. & PAZ-ARES, J. 2014. SPX1 is a phosphate-dependent inhibitor of PHOSPHATE STARVATION RESPONSE 1 in Arabidopsis. *Proceedings of the National Academy of Sciences*, 111, 14947-14952.
- QADIR, M., DRECHSEL, P., JIMÉNEZ CISNEROS, B., KIM, Y., PRAMANIK, A., MEHTA, P. & OLANIYAN, O. Global and regional potential of wastewater as a water, nutrient and energy source. Natural resources forum, 2020. Wiley Online Library, 40-51.
- QI, W., MANFIELD, I. W., MUENCH, S. P. & BAKER, A. 2017. AtSPX1 affects the AtPHR1–DNA-binding equilibrium by binding monomeric AtPHR1 in solution. *Biochemical Journal*, 474, 3675-3687.
- QIU, G. & TING, Y.-P. 2014. Direct phosphorus recovery from municipal wastewater via osmotic membrane bioreactor (OMBR) for wastewater treatment. *Bioresource Technology*, 170, 221-229.
- QUISEL, J. D., WYKOFF, D. D. & GROSSMAN, A. R. 1996. Biochemical characterization of the extracellular phosphatases produced by phosphorus-deprived *Chlamydomonas reinhardtii*. *Plant Physiol*, 111, 839-48.

- RABOY, V. 2020. Low phytic acid crops: Observations based on four decades of research. *Plants*, 9, 140.
- RAGSDALE, D. 2007. Advanced wastewater treatment to achieve low concentration of phosphorus. *EPA Region*, 10, 6-11.
- RAMOS-MARTINEZ, E. M., FIMOIGNARI, L. & SAKURAGI, Y. 2017. High-yield secretion of recombinant proteins from the microalga *Chlamydomonas reinhardtii*. *Plant biotechnology journal*, 15, 1214-1224.
- RAO, I. M., BARRIOS, E., AMÉZQUITA COLLAZOS, E., FRIESEN, D. K., THOMAS, R. J., OBERSON, A. & SINGH, B. 2004. Soil phosphorus dynamics, acquisition and cycling in crop-pasture-fallow systems in low fertility tropical soils: A review from Latin America.
- RAO, N. N., GÓMEZ-GARCÍA, M. R. & KORNBERG, A. 2009. Inorganic Polyphosphate: Essential for Growth and Survival. *Annual Review of Biochemistry*, 78, 605-647.
- RASHID, M. H. & KORNBERG, A. 2000. Inorganic polyphosphate is needed for swimming, swarming, and twitching motilities of *Pseudomonas aeruginosa*. *Proc Natl Acad Sci U S A*, 97, 4885-90.
- RASHID, N., NAYAK, M., LEE, B. & CHANG, Y.-K. 2019. Efficient microalgae harvesting mediated by polysaccharides interaction with residual calcium and phosphate in the growth medium. *Journal of Cleaner Production*, 234, 150-156.
- RAVEN, J. 2013. RNA function and phosphorus use by photosynthetic organisms. *Frontiers in Plant Science*, 4.
- REDFIELD, A. C. 1960. The biological control of chemical factors in the environment. *Sci Prog*, 11, 150-70.
- REES, T. A. V. & RAVEN, J. A. 2021. The maximum growth rate hypothesis is correct for eukaryotic photosynthetic organisms, but not cyanobacteria. *New Phytol*, 230, 601-611.
- REIGNIER, O., BORMANS, M., MARCHAND, L., SINQUIN, C., AMZIL, Z., ZYKWINSKA, A. & BRIAND, E. 2023. Production and composition of extracellular polymeric substances by a unicellular strain and natural colonies of *Microcystis*: Impact of salinity and nutrient stress. *Environmental Microbiology Reports*, n/a.
- REISTETTER, E. N., KRUMHARDT, K., CALLNAN, K., ROACHE-JOHNSON, K., SAUNDERS, J. K., MOORE, L. R. & ROCAP, G. 2013. Effects of phosphorus starvation versus limitation on the marine cyanobacterium *Prochlorococcus* MED4 II: gene expression. *Environmental Microbiology*, 15, 2129-2143.
- RENUKA, N., PRASANNA, R., SOOD, A., AHLUWALIA, A. S., BANSAL, R., BABU, S., SINGH, R., SHIVAY, Y. S. & NAIN, L. 2016. Exploring the

- efficacy of wastewater-grown microalgal biomass as a biofertilizer for wheat. *Environmental Science and Pollution Research*, 23, 6608-6620.
- RIEKHOF, W. R., RUCKLE, M. E., LYDIC, T. A., SEARS, B. B. & BENNING, C. 2003. The sulfolipids 2'-O-acyl-sulfoquinovosyldiacylglycerol and sulfoquinovosyldiacylglycerol are absent from a *Chlamydomonas reinhardtii* mutant deleted in SQD1. *Plant Physiol*, 133, 864-74.
- RIVERA-SOLÍS, R. A., PERAZA-ECHEVERRÍA, S., ECHEVARRÍA-MACHADO, I. & HERRERA-VALENCIA, V. A. 2014. *Chlamydomonas reinhardtii* has a small family of purple acid phosphatase homologue genes that are differentially expressed in response to phytate. *Annals of Microbiology*, 64, 551-559.
- ROCHAIX, J. D. 1995. *Chlamydomonas reinhardtii* as the photosynthetic yeast. *Annu Rev Genet*, 29, 209-30.
- RODRIGUEZ, J., SELF, J. & SOLTANPOUR, P. 1994. Optimal conditions for phosphorus analysis by the ascorbic acid-molybdenum blue method. *Soil Science Society of America Journal*, 58, 866-870.
- ROLEDA, M. Y., SLOCOMBE, S. P., LEAKEY, R. J. G., DAY, J. G., BELL, E. M. & STANLEY, M. S. 2013. Effects of temperature and nutrient regimes on biomass and lipid production by six oleaginous microalgae in batch culture employing a two-phase cultivation strategy. *Bioresource Technology*, 129, 439-449.
- RUBIO, V., LINHARES, F., SOLANO, R., MARTÍN, A. C., IGLESIAS, J., LEYVA, A. & PAZ-ARES, J. 2001. A conserved MYB transcription factor involved in phosphate starvation signaling both in vascular plants and in unicellular algae. *Genes & Development*, 15, 2122-2133.
- RUIZ, F. A., MARCHESINI, N., SEUFFERHELD, M., GOVINDJEE & DOCAMPO, R. 2001. The Polyphosphate Bodies of *Chlamydomonas reinhardtii* Possess a Proton-pumping Pyrophosphatase and Are Similar to Acidocalcisomes*. *Journal of Biological Chemistry*, 276, 46196-46203.
- RUIZ, J., ÁLVAREZ, P., ARBIB, Z., GARRIDO, C., BARRAGÁN, J. & PERALES, J. A. 2011. Effect of Nitrogen and Phosphorus Concentration on Their Removal Kinetic in Treated Urban Wastewater by *Chlorella Vulgaris*. *International Journal of Phytoremediation*, 13, 884-896.
- RUZHITSKAYA, O. & GOGINA, E. 2017. Methods for Removing of Phosphates from Wastewater. *MATEC Web Conf.*, 106, 07006.
- SAGER, R. 1955. Inheritance in the Green Alga *Chlamydomonas Reinhardi*. *Genetics*, 40, 476-89.
- SAIARDI, A., ERDJUMENT-BROMAGE, H., SNOWMAN, A. M., TEMPST, P. & SNYDER, S. H. 1999. Synthesis of diphosphoinositol pentakisphosphate by a newly identified family of higher inositol polyphosphate kinases. *Current Biology*, 9, 1323-1326.

- SALOMÉ, P. A. & MERCHANT, S. S. 2019. A Series of Fortunate Events: Introducing *Chlamydomonas* as a Reference Organism. *The Plant cell*, 31, 1682.
- SANZ-LUQUE, E. & GROSSMAN, A. R. 2023. Chapter 4 - Phosphorus and sulfur uptake, assimilation, and deprivation responses. *In: GROSSMAN, A. R. & WOLLMAN, F.-A. (eds.) The Chlamydomonas Sourcebook (Third Edition)*. London: Academic Press.
- SANZ-LUQUE, E., SAROUSSI, S., HUANG, W., AKKAWI, N. & GROSSMAN, A. R. 2020. Metabolic control of acclimation to nutrient deprivation dependent on polyphosphate synthesis. *Science Advances*, 6, eabb5351.
- SARMA, S. J., DAS, R. K., BRAR, S. K., LE BIHAN, Y., BUELNA, G., VERMA, M. & SOCCOL, C. R. 2014. Application of magnesium sulfate and its nanoparticles for enhanced lipid production by mixotrophic cultivation of algae using biodiesel waste. *Energy*, 78, 16-22.
- SATHYA, R., ARASU, M. V., AL-DHABI, N. A., VIJAYARAGHAVAN, P., ILAVENIL, S. & REJINIEMON, T. S. 2023. Towards sustainable wastewater treatment by biological methods – A challenges and advantages of recent technologies. *Urban Climate*, 47, 101378.
- SATO, N., KAMIMURA, R., KANETA, K., YOSHIKAWA, M. & TSUZUKI, M. 2017. Species-specific roles of sulfolipid metabolism in acclimation of photosynthetic microbes to sulfur-starvation stress. *PLOS ONE*, 12, e0186154.
- SCARSELLA, M., TORZILLO, G., CICCIO, A., BELOTTI, G., DE FILIPPIS, P. & BRAVI, M. 2012. Mechanical stress tolerance of two microalgae. *Process Biochemistry*, 47, 1603-1611.
- SCHACHTMAN, D. P., REID, R. J. & AYLING, S. M. 1998. Phosphorus Uptake by Plants: From Soil to Cell. *Plant Physiology*, 116, 447.
- SCHINDELIN, J., ARGANDA-CARRERAS, I., FRISE, E., KAYNIG, V., LONGAIR, M., PIETZSCH, T., PREIBISCH, S., RUEDEN, C., SAALFELD, S., SCHMID, B., TINEVEZ, J.-Y., WHITE, D. J., HARTENSTEIN, V., ELICEIRI, K., TOMANCAK, P. & CARDONA, A. 2012. Fiji: an open-source platform for biological-image analysis. *Nature Methods*, 9, 676-682.
- SCHMIDT, G., HECHT, L. & THANNHAUSER, S. J. 1946. The enzymatic formation and the accumulation of large amounts of a metaphosphate in bakers' yeast under certain conditions. *J Biol Chem*, 166, 775.
- SCHMIDT, J. J., GAGNON, G. A. & JAMIESON, R. C. 2016. Microalgae growth and phosphorus uptake in wastewater under simulated cold region conditions. *Ecological Engineering*, 95, 588-593.

- SCHÖNBORN, C., BAUER, H.-D. & RÖSKE, I. 2001. Stability of enhanced biological phosphorus removal and composition of polyphosphate granules. *Water Research*, 35, 3190-3196.
- SCHREIBER, C., SCHIEDUNG, H., HARRISON, L., BRIESE, C., ACKERMANN, B., KANT, J., SCHREY, S. D., HOFMANN, D., SINGH, D., EBENHÖH, O., AMELUNG, W., SCHURR, U., METTLER-ALTMANN, T., HUBER, G., JABLONOWSKI, N. D. & NEDBAL, L. 2018. Evaluating potential of green alga *Chlorella vulgaris* to accumulate phosphorus and to fertilize nutrient-poor soil substrates for crop plants. *Journal of Applied Phycology*, 30, 2827-2836.
- SCHRODA, M. 2019. Good News for Nuclear Transgene Expression in *Chlamydomonas*. *Cells*, 8, 1534.
- SECCO, D., WANG, C., SHOU, H. & WHELAN, J. 2012. Phosphate homeostasis in the yeast *Saccharomyces cerevisiae*, the key role of the SPX domain-containing proteins. *FEBS Letters*, 586, 289-295.
- SELLS, M. D., BROWN, N. & SHILTON, A. N. 2018. Determining variables that influence the phosphorus content of waste stabilization pond algae. *Water Research*, 132, 301-308.
- SFORZA, E., CALVARUSO, C., LA ROCCA, N. & BERTUCCO, A. 2018. Luxury uptake of phosphorus in *Nannochloropsis salina*: Effect of P concentration and light on P uptake in batch and continuous cultures. *Biochemical Engineering Journal*, 134, 69-79.
- SHATWELL, T., KÖHLER, J. & NICKLISCH, A. 2014. Temperature and photoperiod interactions with phosphorus-limited growth and competition of two diatoms. *PloS one*, 9.
- SHEBANOVA, A., ISMAGULOVA, T., SOLOVCHENKO, A., BAULINA, O., LOBAKOVA, E., IVANOVA, A., MOISEENKO, A., SHAITAN, K., POLSHAKOV, V., NEDBAL, L. & GORELOVA, O. 2017. Versatility of the green microalga cell vacuole function as revealed by analytical transmission electron microscopy. *Protoplasma*, 254, 1323-1340.
- SHIMOGAWARA, K., WYKOFF, D., USUDA, H. & GROSSMAN, A. 1999. *Chlamydomonas reinhardtii* mutants abnormal in their responses to phosphorus deprivation. *Plant Physiology*, 120, 685-94.
- SIANOUDIS, J., KÜSEL, A. C., MAYER, A., GRIMME, L. H. & LEIBFRITZ, D. 1986. Distribution of polyphosphates in cell-compartments of *Chlorella fusca* as measured by ³¹P-NMR-spectroscopy. *Archives of Microbiology*, 144, 48-54.
- SICKO-GOAD, L. & JENSEN, T. E. 1976. Phosphate Metabolism in Blue-Green Algae. II. Changes in Phosphate Distribution During Starvation and the "Polyphosphate Overplus" Phenomenon in *Plectonema boryanum*. *American journal of botany*, 63, 183-188.

- SIDERIUS, M., MUSGRAVE, A., VAN DEN ENDE, H., KOERTEN, H., CAMBIER, P. & VAN DER MEER, P. 1996. CHLAMYDOMONAS EUGAMETOS (CHLOROPHYTA) STORES PHOSPHATE IN POLYPHOSPHATE BODIES TOGETHER WITH CALCIUM¹. *Journal of Phycology*, 32, 402-409.
- SINGH, N. & DHAR, D. 2006. Sewage Effluent: A Potential Nutrient Source for Microalgae. *Proceedings Indian National Science Academy*, 72, 113-120.
- SLOCOMBE, S. P., ZÚÑIGA-BURGOS, T., CHU, L., MEHRSHAHI, P., DAVEY, M. P., SMITH, A. G., CAMARGO-VALERO, M. A. & BAKER, A. 2023. Overexpression of PSR1 in *Chlamydomonas reinhardtii* induces luxury phosphorus uptake. *Frontiers in Plant Science*, 14.
- SLOCOMBE, S. P., ZÚÑIGA-BURGOS, T., CHU, L., WOOD, N. J., CAMARGO-VALERO, M. A. & BAKER, A. 2020. Fixing the Broken Phosphorus Cycle: Wastewater Remediation by Microalgal Polyphosphates. *Frontiers in Plant Science*, 11.
- SLOMPO, N. D. M., QUARTAROLI, L., FERNANDES, T. V., SILVA, G. H. R. D. & DANIEL, L. A. 2020. Nutrient and pathogen removal from anaerobically treated black water by microalgae. *Journal of Environmental Management*, 268, 110693.
- SMITH, S. A. & MORRISSEY, J. H. 2007. Sensitive fluorescence detection of polyphosphate in polyacrylamide gels using 4', 6-diamidino-2-phenylindol. *Electrophoresis*, 28, 3461-3465.
- SOLOVCHENKO, A., GORELOVA, O., KARPOVA, O., SELYAKH, I., SEMENOVA, L., CHIVKUNOVA, O., BAULINA, O., VINOGRADOVA, E., PUGACHEVA, T. & SCHERBAKOV, P. 2020. Phosphorus Feast and Famine in Cyanobacteria: Is Luxury Uptake of the Nutrient Just a Consequence of Acclimation to Its Shortage? *Cells*, 9, 1933.
- SOLOVCHENKO, A., ISMAGULOVA, T., LUKYANOV, A., VASILIEVA, S., KONYUKHOV, I., POGOSYAN, S., LOBAKOVA, E. & GORELOVA, O. 2019a. Luxury phosphorus uptake in microalgae. *Journal of Applied Phycology*, 31, 2755-2770.
- SOLOVCHENKO, A., KHOZIN-GOLDBERG, I., SELYAKH, I., SEMENOVA, L., ISMAGULOVA, T., LUKYANOV, A., MAMEDOV, I., VINOGRADOVA, E., KARPOVA, O., KONYUKHOV, I., VASILIEVA, S., MOJZES, P., DIJKEMA, C., VECHERSKAYA, M., ZVYAGIN, I., NEDBAL, L. & GORELOVA, O. 2019b. Phosphorus starvation and luxury uptake in green microalgae revisited. *Algal Research*, 43.
- SOLOVCHENKO, A., VERSCHOOR, A. M., JABLONOWSKI, N. D. & NEDBAL, L. 2016. Phosphorus from wastewater to crops: An alternative path involving microalgae.(Report). *Biotechnology Advances*, 34, 550.
- SONZOGNI, W. C., CHAPRA, S. C., ARMSTRONG, D. E. & LOGAN, T. J. 1982. Bioavailability of Phosphorus Inputs to Lakes. *Journal of Environmental Quality*, 11, 555-563.

- STERNLIEB, F. R. & LAITURI, M. 2010. Water, Sanitation, and Hygiene (WASH) Indicators: Measuring Hydrophilanthropic Quality. *Journal of Contemporary Water Research & Education*, 145, 51-60.
- SU, Y., MENNERICH, A. & URBAN, B. 2011. Municipal wastewater treatment and biomass accumulation with a wastewater-born and settleable algal-bacterial culture. *Water Research*, 45, 3351-3358.
- TALBOYS, P., HEPPELL, J., ROOSE, T., HEALEY, J., JONES, D. & WITHERS, P. 2016. Struvite: a slow-release fertiliser for sustainable phosphorus management? *Plant and Soil*, 401, 109-123.
- TANG, C.-C., ZHANG, X., HE, Z.-W., TIAN, Y. & WANG, X. C. 2021. Role of extracellular polymeric substances on nutrients storage and transfer in algal-bacteria symbiosis sludge system treating wastewater. *Bioresource Technology*, 331, 125010.
- TANI, C., OHTOMO, R., OSAKI, M., KUGA, Y. & EZAWA, T. 2009. ATP-Dependent but Proton Gradient-Independent Polyphosphate-Synthesizing Activity in Extraradical Hyphae of an Arbuscular Mycorrhizal Fungus. *Applied and Environmental Microbiology*, 75, 7044-7050.
- TARAYRE, C., DE CLERCQ, L., CHARLIER, R., MICHELS, E., MEERS, E., CAMARGO-VALERO, M. & DELVIGNE, F. 2016. New perspectives for the design of sustainable bioprocesses for phosphorus recovery from waste. *Bioresource Technology*, 206, 264-274.
- TODO, K. & SATO, K. 2002. Directive 2000/60/EC of the European Parliament and of the Council of 23 October 2000 establishing a framework for Community action in the field of water policy. *Environmental Research Quarterly*, 66-106.
- TÓTH, D., SOUJANYA, K., ARON, F., ANDRÉ, V.-M., LÁSZLÓ, K., LIANYONG, W., ZSUZSA, S., EDE, M., KLARA, S., ROLAND, T., JULIANE, N., RALPH, B., MARTIN, C. J., ATTILA, M. & SZILVIA, Z. T. 2023. The chloroplastic phosphate transporter CrPHT4-7 supports phosphate homeostasis and photosynthesis in *Chlamydomonas*. *bioRxiv*, 2023.09.08.556869.
- TSEDNEE, M., CASTRUITA, M., SALOMÉ, P. A., SHARMA, A., LEWIS, B. E., SCHMOLLINGER, S. R., STRENKERT, D., HOLBROOK, K., OTEGUI, M. S., KHATUA, K., DAS, S., DATTA, A., CHEN, S., RAMON, C., RALLE, M., WEBER, P. K., STEMMLER, T. L., PETT-RIDGE, J., HOFFMAN, B. M. & MERCHANT, S. S. 2019. Manganese co-localizes with calcium and phosphorus in *Chlamydomonas* acidocalcisomes and is mobilized in manganese-deficient conditions. *Journal of Biological Chemistry*, 294, 17626-17641.
- UDUMAN, N., QI, Y., DANQUAH, M. K., FORDE, G. M. & HOADLEY, A. 2010. Dewatering of microalgal cultures: A major bottleneck to algae-based fuels. *Journal of Renewable and Sustainable Energy*, 2, 012701.

- UEKI, N., IDE, T., MOCHIJI, S., KOBAYASHI, Y., TOKUTSU, R., OHNISHI, N., YAMAGUCHI, K., SHIGENOBU, S., TANAKA, K., MINAGAWA, J., HISABORI, T., HIRONO, M. & WAKABAYASHI, K.-I. 2016. Eyespot-dependent determination of the phototactic sign in *Chlamydomonas reinhardtii*. *Proceedings of the National Academy of Sciences*, 113, 5299.
- UK-ENVIRONMENT-AGENCY. 2019. *Guidance for Waste water treatment works: treatment monitoring and compliance limits* [Online]. Available: <https://www.gov.uk/government/publications/waste-water-treatment-works-treatment-monitoring-and-compliance-limits/waste-water-treatment-works-treatment-monitoring-and-compliance-limits#contact-the-environment-agency> [Accessed].
- VAN DIJK, K. C., LESSCHEN, J. P. & OENEMA, O. 2016. Phosphorus flows and balances of the European Union Member States. *Science of The Total Environment*, 542, 1078-1093.
- VAN MOOY, B. A. S., FREDRICKS, H. F., PEDLER, B. E., DYHRMAN, S. T., KARL, D. M., KOBLÍŽEK, M., LOMAS, M. W., MINCER, T. J., MOORE, L. R., MOUTIN, T., RAPPÉ, M. S. & WEBB, E. A. 2009. Phytoplankton in the ocean use non-phosphorus lipids in response to phosphorus scarcity. *Nature*, 458, 69-72.
- VAN PUIJENBROEK, P. J. T. M., BEUSEN, A. H. W. & BOUWMAN, A. F. 2019. Global nitrogen and phosphorus in urban waste water based on the Shared Socio-economic pathways. *Journal of Environmental Management*, 231, 446-456.
- VERMEGLIO, A., RAVENEL, J. & PELTIER, G. 1990. Chlororespiration: A respiratory activity in the thylakoid membrane of microalgae and higher plants. In: WIESSNER, W., ROBINSON, D. G. & STARR, R. C. (eds.) *Cell Walls and Surfaces, Reproduction, Photosynthesis*. Berlin, Heidelberg: Springer Berlin Heidelberg.
- VOELZ, H., VOELZ, U. & ORTIGOZA, R. O. 1966. The “polyphosphate overplus” phenomenon in *myxococcus xanthus* and its influence on the architecture of the cell. *Archiv für Mikrobiologie*, 53, 371-388.
- VON SPERLING, M. 2007. *Waste Stabilisation Ponds. Biological Wastewater Treatment Series*. IWA Publishing.
- VON SPERLING, M. & AUGUSTO DE LEMOS CHERNICHARO, C. 2002. Urban wastewater treatment technologies and the implementation of discharge standards in developing countries. *Urban Water*, 4, 105-114.
- WANG, L., JIA, X., XU, L., YU, J., REN, S., YANG, Y., WANG, K., LÓPEZ-ARREDONDO, D., HERRERA-ESTRELLA, L., LAMBERS, H. & YI, K. 2023. Engineering microalgae for water phosphorus recovery to close the phosphorus cycle. *Plant Biotechnology Journal*, 21, 1373-1382.
- WANG, L., JIA, X., ZHANG, Y., XU, L., MENAND, B., ZHAO, H., ZENG, H., DOLAN, L., ZHU, Y. & YI, K. 2021. Loss of two families of SPX domain-

containing proteins required for vacuolar polyphosphate accumulation coincides with the transition to phosphate storage in green plants. *Molecular Plant*, 14, 838-846.

- WANG, L., MIN, M., LI, Y., CHEN, P., CHEN, Y., LIU, Y., WANG, Y. & RUAN, R. 2010. Cultivation of green algae *Chlorella* sp. in different wastewaters from municipal wastewater treatment plant. *Appl Biochem Biotechnol*, 162, 1174-86.
- WANG, L., XIAO, L., YANG, H., CHEN, G., ZENG, H., ZHAO, H. & ZHU, Y. 2020. Genome-Wide Identification, Expression Profiling, and Evolution of Phosphate Transporter Gene Family in Green Algae. *Frontiers in Genetics*, 11.
- WEN, Y., HE, Y., JI, X., LI, S., CHEN, L., ZHOU, Y., WANG, M. & CHEN, B. 2017. Isolation of an indigenous *Chlorella vulgaris* from swine wastewater and characterization of its nutrient removal ability in undiluted sewage. *Bioresource Technology*, 243, 247-253.
- WERNER, T. P., AMRHEIN, N. & FREIMOSER, F. M. 2005. Novel method for the quantification of inorganic polyphosphate (iPoP) in *Saccharomyces cerevisiae* shows dependence of iPoP content on the growth phase. *Archives of Microbiology*, 184, 129-136.
- WERNER, T. P., AMRHEIN, N. & FREIMOSER, F. M. 2007. Inorganic polyphosphate occurs in the cell wall of *Chlamydomonas reinhardtii* and accumulates during cytokinesis. *BMC Plant Biology*, 7, 51.
- WILD, R., GERASIMAITE, R., JUNG, J.-Y., TRUFFAULT, V., PAVLOVIC, I., SCHMIDT, A., SAIARDI, A., JESSEN, H. J., POIRIER, Y., HOTHORN, M. & MAYER, A. 2016. Control of eukaryotic phosphate homeostasis by inositol polyphosphate sensor domains. *Science*, 352, 986.
- WILSON, M. S., LIVERMORE, T. M. & SAIARDI, A. 2013. Inositol pyrophosphates: between signalling and metabolism. *Biochem J*, 452, 369-79.
- WITTKOPP, T. M., SCHMOLLINGER, S., SAROUSSI, S., HU, W., ZHANG, W., FAN, Q., GALLAHER, S. D., LEONARD, M. T., SOUBEYRAND, E., BASSET, G. J., MERCHANT, S. S., GROSSMAN, A. R., DUANMU, D. & LAGARIAS, J. C. 2017. Bilin-Dependent Photoacclimation in *Chlamydomonas reinhardtii*. *The Plant Cell*, 29, 2711.
- WOOD, N. J. 2020. Microalgae for Combined Nutrient Recovery and Biofuel Production from Sewage. *A thesis submitted in accordance with the requirements for the degree of Doctor of Philosophy (PhD)*. University of Leeds, UK.
- WU, Q., GUO, L., LI, X. & WANG, Y. 2021. Effect of phosphorus concentration and light/dark condition on phosphorus uptake and distribution with microalgae. *Bioresource Technology*, 340, 125745.

- WUANG, S. C., KHIN, M. C., CHUA, P. Q. D. & LUO, Y. D. 2016. Use of Spirulina biomass produced from treatment of aquaculture wastewater as agricultural fertilizers. *Algal Research*, 15, 59-64.
- WUNDERLIN, P., MOHN, J., JOSS, A., EMMENEGGER, L. & SIEGRIST, H. 2012. Mechanisms of N₂O production in biological wastewater treatment under nitrifying and denitrifying conditions. *Water Research*, 46, 1027-1037.
- WURST, H. & KORNBERG, A. 1994. A soluble exopolyphosphatase of *Saccharomyces cerevisiae*. Purification and characterization. *Journal of Biological Chemistry*, 269, 10996-11001.
- WURST, H., SHIBA, T. & KORNBERG, A. 1995. The gene for a major exopolyphosphatase of *Saccharomyces cerevisiae*. *Journal of Bacteriology*, 177, 898-906.
- WYKOFF, D. D., GROSSMAN, A. R., WEEKS, D. P., USUDA, H. & SHIMOGAWARA, K. 1999. Psr1, a nuclear localized protein that regulates phosphorus metabolism in *Chlamydomonas*. *Proceedings of the National Academy of Sciences of the United States of America*, 96, 15336-15341.
- WYKOFF, D. D. & O'SHEA, E. K. 2001. Phosphate transport and sensing in *Saccharomyces cerevisiae*. *Genetics*, 159, 1491-9.
- XIE, L. & JAKOB, U. 2019. Inorganic polyphosphate, a multifunctional polyanionic protein scaffold. *Journal of Biological Chemistry*, 294, 2180-2190.
- XU, Y., WU, Y., ESQUIVEL-ELIZONDO, S., DOLFING, J. & RITTMANN, B. E. 2020. Using Microbial Aggregates to Entrap Aqueous Phosphorus. *Trends in Biotechnology*, 38, 1292-1303.
- YAO, B., XI, B., HU, C., HUO, S., SU, J. & LIU, H. 2011. A model and experimental study of phosphate uptake kinetics in algae: Considering surface adsorption and P-stress. *Journal of Environmental Sciences*, 23, 189-198.
- YAO, Z.-F., LIANG, C.-Y., ZHANG, Q., CHEN, Z.-J., XIAO, B.-X., TIAN, J. & LIAO, H. 2014. SPX1 is an important component in the phosphorus signalling network of common bean regulating root growth and phosphorus homeostasis. *Journal of Experimental Botany*, 65, 3299-3310.
- YEHUDAI-RESHEFF, S., ZIMMER, S. L., KOMINE, Y. & STERN, D. B. 2007. Integration of Chloroplast Nucleic Acid Metabolism into the Phosphate Deprivation Response in *Chlamydomonas reinhardtii*. *The Plant Cell*, 19, 1023-1038.
- YI-HSUAN, L., SHOTA, N., TONY, Z. J., FANG, I. Y., ANNA, K., ALEXANDER, F. Y., KOSUKE, F. & PO-HSIANG, W. 2023. One-pot chemo-enzymatic

synthesis and one-step recovery of homogeneous long-chain polyphosphates from microalgal biomass. *bioRxiv*, 2023.08.19.553819.

- YUAN, Z., JIANG, S., SHENG, H., LIU, X., HUA, H., LIU, X. & ZHANG, Y. 2018. Human Perturbation of the Global Phosphorus Cycle: Changes and Consequences. *Environmental science & technology*, 52, 2438-2450.
- YUEH, Y. G. & CRAIN, R. C. 1993. Deflagellation of *Chlamydomonas reinhardtii* follows a rapid transitory accumulation of inositol 1,4,5-trisphosphate and requires Ca²⁺ entry. *Journal of Cell Biology*, 123, 869-875.
- YULISTYORINI, A. 2016. *Phosphorus Recovery from Wastewater through Enhanced Micro-algal Uptake*. University of Leeds.
- ZHANG, N., PAZOUKI, L., NGUYEN, H., JACOBESHAGEN, S., BIGGE, B. M., XIA, M., MATTOON, E. M., KLEBANOVYCH, A., SORKIN, M., NUSINOW, D. A., AVASTHI, P., CZYMMEK, K. J. & ZHANG, R. 2022. Comparative Phenotyping of Two Commonly Used *Chlamydomonas reinhardtii* Background Strains: CC-1690 (21gr) and CC-5325 (The CLiP Mutant Library Background). *Plants*, 11, 585.
- ZHANG, R., PATENA, W., ARMBRUSTER, U., GANG, S. S., BLUM, S. R. & JONIKAS, M. C. 2014. High-Throughput Genotyping of Green Algal Mutants Reveals Random Distribution of Mutagenic Insertion Sites and Endonucleolytic Cleavage of Transforming DNA. *The Plant Cell*, 26, 1398.
- ZHANG, S., KIM, T.-H., HAN, T. H. & HWANG, S.-J. 2015. Influence of light conditions of a mixture of red and blue light sources on nitrogen and phosphorus removal in advanced wastewater treatment using *Scenedesmus dimorphus*. *Biotechnology and Bioprocess Engineering*, 20, 760-765.
- ZHAO, Y., YAN, Z., QIN, J. & XIAO, Z. 2014. Effects of long-term cattle manure application on soil properties and soil heavy metals in corn seed production in Northwest China. *Environmental Science and Pollution Research*, 21, 7586-7595.
- ZHU, W., MIAO, Q., SUN, D., YANG, G., WU, C., HUANG, J. & ZHENG, C. 2012. The mitochondrial phosphate transporters modulate plant responses to salt stress via affecting ATP and gibberellin metabolism in *Arabidopsis thaliana*.
- ZONES, J. M., BLABY, I. K., MERCHANT, S. S. & UMEN, J. G. 2015. High-Resolution Profiling of a Synchronized Diurnal Transcriptome from *Chlamydomonas reinhardtii* Reveals Continuous Cell and Metabolic Differentiation. *The Plant Cell*, 27, 2743.

Appendix

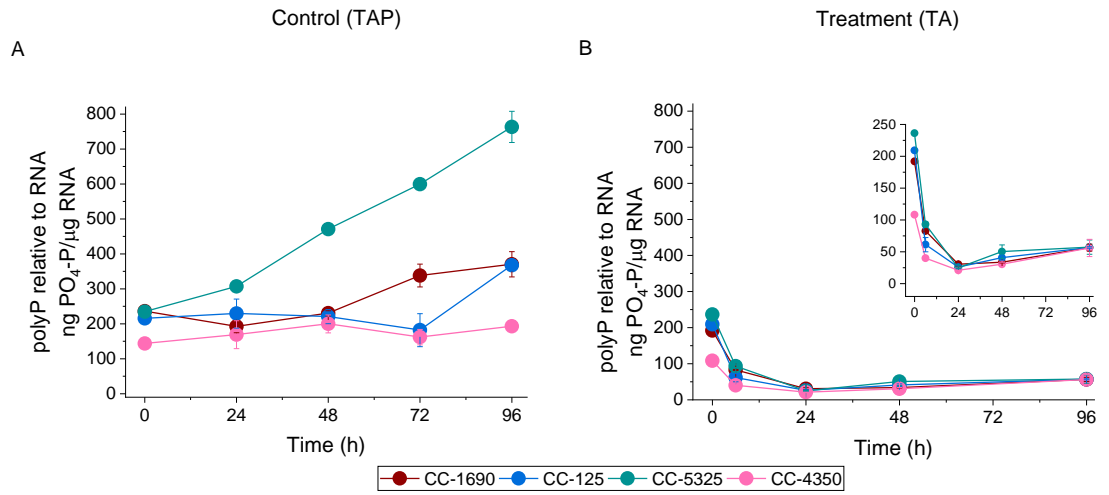


Figure A 1 Polyphosphate quantification of *C. reinhardtii* in proportion to RNA. PolyP quantification may be misinterpreted if expressed as a proportion to RNA content, due to decreased RNA content in biomass over time. and A-B polyP content relative to RNA (ng PO₄-P/μg RNA).

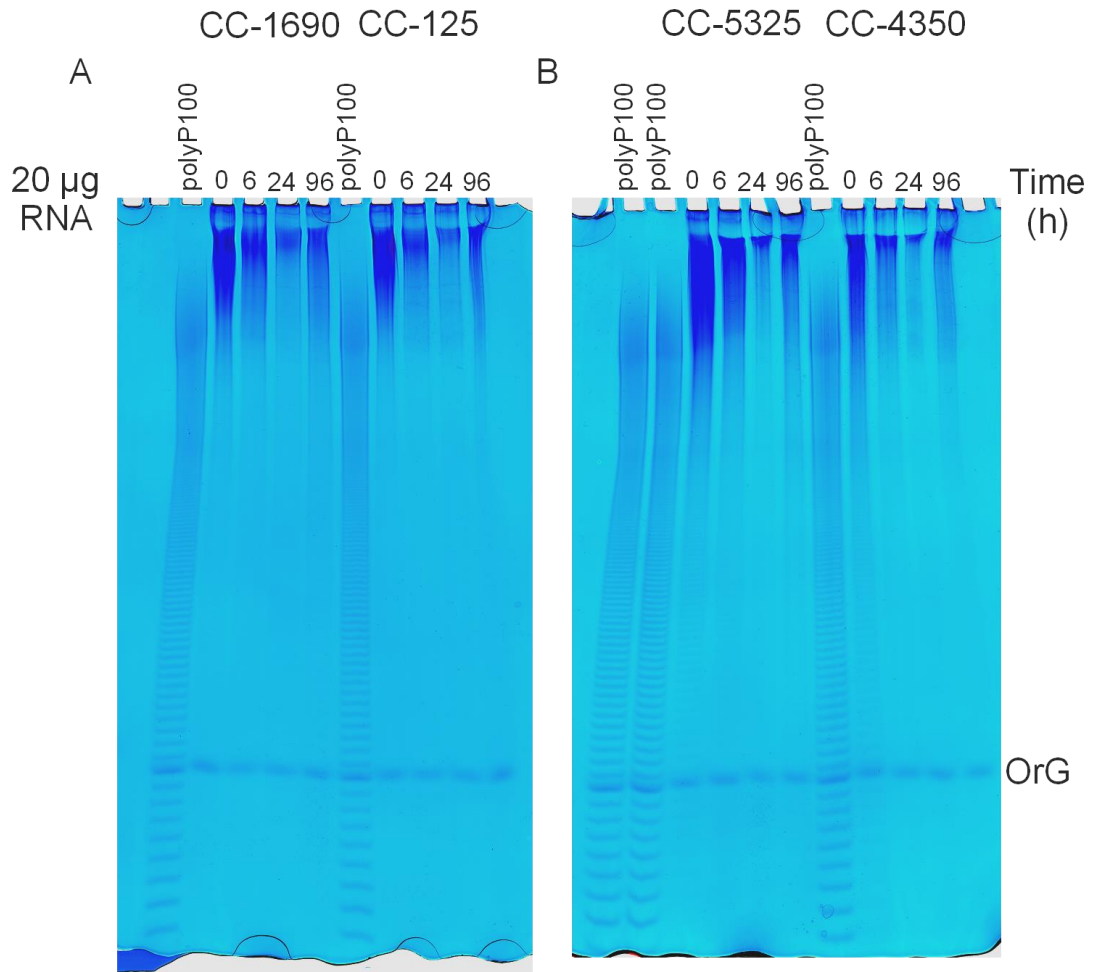


Figure A 2 PAGE polyP visualisation with equal loading of RNA from P-deprivation experiment. Equal loading of RNA on PAGE shows an 'increase' in polyP content after 96 h of P deprivation, leading to result misinterpretations. Visualisation of polyP migration on 20% PAGE shows normalisation of polyP by loading 20 µg RNA on each well. *C. reinhardtii* CC-1690, CC-125, CC-5325 and CC-4350 mid-exponential cells were resuspended in TA media (Treatment) and samples were collected after 6, 24 and 96 h. Orange dye (OrG) on the right indicates migration. polyP100 standard for medium and short-chain polyphosphate. PAGE was stained with Toluidine blue.

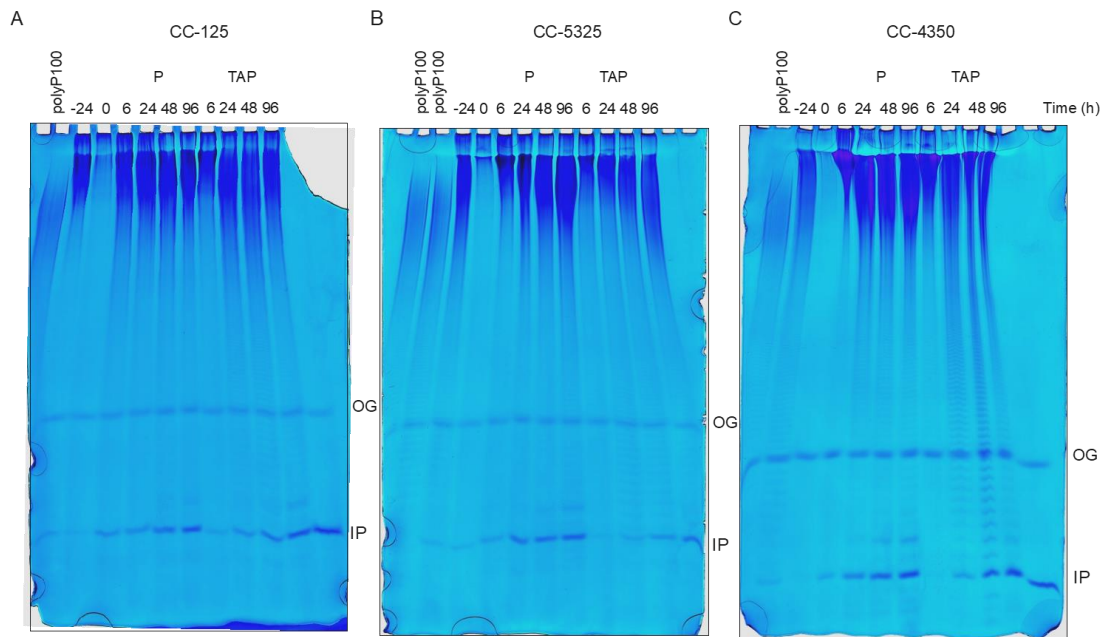


Figure A 3 PAGE with polyP migration during 24 h P deprivation and P repletion as KPO_4 or TAP media. 33% PAGE shows polyP migration of strains A CC-125, B CC-5325 and C CC-4350 mid-exponential cells (-24 h time point) resuspended in TA media (P deprivation) for 24 h and supplied of 1 mM P with either a KPO_4 solution (P repletion) or resuspended in fresh TAP media (TAP repletion) and monitored for 96 h. An equivalent of 500 μg dw per well was loaded. polyP100 was used as a standard (left side of PAGES). OrG indicates Orange G dye migration. IP_6 2 nmol standard confirmed the presence of IP_6 .

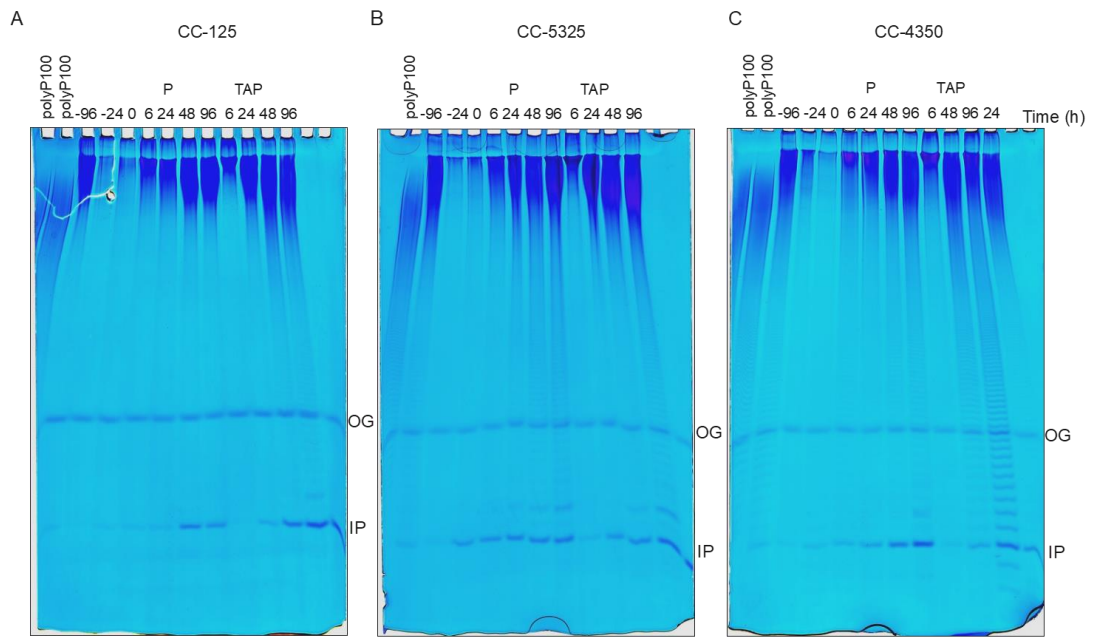


Figure A 4 PAGE with polyP migration during 96 h P deprivation and P repletion as KPO₄ or TAP media. 33% PAGE shows polyP migration of strains A CC-125, B CC-5325 and C CC-4350 mid-exponential cells (-96 h time point) resuspended in TA media (P deprivation) for 96 h (-72 h sample is equivalent to 24 h after P deprivation) and supplied of 1 mM P with either a KPO₄ solution (P repletion) or resuspended in fresh TAP media (TAP repletion) and monitored for 96 h. An equivalent of 500 μ g dw per well was loaded. polyP100 was used as a standard (left side of PAGEs). OrG indicates Orange G dye migration. IP₆ 2 nmol standard confirmed the presence of IP₆.

Day 2

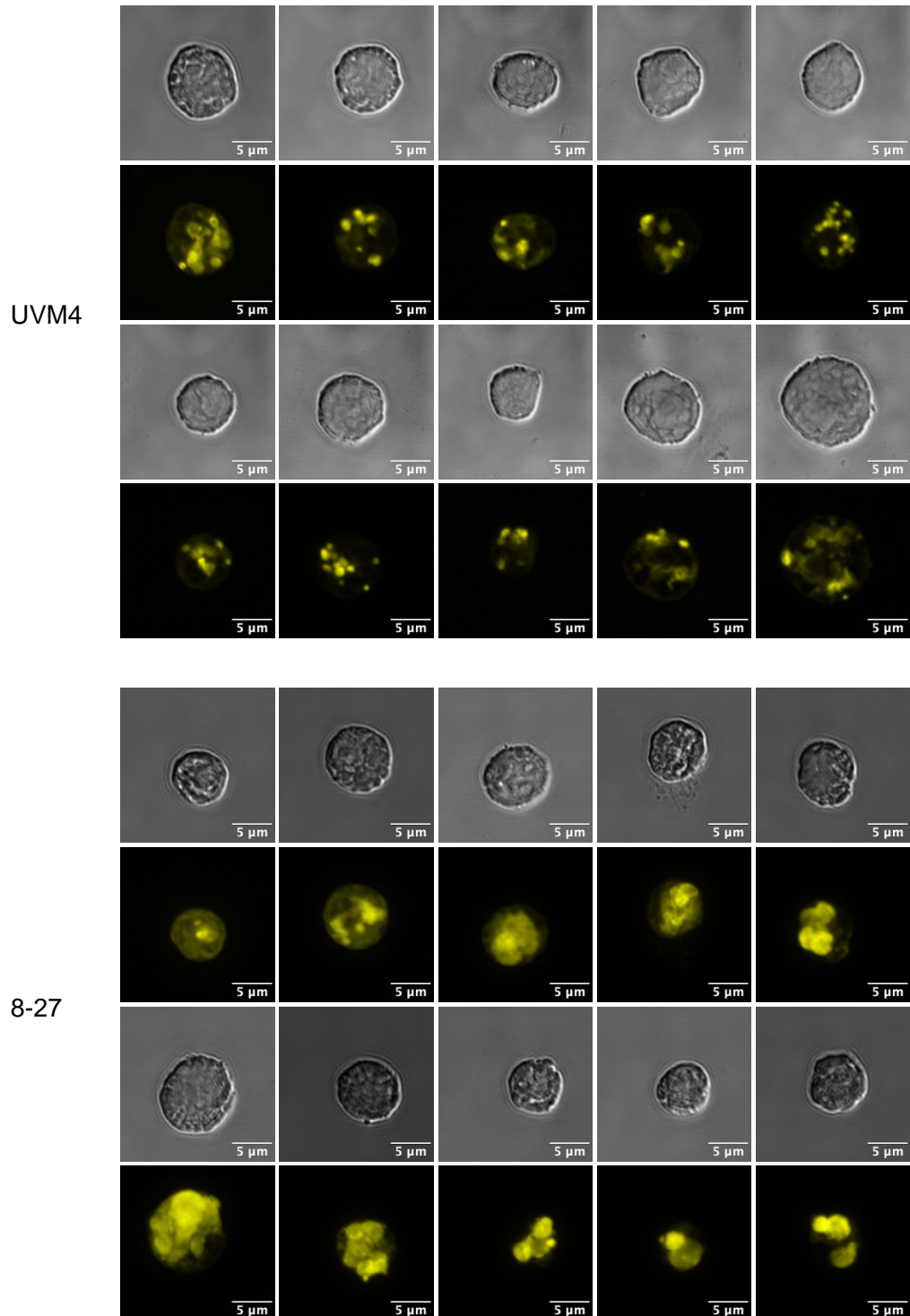


Figure A 5 Confocal images of DAPI stained cells taken after 48 h of cultivation. The images show the non-transformed control, UVM4 and the PSR1 overexpression strain 8-27. For one of the triplicates, 10 cells from each sample were randomly chosen out of 30-50 pictures. Brightfield (top/grey) and DAPI-Poly-P (bottom/yellow) represent the same cell. DAPI-polyP pictures are a projection of 6-12 z-stacks taken with the microscope software.

Day 3

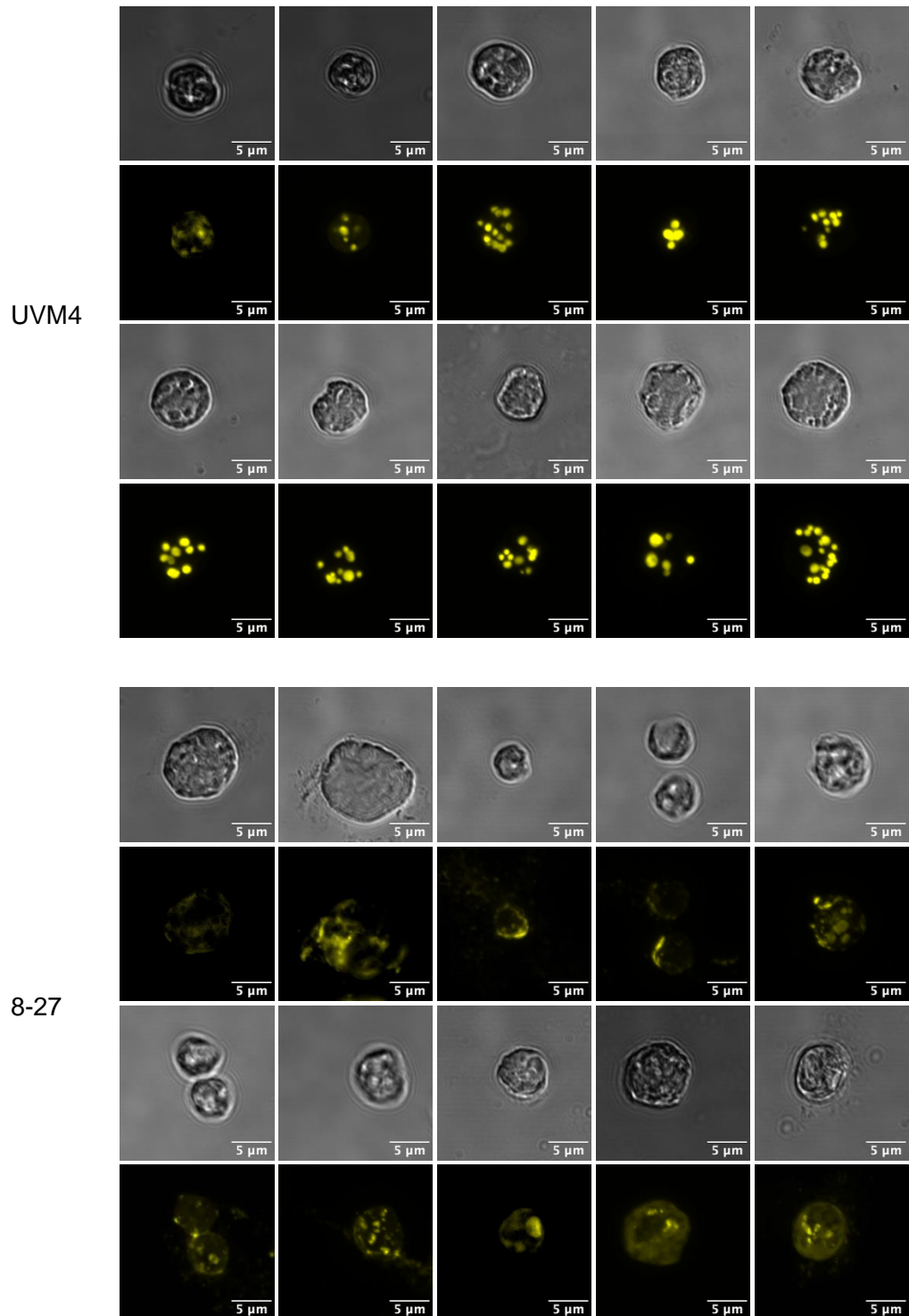


Figure A 6 Confocal images of DAPI stained cells taken after 72 h of cultivation. The images show the non-transformed control, UVM4 and the PSR1 overexpression strain 8-27. For one of the triplicates, 10 cells from each sample were randomly chosen out of 30-50 pictures. Brightfield (top/grey) and DAPI-Poly-P (bottom/yellow) represent the same cell. DAPI-polyP pictures are a projection of 6-12 z-stacks taken with the microscope software.

Day 6

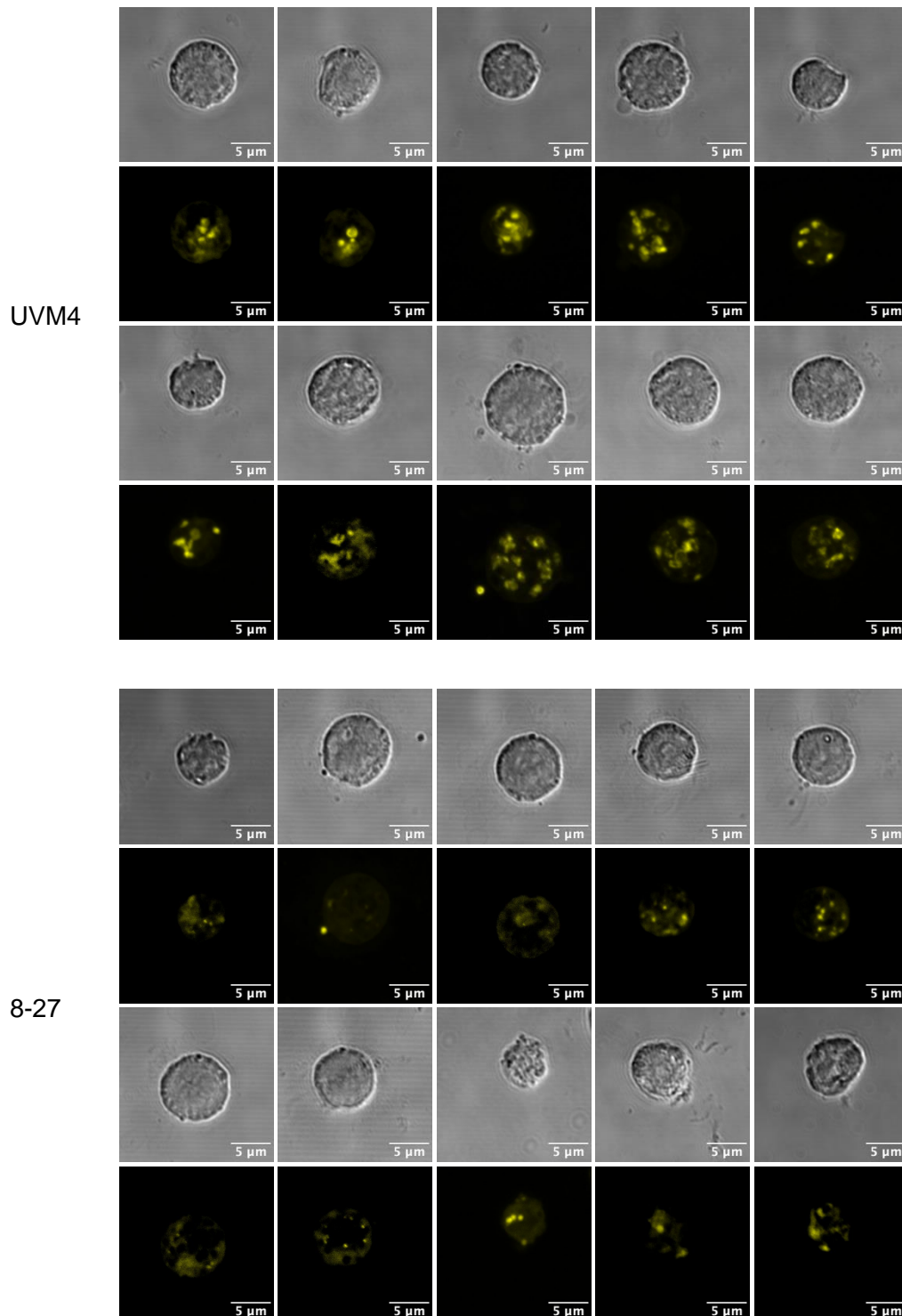


Figure A 7 Confocal images of DAPI stained cells taken after 144 h of cultivation. The images show the non-transformed control, UVM4 and the PSR1 overexpression strain 8-27. For one of the triplicates, 10 cells from each sample were randomly chosen out of 30-50 pictures. Brightfield (top/grey) and DAPI-Poly-P (bottom/yellow) represent the same cell. DAPI-polyP pictures are a projection of 6-12 z-stacks taken with the microscope software.

Table A 1 Changes in nutrient uptake rates by PSR1 overexpression strain and psr1-1 mutant, compared to the control. Average values (n=3) for the strains UVM4, 8-27 and psr1-1 were used \pm SE. nn corresponds to values below 0.1 mg g dw⁻¹ h⁻¹.

A				
Phosphate uptake rate				
mg PO ₄ -P g dw ⁻¹ h ⁻¹				
Strain	0-1 h	1-6 h	6-12 h	12-24 h
UVM4	3.40 \pm 0.27	6.25 \pm 0.16	0.31 \pm 0.11	nn
8-27	9.12 \pm 1.59	5.81 \pm 0.81	nn	nn
psr1-1	1.80 \pm 0.48	0.38 \pm 0.06	0.61 \pm 0.08	0.22 \pm 0.04
B				
Ammonium uptake rate				
mg NH ₄ -N g dw ⁻¹ h ⁻¹				
	0-1	1-6	6-12	12-24
UVM4	2.1 \pm 0.85	8.38 \pm 1.39	2.67 \pm 0.95	0.55 \pm 0.05
8-27	4.34 \pm 2.34	6.28 \pm 0.12	3.35 \pm 0.31	0.13 \pm 0.06
psr1-1	2.15 \pm 1.58	6.13 \pm 0.78	6.7 \pm 0.29	1.35 \pm 0.26
C				
Sulphate uptake rate				
mg SO ₄ -S g dw ⁻¹ h ⁻¹				
	0-1	1-6	6-12	12-24
UVM4	0.11 \pm 0.08	0.59 \pm 0.01	0.20 \pm 0.01	nn
8-27	0.40 \pm 0.27	0.47 \pm 0.02	0.28 \pm 0.02	nn
psr1-1	0.22 \pm 0.07	0.49 \pm 0.06	0.49 \pm 0.01	nn